Lipid-specific IgM antibodies in multiple sclerosis and viral immunity

Lorna Rebecca Hayden

B.A. Natural Sciences (mod. Molecular Medicine)

Submitted in fulfilment of the requirements for the Degree of Doctor of Philosophy

School of Infection, Immunity and Inflammation

College of Medical, Veterinary and Life Sciences

University of Glasgow

September, 2021

Abstract

Multiple sclerosis (MS) is an inflammatory demyelinating disease of the central nervous system (CNS) and the leading cause of disability in young adults. Over the last 20 years, a plethora of drugs have been approved for the treatment of MS, many of which target the immune response to reduce CNS inflammation. Although effective, many of these therapies have been associated with an increased risk of developing progressive multifocal leukoencephalopathy (PML), a fatal infection of the CNS by the John Cunningham virus. As a result, these effective therapeutics are used with caution pending the establishment of reliable risk stratification tools.

A recent association between intrathecal lipid-reactive IgM synthesis and reduced incidence of PML in natalizumab-treated MS prompted our investigation into the antiviral properties of lipid-reactive IgM antibodies. Using murine heterogenous CNS cultures, we investigated the antiviral properties of both human and mouse IgMs. Initial investigations focused on the sulfatide-reactive IgM O4, a major target of the IgM response in MS patients. Using microarray analysis, RT-qPCR, and fluorescence *in situ* hybridisation, alongside genetic knock-out cultures and a range of pharmacological inhibitors, it was deduced that O4 could stimulate microglia to upregulate interferon beta (IFN-ß) in a cGAS-STING-dependent manner, triggering global interferon stimulated gene (ISG) expression in major cell-types of the CNS. This interferon (IFN) response limited the replication of two genetically unrelated viruses, with final experiments focused on developing an *in vivo* model to investigate these antiviral IgMs.

The data presented in this thesis provide a plausible explanation for the association between intrathecal IgM synthesis and reduced incidence of PML in natalizumab-treated MS patients. This research will aid risk stratification of MS patients, allowing safe access to effective therapeutics. Further understanding of the mechanism of this antibody-mediated response could lead to the development of an antiviral therapy for use as a co-treatment in MS or as a broad-spectrum therapeutic for the treatment of viral encephalitis.

Table of Contents

List of tables

List of figures

Acknowledgements

First and foremost, I would like to thank my three wonderful supervisors who have been invaluable in guiding me through my PhD. I always say that you complement each other in both skill and personality. Prof. Christopher Linington being the “big ideas” man with a wealth of knowledge in biochemistry and immunology, Prof. Julia Edgar being the level-headed voice of reason whose expertise in neuroscience and multiple sclerosis undoubtedly made my publication possible, and finally Dr. Marieke Pingen, a savant of all things virology who spent the final year of my PhD teaching me a plethora of new skills which has been invaluable in my pursuit of post-PhD employment. You have all contributed immensely to my progress as a scientist and as a person.

Secondly, I would like to thank my funder Medical Research Scotland (MRS) and Alex Graham, the scientific advisor in charge of MRS PhD students. Not only has MRS supported my PhD project financially but has provided incredible training and networking experiences over the last four years. Thank you to my assessor Carl Goodyear for the wealth of advice over the last four years, and Alain for helping me find an industry placement when I was grasping at straws. Many thanks to Bill, Chris, Robyn, and Chloe at ILC Therapeutics for being so welcoming during my industry placement, it was a fun way to spend the last three months of my PhD. A final scientific acknowledgement to all the wonderful staff at the CRF, both your expertise and top-class banter made dissection days more bearable.

On a more personal note, thank you to the past and present occupants of B319 for the dazzling conversations, banter, and singsongs over the last four years. Thanks to the level 3 gang for all the craic and support. Special thanks to Diana who always helped me out when we were on our own despite being up to her eyes in cultures. More importantly, thank you for always being available for a drink, cup of tea, or a movie night. Glasgow lost a star when you moved! Thank you to Daniel and Liz. We joke that you are somehow my Glasgow family, but I honestly could not have made it through the last four years without you. And finally, thank you to my parents and family for supporting me through this journey. I know you were not so happy to see me leave but with mam’s monthly trips to Glasgow I think we somehow managed…

Author's declaration

I declare that, except where referenced to others, this thesis is the product of my own work and has not been submitted for any other degree at the University of Glasgow or any other institution.

Signature:

Printed name: LORNA HAYDEN

Abbreviations

Abbreviation	Full name
A4CD	non-specific IgM derived from mouse immunised with MOG
AA3	rat anti-proteolipid protein clone AA3
AD	Alzheimer's disease
AIM	apoptosis inhibitor of macrophages
ANOVA	analysis of variance
APO	apolipoprotein
ATP	adenosine triphosphate
Aß	amyloid beta
BBB	blood-brain-barrier
bp	base pair
BSA	bovine serum albumin
BUNV	bunyamwera virus
C(x)	complement component (x)
CB	cerebellum
CCL	C-C motif ligand
CCR	C-C motif receptor
CD	cluster of differentiation
CD5L	CD5-like
cDNA	complementary DNA
cGAS	cyclic GMP-AMP synthase
CIS	clinically isolated syndrome
CNS	central nervous system
CSF	cerebrospinal fluid
CST	cerebroside sulfotransferase
CT	copy number at threshold
CTL	cytotoxic lymphocyte
CX	cortex
CX3CR	C-X3-C motif chemokine receptor
CXCL	C-X-C motif ligand
CXCR	C-X-C motif receptor
DAMP	damage-associated molecular pattern
DAPI	4′,6-diamidino-2-phenylindole
DAVID	database for annotation, visualisation, and integrated discovery
DC	dendritic cell
DDX	DExD/H-box helicase
DEG	differentially expressed gene
dH2O	deionised water
DIV	day *in vitro*
DM	differentiation media
DMEM	Dulbecco's modified Eagle's medium
DMSO	dimethyl sulfoxide
DMT	disease modifying therapy

Continued overleaf

DNA	deoxyribose nucleic acid
DPBS	Dulbecco's phosphate buffered saline
dsDNA	double-stranded DNA
dsRNA	double-stranded RNA
E(x)	embryonic day (x)
EAE	experimental autoimmune encephalomyelitis
EDTA	ethylenediaminetetraacetic acid
efH2O	endotoxin-free water
EGF	epidermal growth factor
ER	endoplasmic reticulum
FA2H	fatty acid-2-hydroxylase
FBS	foetal bovine serum
Fcα/μR	Fc alpha mu receptor
FcμR	Fc mu receptor
F*is*H	fluorescence *in situ* hybridisation
GA	glatiramer acetate
GalC	galactosyl ceramidase
GAPDH	glyceraldehyde-3-phosphate dehydrogenase
GBP	guanylate binding protein
Gd	gadolinium
gDNA	genomic DNA
GFAP	glial fibrillary acid protein
GO	gene ontology
GTP	guanosine-5'-triphosphate
HBSS	Hank's balanced salt solution
hiPSC	human induced pluripotent stem cell
HIV1	human immunodeficiency virus 1
HMGB1	high motility group box protein 1
HSV	herpes simplex virus
i.n.	intranasal
i.p.	intraperitoneal
Iba1	ionized calcium binding adaptor molecule 1
IFI	interferon gamma inducible protein
IFIT	interferon induced protein with tetratricopeptide repeats
IFNAR	interferon alpha/beta receptor
IFNGR	interferon gamma receptor
IFN-I	type-I interferon
IFN-α	interferon alpha
IFN-β	interferon beta
IFN-γ	interferon gamma
IFN-λ	interferon lambda
IFNλR	interferon lambda receptor
Ig	immunoglobulin
IL	interleukin
iNOS	inducible nitric oxide synthase
IRF	interferon regulatory factor
IRG	interferon regulated gene

Continued overleaf

IRGM	immunity related GTPase M
ISG	interferon stimulated gene
iSLE	incomplete systemic lupus erythematosus
J chain	joining chain
JCV	John Cunningham virus
kDa	kilo Dalton
KEGG	Kyoto encyclopaedia of genes and genomes
L-15 medium	Leibovitz's L-15 medium
LCMV	lymphocytic choriomeningitis virus
LMW	low molecular weight
LPS	lipopolysaccharide
MAG	myelin associated glycoprotein
MAP2	microtubule associated protein 2
MAVS	mitochondrial antiviral signalling protein
MDA5	melanoma differentiation associated gene 5
MOG	myelin oligodendrocyte glycoprotein
MOI	multiplicity of infection
mRNA	messenger RNA
MS	multiple sclerosis
MWCO	molecular weight cut off
Mx1	MX dynamin-like GTPase 1
MyD88	myeloid differentiation primary response protein 88
MYRF	myelin regulatory factor
NAWM	normal appearing white matter
NCBI	national centre for biotechnology information
NeuN	neuronal specific nuclear protein
NFκB	nuclear factor kappa-light-chain-enhancer of activated B cells
NK	natural killer
NOD	nitric oxide
NOD	nucleotide-binding and oligomerization domain
NS	non-structural
NT	neurotransmitter
O1	mouse anti-GlaC IgM clone O1
O4	mouse anti-sulfatide IgM clone O4
OAS	oligoadenylate synthase
OCB	oligoclonal band
OFB	olfactory bulb
Olig2	oligodendrocyte transcription factor 2
OSC	organotypic slice culture
PAMP	pathogen-associated molecular pattern
PBMC	peripheral blood mononuclear cell
PBS	phosphate buffered saline
PCR	polymerase chain reaction
Pen/Strep	penicillin-streptomycin
PFA	paraformaldehyde
pfu	plaque forming unit
PI	propidium iodide

Continued overleaf

pIgR	polymeric immunoglobulin receptor
PML	progressive multifocal leukoencephalopathy
poly I:C	polyinosinic:polycytidylic acid
PPMS	primary progressive multiple sclerosis
PRR	pattern recognition receptor
PVM	perivascular macrophage
***q* - value**	adjusted *p* - value
RAC	rac family small GTPase
rhIgM22	recombinant human IgM 22
RIG-I	retinoic acid inducible protein 1
RNA	ribose nucleic acid
RRMS	relapsing-remitting multiple sclerosis
Rsad2	radical S-adenosyl methionine domain-containing protein 2
RT	reverse transcriptase
RT-qPCR	real-time quantitative polymerase chain reaction
S/D	Sprague Dawley
SDS PAGE	sodium dodecyl sulfate polyacrylamide gel electrophoresis
SFV	Semliki forest virus
siRNA	small-interfering RNA
SLE	systemic lupus erythematosus
SP	spleen
SPMS	secondary progressive multiple sclerosis
SRCR	scavenger receptor of the cysteine-rich family
ssRNA	singe-stranded RNA
STING	stimulator of interferon genes
T-75	75 cm^3 tissue culture flask
TAE	tris-acetate-EDTA
TANK	TRAF family member-associated NFκB activator
TBEV	tick-borne encephalitis virus
TBK	TANK binding kinase
TGM	transglutaminase
Th	T helper
TI	T cell-independent
TLR	toll-like receptor
TNF-α	tumour necrosis factor alpha
TRAF	tumour necrosis factor receptor-associated factor
TRAM	translocating chain-associated membrane protein
TRIF	TIR-domain-containing adapter-inducing interferon-β
WT	wild-type
ZC3HAV	zinc finger CCCH-type containing antiviral
ZFP	zinc-finger protein

Chapter 1

Introduction

1 Introduction

1.1 Cells of the central nervous system

1.1.1 Overview

The central nervous system (CNS) consists of the brain, spinal cord, and optic nerve, and is responsible for processing information from the environment, initiating voluntary and involuntary muscle movements, enabling learning, forming memories, and defining our personalities through affective functions. Many cell-types make up the brain, the most predominant of which are: neurons, astrocytes, and oligodendrocytes. The CNS also houses its own immune cell population consisting of several types of myeloid cell. These include microglia, macrophages, monocytes, dendritic cells (DCs), and granulocytes (Goldmann et al. 2016; Chinnery, Ruitenberg, and McMenamin 2010).

1.1.2 Neurons

Neurons are electrically excitable and carry information between the CNS, peripheral nervous system, and effector tissues/organs (Bernhard and Rexed 1945; Gesell, Hunter, and Lillie 1949; Barakan, Downman, and Eccles 1949). Neurons generate and conduct electrical signals in the form of action potentials and communicate with each other through the release of neurotransmitters. A typical neuron has four morphologically defined regions: dendrites, cell body, axon, and pre-synaptic terminals (Eyzaguirre and Kuffler 1955).

Dendrites detect neurotransmitters (NTs) from other neurons through NT receptors (Dale 1934; Lands 1951). Upon NT binding to its receptor, the neuron responds by opening ion channels, allowing ions to enter or exit the neuron (Purpura 1957; Bradbury et al. 1974). Some presynaptic neurons are excitatory, meaning they stimulate the signalling of the next neuron. Others are inhibitory, meaning they inhibit the signalling of the next neuron (Florey 1954).

For the post-synaptic neuron to transmit information downstream of the neurotransmitter-derived signal, positive ions must enter the cell and increase

the neuron's membrane potential from resting state (approximately - 70 mV) to the threshold of excitation (approximately - 55 mV) (Amatniek et al. 1957; Chandler and Hodgkin 1965; Eyzaguirre and Kuffler 1955). This increase in membrane potential is called depolarisation and if this threshold is reached, additional sodium ion channels are opened leading to a massive increase in membrane potential (approximately + 30 mV) initiating an action potential (Eyzaguirre and Kuffler 1955).

Sodium ions diffuse from the neuronal cell body to the axon initial segment, and subsequently to consecutive nodes of Ranvier as voltage-gated sodium channels open downstream. This process of ion diffusion and sodium channel opening continues until the impulse reaches the axon terminus, causing the release of NTs into the synaptic cleft to interact with the next neuron or effector tissue (Goldman and Blaustein 1966; Hutter and Kostial 1955). Following depolarisation, potassium channels open allowing potassium ion egress, returning the membrane potential to resting state (repolarisation) after a brief hyperpolarisation (Eyzaguirre and Kuffler 1955; Akman, Silber, and et al. 1949).

1.1.3 Glia

Astrocytes, oligodendrocytes, and microglia are termed "glial" cells, stemming from the Greek word meaning "glue". Historically these cells were considered purely structural, holding neurons in place within the CNS (Herndon 1964; Dermietzel and Spray 1998). We are now aware of the many functions of glial cells within the CNS, including maintaining homeostasis and facilitating neuronal signalling. Based on their size, glia can be further divided into "macroglia" (astrocytes and oligodendrocytes), and "microglia" (Glees and Hasan 1990).

1.1.4 Astrocytes

Astrocytes have multiple homeostatic functions in the CNS, including those relating directly to neuronal function, and others required to protect the brain from harmful pathogens or substances (Björklund et al. 1984; Vernadakis 1988). Astrocytic functions which directly aid neuronal signalling include the maintenance of extracellular potassium concentration, uptake of neurotransmitters from the synaptic cleft, release of neurotransmitter precursors, and provision of energy substrates to neurons (Hertz and Nissen

1976; Hertz, Wu, and Schousboe 1978; Erecińska and Silver 1990; R.P. Shank and Aprison 1979; R. P. Shank and Campbell 1984). Other functions include reinforcement of the blood-brain-barrier (BBB), scavenging of reactive oxygen species, and working with microglia to mount an immune response against pathogens (Brightman and Reese 1969; Lucius and Sievers 1996; Pinteaux et al. 1996; Schreiner et al. 2015; J.S. Park et al. 2021).

Astrocytes have specialised end-feet that cover nearly the entire surface of CNS microvessels (Liebner et al. 2018). End-feet proteins aquaporin-4 and Kir4.1 regulate water homeostasis at the neurovascular unit whilst secreted proteins Wnt, sonic hedgehog, retinoic acid, glial-derived neurotropic factor, and angiopoietin upregulate endothelial tight junction protein expression (Eid et al. 2005; Bosco et al. 2005; Igarashi et al. 1999; Alvarez et al. 2011; Mizee et al. 2014; Y. Zhou et al. 2014; Gurnik et al. 2016). Loss of contact or disruption to astrocytic end-feet causes expansion of blood vessel diameter, downregulation of tight junction proteins, and an increase in BBB permeability (S. Ma, Kwon, and Huang 2012; Lien et al. 2012; Menezes et al. 2014).

Astrocyte-microglia crosstalk is mediated by a variety of signalling pathways and can lead to an effective immune response in the event of infection. However chronic activation can contribute to pathology in neurological disease. Due to the complex nature of the CNS and the multiple effector molecules released in response to infection/injury, it is difficult to describe the impact of a single signalling pathway in the context of disease.

However, some inter-glial pathways have been described in detail including the complement pathway whereby astrocytic C3 interacts with microglial C3aR to mediate amyloid beta pathology and neuroinflammation in Alzheimer's disease, and the IL-18 and IL-18R pathway where microglial IL-18 induces astrocytic hypertrophy and proinflammatory cytokine release through IL-18R in traumatic brain injury (Lian et al. 2016; Miyoshi et al. 2008). Furthermore, an array of cytokines and proinflammatory molecules have been implicated in astrocyte-microglial crosstalk, though their exact mechanisms of action have not been elucidated. These include the cytokine CCL2 and the apolipoprotein serum amyloid A (Barbierato et al. 2017; Xu et al. 2017).

1.1.5 Oligodendrocytes

The principal role of oligodendrocytes is to produce myelin which ensheaths the axons of neurons. Oligodendrocytes wrap their processes tightly around neurons forming a spiral with multiple layers of membrane surrounding the axon (Raine 1984). On a typical myelinated neuron, oligodendrocytes ensheath uniform sections of the neuron, leaving regular gaps along the axon called nodes of Ranvier (Ranvier 1871). These gaps leave the axolemma exposed to extracellular fluid, including sodium ions which influx through voltage-gated sodium channels to potentiate action potentials (Mueller 1958). The compact layers of myelin insulate the axon and reduce internodal capacitance. Action potentials "jump" from node to node, drastically increasing the rate of electrical pulse transmission along the axon (Funch and Faber 1984).

The tight compact barrier formed by myelin allows for rapid electrical conductance but also disconnects the axon surface from the extracellular milieu, limiting uptake of energy substrates through the axonal membrane. It has been suggested that the limited axonal membrane exposure at nodes of Ranvier is insufficient surface area for the uptake of energy substrates required for axonal function (Saab, Tzvetanova, and Nave 2013; Philips and Rothstein 2017; Stadelmann et al. 2019). This has led to the hypothesis of metabolic coupling between axons and oligodendrocytes whereby oligodendrocytes syphon energy substrates to the axon through the cytoplasmic myelinic channel that runs from the oligodendrocyte soma to the inner most layer of the myelin sheath. This is further supported by the capacity of the oligodendrocyte to produce large quantities of lactate, and the presence of monocarboxylate transporters (MCTs) at the adaxonal membrane of the myelin sheath (Y. Lee et al. 2012; Fünfschilling et al. 2012; Peachey et al. 2018). Indeed, oligodendrocyte-specific knock-down of MCT1 induces axonal injury and degeneration with no visible alterations to myelin integrity (F. Dong et al. 2017; Y. Lee et al. 2012).

In addition to conductance and metabolic coupling, specific myelin proteins are known to contribute to axonal integrity, with their absence leading to late-onset axonal pathology. Examples of such proteins include proteolipid protein, 2',3'-cyclic nucleotide 3'-phosphodiesterase, and myelin-associated glycoprotein, with genetic knock-out mice displaying axonal pathology in the absence of any

disturbances to the myelin sheath (Klugmann et al. 1997; Lappe-Siefke et al. 2003; Yin et al. 1998). *In vivo* observations suggest that these proteins might be involved in the transportation of cargo within the myelin sheath as well as organelle transport within the axon by way of influencing neurofilament function (Sousa and Bhat 2007; H.B. Werner et al. 2007). This is further supported by peroxisomal and mitochondrial perturbations in oligodendrocytes and neurons respectively leading to late-onset axonal degeneration (Kassmann et al. 2007; Woolums et al. 2020).

Loss of function mutations in single myelin proteins are observed in a heterogenous group of neurodegenerative disorders termed hereditary spastic paraplegia (HSP) whereby patients experience progressive spasticity and weakness of lower limbs. Although HSP is a genetically diverse group of disorders, they have a common feature whereby axonal pathology occurs whilst surrounded by an intact myelin sheath (Salinas et al. 2008). In contrast, the degradation of myelin in inflammatory demyelinating diseases such as MS and neuromyelitis optica spectrum disorder exposes axons to lysis by peripheral immune cells as well as cytotoxic molecules released by CNS-resident macrophages and microglia (Lumsden 1971; Putnam 1934; Yamasaki and Kira 2019; Kitley et al. 2014). Therefore, the myelin sheath not only provides insulation and trophic support to the axon but acts as a protective barrier preventing axonal degeneration by cytotoxic extracellular factors.

1.1.6 Myeloid cells

A variety of myeloid cells are present in the CNS, each occupying specific anatomical niches within the brain and spinal cord. The primary function of these myeloid cells is immune surveillance, with microglia occupying the CNS parenchyma, and other myeloid cells surveying the meninges, choroid plexus, and perivascular space. Each region-specific myeloid cell-type has additional homeostatic functions depending on location. These cells also vary in their contribution to neuropathology in the event of infection, injury, autoimmunity, and neurodegeneration (Goldmann et al. 2016; Chinnery, Ruitenberg, and McMenamin 2010).

1.1.7 Microglia

Microglia are the most prominent myeloid cell-type of the CNS. Derived from, erythomyeloid precursors in the extra-embryonic yolk sac, these tissue-resident macrophages occupy the brain in early embryonic development and remain there throughout adulthood (Streit, Graeber, and Kreutzberg 1988; Akiyama et al. 1994; Kierdorf et al. 2013; Ginhoux et al. 2010). Microglia undergo coupled apoptosis and local proliferation to maintain appropriate cell numbers in the parenchyma and, in contrast to non-CNS tissues, are not replenished by peripheral monocytes (Ajami et al. 2007; Askew et al. 2017).

Homeostatic functions of microglia include dictating neural progenitor fate decisions, synaptogenesis, synaptic pruning, neurite formation, and clearance of cellular debris (Wake et al. 2009; Jonakait et al. 2000; Blinzinger and Kreutzberg 1968; Hung et al. 2010; Paolicelli et al. 2011; Lemkey-Johnston, Butler, and Reynolds 1976). Microglial processes are dynamic, continually surveying their environment for perturbations including damage-associated molecular patterns (DAMPs), pathogen-associated molecular patterns (PAMPs), cytokines, chemokines, and changes in pH, with evidence of their processes extending to cover 10 times the size of their cell bodies (Nimmerjahn, Kirchhoff, and Helmchen 2005; DuBois, Bolton, and Cuzner 1986; Esen and Kielian 2006; Edye et al. 2013).

Given their role in maintaining synaptic integrity and neuronal circuitry, it is unsurprising that mice with mutant microglial phenotypes have severe developmental deficits. Important microglial proteins involved in synaptic pruning and neuronal maintenance include C3, C1q, C3R, and CX3CR1, with mice deficient in these proteins presenting with an increase in apoptotic neurons and a decrease in synaptic transmission, functional connectivity, and cognitive performance (Stevens et al. 2007; Schafer et al. 2012; Paolicelli et al. 2011; Zhan et al. 2014).

Recent advances have allowed for CNS-resident microglia to be differentiated from perivascular macrophages (PVMs) in *in vivo* models of CNS disease. In the mouse model of MS, experimental autoimmune encephalomyelitis (EAE), microglia have a protective role clearing tissue debris and aiding recovery. In

contrast, infiltrating monocyte-derived macrophages promote demyelination, contributing to EAE pathology (Yamasaki et al. 2014; N.D. Lewis et al. 2014).

However, in mouse models of neurodegenerative diseases such as dementia, microglia contribute to pathology through excessive phagocytosis of synapses, triggered by the presence of protein aggregates. This pathological characteristic is attributed to an age-associated decline in microglial function (Hong et al. 2016; Herz et al. 2017). In infection, microglia have positive roles in pathogen phagocytosis and cytokine production, leading to leukocyte infiltration and pathogen clearance. However, the secretion of cytokines can also negatively affect neurogenesis and cause neurotoxicity (Braun et al. 1999).

1.1.8 Macrophages, monocytes, dendritic cells, and granulocytes

Non-parenchymal macrophages of the meninges, choroid plexus, and perivascular areas of the CNS have important roles in sampling local debris and dying cells, as well as macromolecules draining through the CNS lymphatic system (Louveau et al. 2015). Furthermore, non-parenchymal macrophages are involved in amyloid beta clearance in Alzheimer's disease (Mendes-Jorge et al. 2009; Maat-Schieman et al. 1997; Hawkes and McLaurin 2009; Goldmann et al. 2016). PVMs have additional homeostatic functions in preserving endothelial cell health including promotion of capillary stability, regulation of vascular constriction, and maintenance of blood-brain-barrier integrity (Mendes-Jorge et al. 2009; He et al. 2016). PVMs are transcriptionally related to microglia, with PVMs displaying similar characteristics to microglia including longevity and lack of replenishment by peripheral monocytes (Goldmann et al. 2016).

In the context of disease, infiltrating macrophages cause oxidative stress, cytotoxicity, and the recruitment of immune cells such as neutrophils and monocytes (Fischer et al. 2012; Mildner et al. 2008). In MS, PVMs have been shown to reactivate infiltrating autoreactive T cells, allowing T cell entry to the parenchyma (Tran et al. 1998; Bartholomäus et al. 2009). Monocytes are rarely found in the CNS under homeostatic conditions but can infiltrate during disease (Mildner et al. 2008). Monocyte infiltration has been implicated in the pathology of several CNS diseases with proinflammatory factors central to their pathological mechanisms. These factors include proteolytic enzymes, reactive

oxygen species, and cytokines which breakdown the BBB (Mildner et al. 2008; Herz et al. 2017).

Other myeloid cells of the CNS include DCs and granulocytes (Chinnery, Ruitenberg, and McMenamin 2010). DCs, neutrophils, and mast cells are all found in the meninges, with DCs also found in the choroid plexus, and mast cells in the parenchyma (Serot et al. 1997; Kiernan 1976; Chinnery, Ruitenberg, and McMenamin 2010). Mast cells have homeostatic functions as sources of serotonin, but the basal function of resident DCs and neutrophils remains obscure (Nautiyal et al. 2012; Cronk et al. 2015; Herz et al. 2017).

The role of DCs under disease conditions has been well described in the CNS. In MS, DCs are known to sample and process CNS antigens, present myelin antigen to T cells in draining lymph nodes, reactivate meningeal T cells, and directly cause CNS tissue damage (Matsumoto et al. 1986; Risau, Engelhardt, and Wekerle 1990; Ifergan et al. 2008; Keller et al. 2017; von Glehn et al. 2018).

The CNS is a complex organ that not only comprises of nerves and macroglia, but a host of immune cells with integral homeostatic functions critical for the maintenance of CNS integrity. In the event of disease, immune cells can protect the CNS and aid recovery, but can also inadvertently contribute to disease pathology. MS is an example of one such disease which will be discussed in the next section.

1.2 Multiple sclerosis

1.2.1 Overview

MS is an inflammatory demyelinating disease of the CNS whereby the myelin sheath is focally degraded leading to perturbed neuronal signalling, axonal degeneration, and neuronal cell death (Putnam 1934; Périer and Grégoire 1965; Lumsden 1971). There are different MS phenotypes including clinically isolated syndrome (CIS), relapsing remitting MS (RRMS), primary progressive MS (PPMS), and secondary progressive MS (SPMS) (F.D. Lublin et al. 2014). Symptoms range from visual/gait disturbances in early stages of disease, to permanent disability

and death in later stages (Lumsden 1971). The cause of MS is unknown and there is no cure (Yamout and Alroughani 2018). Many disease modifying therapies (DMTs) have been approved for the treatment of MS which aim to reduce the frequency and severity of relapses in RRMS patients, limit disease progression, and prevent further neurological deficits for all MS patients (Hauser and Cree 2020). For a list of DMTs approved for the treatment of MS, see Table 1.1.

1.2.2 Epidemiology

Approximately 100,000 people are living with MS in the UK alone, with worldwide figures estimated at 2.8 million (GBD-2016-Multiple-Sclerosis-Collaborators 2019; Walton et al. 2020). Although the cause of MS is unknown, it is generally considered a complex disorder where environmental factors initiate disease in genetically susceptible individuals.

Currently, 200 genetic loci are linked with susceptibility to MS (Haines et al. 1998; Baranzini and Oksenberg 2017). Of these, ~ 90 are HLA loci, implicating antigen recognition in the pathogenesis of MS. HLA loci account for approximately 20 – 30 % of the genetic susceptibility in MS, examples of which include HLA-DRB1*1501, HLA-DQB1*0301, and HLA-DQB1*0602 (Barcellos et al. 2006; Zivadinov et al. 2007).

Other immunological genes contribute minor susceptibility, including *IL2RA*, *IL17RA*, and *TNFRSF1A* (Hafler et al. 2007; De Jager et al. 2009; Haines et al. 1998). Furthermore, females are approximately three times more likely to develop MS than males, highlighting sex differences in the development of MS (Beeson 1994; Jacobson et al. 1997). Biological factors alone do not cause MS indicating a significant environmental component to the disease. Factors such as vitamin D deficiency, Epstein Barr virus infection, and smoking are associated with an increased risk of developing MS (Compston and Coles 2008). Thus, researching gene-environmental interactions in the context of MS could lead to the identification of the true cause of MS and improve understanding of other autoimmune and inflammatory diseases.

Table 1.1 Disease modifying therapies approved for multiple sclerosis

Drug name	Brand name	Route	Mechanism	Approved
Interferon ß-1b	Betaferon	Injection	Unknown	(1993) US (2007) EU (2002) UK
Interferon ß-1a	Avonex	Injection	Unknown	(1996) US (1997) EU (2002) UK
Glatiramer acetate	Copaxone	Injection	Unknown	(1996) US (2000) EU (2002) UK
Mitoxantrone	Novantrone	Infusion	Type II topoisomerase inhibitor	(2000) US (2002) EU (2002) UK
Natalizumab	Tysabri	Infusion	α4ß1 integrin mAb	(2004) US (2006) EU (2007) UK
Fingolimod	Gilenya	Oral	Sphingosine-1-phosphate receptor inhibitor	(2010) US (2011) EU (2012) UK
Teriflunomide	Aubagio	Oral	Unknown	(2012) US (2013) EU (2014) UK
Dimethyl fumarate	Tecfidera	Oral	Unknown	(2013) US (2014) EU (2014) UK
Alemtuzumab	Lemtrada	Infusion	CD52 mAb	(2014) US (2013) EU (2014) UK
Ocrelizumab	Ocrevus	Infusion	CD20 mAb	(2016) US (2018) EU (2018) UK
Cladribine	Mavenclad	Oral	Purine analogue	(2019) US (2017) EU (2017) UK
Siponimod	Mayzent	Oral	Sphingosine-1-phosphate receptor inhibitor	(2019) US (2020) EU (2020) UK
Ozanimod	Zeposia	Oral	Sphingosine-1-phosphate receptor inhibitor	(2020) US (2020) EU (2021) UK
Ofatumumab	Kesimpta	Injection	CD20	(2020) US (2021) EU (2021) UK
Ponesimod	Ponvory	Oral	Sphingosine-1-phosphate receptor inhibitor	(2021) US (2021) EU (-----) UK

mAb = monoclonal antibody. Approval years acquired from U.S. Food and Drug Administration (US), European Medicines Agency (EU), and National Health Service (UK) websites.

1.2.3 Pathophysiology

The pathophysiology of MS varies depending on the type of MS. CIS is characterised by an acute or sub-acute neurological disturbance lasting greater than 24 hrs, with peak severity occurring 2-3 weeks after symptom onset (D.H. Miller et al. 2008). A CIS episode is defined as being isolated in both space and time, meaning that the episode is caused by a single demyelinating lesion, usually on the optic nerve, brain stem, or spinal cord, and that the incident occurred once, i.e. the patients did not relapse (Thompson et al. 2018). To rule out infection, the episode must occur in the absence of fever or clinical symptoms of encephalopathy (D.H. Miller et al. 2008). Neurological symptoms of a CIS event include visual impairment, ataxia, or limb weakness depending on the location of the lesion. CIS is often the first clinical symptom of RRMS, with CIS conversion to clinically definite RRMS varying between 10 - 85 % of CIS cases depending on other MS-associated risk factors (D.H. Miller, Chard, and Ciccarelli 2012).

RRMS is characterised by periods of neurological impairment followed by functional recovery and accounts for 85 % of MS diagnoses. Typical age of onset of RRMS is 20 – 40 years of age, with 60 – 70 % of patients converting to SPMS within 10 - 20 years of RRMS diagnosis (Confavreux and Vukusic 2006). Both PPMS and SPMS are characterised by gradual functional decline with no periods of remission (Kurtzke 1956). Approximately 15 % of MS patients are diagnosed with PPMS, having a later age of onset than RRMS at approximately 50 years of age (Confavreux and Vukusic 2006). Again, functional decline is relentless but this particular type of MS does not show sex bias, meaning males are equally likely to develop PPMS compared to females (Polliack, Barak, and Achiron 2001). All clinically definite types of MS are characterised by disseminated demyelinating lesions in the brain and spinal cord, but there are distinct differences in the pathological mechanisms of relapsing remitting and progressive forms of MS (Confavreux and Vukusic 2006).

1.2.4 Pathogenesis overview

CNS inflammation is a characteristic of both relapsing remitting and progressive MS; however, progressive MS (PMS) is often described as an inflammatory CNS

disease contained within an intact BBB. In contrast, BBB disruption is highly pronounced in RRMS and is associated with peripheral immune cell infiltration. As a result, both MRI and CNS pathology differ between RRMS and PMS patients (Hochmeister et al. 2006; Lassmann 2008). During a relapse event, RRMS patients present with focal active demyelinating lesions, characterised by an abundance of macrophages/microglia throughout the lesion, perivascular cell cuffing, and local BBB permeability (Babbe et al. 2000; Lassmann et al. 1998). BBB permeability allows lesions to be visualised by gadolinium (Gd) enhancement, and normal appearing white matter (NAWM) outwith the lesion site lacks abnormal immunopathology. In contrast, lesions of PMS patients cannot be visualised by normal Gd enhancement procedures due to the BBB retaining some integrity (Hochmeister et al. 2006; Lassmann 2008). However, demyelination and axonal degeneration is diffuse throughout the parenchyma, with an abundance of active microglia and low level $CD4^+$ T cell infiltration (Babbe et al. 2000). Even NAWM of PMS patients shows signs of immunopathology with abnormal levels of activated microglia (Kutzelnigg et al. 2005).

1.2.5 RRMS pathogenesis

The pathogenesis of RRMS is better understood than that of PPMS. However, it is difficult to make definitive statements regarding RRMS pathogenesis with molecular research limited to post-mortem brain tissue and animal models that fail to recapitulate all aspects of this human disease. The current hypothesis for RRMS is that naïve T cells are sensitised by myelin antigens in peripheral lymph nodes, causing them to differentiate into myelin-specific Th1 or Th17 cells. During a relapse event, these peripherally activated T cells increase their expression of adhesion molecules such as α4ß1 integrin, allowing their extravasation across the BBB into the perivascular space through vascular cell adhesion molecule 1.

Antigen presentation to autoreactive T cells by perivascular myeloid cells is required to reactivate T cells, allowing penetration into the CNS parenchyma and secretion of proinflammatory cytokines, causing further immune cell recruitment to the CNS. This aggressive inflammatory response results in demyelination, axonal injury, and degeneration mediated by infiltrating macrophages, activated microglia, and neutrophils (Yamasaki and Kira 2019).

Although originally considered a T cell-mediated disease, it is now recognised that B cells play a critical yet poorly understood role in MS disease pathogenesis. Intrathecal immunoglobulin synthesis, or the presence of oligoclonal bands (OCBs), has long been associated with MS indicating that antibody-secreting B cells are present in the cerebrospinal fluid (CSF) and that they are producing abnormally large quantities of antibody such that bands representing specific antibody clones can be visualised on an isoelectric gel (Lowenthal and Karcher 1979; Cutler, Merler, and Hammerstad 1968; Kabat and Freedman 1950).

CIS patients positive for intrathecal OCBs have an increased risk of converting to RRMS, even more so if these antibodies show specificity for viruses such as measles, rubella, and varicella zoster virus (Tintoré et al. 2008; Brettschneider et al. 2009). Other B cell abnormalities associated with RRMS conversion include increased CSF CXCL13 and increased CD5-expressing B cells in peripheral blood (Brettschneider et al. 2010; Villar et al. 2011).

It is evident that B cells play a role in RRMS as B cell-depleting therapeutics rituximab and ocrelizumab reduce relapse rates and new lesion development in MS. Furthermore, it has been shown that it is the reduction of B cells, not CSF antibody levels, that correlate with a reduction in relapse rate. This may indicate that B cells exacerbate MS through cytokine production or antigen presentation to T cells, rather than antibody production (Hauser et al. 2008; Montalban et al. 2017).

It is unclear whether the initiating event of MS is oligodendrocyte apoptosis, leading to drainage of myelin antigens to the lymph nodes, or whether CNS invasion of autoreactive T cells initiates CNS damage (Barnett and Prineas 2004). Nevertheless, each acute relapse during RRMS has limited effects on overall disease progression. Functional decline occurs predominantly in the progressive phase, with patients experiencing similar rates of decline during both PPMS and SPMS (Confavreux et al. 2000; Kremenchutzky et al. 2006).

1.2.6 PMS pathogenesis

PMS lacks the florid perivascular inflammatory infiltrates observed in RRMS but retains a major inflammatory component. Meningeal inflammation, ectopic B cell follicles, diffuse microgliosis, and peripheral lymphocytes are all present in

the CNS, but to a lesser extent than in RRMS patients (Serafini et al. 2004; Magliozzi et al. 2007; Lovato et al. 2011). Grey matter pathology is diffuse and pronounced, correlating better with disability than white matter lesions (Bozzali et al. 2002). Unlike RRMS, PMS is generally nonresponsive to immunomodulatory DMTs, leading to the concept that accumulation of disability in PMS is due to axonal degeneration, which is driven by inflammatory activity sequestered in CNS behind an "intact" BBB (Hochmeister et al. 2006; Lassmann 2008).

Meningeal B cell follicle-like structures are particularly pronounced in SPMS patients, existing independent of the peripheral B cell pool and containing proliferating B cells, plasma cells, helper T cells, and follicular DCs (Frischer et al. 2009; Serafini et al. 2004; Magliozzi et al. 2007). Approximately 40 – 70 % of SPMS patients present with these structures which are usually found adjacent to underlying grey matter pathology (Serafini et al. 2004; Magliozzi et al. 2007; Lovato et al. 2011). It is likely that these ectopic germinal centres contribute to the CNS inflammatory milieu of SPMS patients through the production of cytokines and other pro-inflammatory molecules (Magliozzi et al. 2007; Lovato et al. 2011). This is supported by the efficacy of B cell-depleting therapies in PMS, an outcome that is not observed with T cell-targeted therapies. However, this efficacy might be restricted to a subset of PMS patients with ongoing RRMS-like inflammation (Montalban et al. 2017; F. Lublin et al. 2016).

Although many researchers consider MS as a primarily immune-mediated disease, our current understanding of PPMS may suggest that MS is a predominantly neurodegenerative disease, and that relapsing remitting forms bear an additional immunological component. PPMS is characterised by diffuse, widespread demyelination and axonal pathology accompanied by microglial activation (Haider et al. 2014; Kutzelnigg et al. 2007; Bramow et al. 2010). It is possible that those with RRMS have additional genetic/immunological susceptibilities which add a peripheral immunological component. Such susceptibilities could be related to autoreactive T and B cells, vascular and immunological cell adhesion molecules, or proteins involved in BBB integrity (Durán et al. 1999). This is further supported by the female bias observed in RRMS, which does not transcend to PPMS (Beeson 1994; Jacobson et al. 1997; Polliack, Barak, and Achiron 2001).

RRMS is not the only immune-mediated disease with a female bias, with rheumatoid arthritis, systemic lupus erythematosus, and psoriasis all showing increased prevalence in women (Engel and Burch 1967; McCarty et al. 1995; Sampogna et al. 2006). In the absence of a peripheral autoreactive immune response, temporarily amplifying neurological disturbances, CNS destruction could go unnoticed and present as a gradual functional decline rather than dramatic functional deficits followed by recovery.

1.2.7 MS treatment

Pre-1990, there were no effective therapies for the treatment of MS (Table 1.1). The first therapies introduced (interferon beta, glatiramer acetate, and mitoxantrone) decreased inflammation but their efficacy was limited, and their mechanisms of action remain unknown (K.P. Johnson et al. 1995; Jacobs et al. 1996; Millefiorini et al. 1997). In 2004, the first monoclonal antibody therapy was approved for the treatment of MS, leading to an explosion of targeted therapies being developed from 2010 to the present day (Table 1.1) (Polman et al. 2006). The majority of these new therapeutics aimed to prevent immune cell migration into the CNS and had increased efficacy compared to the aforementioned first-line therapies (Berger 2017). Efficacy varies from as little as a 30 % reduction in relapse rate, up to 70 % with newer therapies. However, therapies with higher efficacy tend to have more serious side effects (Jacobs et al. 1996; Polman et al. 2006; Kappos et al. 2010). As such, it is the general recommendation to initiate treatment with a lower risk first-line therapeutic, then move on to higher risk DMTs if the patient does not respond (Yamasaki and Kira 2019).

First-line therapies, interferon-beta (IFN-ß) and glatiramer acetate (GA), have similar efficacies with a 30 % reduction in relapse rate and 50 % reduction in new expanding lesions (K.P. Johnson et al. 1995; Jacobs et al. 1996). Although serious side effects are minimal, IFN-ß causes influenza-like symptoms around the time of injection, making it an unpopular choice amongst MS patients (Jacobs et al. 1996). The mechanism of action of these therapeutics is unknown, however, both have been shown to correct the Th1/Th17 shift, suppress antigen presentation, and limit T cell proliferation. Approximately 30 % of RRMS patients do not respond to either IFN-ß or GA, meaning higher risk therapies are required

to limit disease progression. Patients with an aggressive MS disease course might also require higher efficacy therapies immediately after diagnosis, with IFN-β and GA unlikely to make significant impact on the disease course (K.P. Johnson et al. 1995; Jacobs et al. 1996).

Unlike IFN-β and GA, most second-line therapies have well described mechanisms of action. These include fingolimod, natalizumab, and ocrelizumab. Fingolimod is a sphingosine-1-phosphate inhibitor which prevents T cell egress from the lymph node (Kappos et al. 2010). Natalizumab is an α4β1 integrin inhibitor which prevents T cell extravasation across the BBB (Coisne, Mao, and Engelhardt 2009). Ocrelizumab is a monoclonal antibody against CD20, depleting peripheral B cells (Montalban et al. 2017). Each of these therapeutics reduces relapse rates by 50 – 70 % and reduces new expanding lesions by 80 – 95 % (Polman et al. 2006; Kappos et al. 2010; Montalban et al. 2017). In PMS patients, ocrelizumab offers a 24 % reduction in clinical disability progression (Montalban et al. 2017).

As mentioned previously, with increased efficacy comes an increased risk of serious side effects. The most deadly of these is progressive multifocal leukoencephalopathy (PML) caused by productive infection of oligodendrocytes by the John Cunningham virus (JCV). Each of the second-line therapies above confer an increased risk of developing this disease, which can be fatal in 30 % of cases (Biogen 2020; Berger et al. 2018; Patel et al. 2021). Many other MS therapies have been shown to increase risk of PML including dimethyl fumarate and rituximab (Clifford et al. 2011; Berger 2017).

1.3 Progressive multifocal leukoencephalopathy

1.3.1 John Cunningham virus

PML is a severe demyelinating disease of the CNS caused by JCV (Astrom, Mancall, and Richardson 1958; Itoyama et al. 1982). JCV is a double-stranded DNA (dsDNA) human polyomavirus of the *Polyomaviridae* family and is extremely common amongst the general population (Field et al. 1974). Depending on the country in question, approximately 40-90% of the general population are

seropositive for the virus, meaning they have been exposed to the virus at some point in their lives and have developed antibodies against JCV (Taguchi, Kajioka, and Miyamura 1982; Major and Neel 1998; Gu et al. 2003; Kean et al. 2009). Initial infection predominantly occurs in childhood due to close interpersonal contact as seen with members of the same household. The vast majority of JCV infections yield no clinically evident symptoms and the infection itself is self-limiting with blood virus particles eventually becoming undetectable over time (Pietropaolo et al. 2018). After initial infection, JCV lies dormant in the kidneys, tonsils, or peripheral blood leukocytes (Yogo et al. 1990; Dörries et al. 1994; A. Kato et al. 2004). Low-level viral replication can occur in the kidneys leading to urinary viral shedding. It is estimated that approximately 20 % of those seropositive for the virus experience this low-level persistent infection of the kidneys but remain asymptomatic (Wollebo et al. 2015).

1.3.2 Epidemiology

The first incidence of PML was reported as a complication in patients with chronic lymphatic leukaemia and Hodgkin's lymphoma (Astrom, Mancall, and Richardson 1958). Since then, it has been deduced that PML occurs when the immune system is suppressed or compromised, typically from haematological malignancies including leukaemia and lymphoma, viruses which infect immune cells such as human immunodeficiency virus 1 (HIV-1), or in patients with inflammatory disease in receipt of immunosuppressive therapies, including those receiving immunosuppressants due to organ transplant (Brooks and Walker 1984).

In the context of MS, the baseline risk of developing PML when treated with certain DMTs varies from 2 per 100,000 for dimethyl fumarate, 3 per 100,000 for fingolimod, to an alarming 4.19 per 1,000 when receiving natalizumab (Berger 2017). These statistics are calculated based on patients who have not received any other DMTs previously and are negative for JCV antibodies. The risk of developing PML increases if the patient has received other DMTs previously and increases with duration of DMT use (Cutter and Stüve 2014; M.H. Werner and Huang 2016). Symptom manifestation occurs weeks/months after establishment of infection within the CNS and can affect multiple areas of the brain leading to an array of symptoms including sensory, motor, cognitive, behavioural, and psychiatric effects. Examples of symptoms include vision and speech

impairment, headache, gait disturbances, and seizures (Brooks and Walker 1984).

1.3.3 Pathogenesis

Although the mechanism by which immunosuppression contributes to PML remains unclear, a two-hit model has been proposed (Mills and Mao-Draayer 2018). First, the altered ratio of pro-/anti-inflammatory T cells and decreased immunosurveillance allows the archetypal, non-pathogenic JCV to proliferate, leading to the accumulation of mutations necessary to productively infect oligodendrocytes (Bellizzi et al. 2012). Specifically, rearrangements to JCV's non-coding regulatory region are associated with PML, leading to increased expression of early viral genes, enhancing the rate of viral replication (Gosert et al. 2010). Second, the inability of the immunosuppressed CNS to clear the active viral infection leads to oligodendrocyte death and subsequent demyelination and neurodegeneration (Mills and Mao-Draayer 2018). Incidences are fatal in 30% of cases, with less than 5% recovering fully without lasting disability or illness. As a result, immunosuppressive therapies such as natalizumab are restricted to patients in advanced disease states or unresponsive to lower risk therapies (Brown 2009).

The increased efficacy of DMTs such as natalizumab compared to first-line therapies IFN-ß and GA has fuelled investigations to improve risk stratification for MS patients, allowing more patients safe access to high efficacy drugs without the risk of developing a fatal viral infection. As such, studies were performed to identify serum or CSF biomarkers that were common to patients who were more susceptible to PML, or those who did not develop PML over the course of DMT treatment. As a result, it was discovered that natalizumab-treated MS patients who were positive for intrathecal lipid-reactive IgM antibodies had a dramatically reduced risk of developing PML compared to those with no IgM oligoclonal bands in their CSF (Villar et al. 2015).

1.3.4 Antibodies in MS

Antibodies, also known as immunoglobulins (Ig), are glycoproteins produced by terminally differentiated cells of the B lymphocyte lineage, namely plasmablasts and plasma cells (Rosevear and Smith 1961; Bjorneboe, Gormsen, and Lundquist

1947). There are five antibody isotypes: IgG, IgA, IgD, IgE, and IgM, each with a variety of functions including complement fixation, antibody-dependent cytotoxicity, and mast cell sensitising (Rowe et al. 1968). IgG, IgD, and IgE antibodies are secreted as monomers, whilst IgA and IgM antibodies are multimeric (Abdou and Abdou 1973).

Abnormal antibody production is a hallmark of MS with > 90 % of clinically definite MS patients positive for OCBs in the CSF (Kabat and Freedman 1950; McLean, Luxton, and Thompson 1990). Antibody-secreting B cells in MS patient CSF have been identified as clonally expanded B cells which have undergone somatic hypermutation, suggesting clonal expansion was driven by antigen binding (Obermeier et al. 2008; Y. Qin, Duquette, et al. 1998). Intrathecal IgG bands are found in almost all MS patients, whilst IgM bands are present in approximately 30 – 40 % of patients (Villar, Masjuan, et al. 2005).

Although excessive antibody production is observed in MS patients, B cell clones tend to differ widely between individuals (Colombo et al. 2000). As a result, identifying CNS-reactive antibodies common to all MS patients has been unsuccessful (Hohlfeld et al. 2016). This is in stark contrast to other CNS inflammatory conditions where CNS-specific antibodies play a central pathological role. Examples of such antibody-mediated diseases include aquaporin-4 antibody (Ab) positive neuromyelitis optica spectrum disorder, *N*-methyl-D-aspartate Ab mediated encephalitis, and myelin oligodendrocyte glycoprotein Ab associated disorders (Baumann et al. 2015; Baumann et al. 2016; Hacohen et al. 2017; Jarius et al. 2018; Ketelslegers et al. 2015; Kitley et al. 2014; Y. Takahashi et al. 2005).

There are some common antibody targets amongst MS patients although not present in all diagnosed individuals. IgG antibodies to Kir4.1 are found in approximately half of MS patients, whilst antibodies to myelin proteins and lipids have been identified in some MS patients (Srivastava et al. 2012; Brennan et al. 2011). Examples of such myelin components include myelin oligodendrocyte glycoprotein, myelin basic protein, sulfatide, and galactosyl ceramidase (Brennan et al. 2011; Hohlfeld et al. 2016). Furthermore, antibodies against intracellular self-proteins including DNA, RNA, cholesterol, cardiolipin, phosphatidylcholine, and phosphatidylserine have all been identified in MS

patients (Brennan et al. 2011; Villar, Sadaba, et al. 2005; Brändle et al. 2016; F. Lu and Kalman 1999). The presence of antibodies against intracellular self-proteins suggest that CSF antibodies might develop secondary to CNS pathology, with the release myelin and intracellular debris into the extracellular space leading to the production of antibody to remove said debris (Brändle et al. 2016; R. Li, Patterson, and Bar-Or 2018).

Despite evidence of antibody production being a secondary event in MS, *in vitro* and histopathological studies have shown that these antibodies can contribute to MS pathology, with immunoglobulin and complement deposits present in post-mortem MS lesions, and MS-derived antibodies inducing complement-dependent demyelination *in vitro* (Storch et al. 1998; Rodriguez et al. 1988; Lucchinetti et al. 1996; Elliott et al. 2012). But, as mentioned previously, B cells are more damaging in MS than the antibodies that they produce, which begs the question as to whether lipid-reactive IgM antibodies truly have a function beyond the clearance of debris.

Unlike subsets of IgG, lipid-reactive IgM antibodies have been specifically associated with a more aggressive MS disease course and reduced risk of developing PML (Villar, Sadaba, et al. 2005; Villar et al. 2015). This thesis will investigate whether MS-relevant lipid-reactive IgM clones can protect against CNS viral infection, and whether this antiviral response is also responsible for the more aggressive disease course observed in IgM-positive MS patients. To do this, we must understand the normal antiviral response of the CNS to viral infection.

1.4 Immune response to virus

1.4.1 Overview

Viruses are obligate intracellular parasites which require host cell machinery to replicate and spread to new cells or other individuals (Gelderblom 1996). In humans, viral infections are rarely lethal due to our efficient immune systems quashing virus infection before causing severe clinical symptoms (Lilienfeld 1973). The human immune system can be broadly separated into the “innate”

and “adaptive” immune systems, both of which have crucial functions in combatting viral infection (Rinaldo and Torpey 1993).

1.4.2 Innate immune response

The role of the innate immune response in viral infection is to block initial infection or to eliminate virus-infected cells (Horisberger, Haller, and Arnheiter 1980). This is achieved through pattern recognition receptors (PRRs) which recognise PAMPs and initiate an immune response accordingly (Krieger 1997; Bowie et al. 2000; Kurt-Jones et al. 2000; Ferguson et al. 2000; Pulendran, Palucka, and Banchereau 2001).

PRRs involved in innate antiviral defence can be broadly separated into two categories, membrane-bound receptors of which the toll-like receptor (TLR) family are the most prominent, and cytosolic DNA/RNA sensors which encompasses numerous receptor families, as well as an array of unrelated nucleotide-binding receptors. These receptors are activated upon recognition of either double- or single-stranded RNA (dsRNA/ssRNA) or dsDNA (Shinobu et al. 2002; Sivori et al. 2004; Heil et al. 2004; Yun, Tsao, and Der 2011).

TLRs can be found on cellular and endosomal surfaces, with those linked to virus recognition including TLRs 3, 4, 7, 8, and 9 (Medzhitov, Preston-Hurlburt, and Janeway 1997; Loré et al. 2003; Sirén et al. 2005). These receptors are constitutively expressed at high levels by certain immune cells such as plasmacytoid DCs, but their expression can be upregulated by most cell types in the event of infection (Kaisho and Akira 2000). The above-mentioned TLRs can be further divided into MyD88-depenedent TLRs (TLRs 4, 7, 8, and 9) and MyD88-independent TLRs (TLRs 3 and 4), whereby TLR4 can signal by MyD88-dependent and independent mechanisms (Yamamoto 2003).

As mentioned above, there are a vast array of cytosolic DNA/RNA sensors including members of the retinoic acid-inducible gene I (RIG-I)-like receptor family (RIG-I, melanoma differentiation-associated gene 5 (MDA5)), members of the pyrin and HIN200 domain-containing protein (PHYIN) family (absent in melanoma 2 (AIM2), gamma interferon inducible protein 16 (IFI16)), DExD/H-Box helicase (DDX/DHX) family members (DHX9, DHX36, and DDX60), and other unrelated receptors such as RNA polymerase III, DNA-dependent activator of IRFs

(DAI), cyclic GMP-AMP synthase (cGAS), and stimulator of interferon signalling (STING) (Bowie et al. 2000; Yoneyama et al. 2004; D.C. Kang et al. 2002; Fernandes-Alnemri et al. 2009; Unterholzner et al. 2010; T. Kim, Pazhoor, et al. 2010; Miyashita et al. 2011; Chiu, Macmillan, and Chen 2009; Sun et al. 2013; Takaoka et al. 2007)

PRR activation in the event of viral infection leads to an upregulation of cytokines required for viral defence. The most potent and well-described of these cytokines are type-I interferons (IFN-I). A diagram showing PRR induction of IFN-I signalling can be found in Fig 1.1. There are five subtypes of IFN-I, the most studied of which are interferon alpha (IFN-α) and IFN-β (Pestka, Krause, and Walter 2004).

Upon IFN-I release by a stimulated cell, IFN-I engages with its receptor, the interferon alpha/beta receptor (IFNAR) (Aguet et al. 1982). IFNAR is a heterodimer consisting of IFNAR alpha and beta chains (IFNAR1 and IFNAR2 respectively) (Pestka 1997). IFN-I binding to IFNAR initiates a JAK/STAT pathway leading to the upregulation of ISGs, of which there are over 1,000 (Pestka 1997; Der et al. 1998). These genes encode proteins which act both intra- and extracellularly to block virus infection and limit virus spread to neighbouring cells. Other ISGs encode proteins involved in apoptosis and cell cycle cessation to kill virus-infected cells and stop cell proliferation (Der et al. 1998; Levy et al. 1990). Halting cell proliferation prevents the virus from taking advantage of host cell transcription and translation machinery required for virus replication. Examples of proteins encoded by ISGs include cytokines such as CXCL10, intracellular antiviral proteins such as MX1 and RSAD2, pro-apoptotic factors including BAX and BAK, and anti-proliferative genes such as *p53* (Tamassia et al. 2008; Ahn et al. 2002; Arany et al. 1996; Dreiding, Staeheli, and Haller 1985; Chin and Cresswell 2001).

1.4.3 Adaptive immune response

In the event of a virus infection, the innate immune system is triggered instantly and can upregulate antiviral ISGs in a matter of hours. However, the proteins encoded by ISGs provide a generalised antiviral response, which can slow viral replication but does not always eliminate virus completely. The adaptive immune response takes time to develop but provides a targeted attack of both

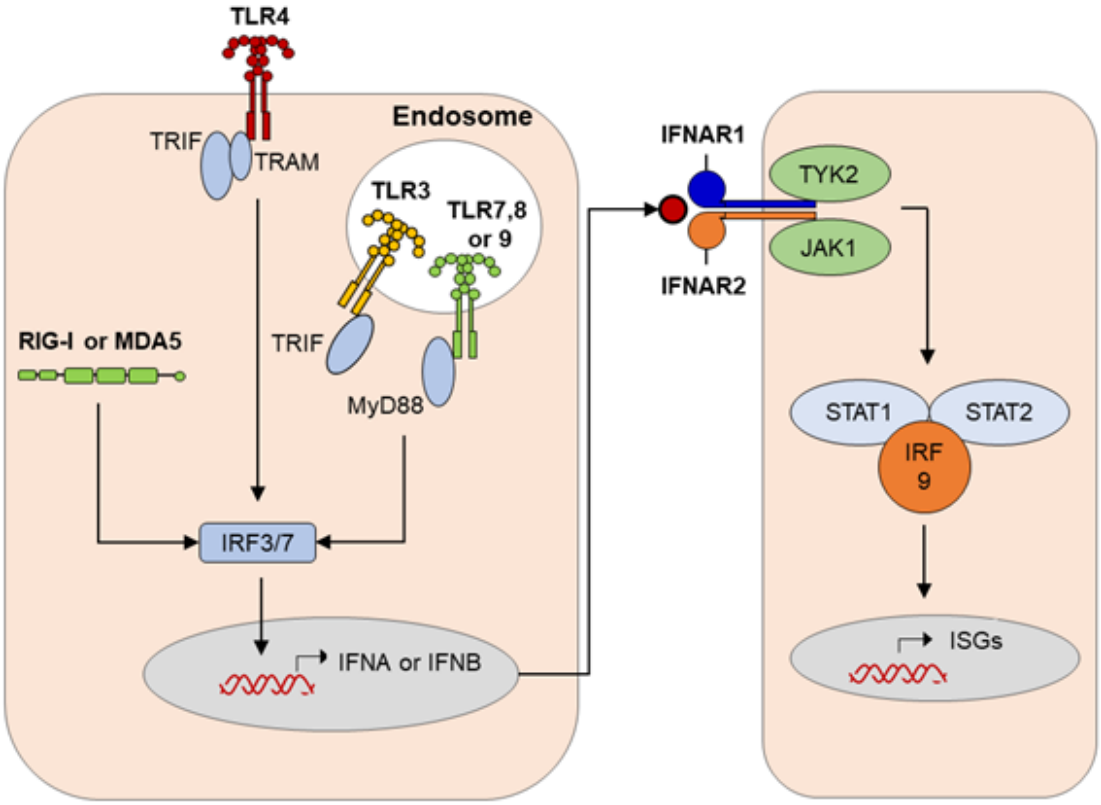

Figure 1.1 Diagram of interferon-inducing pattern recognition receptors and ISG upregulation by IFNAR1/2.

virus and virus-infect cells. The two main cell types involved in the adaptive immune response are T cells and B cells (Kindred and Shreffler 1972).

1.4.4 T cells

During primary virus infection, T cells are the most critical cell types and can efficiently recognise and kill virus-infected cells (Perlmann and Holm 1969). This is important as after the establishment of infection, viruses mainly spread through cell-cell contact rather than egress into the extracellular milieu, making purely antibody-dependent responses ineffective (Phillips and Bourinbaiar 1992; Hummel, Bellini, and Offermann 1998).

Although the innate and adaptive immune systems are often discussed separately, the adaptive immune response could not function without cells of the innate immune system (Rinaldo and Torpey 1993). Antigen presenting cells such as DCs phagocytose viral particles and present viral antigens to T cells using MHC class I or class II molecules (Nussenzweig et al. 1980; Zinkernagel and Doherty 1975; Steinman et al. 1979). Recognition and processing of antigen typically occurs in peripheral tissues, after which DCs migrate to lymphoid tissues by following cytokine and chemokine gradients (Steinman et al. 1979; Szakal, Holmes, and Tew 1983; Cumberbatch and Kimber 1992; Morikawa et al. 1995). Upon entering lymphoid tissues, DCs interact with $CD4^+$ or $CD8^+$ T cells to facilitate T cell activation, a process which can take several days to achieve (Morikawa et al. 1995). $CD4^+$ T cells recognise antigen presented on MHC class II molecules whilst $CD8^+$ T cells recognise MHC class I antigen complexes (Green and Jotte 1985; P. Johnson and Williams 1986). Circulating $CD8^+$ T cells can also recognise viral antigen presented on MHC class I molecules on virus-infected cells (Koszinowski, Gething, and Waterfield 1977).

Alongside antigen presentation, co-stimulatory molecule engagement (CD28 and CD80/86) and proinflammatory cytokines are required for T cell activation (Pierrès et al. 1988; Wahl et al. 1975). Once these specifications are met, T cells proliferate rapidly and differentiate into effector cells (Schmitz and Radbruch 1992). $CD4^+$ T cells are activated during viral infection, but their role is not as critical as that of $CD8^+$ T cells. $CD4^+$ T cells primarily act as helper cells which facilitate effective antibody production and promote $CD8^+$ T cell responses

(Creemers, O'Shaughnessy, and Boyko 1986; D.E. Lewis, Gilbert, and Knight 1986; Kabelitz et al. 1987; Buller et al. 1987).

After proliferation and activation, $CD8^+$ T cells exit the lymphoid tissues into the efferent lymph and bloodstream and travel throughout the body to target both primary and secondary infection sites (Bode et al. 1999; Lawrence and Braciale 2004). $CD8^+$ T cells, also known as cytotoxic lymphocytes (CTLs), kill virus-infected cells by a variety of methods. These include the use of perforins to lyse cells, granzymes to induce necroptosis, and engagement of Fas on target cells which induces apoptosis (Fruth et al. 1987; Krähenbühl et al. 1988; Young et al. 1989; Miyawaki et al. 1992). CTLs can also clear virus from infected cells without killing the host cell by way of cytokine secretion. Production of IFN-γ, TNF-α, lymphotoxin-α, and CCL5 all facilitate this process which is important in non-rejuvenating cells such as neurons. It is thought that these cytokines synergise to enhance the intracellular ISG response, thus preventing virus replication and promoting the destruction of viral genetic material and viral proteins (Wong and Goeddel 1986; Cantin et al. 1995; Guidotti, Borrow, et al. 1999; Guidotti, Rochford, et al. 1999; Kumaraguru et al. 2001; Losana et al. 2002; D.J.J. Carr et al. 2006).

After resolution of virus infection, approximately 95 % of CTLs undergo activation-induced cell death, with the remaining T cells differentiating into resting memory T cells (Orchansky and Teh 1994; Akbar et al. 1993). Memory T cells, alongside memory B cells provide rapid enhanced protection upon reinfection, with these cell populations remaining stable in the body for many years post-infection (Rickinson et al. 1981; Nossal and Makela 1962; Biberfeld, Biberfeld, and Sterner 1974).

1.4.5 B cells

The primary function of B cells is to produce antibody. It is important to note that antibodies can only bind virions located in the extracellular space, therefore the role of B cells in viral immunity is more critical in the event of reinfection where antibody can prevent virus attachment and internalisation into host cells (Gollins and Porterfield 1984).

Naïve B cells circulate in peripheral blood or reside in the germinal centres of lymphoid tissues where they recognise antigen through their B cell receptors, formed of membrane-bound IgM or IgD molecules (Abdou and Abdou 1973; Melcher and Uhr 1976; Boonpucknavig et al. 1976). B cells internalise antigen and process it for presentation to T helper cells (Watson, Trenkner, and Cohn 1973; Katz and Unanue 1973). Upregulation of MHC class II molecules alongside CD80/CD86 on B cells stimulates T cells to "help" the B cell mount an immune response (Azuma et al. 1993). Reciprocal signalling by T cells through the CD40 ligand induces isotype switching and somatic hypermutation in B cells, allowing B cells to produce antibodies of the correct structure and binding affinity for their immunological purpose (Noelle et al. 1992; Hodgkin, Castle, and Kehry 1994; Zan et al. 2000).

Isotype switching is the process of switching from IgD/IgM to a more appropriate isotype to exert the correct immunological function (Kearney, Cooper, and Lawton 1976). These functions include complement fixation, mucosal defence, and allergy response. T cell-derived cytokines dictate the isotype which is ultimately produced by the B cell (Mongini, Paul, and Metcalf 1982; Isakson et al. 1982). Somatic hypermutation is the process whereby mutations randomly occur in the antigen binding portion of the immunoglobulin to improve the binding affinity to the antibody to its target antigen (S. Kim et al. 1981). If the mutation leads to increased antigen binding affinity, that B cell clone receives a proliferative advantage over other B cells in the germinal centre pool (Berek, Griffiths, and Milstein 1985; Manser et al. 1985). If the mutations result in decreased binding affinity, the B cell fails to receive survival signals and dies (Jerne 1974).

B cell-derived antibodies have many functions including pathogen neutralisation, complement fixation, and antibody-dependent cellular cytotoxicity. Neutralisation is the process by which the antibody itself inhibits infection or the pathogenic mechanisms of an extracellular pathogen, typically by preventing pathogen attachment to host tissue (Forthal 2014). This can occur through aggregation as observed in mucosal tissues whereby IgA or IgM bind to the pathogen and the resultant aggregate is simply removed from the mucosa by peristalsis (Phalipon et al. 2002). Antibodies can also neutralise through pathogen immobilisation, binding to the pathogen's host-binding ligand, or can

neutralise post-internalisation by preventing virus-host membrane fusion (Greenbury and Moore 1966; McCullough et al. 1987; Barbey-Martin et al. 2002; Binley et al. 2004; Campodónico et al. 2010).

Complement-dependent antibody functions include the lysis of pathogens or infected cells and aiding phagocytosis (Wardlaw 1962; Fawwaz, Tenforde, and Mehlberg 1975; Howard and Wardlaw 1958; Kosugi et al. 1987). The latter function can lead to T cell activation, promoting further antibody production through T-B cell interactions. Many pathogens have developed strategies to evade complement including *Neisseria meningitidis*, *Neisseria gonorrhoeae*, and *Haemophilus influenzae* (Ram et al. 1999; Hallström et al. 2007; Ram, Lewis, and Rice 2010). Therefore, coupling complement with pathogen-specific antibodies ensures that the pathogen can be killed or cleared by the host.

Fc receptors on immune cells allow for antibody-dependent cellular cytotoxicity. In this process, the antibody forms a bridge between the immune cell and the pathogen or infected cell. This interaction licences the immune cell to kill the pathogen or infected cell by cell lysis or apoptosis (Pudifin, Harding, and MacLennan 1971; MacLennan and Howard 1972; N.H. Stacey et al. 1985). This mechanism is very effective, even against large pathogens such as parasites (Kazura 1981).

1.4.6 IgM

IgM production is robust at the start of infection but wanes after isotype switching, with B cells favouring IgG secretion over IgM. Despite this, IgM antibodies have very specific antiviral functions that are crucial in the event of viral infection. Secreted IgM polymerises to form pentamers or hexamers and can be defined as “natural” or “induced” (Brewer et al. 1994).

Natural IgM (nIgM) is found circulating in the absence of injury or infection and is produced by long-lived, self-renewing $CD5^+$ B cells termed B1 cells (Mouthon et al. 1995; Hashimoto et al. 1978; Kawahara et al. 2003; Tornberg and Holmberg 1995). nIgM does not undergo somatic hypermutation making it highly conserved with limited variation from germline sequences (Mouthon et al. 1995; Tornberg and Holmberg 1995; Kawahara et al. 2003). nIgMs are low affinity, autoreactive, and polyreactive antibodies, binding to protein, lipid, and carbohydrate antigens

such as DNA, RNA, phosphatidylcholine, and sphingolipids (Nakamura et al. 1988; Hayakawa et al. 1999; D.N. Glass et al. 1973; Mercolino, Arnold, and Haughton 1986; J.C. Lee et al. 1974; M. Kato, Kubo, and Naiki 1978). nIgM provides broad protection against pathogens without having encountered them previously and clears apoptotic and necrotic cells from the circulation (Nakamura et al. 1988; Blandino and Baumgarth 2019).

Induced IgM (iIgM) is produced by B2 cells in response to an antigen and has a more restricted, higher affinity antigen binding domain due to somatic hypermutation (Manivel et al. 2000; Baumgarth et al. 1999). Although iIgM is not considered to be critical for long-term humoral immunity, long-lived IgM-producing plasma cells have been identified in humans suggesting important long-term functions (Magri et al. 2017; Price et al. 2019; Wilson et al. 2019)

1.4.7 Antiviral responses in the CNS

The CNS has a unique immunological status and has long been considered an immune privileged organ (Medawar 1948). Although this concept of immune privilege has been disproved with the discovery of the brain lymphatic system, the BBB is effective at excluding most blood-borne pathogens from the meninges, parenchyma, and ventricular system (Weller et al. 2009; Aspelund et al. 2015; Klein and Hunter 2017; Louveau et al. 2015). The exception is pathogens with specific neurotropism, though in most cases, infection of the CNS is not beneficial to the pathogen as host fatality discontinues the pathogen's life cycle (Klein and Hunter 2017). Viruses can enter the CNS by retrograde transmission along axons, trans-endothelial entry from the CSF, transcytosis at the BBB, or by hi-jacking infiltrating mononuclear cells (Ren and Racaniello 1992; Lane et al. 1996; Romero et al. 2000; F. Li et al. 2015; H. Liu et al. 2019).

In a typical CNS viral infection, the initial site of infection is in the periphery leading to antigen presentation by peripheral DCs to $CD4^+$ and $CD8^+$ T cells in peripheral lymph nodes (Klein and Hunter 2017). If virus migrates to the CNS prior to establishment of an adaptive immune response, the neurovascular unit and choroid plexus are armed with a plethora of PRRs which initiate an innate immune response and trigger the recruitment of peripheral immune cells (Nagyoszi et al. 2010; Nyúl-Tóth et al. 2017; Hwang and Bergmann 2018b; Yu et al. 2019). Furthermore, all neural cells have basal PRR expression including the

expression of TLRs and DNA/RNA sensors, although the level of expression varies with cell-type and brain region (Bsibsi et al. 2002; Préhaud et al. 2005; Zhao et al. 2016). This heterogeneity influences viral spread and immunopathology in a virus-specific manner, for example, low RIG-I and MDA5 expression by cortical neurons leads to increased West Nile virus (WNV) load in the cortex compared to other brain regions (Daffis et al. 2007).

As in the periphery, IFN-I's have a key role in the defence against CNS viral infection. Alongside the antiviral functions mentioned in 1.4.2, IFN-I's aid BBB stabilisation, limiting virus and immune cell entry to the CNS and reducing immunopathology (Daniels et al. 2014; Daniels et al. 2017). Again, basal levels of IFN response proteins influence the tropism of different viruses to different cell-types and brain regions. For example, the murine cerebellum has particularly high basal levels of TLR7, MDA5, IFN-α, STAT1, MX1, and RSAD2, which has been shown to restrict neurotropic virus infection in this region (Cho et al. 2013).

As described in the context of MS, pathogen-specific T cells require antigen presentation by perivascular myeloid cells to access the parenchyma and initiate local T cell expansion/retention in the CNS (Tschen et al. 2006). However, there have been reports of T cells migrating to the uninflamed CNS, supporting the idea of homeostatic immune surveillance in the absence of infection (Wekerle et al. 1986). Furthermore, memory T cells are retained in perivascular space of the CNS years after infection, supporting the idea of long-term immunity in the CNS (Hawke et al. 1998).

One key difference in viral responses of the CNS is how $CD8^+$ T cells interact with neurons. Although it is evident that neurons can limit viral replication through ISG expression, there is little evidence of $CD8^+$ T cell-mediated lysis of neurons. Instead, $CD8^+$ T cells work with microglia to eradicate virus by non-cytopathic means. As described previously, this mechanism is a synergistic feat between cytokines and intracellular neuronal ISGs which destroy viral genetic material. Furthermore, microglia support T cell proliferation and antiviral activity whilst maintaining an intact BBB and limiting neutrophil infiltration, thus preventing CNS immunopathology (Oldstone et al. 1986; Binder and Griffin 2001; Herz et al. 2017).

Therefore, the immune response to viruses is a multifaceted endeavour, with several cell-types of the innate and adaptive immune systems critical for efficient pathogen clearance. This immune response is further complicated in the CNS, where the BBB limits immune cell entry and $CD8^+$ T cells cannot clear virus in long-lived neuronal cells by cell lysis. This makes the notion of a protective lipid-reactive IgM even more intriguing with multiple means for the antibody to execute its function under normal circumstances, but also that this IgM-mediated protection might be a CNS-specific phenomenon developed due to the limited potential of $CD8^+$ T cells to remove virus from the CNS. To test the hypothesis that lipid-reactive IgM antibodies elicit an antiviral response in the CNS, we required a suitable *in vitro* model that could withstand exogenous antibody stimulation and virus infection.

1.5 Modelling the CNS in vitro

1.5.1 Overview

The complexity of the human brain poses a great challenge to the establishment of models to the study the CNS and associated diseases. Although *in vivo* models study the intact CNS, the human brain has unique features that are not found in other animals (Nikolakopoulou et al. 2020). Therefore, reliance on animal models to interpret the human CNS might cause more harm than good, with high cost and ethical concerns associated with *in vivo* studies and a staggeringly low success rate of CNS drugs tested in animals prior to clinical trial (Kesselheim, Hwang, and Franklin 2015; Gribkoff and Kaczmarek 2017).

Although *in vitro* systems cannot fully recapitulate the complexity of the CNS, recent advances in cell culture have led to the development of a variety of systems to explore neural cell function. These culture systems vary in cost, complexity, physiological relevance, ease of manipulation, and time required for generation and maintenance. Importantly, using *in vitro* models can reduce the number of animals used in a study, and human relevance can be explored using human cell lines or stem cells (Nikolakopoulou et al. 2020). Additionally, the use of three-dimensional cultures has allowed for complex cell-cell interactions to be explored, with some researchers developing *in vitro* CNS-BBB three-

dimensional models (Choi et al. 2014; Maoz et al. 2018). These models have revolutionised the field of neuroscience and have made an important step forward in improving pharmacological research for diseases of the CNS.

1.5.2 Cell lines

In general, the more basic the cell culture system, the cheaper and less time-consuming they are to maintain. Basic cell culture systems are also more easily manipulated pharmacologically and can be readily transfected for the purpose of siRNA silencing. The downside is that culture systems that are easy and cheap to grow, often do not resemble the physiology of cells *in vivo* (Gordon, Amini, and White 2013).

Cell lines are considered the most basic cell culture system. However, they have proved important in the study of neural cells as mature neurons do not undergo cell division, making neuronal cell culture difficult compared to other cell-types (Gordon, Amini, and White 2013). Neural cell lines are often tumour-derived or have been immortalised using oncogenic viruses or by serial passage leading to an oncogenic mutation. As a result, these cells can undergo several rounds of cell division, with some being able to proliferate indefinitely (Nilsson and Pontén 1975). These cells can be grown very easily, yield vast cell numbers, and have minimal interculture variability (G.N. Stacey, Bolton, and Doyle 1991). The disadvantage is that these cells are essentially cancer cells and have lost many of their natural phenotypic properties, devoting much of their energy to cell division rather than their normal physiological functions (Sapp and Yeh 1998; Frisa et al. 1994). Cell lines are also homogenous, which can be useful when studying cell autonomous properties of neural cells but lose physiological relevance when considering the brain as a whole (G.N. Stacey, Bolton, and Doyle 1991; Nikolakopoulou et al. 2020). Examples of neural cell lines include CATH-a (neuron), OLN-93 (oligodendrocyte), C8-S (astrocyte), and BV2 (microglia) (Blasi et al. 1990; Suri et al. 1993; Thomsen and Lade Nielsen 2011; Richter-Landsberg and Heinrich 1996).

Human neuroblastoma and teratocarcinoma cell lines are also used where cells proliferate as progenitor cells and are then differentiated into neurons or glial cells to conduct experiments. Examples of such cell lines are SH-SY5Y and NT2 (Perez-Polo, Werbach-Perez, and Tiffany-Castiglioni 1979; Andrews 1984). To

differentiate into “neuron-like” cells, specific reagents are added to the media such as retinoic acid, phorbol esters, and inhibitors of mitosis. Differentiated cells decrease their rate of proliferation, exiting cell cycle and entering G_0 phase. They also express markers for mature neurons such as ßIII-tubulin, synaptophysin, microtubule-associated protein 2 (MAP2), and neuronal specific nuclear protein (NeuN). It is important to note that although these differentiated cells express neuronal markers, most scientists consider them to be “neuron-like” cultures, rather than true neurons (Perez-Polo, Werbach-Perez, and Tiffany-Castiglioni 1979; Andrews 1984; Påhlman et al. 1984).

1.5.3 Primary cell culture

Primary cells are made directly from tissues and have not undergone subculturing. As primary cells are not tumour-derived or transformed by oncogenic processes, they more accurately represent the properties of neural cells *in vivo* (Asch, Medina, and Brinkley 1979; Koch and Leffert 1980). However, the number of cells that can be obtained from a specific tissue is limited, giving rise to ethical concerns as additional human or animal subjects are required to reach the desired cell yield, number of technical replicates, and number of biological replicates (Gordon, Amini, and White 2013). That being said, repetition of an experiment with the same cell line does not create any biological replication, making the results derived from primary cells more biologically meaningful (Lazic, Clarke-Williams, and Munafò 2018).

Primary cells are not immortal, meaning they remain viable for a shorter length of time compared to cell lines, with sub-culturing affecting their physiological characteristics. This gives rise to an additional concern whereby primary cells might not stay viable for a sufficient length of time to become fully differentiated and matured, or that rate and extent of differentiation might vary between biological replicates (Gordon, Amini, and White 2013; Nikolakopoulou et al. 2020). This is of concern when modelling neurodegenerative diseases, where age is an important risk factor in the human disease.

An array of protocols exists for the culture of pure, homogenous neural cells including neurons, astrocytes, oligodendrocytes, and microglia (Lindsay et al. 1982; Giulian and Baker 1986; Dotti, Sullivan, and Banker 1988; Nussbaum et al. 1988). Many researchers also take advantage of heterogenous systems such as

simple co-cultures of two cell types, and more complex systems including mixed neuronal-glial cultures containing all major cell types of the CNS (Whittemore, Sanon, and Wood 1993; Hamilton and Rome 1994; Kenigsberg and Mazzoni 1995; Thomson et al. 2008; Bijland et al. 2019). Although primary cell cultures can be pharmacologically manipulated, the lack of proliferation makes these cells difficult to transfect by conventional means (Tur-Kaspa et al. 1986; Rakotoarivelo et al. 2007).

Both heterogenous and homogenous cultures have their benefits depending on the scientific question at hand. Heterogenous cultures, especially those containing all major CNS cell types, provide a useful tool to investigate how the brain as a whole might react to a stimulus. In contrast, homogenous cultures can help identify which specific cell type contributes to certain aspects of a response. Co-culturing cell-types highlights interdependent functions.

1.5.4 Myelinated cultures

Researchers at the University of Glasgow pioneered the development of a primary heterogenous CNS culture system derived from rodent embryonic spinal cord containing all major cell types of the CNS. These cultures, herein referred to as “myelinated cultures”, remain viable up to day *in vitro* (DIV) 40, with the process of myelination beginning at approximately DIV18 and experiments typically being performed on DIV24 if examining the effect of axons with a considerable amount of myelin (Arseni 2020; Bijland et al. 2019; Thomson et al. 2008). At this stage, the cultures are considered “mature” and possess many *in vivo*-like properties including spontaneous neuronal electrical activity, response to inflammatory stimuli, and microglial migration and phagocytosis.

One pregnant dam can yield up to 30 million cells in mice, and approximately 60 million cells in rats. This equates to ~ 64 individual cultures from one biological n in mice and 120 in rat, each of which can be used for a different treatment condition (Thomson et al. 2008; Bijland et al. 2019). A standard rule of thumb is that one whole embryonic spinal cord can yield up to 3.6 million cells, or 8 individual cultures. Cells can be cultured on coverslips contained within 35 mm dishes (3 coverslips per dish) or in 24-well plates. Cells can also be contained within 96-well plates to allow for semi-high throughput drug screening.

Since the establishment of this culture method, specific protocols have been developed for siRNA silencing and live-cell imaging of myelinated cultures, alongside the development of CellProfiler pipelines for the quantification of axon/myelin density, and nuclear cell markers including DAPI, Olig2, and NeuN (Thomson et al. 2008; Bijland et al. 2019). The disadvantages of this culture system include the lack of human relevance and the two-dimensional structure of the cultures which can hinder their *in vivo* relevance. However, the presence of other *in vivo*-like features makes this an attractive, low-cost, flexible, and reproducible model to study the CNS.

1.5.5 Organotypic slice cultures

Although heterogenous primary cultures are more physiologically relevant than cell lines and demonstrate cell-cell interactions, the brain is a three-dimensional organ with distinct regions and circuitry that are not recapitulated in a two-dimensional system.

Organotypic slice cultures (OSCs) are *ex vivo* cultures where the brains of young (post-natal day ≤ 12) rodents are thinly sliced and mounted onto semi-porous membranes contained within cell culture dishes (Croft et al. 2019; De Simoni, Griesinger, and Edwards 2003). The membrane suspends the tissue within the cell culture well, and OSC medium is taken up by the tissue from the well floor through the semi-porous membrane by capillary action (Stoppini, Buchs, and Muller 1991).

The advantage of using a slice culture system is that the cells are not disassociated and remain intact, maintaining the complex neuronal circuits and regional brain differences observed *in vivo*. Compared to other three-dimensional *in vitro* models such as organoids, OSCs are relatively straightforward and inexpensive. Unlike organoids, OSCs have anatomically relevant cytoarchitecture and are substantially less variable as their three-dimensional structure is not dependent on artificially administered growth factors (Croft et al. 2019).

OSCs have been revolutionary in electrophysiological and network connectivity studies, with many aspects of *in vivo* inter-neuronal functions being fully recapitulated in OSC models (Soares et al. 2013; De Simoni, Griesinger, and

Edwards 2003; Finley et al. 2004; Mielke et al. 2005). These include the development of neuronal morphology, dendritic spine branching, synaptic density, and electrical connectivity (De Simoni, Griesinger, and Edwards 2003; Finley et al. 2004). Given the number of slices that can be made from one rodent brain, laboratories focused on electrophysiology and neuronal connectivity would greatly reduce the animal numbers required for experiments through implementation of OSC systems (Croft et al. 2019).

In contrast, OSCs have been less successful in modelling neurodegenerative diseases, with very few OSC observations being successfully validated *in vivo*. In addition, OSCs require a high concentration of serum in their media to survive (~ 25 %) which can interfere with many stimuli or pharmacological agents administered to the media (Croft et al. 2019). Therefore, OSCs provide an excellent model for electrophysiological studies but further protocol developments would be required for their application to other aspects of CNS disease modelling.

1.5.6 Human-derived culture systems

As mentioned previously, there are substantial differences between the human and rodent brain and over-reliance on rodent systems is thought to contribute to the low success rate of CNS drug development (Kesselheim, Hwang, and Franklin 2015; Gribkoff and Kaczmarek 2017; Nikolakopoulou et al. 2020). Differentiation of human stem cells was first demonstrated using embryonic tissue; however, this process comes with major ethical concerns (Migliaccio and Migliaccio 1988). Recent advances in stem cell culture have allowed for somatic human cells, such as epidermal fibroblasts, to be reprogrammed back to a pluripotent stem cell state, overriding the aforementioned ethical concerns and allowing human induced pluripotent stem cells (hiPSCs) to be generated from patients and healthy controls (K. Takahashi and Yamanaka 2006).

hiPSCs can be maintained as two-dimensional cultures or three-dimensional organoids (Penney, Ralvenius, and Tsai 2020). Differentiation protocols have been developed for astrocytes, oligodendrocytes, microglia, and multiple sub-types of neurons (Hu, Du, and Zhang 2009; Soldner et al. 2009; Krencik et al. 2011; Maroof et al. 2013; Nicholas et al. 2013; Muffat et al. 2016). Co-culturing protocols also exist for both two-dimensional and three-dimensional systems,

however these techniques are in their infancy and require further optimisation (Odawara et al. 2014; Wevers et al. 2016; Nikolakopoulou et al. 2020; Penney, Ralvenius, and Tsai 2020).

hiPSCs are highly variable, with the same differentiation protocol used on the same hiPSC line often yielding clones with considerable differences in morphology and gene expression (K. Kim, Doi, et al. 2010; Volpato et al. 2018). Differentiated hiPSCs often have immature functional characteristics representative of embryonic tissue and retain epigenetic memory from the somatic cell donors, leading to bias towards specific cell lineages (J.D. Miller et al. 2013; K. Kim, Doi, et al. 2010; Polo et al. 2010). The latter issue can be overcome by extensive genome editing, however, hiPSCs are intrinsically unstable compared to primary cells, with studies specifically referencing the instability of the hiPSC genome (Komor et al. 2016; Mayshar et al. 2010; Ji et al. 2012).

Furthermore, hiPSCs are usually differentiated into single cell-types first then co-cultured (J. Park et al. 2018). This approach does not consider developmental cues that are delivered from other cells of the CNS (Cahoy et al. 2008; Gosselin et al. 2017). Finally, as differentiation protocols are dependent on exogenously administered reagents based on our current understanding of developmental cues, there is some debate as to whether certain differentiated clones are truly the desired cell type. One example is a report on hiPSC-derived brain microvascular endothelial cells which the authors state did not recapitulate the BBB as desired, but the immature embryonic neuroectodermal epithelium (T.M. Lu et al. 2021).

Although organoids show *in vivo* features that are not observed in two-dimensional systems, these three-dimensional cultures have their own downsides (Choi et al. 2014). Alongside the disadvantages mentioned above for two-dimensional hiPSCs, organoids spontaneously self-assemble, leading to high variability and issues with reproducibility (Nikolakopoulou et al. 2020). Additionally, their spheroid nature leads to cells in the centre of the organoids experiencing hypoxia, nutrient deprivation, cytotoxicity, and cell death (Qian et al. 2016; Penney, Ralvenius, and Tsai 2020).

Despite the disadvantages listed above, patient-derived hiPSCs have shown great promise in understanding functional cellular differences between cells of the neurodegenerative brain and those of healthy controls. Given that the majority of animal models are based on gene over-expression or induction of a disease state that does not reflect how the disease naturally occurs in human, hiPSC technology would certainly allow for disease relevant cellular perturbations to be discovered (Choi et al. 2014; Penney, Ralvenius, and Tsai 2020).

However, if investigating an exogenous effect on the normal human brain, the lack of established co-culturing protocols, alongside the vast cost and time required to reprogramme and differentiate cells, makes this an unattractive model for exploratory experiments (J.D. Miller et al. 2013; J. Park et al. 2018; Nikolakopoulou et al. 2020; Penney, Ralvenius, and Tsai 2020). Nonetheless, if a pharmacological target or agent is unveiled using a rodent system, examining its effect in a human system prior to clinical trial would undoubtedly save considerable time and money (Kesselheim, Hwang, and Franklin 2015; Gribkoff and Kaczmarek 2017; Nikolakopoulou et al. 2020).

1.5.7 Choosing the correct in vitro model

From the models described above, it is evident that each model has their benefits depending on the scientific question at hand. Cell lines prove useful and cost effective for simple, preliminary experiments, addressing questions such as “can virus X infect cell-type Y?” (Geller 1991). Rodent primary cells, both homogenous and heterogenous, can provide insights into how cells of the CNS might react individually or as a network to a stimulus. After exploratory experiments in rodent models, leading to identification of a cell-type or protein of interest, one could proceed to hiPSCs to confirm human relevance. As mentioned above, hiPSC cultures would prove more useful in determining human disease relevant cellular anomalies which are not observed in rodent animal models (Penney, Ralvenius, and Tsai 2020). Lastly, although OSCs are immensely useful for connectivity and electrophysiological studies, their limitations regarding exogenous stimulation and failure to recapitulate neurodegenerative disease states makes them an unattractive option when investigating external stimuli on the CNS (De Simoni, Griesinger, and Edwards 2003; Soares et al. 2013; Croft et al. 2019).

Taking the above information into consideration, the experiments performed in the current thesis utilised myelinated cultures to explore the antiviral properties of lipid-reactive IgM antibodies (Thomson et al. 2008; Bijland et al. 2019). Given the high cost and variability associated with hiPSC cultures and the inherent issues of oxygen, nutrient, and stimulus distribution in three-dimensional systems, myelinated cultures present a highly useful and reliable tool in exploring the effects of exogenous stimuli such as antibodies on cells of the CNS (K. Kim, Doi, et al. 2010; Volpato et al. 2018; Qian et al. 2016). This conclusion was based on the quantity of cells that could be produced from a single dam making exploratory experiments feasible given the number of conditions that can be tested simultaneously, the improved physiological relevance compared to cell lines making results more biologically meaningful, the lower cost and reproducibility compared to organoid models, and the lack of serum required in cell culture media which allows for a broad range of stimuli to be tested without interference in contrast to OSCs. Furthermore, myelinated cultures have been used previously to study virus infection in the context of Zika virus, making it an established model to investigate neurotropic viruses (Cumberworth et al. 2017; V. Schultz et al. 2021).

1.5.8 Choice of model neurotropic virus

The hypothesis that intrathecal lipid-reactive IgM antibodies found in MS patients protect the CNS from neurotropic viral infection was inspired by the finding that MS patients positive for these antibodies had a dramatically reduced risk of developing PML during Natalizumab treatment (Villar et al. 2015). As mentioned in section 1.3, PML is caused by JCV, an obligate human pathogen which infects cells of the oligodendroglial lineage in the CNS. As research into this hypothesis was in its infancy, with many exploratory experiments required to ascertain a mechanism of action, it was decided to proceed with rodent myelinated cultures and substitute JCV with two alternative neurotropic viruses.

Bunyamwera virus (BUNV) is a negative-sense ssRNA virus for the *Orthobunyavirus* genus and *Peribunyaviridae* family, being the first *Bunyaviridae* family member to be successfully rescued from cloned cDNAs (Bridgen and Elliott 1996). It is a human-relevant, arthropod-borne virus with a segmented genome, causing haemorrhagic fever in humans and encephalitis in domestic animals

(Hughes et al. 2020; Tauro et al. 2015). Other related viruses include Cache Valley and La Crosse viruses (Holden and Hess 1959; Balfour et al. 1973). Due to the presence of BUNV experts within the University of Glasgow, any results obtained from BUNV experiments could be assessed using full understanding of BUNV literature which might not have been possible if another virus had been chosen. This knowledge base at the University of Glasgow alongside the human relevance of BUNV and its ability to infect cells of the CNS provided the reasoning behind selecting this virus for experiments within this thesis.

Semliki Forest virus (SFV) strain A7(74) is a mouse-adapted positive-sense ssRNA virus of the *Togaviridae* family and *Alphavirus* genus. The SFV A7(74) strain was originally isolated in 1961 from *Aedes argenteopunctatus* in Namacurra, Mozambique (McIntosh, Worth, and Kokernot 1961). Although this virus lacks human relevance, SFV A7(74) is neurotropic, infecting oligodendrocytes resulting in demyelination. Therefore, the pathogenesis of this virus is functionally similar to JCV despite being of different origin. Furthermore, SFV A7(74) has been well described *in vitro* and *in vivo*, meaning that results from experiments described herein could be compared to the existing literature, allowing for well-informed conclusions to be drawn (Fazakerley and Webb 1987).

Although JCV was not used in this thesis, this does not reflect a lack of desire by the Linington laboratory to use JCV in the future. As will be detailed in the final discussion of this thesis, the knowledge obtained from this thesis will allow for concise, high impact experiments to be performed using human iPSC's and human polyoma viruses including JCV. The experiments performed in this thesis laid the groundwork for future experiments by delving into the mechanism of action of lipid-reactive IgMs, allowing us to understand the cell types and immune pathways involved in this response.

1.6 Aims of thesis

The overarching aim of this thesis was to investigate whether lipid-reactive IgM antibodies, similar to those found in MS patients, could elicit an antiviral response in myelinated cultures. The ultimate goal of this work was to improve

our understanding of and aid risk stratification in MS, allowing patients safe access to high efficacy therapies. To address this overarching aim, three main experimental avenues were pursued.

1. To investigate whether lipid-reactive IgM antibodies trigger an antiviral transcriptional signature in myelinated cultures.

2. To determine the mechanism of action of any antiviral response induced.

3. To ascertain whether pre-treatment with lipid-reactive IgM could limit neurotropic virus replication.

To address these aims, we selected a candidate lipid-reactive IgM antibody and two well-described neurotropic viruses to model the effect of IgM in the context of MS and viral encephalitis using the myelinated culture system.

The sulfatide-reactive IgM O4 was selected as previous studies by our laboratory have shown that sulfatide is the major target of intrathecal lipid-reactive antibodies found in MS patients (Brennan et al. 2011). O4 is an antibody clone generated by mouse hybridoma cells which have been in the possession of the Linington laboratory for many years (Sommer and Schachner 1981). As such, protocols have been developed to produce high concentrations of O4 in bioreactor flasks under ultra-low endotoxin conditions (Hayden et al. 2020).

As mentioned in section 1.5.8, the model neurotropic viruses BUNV and SFV A7(74) were selected for use in this thesis, BUNV as a human-relevant pathogen with neurotropic properties and SFV A7(74) as a virus with pathogenesis functionally similar to JCV (Fazakerley and Webb 1987; Pekosz et al. 1995; Tauro et al. 2015). JCV could not be used in this thesis as this and other related polyoma viruses are obligate human pathogens which do not replicate in rodent cultures (Tan and Koralnik 2010).

The above aims were achieved using microarray and pathway analysis followed by real-time quantitative polymerase chain reaction (RT-qPCR) to ascertain the O4-induced transcriptional profile. Investigation into the mechanism of action utilised genetic knock-out cultures alongside pharmacological inhibitors of innate immune pathways. Efficacy of O4 against neurotropic viral infection was assessed using immunocytochemistry for virus positive cells alongside plaque assays for infectious virus supernatant.

Together the experimental aims described above identified a subset of lipid-reactive IgM antibodies with antiviral properties, partially unravelled the mechanism of action of these IgMs, and demonstrated their functional efficacy *in vitro* using model neurotropic viruses.

Chapter 2

Materials and methods

2 Materials and methods

2.1 Cell culture

All cell culture procedures, except tissue harvesting, were performed in sterile laminar flow cabinets. Incision sites of animals to be dissected and all materials required for cell culture were sterilised with 70 % methylated spirits prior to procedure. All cells were maintained at 37°C, 7 % CO_2/93 % air in a humidified incubator unless otherwise stated.

2.1.1 Animals

Primary cultures were generated from Sprague Dawley (S/D) rats (Harlan Laboratories), *Cst*$^{+/-}$ mice on a C57Bl/6 background (Prof. Hugh Willison) and wild-type and *Ifnar1*$^{-/-}$ mice on a 129S7/SvEvBrdBklHprtb-m2 background (B&K Universal). S/D rats and *Cst*$^{+/-}$ mice were maintained at the University of Glasgow Central Research Facility and wild-type and *Ifnar*$^{-/-}$ mice at the Vet Research Facility, all under a 12-hour light/dark cycle with food and water *ad libitum*.

2.1.2 Neurospheres

Post-natal day 1 S/D rats were euthanised by lethal intraperitoneal (i.p.) injection of Euthatal and death confirmed by severing the femoral artery. Brains were removed from skull, striata collected and placed in a bijou (Thermo Scientific™) containing 1.5 ml Leibovitz's L-15 Medium (L-15 medium, Gibco™) at a concentration of three striata per bijou. Striata were mechanically dissociated by glass Pasteur pipette and cell suspension from each bijou transferred to a 15 ml centrifuge tube (Greiner). Tubes were centrifuged at 86 rcf (800 rpm) for 5 mins and supernatant removed. Pellet from each tube was resuspended 20 ml neurosphere media [Dulbecco's modified Eagle medium (DMEM)/F12 (Gibco™), supplemented with 0.66 % D-(+)-glucose, 0.124 % sodium bicarbonate, 2 mM L-glutamine, 1x penicillin-streptomycin (Pen/Strep), 5.5 mM HEPES, 0.01 % bovine serum albumin (BSA), 25 µg/ml human insulin solution, 100

µg/ml human apo-transferrin, 60 µM putrescine dihydrochloride, 20 nM progesterone, and 30 nM sodium selenite (all from Sigma)], plated in a 75 cm^3 tissue culture (T-75) flask supplemented with 20 ng/ml recombinant murine epidermal growth factor (EGF, Peprotech) and placed in a humidified incubator. Cells were fed every 3-4 days by adding 5 ml neurosphere media and 4 µl EGF to each flask until large round neurospheres were formed (approximately 7 days).

2.1.3 Neurosphere-derived astrocytes

Prior to experiment, 13 mm diameter glass coverslips (thickness 0, VWR™) were sterilised by autoclaving and coated with poly-L-lysine hydrobromide (13.2 µg/ml in sterile water, Sigma) for a minimum of 2 hrs at 37°C. Coverslips were then washed 3 times with sterile water, inserted into the wells of 24-well plates (one coverslip per well) and allowed dry in a sterile laminar flow cabinet. To generate neurosphere-derived astrocytes, each mature neurosphere flask was scraped with a sterile cell-scraper (Grenier) and cell suspension transferred to 50 ml centrifuge tube (Greiner). Neurospheres were centrifuged at 86 rcf for 5 mins and resuspended in astrocyte media [DMEM (1 g/L glucose with GlutaMAX™, Gibco™) supplemented with 10 % foetal bovine serum (FBS), 1 mM L-glutamine and 1x Pen/Strep (all Sigma)]. Cell suspension from each flask was divided amongst five 24-well plates and volume of media brought up to 1.5 ml per well. Cells were fed every 3-4 days by removing half old media and replacing with fresh astrocyte media until they formed a confluent monolayer.

2.1.4 Rat myelinated cultures

S/D rats were time-mated, with the day of plugging denoted as embryonic day 0.5 (E0.5). Pregnant females were sacrificed at E15.5 by rising concentration of CO_2 and death confirmed by severing the femoral artery. Embryos were excised and embryonic spinal cords extracted. Meninges was removed from each spinal cord and discarded. Cords were placed in 1ml Hank's Balanced Salt Solution (HBSS, no calcium, no magnesium, Gibco™) at a density of $\leq$ 6 cords per ml of HBSS. The cords were enzymatically digested with 1x trypsin (from porcine pancreas, Sigma) and 100 µg/ml collagenase type I (Gibco™) for 15 mins at 37°C. Enzymatic activity was stopped by adding 2 ml of SD inhibitor [L-15 medium supplemented with 0.52 mg/ml soybean trypsin inhibitor, 0.04 mg/ml

deoxyribonuclease I from bovine pancreas and 3.0 mg/ml BSA (all Sigma)] per 1ml HBSS. The cords were then triturated, centrifuged at 196 rcf (1,200 rpm) for 5 mins and resuspended in plating media [50 % DMEM (4.5 g/L glucose with GlutaMAX™), 25 % horse serum (Gibco™), 25 % HBSS (with sodium bicarbonate, Sigma), supplemented with 2 mM L-glutamine and 0.5x Pen/Strep] at a concentration of 3 x 10^6 cells per ml. The aforementioned astrocyte coverslips were carefully removed from the 24-well plates and placed in 35 mm Petri dishes (Corning), 3 coverslips per dish. 150,000 spinal cord cells were plated onto each astrocyte coverslip and dishes were placed in a humidified incubator for 2 hrs. Each dish was then topped up with 450 µl of plating media and 600 µl of differentiation media [DMEM (4.5 g/L glucose with GlutaMAX™, Gibco™), 1 mM sodium pyruvate, 10 ng/ml biotin, 0.5x N1 Medium Supplement, 50 nM hydrocortisone, 0.1 µg/ml insulin from bovine pancreas and 1 % Pen/Strep (all from Sigma)]. Cells were fed every 2-3 days by removing 500 µl of old media and replacing with 600 µl of fresh differentiation media. From Day *in vitro* (DIV) 13, cells were fed with differentiation media without added insulin (DM-). An astrocyte monolayer was required as the spinal cords of E15.5 rats do not contain sufficient astroglial progenitors. Rat myelinated cultures were used for the majority of experiments due to higher cell yield, reliable reproducibility, and generally higher myelination rates than mouse myelinated cultures. The latter two qualities were aided by the astrocyte monolayer which provides the cultures with added stability and trophic support.

2.1.5 Mouse myelinated cultures

Mice were time-mated and pregnant females sacrificed at E13.5 by rising concentration of CO_2, death confirmed by severing the femoral artery. Spinal cords were extracted from embryos and processed as per rat myelinating culture protocol with some amendments. Cords were enzymatically digested with 1x trypsin for 15mins at 37°C. Enzymatic activity was stopped by adding 2ml SD inhibitor per ml of HBSS. Cords were triturated, centrifuged at 181 rcf (1,000 rpm) and resuspended in plating medium. Cells were plated onto coverslips coated with poly-L-lysine hydrobromide (13.2 µg/ml in boric acid buffer, pH 8.4) at a density of 165,000 cells per coverslip. Coverslips were contained in 35 mm Petri dishes, 3 coverslips per dish, and incubated for a minimum of 4 hrs to

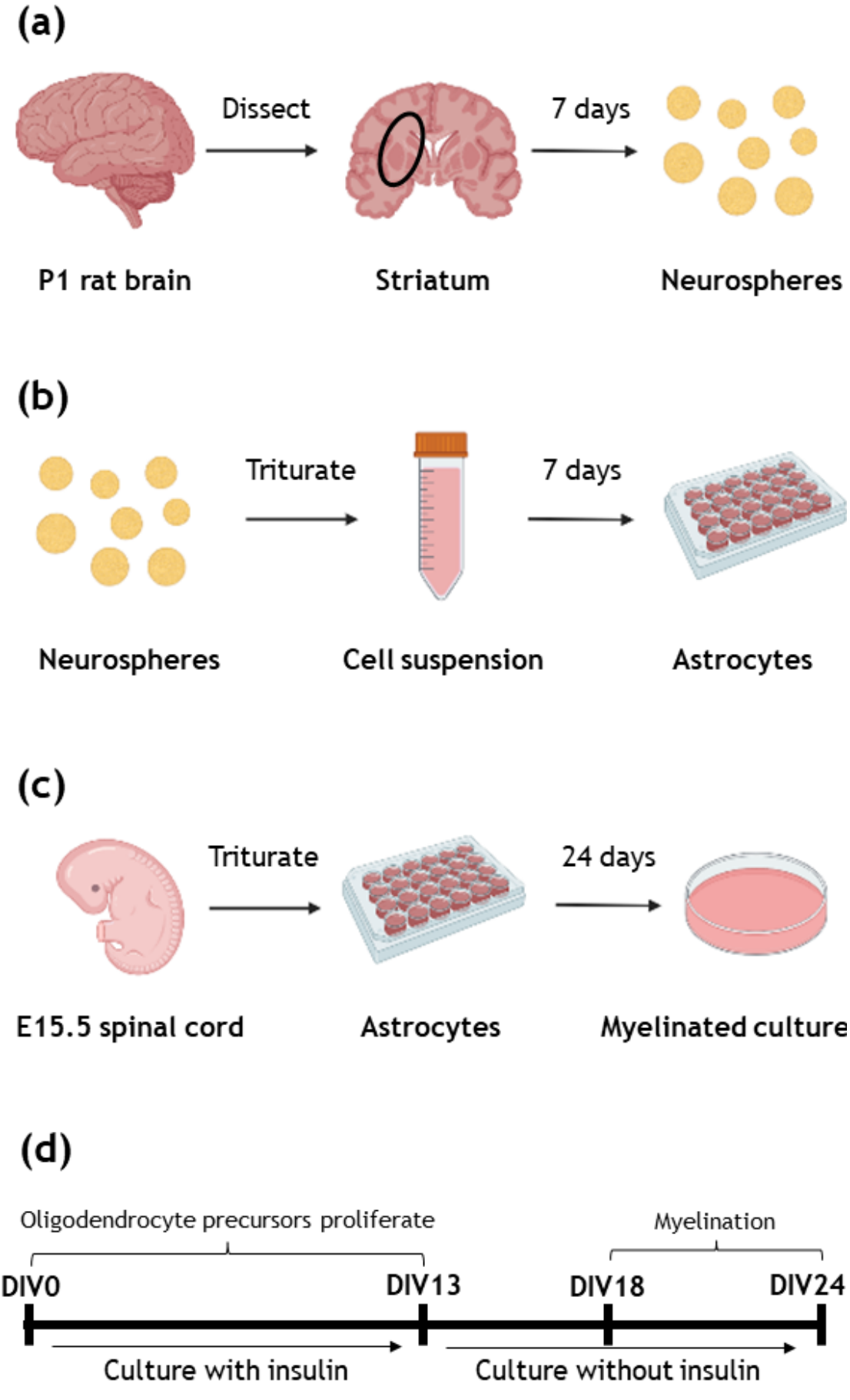

Figure 2.1 Schematic for the culture of rat myelinated cultures. (a) neurospheres (b) neurosphere-derived astrocytes (c, d) myelinated cultures.

attach. Once visibly attached, dishes were topped up with 300 µl plating media and 600 µl differentiation media. Cells were fed and maintained as per the rat culture protocol. Mouse myelinated cultures were used to explore the effect of specific gene deletion on the lipid-reactive IgM response.

2.1.6 Mixed glial cultures

Post-natal day 1 S/D rats were euthanised by lethal (i.p.) injection of Euthatal and death confirmed by severing the femoral artery. Rats were decapitated, heads submerged in cold 70 % ethanol and transferred to a 50 ml centrifuge tube containing Dulbecco's phosphate buffered saline (DPBS, Gibco™). Heads were then transferred to a 90 mm Petri dish (Thermo Scientific™) containing L-15 medium and kept on ice for the duration of the dissection. Brains were removed from skull with caution to ensure brain tissue was not damaged. Meninges was removed from brain using fine tweezers and brain tissue placed in a new 90 mm Petri dish containing 5 ml chilled L-15 medium. Brains were transferred to a 50 ml centrifuge tube using a 10 ml pipette and centrifuged at 2,500 rcf for 5 mins. Supernatant was discarded and 5 ml fresh medium added. Tissue was triturated by pipetting up and down 10 times with a 10 ml pipette and once with a 5 ml pipette. Cell suspension was passed through an EASYstrainer™ cell sieve (70 µm, Greiner) into a 50 ml centrifuge tube and strainer rinsed with 5 ml of L-15 medium. The strained cell suspension was the centrifuge at 2,500 rcf for 5 mins. Meanwhile, 12 ml of pre-warmed mixed glial media [DMEM (4.5 g/L glucose with GlutaMAX™), supplemented with 10 % FBS and 1 % Pen/Strep] was added to each T-75 flask. For the number of brains dissected (n), n-1 flasks were generated. Supernatant was discarded and cells resuspended in mixed-glial media by pipetting up and down 10 times using a 10 ml pipette. Cell suspension was divided amongst the T-75 flasks and flasks placed in a humidified incubator for 5 days. Media was removed from each flask and replaced with 12 ml fresh pre-warmed mixed glial media. Media was changed every 3 days until a confluent monolayer was achieved (approximately 14 days).

2.1.7 Primary microglia

Once mixed glial cultures formed a confluent monolayer, flasks were sealed with parafilm, placed in a pre-warmed shaking incubator and shaken at 100 rpm for 1

hr at 37°C. Media was collected from each flask and transferred to a 50 ml centrifuge tube. Media was centrifuged at 2,500 rcf for 5 mins and supernatant discarded. Cells were resuspended in microglia media [DMEM (4.5 g/L glucose with GlutaMAX™), supplemented with 10 % horse serum and 1 % Pen/Strep] at a concentration of 400,000 cells per ml. Cells were plated onto uncoated glass coverslips (13mm diameter), one coverslip per well of a 24-well plate, at a concentration of 180,000 cells per well. Cells were returned to incubator to adhere overnight, after which media was removed and replaced with serum-free microglia containing stimulant of interest.

2.1.8 Hybridoma cell culture

O4 and A4CD hybridoma cells were originally received from Prof. Ilse Sommer (University of Heidelberg) and Prof. Robert S. Fujinami (University of Utah) respectively. The O4 hybridoma clone was originally produced by fusing mouse myeloma P3-NS1/1-Ag4-1 with spleen cells from BALB/c mice immunized with white matter from bovine corpus callosum (Sommer and Schachner 1981). The resultant hybridoma produced a polyreactive mouse IgM with high immunoreactivity to the glycosphingolipid sulfatide. The A4CD hybridoma clone was originally derived from the splenocytes of an A.SW mouse immunised with MOG_{92-106} peptide to induce progressive stage EAE. Splenocytes were fused with SP2/0-Ag14 myeloma cells producing an IgM with nIgM properties exhibiting poly- and auto-reactivity (Peterson et al. 2007).

Cells were stored in freezing medium [OptiMem™ (Reduced serum medium, no phenol red, Gibco™) supplemented with 50 % FBS, 10 % DMSO] in cryogenic vials in liquid nitrogen until use. To culture, cells were removed from liquid nitrogen and immediately placed in a water bath at 37°C. Once thawed, cells were resuspended in 1 ml FBS then transferred to a 15 ml centrifuge tube containing 8 ml OptiMem™ supplemented with 50 % FBS, 1 % Pen/Strep. Cells were centrifuged at 86 rcf (800 rpm) for 5 mins, resuspended in 5 ml 50 % FBS-OptiMem™ and placed into a 25 cm^3 tissue culture flask. Cells were incubated overnight at 5 % CO_2/37°C then transferred to a T-75 flask. Cells were gradually weaned down to 10 % FBS-OptiMem™ over 3 weeks, splitting 2-3 times a week. Once proliferating at a stable rate in 1 0% FBS, cells were transferred to a CELLine™ Bioreactor Flask (DWK Life Sciences). At this point, media was

switched to ultra-low endotoxin media [OptiMem™ supplemented with 10 % ultra-low endotoxin FBS (Biowest) and 1 % Pen/Strep]. Briefly, 50 ml media was added to media compartment of flask for 30 mins. Cells were centrifuged, all media removed and resuspended in ultra-low endotoxin media to a density of 1.5 x 10^6 cells per ml. 15 ml of cells were introduced to the cell compartment of the flask and 200 ml media added to the media compartment. Cells were split either 1:5 or down to 1.5 x 10^6 cells per ml every 2-3 days by removing the appropriate volume of cells from cell compartment and replacing with the same volume of fresh media. Cells were centrifuged at 181 rcf (1,000 rpm) for 5 mins, supernatants collected and stored at -20°C until use. Half media was removed from media compartment and replaced with 100 ml fresh media. Once a week, all media from media compartment was removed and replaced with fresh media.

2.2 IgM antibody purification

2.2.1 Purification

O4 and A4CD antibodies were purified under sterile conditions from hybridoma supernatants using Hi-Trap IgM purification HP columns (GE Healthcare) as per manufacturer's instructions. Prior to every purification, fresh binding buffer [20 mM sodium phosphate, 0.8 M ammonium sulphate in cell culture grade endotoxin-free water (efH_2O, HyClone™)], elution buffer [20 mM sodium phosphate in efH_2O] and regeneration buffer [20 mM sodium phosphate in 30 % propan-2-ol (efH_2O)] were prepared in a sterile laminar flow hood, pH adjusted to 7.5 and sterile-filtered. All equipment required for purification were sterilised by UV light before use. Peristaltic pump was set at a flow rate of 1 ml per minute and tubing was sterilised by passing through 10 ml 70 % ethanol (in efH_2O) followed by 20 ml binding buffer. Meanwhile, 35-50 ml supernatant was thawed and passed through a 0.45 µm filter. Ammonium sulphate was slowly added to supernatant while stirring by magnetic stirrer to form a 0.8 M ammonium sulphate solution. Column was attached to tubing, new columns were first calibrated by passing through 5 ml binding buffer, followed by 5 ml elution buffer and 5 ml regeneration buffer. 5 ml binding buffer was then passed through column followed by the supernatant and a further 15 ml binding buffer

to remove unbound protein from the column. Flow through was collected. Bound protein was eluted with 10 ml elution buffer and collected in 10 fractions of 1 ml each. Column was regenerated with 7 ml regeneration buffer. Process was repeated with flow through. Column was stored in 20 % ethanol (in efH_2O) and re-used a maximum of 3 times. Concentration of protein fractions was measured using a Nanodrop (Denovix DS-11). Fractions with highest protein concentration were pooled and dialysed in a Spectra/Por 6 Regenerated Cellulose Dialysis Membrane (Spectrum Labs) against DPBS (> 100x volume of protein) for 24 hrs at 4°C. Final antibody concentration was determined by Nanodrop and diluted to 1 mg/ml in DPBS.

2.2.2 Sodium dodecyl sulfate polyacrylamide gel electrophoresis (SDS PAGE)

Samples of supernatant, supernatant flow-through, pooled purified protein and control IgM were analysed by SDS PAGE to ensure IgM bands were present. All materials required for SDS PAGE were purchased from Invitrogen™. For every sample, a 1.5 ml Eppendorf was prepared containing 15 µl sample, 5 µl NuPAGE™ LDS Sample Buffer (4X) and 2 µl NuPAGE™ sample Reducing Agent (10X). Eppendorf lids were pierced with a needle and tubes placed in a pre-warmed heating block at 70°C for 10 mins. Running buffer was prepared by adding 50 ml NuPAGE™ MES SDS Running Buffer (20X) to 950 ml dH_2O and mixing gently by inversion. Buffer was added to gel tank and 10 µl boiled sample loaded into each well of a pre-cast NuPAGE™ 4-12 % Bis-Tris Mini Protein Gel. 5 µl SeeBlue™ Plus2 Pre-stained Protein Standard was added to outermost wells. Gel was run for 1.5 hrs at 100 V then stained with Coomassie Blue for 2 hrs on an orbital shaker. Coomassie Blue was removed and de-stain solution [50 % methanol, 10 % acetic acid in dH_2O] added. Gel was returned to shaker and de-stain solution changed every 30 mins until protein bands were clearly visible.

2.3 Virus production and infection

2.3.1 BUNV

Wild-type BUNV stock was kindly produced and supplied by Xiaohong Shi, University of Glasgow. Briefly, plasmids pTM1BUNL, pTM1BUNM, and pTM1BUNN,

encoding BUNV proteins L, M (polyprotein precursor), and N, respectively, and pT7riboBUNLRen(−), pT7riboBUNMRen(−), and pT7riboBUNSRen(−), were used to generate viral genomic-sense minigenomes (Weber 2001). BSR-T7/5 cells were transfected with the above plasmids for 5 hrs, after which time, the inoculum was removed and replaced with growth media [Glasgow Minimum Essential Medium supplemented with 10% tryptose phosphate broth, 10% FBS, and (Gibco) and 1 mg/ml Geneticin (G418) sulfate (Calbiochem)]. Cells were incubated for 5–11 days at 33 °C until cytopathic effect was observed. Supernatant was clarified and stored at − 70 °C until use.

2.3.2 SFV A7(74)-mCherry

The mCherry marker gene was inserted in the nsP3 protein of SFV A7(74) using a naturally occurring XhoI site, resulting in plasmid pCMV-SFVA774(XhomCherry). This plasmid was generated and kindly provided by Andres Merits, University of Tartu, the backbone of which has been previously described (Saul et al. 2015). Virus stocks were generated by electroporating this plasmid in BHK cells and propagated in Glasgow Minimum Essential Medium (Gibco) with 5% FBS, 10% tryptose phosphate broth (Gibco), 1% Pen/Strep at 37 °C in 5% CO2. When severe cytopathic effect was observed, virus-containing supernatant was centrifuged 500 × g for 30 min to remove cellular debris and cell-free virus stored in small aliquots at − 70 °C. Stocks were titrated by plaque assay as described below.

2.3.3 Quantification of virus by plaque assay

To quantify BUNV stocks and supernatant of BUNV-infected myelinated cultures, Vero E6 cell monolayers were incubated with serially diluted supernatant for 1 h at 37 °C then covered with 0.6% Avicel (FMC Biopolymer)-minimum essential medium overlay medium supplemented with 2% FBS. Cells were incubated for four days and fixed with 4% formaldehyde-PBS and stained with 0.5% (w/v) methyl violet. Virus titres were calculated and presented as plaque forming units (PFU)/ml. A similar assay was used for SFV, with the following adaptations: BHK cells were infected and maintained as described, and at 2 days post infection fixed in 10% formaldehyde-PBS and stained with 0.1% toluidine blue (Sigma).

2.3.4 Infection of myelinated cultures with BUNV

Myelinating cultures were treated with either media alone, A4CD or O4 for 24 hrs. All media was removed, and cells inoculated with 0.75 % BSA (Sigma) in PBS alone or with BUNV (MOI = 1). Cells were incubated for 1hr at 5 % CO_2/95 % air, shaking gently every 15 mins. Inoculum was removed and fresh DM- added. Cells were returned to the incubator for a further 24 hrs at which point supernatant was collected for plaque assay, cells washed with 0.75 % BSA-PBS and fixed with 4 % formaldehyde-2 % sucrose in PBS for 10 mins. Fixative was removed, 0.75 % BSA-PBS added, and cells stored at 4°C until immunocytochemistry was performed

2.3.5 Intranasal SFV-A7(74)-mCherry infections

Nine-week-old male C57Bl/6 mice were anaesthetised with isoflurane and infected intranasally (i.n) with 1 x 10^5 pfu SFV-A7(74)-mCherry in 20 µl PBSA [0.75% bovine serum albumin in PBS]. Mice were returned to home cage for 24, 48, and 72 hrs with weight being measured every 24 hrs. At the appropriate time-points, mice were euthanised, blood drawn from the hepatic vein, and the following tissues harvested for RT-qPCR: olfactory bulb (OFB), cortex (CX), cerebellum (CB), and spleen (SP).

2.4 Cell culture treatments

2.4.1 General antibody treatments

Once A4CD and O4 antibodies were purified and the presence of IgM was confirmed by SDS PAGE, antibodies were tested for anti-viral activity by treating DIV24 myelinating cultures with 20 µg/ml of antibody for 6 or 24 hrs and processed for RT-qPCR to assess *Ifnb1* or ISG induction respectively. As a negative control, cultures were treated with commercial IgM form mouse myeloma (20 µg/ml, Sigma). As a positive control, cultures were treated with polyinosinic:polycytidylic acid (poly I:C, 5 µg/ml, Sigma). To treat cultures, 500 µl of media was removed and 500 µl of treatment added. Treatments were

diluted in DM-. For all IgM antibody experiments thereafter, myelinating cultures were treated at DIV24 and antibodies were used at final concentration of 20 µg/ml. Other IgM antibodies used in this thesis include: O1 (R&D Systems) and A2B5 (Abcam). Untreated controls were given DM- alone.

2.4.2 IFN-β neutralisation

Rat myelinating cultures were treated with media alone, A4CD or O4 in combination with either rabbit anti-rat IFN-β neutralising antibody or normal rabbit IgG control (10 µg/ml, both R&D Systems) for 24 hrs. Cells were then lysed for RNA isolation.

2.4.3 Supernatant sub-fractionation

This experiment was conducted to investigate whether O4-induced IFN-I response was mediated directly by the antibody (~ 970 kDa) or was due to the secondary release of DAMPs (< 50 kDa) by the cultures upon O4 binding. Rat myelinating cultures were treated with media alone (2 x dishes), A4CD (5 x dishes), O4 (5 x dishes) and poly I:C (2 x dishes) for 2 or 6 hrs. During the 2 hr incubation, 2 x 50 kDa molecular weight cut-off (MWCO) Amicon® Ultra-4 Centrifugal Filter Units were sterilised by adding 4 ml 70 % ethanol (in efH_2O) to the units and centrifuging at 4,000 rcf for 20 mins at 4°C. Sterile DPBS was added to the filters until required at which time the filter units were centrifuged as above to rinse the filter. Supernatants were collected from 4 x A4CD and 4 x O4 dishes (4 ml supernatant per condition). 1 ml of each supernatant was removed and placed in labelled Eppendorfs on ice. The remaining 3 ml supernatant was placed in the filter unit, 1 unit per condition, and centrifuge a described above. Whilst the A4CD and O4 supernatants were centrifuging, supernatant was removed from 1 x untreated and 1 x poly I:C treated culture and placed in Eppendorfs on ice. Once filter units had been centrifuged, the > 50 kDa and < 50 kDa fractions were removed and placed in sterile bijous on ice. The volume of each fraction was calculated and brought back up to 3 ml with cold DM-. Naïve cells were removed from incubator, media discarded, and replaced with the following chilled supernatants: untreated (uncentrifuged), A4CD (uncentrifuged), A4CD (>50 kDa), A4CD (< 50 kDa), O4 (uncentrifuged), O4 (> 50 kDa), O4 (< 50 kDa) and poly I:C (uncentrifuged). Cells were returned to the

incubator for 4 hrs. Cells were then lysed for RNA isolation along with the remaining cultures that were treated undisturbed for 6 hrs.

2.4.4 Signalling pathway inhibition

Rat cultures were treated 6 hrs with media alone, A4CD or O4 with simultaneous administration of either dimethyl sulfoxide (DMSO, Sigma) or 10 μM of one of the following inhibitors: ST2825 (MedChemExpress®), RU.521 (Invivogen), C-176 (Biovision) and BX795 (Invivogen). Cells were lysed for RNA isolation or fixed for immunocytochemistry.

2.4.5 Microglia depletion

Rat cultures were treated from DIV18-28 with PLX3397 (Selleckchem) or an equivalent volume of DMSO every 2-3 days. Final concentration of PLX3397 in cell culture dish was maintained at 1 μM and volume of DMSO maintained at 0.1 % of total media volume. On DIV28, cells were treated for 6 hrs with media alone, A4CD or O4 in combination with either PLX3397 or DMSO. Cells were lysed for RNA isolation or fixed for immunocytochemistry.

2.5 Molecular biology

2.5.1 RNA isolation

Prior to RNA isolation procedures, bench was cleaned with 70 % ethanol and RNase*Zap*™ RNase Decontamination Solution (Invitrogen™). RNA was extracted from rat cultures using the RNeasy® Plus Micro kit (Qiagen) as per manufacturer's instructions. Media was removed, 350 μl of Buffer RLT Plus added to dish and allowed to incubate for a few minutes. Coverslips were scraped using sterile scrapers, lysate transferred to labelled Qiashredders (Qiagen) and centrifuged at 8,000 rcf for 1 min. Tubes containing homogenised lysate were sealed and stored at -80°C until use. Lysates were thawed on ice, transferred to a gDNA Eliminator spin column and centrifuged at 12,000 rcf for 30 secs. 350 μl 70 % ethanol (in nuclease-free water) was added to each tube

and the contents mixed briefly by pipetting. Lysate was then transferred to an RNeasy® MinElute spin column and centrifuged at 8,000 rcf for 30 secs. Flow-through was discarded and column washed with 700 µl Buffer RW1 (8,000 rcf, 30 secs), followed by 500 µl Buffer RPE (8,000 rcf, 30 secs) and 500 µl 80 % ethanol (in nuclease-free water) (8,000 rcf, 2 mins), discarding flow-through each time. Column lids were removed using a sterile scissors and column membranes dried by centrifuging at 13,200 rcf for 5 mins. Columns were placed in 1.5 ml collection tubes and 14 µl RNase-free water pipetted directly onto column membrane. Water was allowed incubate on membrane for 2 mins before centrifuging at 16,000 rcf for 1 min. Collection tubes were immediately placed on ice and RNA concentration determined by Nanodrop.

The PureLink™ RNA Mini Kit (Invitrogen™) and TRIzol® Reagent (Invitrogen™) was used to extract RNA from mouse cultures and virus-infected cultures and tissues. For tissues, perfused brains were placed in RNase-free microfuge tubes containing ice-cold RNA*later*® and stored at 4°C for 24 hrs. The brains were subsequently divided into cerebellum, cortex, hippocampus, and olfactory bulb, and placed in RNase-free microfuge tubes containing one stainless steel ball. 1 ml TRIzol® Reagent was added and tubes placed in a homogeniser at maximum speed for 10 mins.

For extraction of RNA from cultures, all media was removed from cells and 1ml TRIzol® Reagent added per dish. Cultures were incubated for 10 mins in a fume hood and lysates transferred to RNase-free microfuge tubes and stored at -80°C until use. From this point onwards, both tissue- and culture-derived TRIzol® samples were treated in the same way as per manufacturer's instructions.

200 µl chloroform (VWR) was added to each tube of lysate, tubes resealed, and lysates shaken by hand for 15 secs. Samples were left undisturbed for 2-3 mins before centrifuging at 12,000 rcf for 15 mins at 4°C. 500 µl of aqueous layer was transferred to an RNase-free microfuge tube containing 500 µl 70 % ethanol (in nuclease-free water). Samples were vortexed to mix, 500 µl of contents were transferred to a Spin Cartridge and centrifuged at 12,000 rcf for 15 secs. Flow-through was discarded and process repeated until all sample was loaded onto column. Cartridge was washed once with 700 µl of Wash Buffer I followed by 2 x 500 µl Wash Buffer II (all at 12,000 rcf for 15 secs, flow-through discarded after

each wash). Cartridge lids were removed, and membrane dried by centrifuging at 12,000 rcf for 1 min. Cartridge was transferred to a Recovery Tube and 14 µl RNase-free water pipetted directly onto membrane. Water was incubated for 2 mins and cartridge centrifuged at 16,000 rcf for 2 mins. Recovery Tubes were immediately placed on ice and concentration of RNA was determined by Nanodrop.

2.5.2 cDNA synthesis

cDNA was synthesised from a maximum of 1µg RNA using a QuantiTect® Reverse Transcription Kit (Qiagen) following the manufacturer's instructions using a Biometra T3 Thermocycler (Thermofisher). Within each individual experiment, the same amount of RNA was used for all conditions in that experiment. For every sample, a maximum of 12 µl RNA was added to a 0.2 ml PCR tube (Star Lab). Volume was made up to 12 µl with RNase-free water. 2 µl gDNA Wipeout Buffer was added to each tube and tubes incubated at 42°C for 2 mins then immediately placed on ice. To each tube, 4 µl Quantiscript RT Buffer (5X), 1 µl Qunatiscript Reverse Transcriptase and, 1 µl RT Primer Mix were added. Tubes were centrifuged to mix and incubated for 15 mins at 42°C. Synthesised cDNA was diluted to appropriate volume using RNase-free water (1:200 for 1µg starting RNA) and stored at 4°C for short-term or -20°C long-term.

2.5.3 Primer design

Primers were designed using mRNA sequences obtained from NCBI nucleotide data base. Primer 3 software (http://biotools.umassmed.edu/bioapps/primer3_www.cgi) (Rozen and Skaletsky 2000) was used to find suitable primer sequences. Primer sequences were checked for specificity using BLAST (http://blast.ncbi.nlm.nih.gov/Blast.cgi). Primers were purchased from Integrated DNA Technologies and reconstituted to 100µM in RNase-free water. A list of primers used in this thesis can be found in Table 2.1.

2.5.4 End-point polymerase chain reaction (PCR)

To test primer pairs before use in Real-Time PCR, end-point PCR was performed using cDNA where the target gene was likely to be highly expressed. Primers

Table 2.1: Primer sequences

Gene	Species	Forward sequence	Reverse sequence
GAPDH	Rat	AGATGGTGAAGGTCGGTGTG	TGAAGGGGTCGTTGATGG
Ifnb1	Rat	GCTGAATGGAAGGCTCAAC	GAATGGCAAAGGCAGTGTAA
Cxcl10	Rat	GCAAGTCTATCCTGTCCGCA	CTAGCCGCACACTGGGTAAA
Mx1	Rat	TGAGGAGACGAAGAGAGGAG	GCAGTTAGGAGCAGGAAGGA
Rsad2	Rat	ACTGGGAAGGGGGATTTACTT	TTTTTACCGCCGAACACATT
Oasl	Rat	GCCGAGGTCTATGTGAATCTG	TCGCTGAAGGAAGGAGAGAA
18S	Rat	CTCAACACGGGAAACCTCAC	GACAAATCGCTCCACCAACT
Ifit2	Rat	CCTGTGCTTGACTGTGAGGA	AGTGGATTCTGGGTTCTTTGG
Isg15	Rat	GGATGGTGTTGCCCTTATC	GCCCCTTTCATTCCTCAC
Isg20	Rat	CTGAGGGTCTGAGGAGCA	CGCTGACTTGGGTTCTGTAGT
Ccl5	Rat	CTTTGCCTACCTCTCCCTCG	TCCCCAGCTGGTTAGGACT
Ifna4	Rat	CTCATCTGCTGCTTGGAATG	TTCTTGGGTTAGGGGAGGTT
Ifng	Rat	GCCCTCTCTGGCTGTTACTG	CCAAGAGGAGGCTCTTTCCT
BUNM	BUNV	GGGGAAGATACAGGCAATGA	CCCACACACAGTCAGTAACAACA
18S	Mouse	GACTCAACACGGGAAACCTC	TAACCAGACAAATCGCTCCAC
Cxcl10	Mouse	GCTCAAGTGGCTGGGATG	GAGGACAAGGAGGGTGTGG
Mx1	Mouse	GGTCGGCTTCTGGTTTTGT	TGATGGGTGGTGGGCTAA
Rsad2	Mouse	AAATGTGGCTTCTGCTTCCA	CCAAGTATTCACCCCTGTCCT
Oasl1	Mouse	AGGGGGTGTGAGAAGTCGT	GATTGGTTAGGAAGATGGTTTGG
Ifnb1	Mouse	CACAGCCCTCTCCATCAACT	GCATCTTCTCCGTCATCTCC

tested were related to the IFN-I response so cDNA from poly I:C-treated myelinating cultures was used. As controls, nuclease-free water and cDNA from untreated cultures were also used. 0.2 ml PCR tubes were placed on ice and 3 µl of cDNA or water added. To each tube, 5 µl REDTaq® ReadyMix™ PCR Reaction Mix (Sigma), 1.5 µl nuclease-free water and 0.6 µl primer mix was added. Tubes were centrifuged to mix and placed in a Thermocycler. Cycle settings were as follows: 50°C for 5 mins, 95°C for 10 mins, followed by 40 cycles of 95°C for 15 secs, 60°C for 1 min, and a final dissociation step at 95°C for 15 secs. Samples were stored at 4°C until use.

2.5.5 Agarose gel electrophoresis

150 g UltraPure™ Agarose (Invitrogen™) was dissolved in 1X TAE buffer (40 mM Tris base, 20 mM acetic acid, 1 mM ethylenediaminetetraacetic acid in dH_2O) by heating and 0.5 µg/ml ethidium bromide added. Solution was swirled to mix, poured into a gel mould and allowed to set for 1 hr. 10 µl cDNA samples were loaded into wells of gel and 5 µl 100 bp DNA ladder (Promega) loaded into the outermost wells of gel. Gel was run at 100 V for 1.5 hrs and imaged.

2.5.6 Microarray and Partek Genomic Suite analysis

RNA was extracted from myelinating cultures (biological n = 3) treated 24 hrs with media alone, commercial non-specific IgM (Sigma) or commercial anti-sulfatide IgM O4 (R&D Systems). RNA quality and integrity was assessed using Agilent Bioanalyser 6000 Nano LabChip platform system at Edinburgh Genomics, Roslin Institute, University of Edinburgh. This system utilises the RNA Integrity Number (RIN) algorithm to analyse RNA electropherograms for degradation products, where an RIN score of 1 indicates a completely degraded RNA sample and 10 indicates a totally intact RNA sample. An RIN score of > 8 was deemed acceptable for analysis, with all submitted samples being ≥ 8.7.

Total RNAs were processed and labelled with biotin using Ambion WT Expression Kit following the Affymetrix GeneChip WT Terminal Labeling and Hybridization protocol. The processed RNAs were hybridized to Affymetrix GeneChip® Rat Gene 2.1 ST Arrays which comprised of 28,407 distinct RefSeq probes that equated to 16,771 well-annotated gene transcripts. Hybridisation was performed

as per manufacturer's instructions for using the Fluidics Station 450. The hybridized arrays were scanned on the Gene Array Scanner 3000-7G and the resultant data analysed using Partek Genomics Suite and PathwayTM software (version 6.6, Partek Inc., St. Louis, MO, USA). Probeset level data were normalised on a chip-by-chip basis using the GC content-adjusted robust multi-array average (GCRMA) algorithm and summarised to transcript cluster level using One-Step Tukey's Biweight method.

2.5.7 Real-time quantitative PCR (RT-qPCR)

Quantitative real-time PCR was performed in MicroAmp Fast Optical 96-well reaction plates (0.1ml) (Invitrogen™) with each sample being run in triplicate. Reagents per well were as follows; 7.5 µl Power SYBR™ Green PCR Master Mix (Applied Biosystems), 5.2 µl RNase-free water, 0.3 µl primer mix (100 µM stock) and 2 µl cDNA. Plates were run in an Applied Biosystems Fast Real-Time PCR System (ABI 7500) and quantified using the comparative CT (ΔΔCT) method or standard curve method. Cycle settings were as follows; 50°C for 5 mins, 95°C for 10 mins, followed by 40 cycles of 95°C for 15 secs, 60°C for 1 min, and a final dissociation step at 95°C for 15 secs. *18S* was used as the housekeeping gene for mouse and virus experiments. *Gapdh* was used as the housekeeping gene for all other rat experiments.

2.6 Immunocytochemistry

For live-staining with IgM antibodies, live cells were incubated with antibody (20 µg/ml) for 30 mins at 4°C, fixed with 4 % PFA for 10-20 mins and washed with 1x PBS. For all other immunocytochemistry experiments, live cells were fixed with 4 % PFA without prior antibody incubation and washed with 1x PBS. After fixation, cells were permeabilised with 0.5 % Triton™ X-100 (in 1x PBS, Sigma) for 10 mins, washed with 1x PBS and blocked with blocking buffer [1 % BSA, 10 % horse serum in 1x PBS] for 45 mins. Primary antibodies were diluted in blocking buffer and incubated with cells for 45 mins. Cells were then washed with 1x PBS and incubated for 15 mins protected from light with appropriate secondary antibody diluted 1:400 in blocking buffer. Coverslips were then washed in 1x PBS

followed by dH_2O and mounted onto glass slides with Mowiol 4-88 mounting medium [33 % w/v Mowiol® 4-88, 13.2 % w/v glycerol (both Sigma), 0.05 % v/v DAPI (Invitrogen) in 0.13 M Tris pH 8.5]. Mounted slides were stored at 4˚C protected from light until imaged. Full list of primary and secondary antibodies including host species and working dilution can be found in Table 2.2.

2.7 Fluorescence in situ hybridisation (FisH)

F*is*H was performed on rat myelinating cultures treated with A4CD or O4, using the ViewRNA Cell Plus Assay kit (Invitrogen™) as per manufacturer's instructions. First, immunocytochemistry was performed on cells using nuclease-free reagents that accompany the kit. The procedure for immunocytochemistry was the same as described in the previous section with some amendments. All washes were performed with nuclease-free 1X PBS [10 % ViewRNA Cell Plus PBS (10X), 1 % ViewRNA Cell Plus RNase Inhibitor (100X) in nuclease-free water].

Cells were fixed and permeabilised simultaneously for 30 mins with ViewRNA Cell Plus Fixation/Permeabilisation Solution [50 % ViewRNA Cell Plus Fixation/Permeabilisation Component A, 50 % ViewRNA Cell Plus Fixation/Permeabilisation Component B, equilibrated to room temperature]. Blocking buffer was replaced with ViewRNA Cell Plus Blocking/Antibody Diluent Solution [1 % ViewRNA Cell Plus RNase Inhibitor (100X) in ViewRNA Cell Plus Blocking/Antibody Diluent]. Cells were blocked for 20 mins and incubated with primary and secondary antibodies for 1 hr each. After secondary antibody incubation, cells were washed 3 times with nuclease-free 1X PBS and fixed with ViewRNA Cell Plus Fixation Solution [12.5 % ViewRNA Cell Plus Solution A Fixative, 87.5 % ViewRNA Cell Plus Solution B Fixative] for 1 hr. ViewRNA cell plus type 6 probe sets against the following genes: *Cxcl10*, *Mx1*, *Rsad2* and *Oasl*, were thawed at room temperature before being placed on ice. ViewRNA Cell Plus Probe Set Diluent was pre-warmed in a HybEZ 241000ACD Hybridisation Oven (Advanced Cell Diagnostics) at 40°C. Probe sets were diluted 1:100 in pre-warmed ViewRNA Cell Plus Probe Set Diluent and incubated with cells for 2 hrs in hybridisation oven set at 40°C ± 1°C. Cells were washed 5 times with ViewRNA Cell Plus RNA Wash Buffer Solution [0.3 % ViewRNA Cell Plus RNA Wash

Table 2.2: Primary and secondary antibodies for immunocytochemistry

Description [clone]	Source	Species/Isotype	Dilution
Anti-sulfatide [O4]	Linington Lab	Mouse IgM	20 µg/ml
Anti-myelin oligodendrocyte glycoprotein (MOG) [A4CD]	Linington Lab	Mouse IgM	20 µg/ml
Anti-galactosylceramidase (GalC) [O1]	R&D Systems	Mouse IgM	20 µg/ml
Anti-A2B5 [105]	Abcam	Mouse IgM	20 µg/ml
Anti-NeuN [A60]	Millipore	Mouse IgG1	1:200
Anti-nestin [rat-401]	Millipore	Mouse IgG1	1:100
Anti-glial fibrillary acid protein (GFAP) [G-A-5]	Sigma	Mouse IgG1	1:250
Anti-olig2 [211F1.1]	Millipore	Mouse IgG2a	1:200
Anti-olig2	Millipore	Rabbit IgG	1:500
Anti-iba1	Wako	Rabbit IgG	1:500
Anti-CD68 [ED1]	Abcam	Mouse IgG1	1:200
Anti-BUN	Elliott Lab	Rabbit IgG	1:500
Anti-proteolipid protein [AA3]	Barnett Lab	Rat IgG	1:200
Anti-Mouse IgG, IgM (H+L) Secondary Antibody, Alexa Fluor 488	Invitrogen	Goat IgG	1:400
Anti-Mouse IgG1 Cross-Adsorbed Secondary Antibody, Alexa Fluor 568	Invitrogen	Goat IgG	1:400
Anti-Mouse IgG2a Cross-Adsorbed Secondary Antibody, Alexa Fluor 488	Invitrogen	Goat IgG	1:400
Anti-Rabbit IgG (H+L) Cross-Adsorbed Secondary Antibody, Alexa Fluor 488	Invitrogen	Goat IgG	1:400
Anti-Rat IgG (H+L) Cross-Adsorbed Secondary Antibody, Alexa Fluor 488	Invitrogen	Goat IgG	1:400

Component 1, 0.5 % ViewRNA Cell Plus RNA Wash Component 2 in nuclease-free water], left covered with a final layer of with ViewRNA Cell Plus RNA Wash Buffer Solution and stored in a sealed humidified chamber at 4°C overnight, protected from light. Samples were brought to room temperature and ViewRNA Cell Plus Amplifier Diluent and Label Probe Diluent were pre-warmed to 40°C in the hybridisation oven for 30 mins. ViewRNA Cell Plus PreAmplifier Mix, Amplifier Mix and Label Probe Mix were thawed at room temperature then placed on ice until use. Cells were incubated with ViewRNA Cell Plus PreAmplifier Solution [4 % ViewRNA Cell Plus PreAmplifier Mix in ViewRNA Cell Plus Amplifier Diluent] for 1 hr at 40°C ± 1°C and washed 5 times with ViewRNA Cell Plus RNA Wash Buffer Solution. This process was repeated with ViewRNA Cell Plus Amplifier Solution [4 % ViewRNA Cell Plus Amplifier Mix in ViewRNA Cell Plus Amplifier Diluent] followed by ViewRNA Cell Plus Label Probe Solution [4 % ViewRNA Cell Plus Label Probe Mix in ViewRNA Cell Plus Label Probe Diluent]. Cells were left for 10 mins in final wash then rinsed with 1X PBS and mounted onto glass slides using Mowiol 4-88 mounting medium. Mounted slides were stored overnight at 4˚C protected from light and imaged.

2.8 Image capture and analysis

Immunocytochemistry and F*is*H experiments were analysed blind by capturing 10 random images per coverslip, 3 coverslips per condition for every biological replicate. Slides were blinded by a colleague by covering the slide label with opaque tape and assigning letters to each slide in a random order. A note of which condition corresponded to each letter was recorded and put aside until after all imaging and quantification was complete.

Coverslips from BUNV infection, microglia depletion, signalling pathway inhibitor experiments were imaged using an Olympus BX51 microscope (Olympus Lifescience), a Retiga R6 camera and Ocular 2.0 software (both Teledyne Qiamging). Images were saved as tif files. Myelin, axonal, and astroglial density were quantified using the CellProfiler (Carpenter et al. 2006) pipeline “myelin.cp”. Astrocyte density was expressed as the threshold level pixel value for GFAP immunoreactivity, whereas axonal density was expressed as the

threshold level pixel value SMI31 immunoreactivity divided by the total number of pixels to yield percent axonal density. Quantification of myelin density utilised pattern recognition software to distinguish between linear myelinated internodes and oligodendrocyte cell bodies. Myelin density was expressed as percent myelin whereby the myelin pixel value was divided by the total number of pixels, as well as percent myelination whereby the myelin pixel value was divided by the axonal pixel value. To quantify dapi, tif files were first converted to png using CellProfiler pipeline "Ocular.cpproj" and then processed by the "dapi mono.cp" pipeline whereby blue objects between 12 and 60 pixels in diameter were counted. CellProfiler pipelines can be found at https://github.com/muecs/cp/tree/v1.1. $BUNV^+$, $Iba1^+$, $NeuN^+$ and $Olig2^+$ cells were counted manually using cell counter plugin (https://imagej.nih.gov/ij/plugins/cell-counter.html) with ImageJ (Schneider, Rasband, and Eliceiri 2012).

Coverslips from FISH experiments were imaged using a Zeiss Axio Imager 2 and Zen 2012 (blue edition) software. Images were saved as czi files. To quantify total dapi, images were saved as png files using Zen software and processed using the "dapi mono.cp" CellProfiler pipeline. Cells positive for mRNA of interest were quantified manually using the cell counter plugin in Fiji (Schindelin et al. 2012).

2.9 Statistical analysis

Statistical details of experiments including statistical tests used, n values, definition of centre, dispersion and precision measures are reported in the figure legends. Unless otherwise stated, n represents biological replicates. For cell culture experiments, biological replicates are when an experiment is repeated with cultures derived from embryos from different pregnant dams, which each dam contributing one biological n. For *in vivo* experiments, n represents individual mice. As cells were generated from embryos, the gender of cells could not be determined. Spinal cords from all embryos harvested from a pregnant dam were pooled therefore the final cell culture suspension would contain a

mixture of male and female cells. *In vivo* experiments were performed on male mice only.

Selection of cells or mice for each condition was performed randomly, with cells required to be of good quality (no gaps on coverslips with well-established neurites and myelin sheaths). Immunocytochemistry was performed on a representative culture for each n to ascertain relative proportion of myelin, neurite, astrocyte, and microglial density. Normal percent myelination at DIV24 is deemed to be > 5 % as determined using the CellProfiler myelin pipeline. Normal microglial density ranges between 5 and 10 % of total DAPI counts.

Statistical significance was determined using one of the following tests depending on number of samples and variables: two-tailed *t*-test for data with one variable and two conditions, one-way ANOVA with Tukey's *post hoc* test for data with one variable and greater than two conditions, and two-way ANOVA with Sidak's *post hoc* test for data with two variables and two conditions. Data were deemed significant when *p*-value was less than 0.05 and are denoted in figures as $*p < 0.05$, $**p < 0.01$, $***p < 0.001$, $****p < 0.001$.

Statistical analysis was performed in GraphPad Prism 8. Pathway enrichment analysis was performed using Database for Annotation, Visualisation, and Integrated Discovery (DAVID) version 6.8 (Huang da, Sherman, and Lempicki 2009). Interferome version 2.01 was used to identify interferon regulated genes in microarray datasets (Rusinova et al. 2013).

Chapter 3

O4 induces antiviral immune signature in CNS cultures

3 O4 induces antiviral immune signature in CNS cultures

3.1 Introduction

Microarray data previously generated by our laboratory indicated that the sulfatide-reactive IgM O4 induced an antiviral transcriptional signature in rat myelinated cultures (Hayden et al. 2020; Semenoff 2014). This analysis was performed originally in 2014 using pathway enrichment based solely on KEGG annotation terms. Since then, great advances have been made in pathway enrichment analysis and an increasing number of online analysis tools are now freely available. Therefore, the aims of this chapter are to:

1 provide an updated *in silico* analysis of rat myelinated cultures treated 24 hrs with control IgM or O4 and

2 compare the transcriptional signature of O4-treated myelinated cultures in the presence and absence serum, modelling the brain under homeostatic and disease conditions.

3.2 O4 induces immune signature in the absence of serum

Microarray analysis undertaken by Tiia Semenoff identified 259 genes differentially expressed in cultures treated with O4 in the absence of serum compared to cultures treated with control IgM (245 upregulated, 14 downregulated; analysed by one-way ANOVA; fold-change ≥ ±2.0; FDR-adjusted $p \leq 0.05$; n = 3; Appendix 8.1). No significant difference was observed between untreated and IgM control-treated cultures (Hayden et al. 2020; Semenoff 2014).

Pathway analysis of these differentially expressed genes (DEGs) was performed using DAVID (Database for Annotation, Visualisation and Integrated Discovery) (Huang da, Sherman, and Lempicki 2009), identifying functional annotation terms associated with the DEGs using gene ontology (GO), KEGG, and Reactome databases. *p* - values for enrichment scores were adjusted using Bonferroni post

Table 3.1: Gene ontology (GO) analysis of genes differentially regulated by O4

BIOLOGICAL PROCESSES			
GO term	**Count**	***q*-value**	**Enrichment**
Inflammatory response	38	2.7E-23	10.2
Defense response to virus	23	5.4E-16	14.4
Immune response	29	5.2E-15	8.7
Response to virus	19	1.0E-14	18.6
Innate immune response	28	3.1E-14	8.6
Cellular response to tumor necrosis factor	21	3.3E-13	12.6
Cellular response to interferon-gamma	16	9.8E-13	21.0
Response to lipopolysaccharide	27	2.0E-12	7.7
Neutrophil chemotaxis	15	1.3E-11	20.7
Cellular response to interleukin-1	17	1.1E-10	13.9
Chemokine-mediated signalling pathway	14	2.6E-10	19.7
Cellular response to lipopolysachharide	20	4.0E-10	9.6
Negative regulation of viral genome replication	11	2.6E-9	29.4
Positive regulation of ERK1 and ERK2 cascade	20	2.8E-9	8.6
Positive regulation of tumor necrosis factor production	13	5.1E-9	18.6
Defense response	12	1.9E-8	20.0
Lymphocyte chemotaxis	9	2.0E-7	32.8
Cellular response to interferon-beta	10	4.7E-7	22.9
Lipopolysaccharide-mediated signalling pathway	9	4.6E-6	23.2
Monocyte chemotaxis	9	6.0E-6	22.5
Chemotaxis	11	8.9E-6	13.8
Response to interferon-gamma	8	7.6E-5	22.1

CELLULAR COMPONENT			
GO term	**Count**	***q*-value**	**Enrichment**
External side of plasma membrane	18	7.7E-6	5.4
Extracellular space	39	1.6E-5	2.4

MOLECULAR FUNCTION			
GO term	**Count**	***q*-value**	**Enrichment**
Chemokine activity	15	1.5E-15	33.4
CCR chemokine receptor binding	8	6.8E-7	33.7
Peptide antigen binding	9	5.2E-6	19.5
Double-stranded RNA binding	10	6.6E-5	11.6

Table 3.1: Gene ontology (GO) analysis of genes differentially regulated by O4. Table showing GO analysis of genes differentially regulated by O4 (259 transcripts, fold change ≥2, $p < 0.05$). Count = number genes in dataset associated with that term, q – value = Bonferroni adjusted p – value, n = 3.

hoc test to account for multiple comparisons. Only annotation terms with an adjusted *p* – value (*q* – value) of < 0.0001 were shown.

3.2.1 Gene ontology analysis

GO analysis ("The Gene Ontology resource: enriching a GOld mine" 2021; Ashburner et al. 2000) identifies functional terms that are over-represented in a dataset compared to their normal frequency in the genome. These terms include biological processes and molecular functions that might be enriched in a condition, as well as the cellular locations where the DEGs execute their function.

Twenty-two biological processes were enriched with O4-treatment ($p < 0.0001$), all of which were related to immune, inflammatory and/or antiviral pathways. These included cellular response to interferon beta (IFN-ß) and gamma (IFN-γ), immune cell chemotaxis, and defence response to virus (Table 3.1). Cellular component analysis indicated that these biological processes occurred at the external side of the plasma membrane and/or within the extracellular space (Table 3.1). This emphasises the chemokine component of this response, with molecular functions “chemokine activity” and “CCR chemokine receptor binding” being highly enriched (enrichment score 33.4 and 33.7 respectively). Additionally, molecular functions relating to peptide antigen and dsRNA binding were enriched, suggesting the involvement of intracellular mechanisms relating to virus detection and antigen processing (Table 3.1).

These data support our proposal that myelinated cultures treated with O4 upregulate an innate immune signature which includes an antiviral component, supporting our hypothesis that lipid-reactive IgM elicits an antiviral response in the CNS.

3.2.2 KEGG and Reactome pathways

KEGG (Kanehisa and Goto 2000) and Reactome (Jassal et al. 2020) databases use knowledge of how different gene products interact, react, and relate to each other to suggest biological networks that could be enriched in a dataset. Examples of networks include metabolic, human disease, and cell signalling pathways.

Table 3.2: KEGG and Reactome analysis of genes differentially regulated by O4

KEGG PATHWAYS			
KEGG term	**Count**	***q*-value**	**Enrichment**
Herpes simplex infection	28	9.1E-14	7.2
Influenza A	24	3.1E-12	7.8
Phagosome	25	4.7E-12	7.2
Chemokine signalling pathway	22	5.6E-10	6.9
Antigen processing and presentation	17	1.5E-9	9.7
Legionellosis	14	1.9E-9	13.6
Cell adhesion molecules (CAMs)	21	2.8E-9	6.8
Viral myocarditis	16	6.0E-9	9.8
Graft-versus-host disease	14	1.4E-8	11.7
NOD-like receptor signalling	13	3.3E-8	12.6
Cytokine-cytokine receptor interaction	21	4.0E-8	5.8
Rheumatoid arthritis	15	7.1E-8	9.2
Type I diabetes mellitus	14	9.0E-8	10.2
TNF signalling pathway	16	9.9E-8	8.1
Toll-like receptor signalling pathway	15	2.0E-7	8.6
Cytosolic DNA-sensing pathway	12	4.3E-7	11.9
Staphylococcus aureus infection	11	4.2E-6	11.3
Allograft rejection	12	5.0E-6	9.5
Leishmaniasis	12	6.8E-6	9.2
NF-kappa B signalling pathway	13	6.9E-6	8.1
Epstein-Barr virus infection	16	7.1E-6	6.0
Autoimmune thyroid disease	12	1.4E-5	8.6
Tuberculosis	17	1.8E-5	5.2
Pertussis	11	8.1E-5	8.3

REACTOME PATHWAYS			
Reactome term	**Count**	***q*-value**	**Enrichment**
Immunoregulatory interactions between a lymphoid and a non-lymphoid cell	18	4.3E-10	9.6
Chemokine receptors bind chemokines	13	2.8E-9	15.7
Antigen Presentation: Folding, assembly and peptide loading of class I MHC	11	5.3E-7	14.1

Table 3.2: KEGG and Reactome analysis of genes differentially regulated by O4.

Table showing KEGG and Reactome analysis of genes differentially regulated by O4 (259 transcripts, fold change ≥2, $p < 0.05$). Count = number genes in dataset associated with that term, q – value = Bonferroni adjusted p – value, n = 3.

Analysis of KEGG pathways enriched with O4-treatment showed a high proportion of human disease pathways that included viral diseases such as herpes simplex virus (HSV), influenza A, and Epstein-Barr virus infection (Table 3.2). Many autoimmune disease pathways were also enriched as well as various immune response pathways such as antigen presentation, NOD-like receptor signalling, TLR signalling, and cytosolic DNA sensing pathways, all of which are associated with immune defence against pathogens (Table 3.2).

These results imply that O4 stimulates a broad immune response with an antiviral component in myelinated cultures. This finding was reiterated in Reactome analysis which identified significant enrichment in immunoregulatory interactions between lymphoid and non-lymphoid cells, chemokine receptor binding, and antigen presentation (Table 3.2).

3.2.3 Functional annotation clustering

GO, KEGG, and Reactome analysis identified a plethora of interdependent immune pathways and terms that were enriched following O4-treatment. To condense these results, counteracting the redundancy of multiple related terms, functional annotation clustering was performed. This tool combines data obtained from GO, KEGG, and Reactome analyses, as well as analysis of protein domains using databases such as InterPro (Hunter et al. 2009; Lund et al. 2004) and SMART (J. Schultz et al. 1998), to group similar annotation terms together into clusters.

Functional annotation clustering identified 13 significantly enriched clusters in O4-treated cultures ($p < 0.05$) (Fig 3.1). The four most highly enriched clusters represent major immunological processes: innate immunity, viral defence, inflammatory response, and antigen presentation by MHC class I. Other clusters identified in this analysis represent pathways embedded within these broader immunological processes. For example, response to IFN-β and dsRNA binding are key viral defence pathways (Friedman 1970; Baltimore 1971), and the CCR and CXCR3 chemokine families contribute to innate immunity and inflammatory responses. For a full list of genes and functional annotation terms associated with each cluster, see Appendix 8.2.

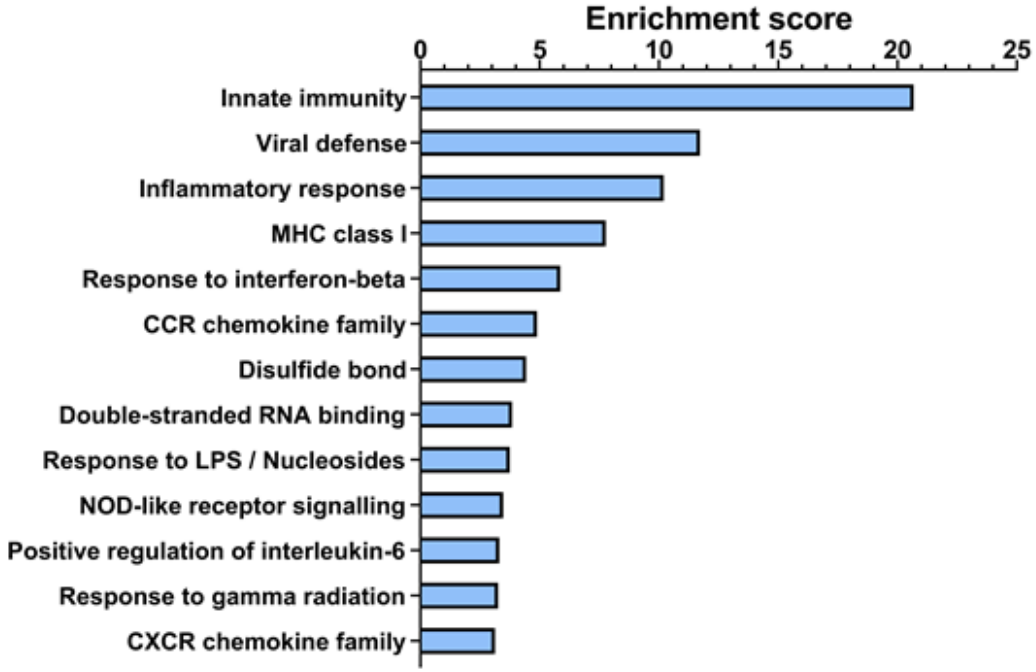

Figure 3.1 Functional annotation clustering of genes differentially expressed by O4. Graph showing functional annotation clusters significantly enriched in O4-treated CNS cultures. Data presented as enrichment score. All clusters enriched with a *p*-value of < 0.05 are displayed. *p*-value adjusted using Bonferroni post *hoc* test to account for multiple comparisons. n = 3.

Although DAVID defines these processes as distinct clusters, there is a clear functional connection between these terms. Consequently, there is substantial overlap between genes associated with each of these clusters. Within the first four clusters, 145 DEGs are represented (56 % of total DEGs), and a third of these are present in two or more of the clusters (Fig 3.2). The proportion genes associated with these clusters increases as we focus on the top 50 transcripts upregulated by O4, where 74 % of transcripts are associated with at least one of the four clusters (Fig 3.3). This indicates that this broad immunological response is a dominant transcriptional feature in O4-treated cultures.

Of the remaining 9 clusters enriched in this analysis, several are associated with viral defence including response to IFN-β, dsRNA binding, response to nucleosides, and NOD-like receptor signalling (Friedman 1970; Baltimore 1971; Allen et al. 2009; Schaeffer et al. 1978). Detailed representations of genes and annotation terms associated with clusters "response to IFN-β" and "dsRNA binding" are found in Fig 3.4 a & b, with reference to intracellular innate antiviral processes such as GTPase activity, nucleoside triphosphate hydrolase, and 2'-5'-oligoadenylate synthetase activity (Cheng, Colonno, and Yin 1983; MacDonald et al. 2013; Rutherford, Hannigan, and Williams 1988). Genes associated with these clusters include *Mx1*, *Oasl*, *Tlr3* and *Gbp1* (Fig 3.4 a & b).

Chemokine signalling is another prominent feature of this analysis, with enrichment of genes encoding ligands for CCR and CXCR chemokine families including *Ccl5*, *Ccl7*, *Cxcl10* and *Cxcl11* (Fig 3.4 c & d). In fact, four of the five genes most upregulated by O4 encode ligands for CXCR3, indicating that this chemokine response is robustly upregulated by O4 at the transcriptional level (Fig 3.3). Although chemokine signalling is complex and *in vivo* studies would be required to determine the functional outcome of this response, these analyses suggest O4 could induce or enhance lymphocyte, monocyte, and/or eosinophil chemotaxis to the CNS (Fig 3.4 c).

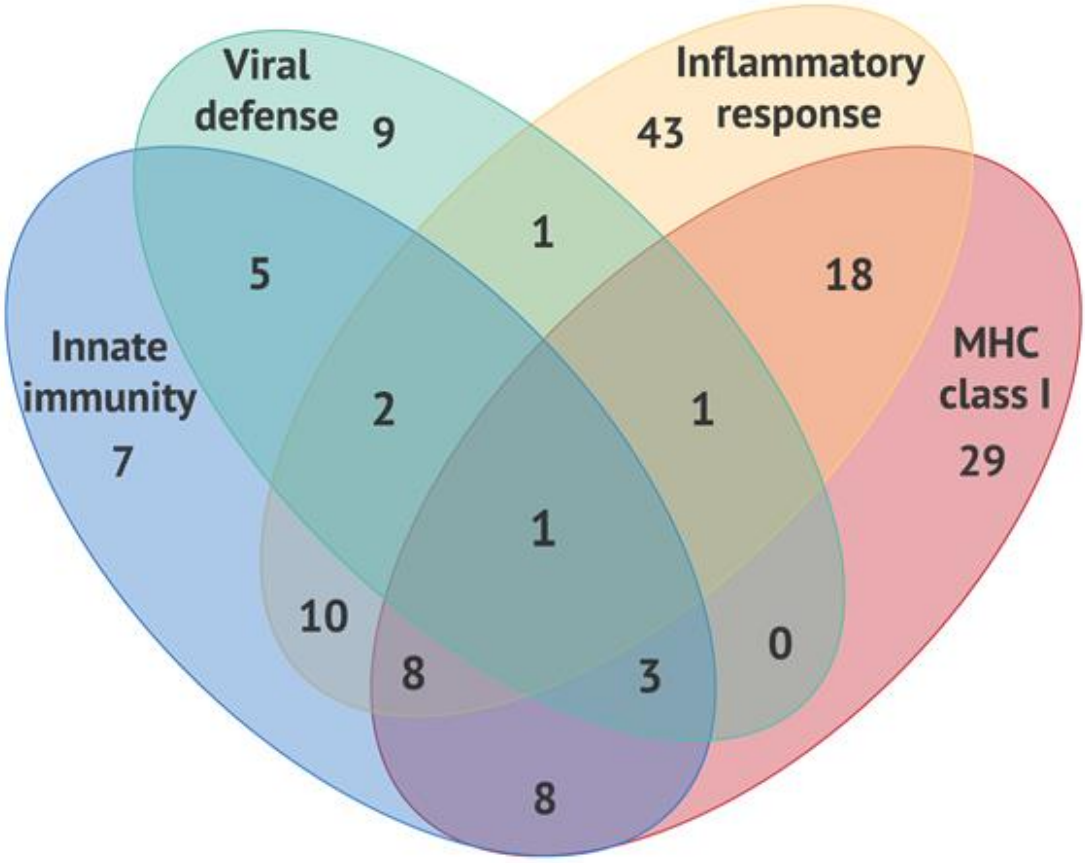

Figure 3.2 Interdependent relationship between clusters 1-4 of functional cluster analysis. Four-set Venn diagram showing the four clusters most enriched by O4. Numbers indicate number of genes in each subset. n = 3.

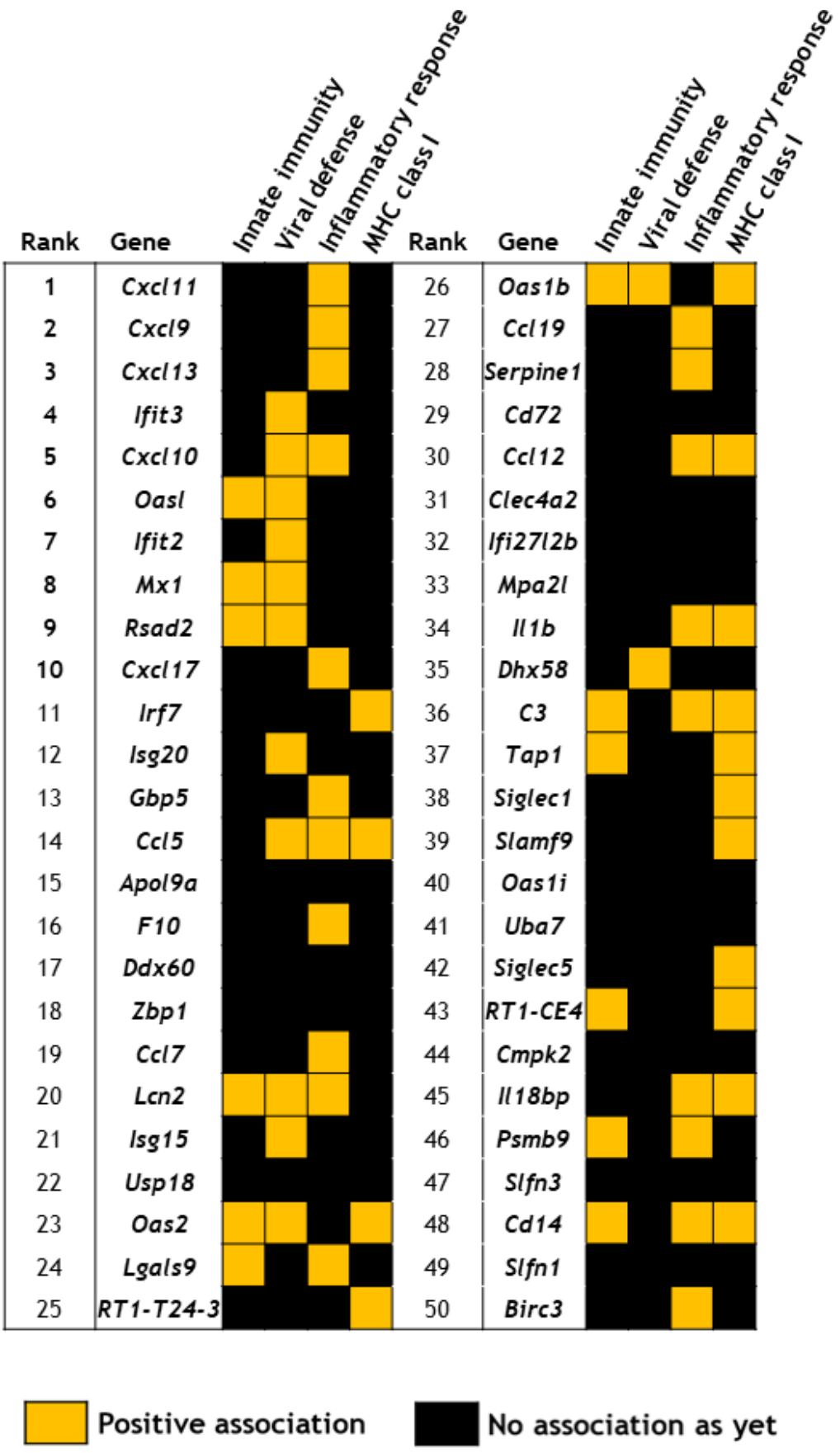

Figure 3.3 Association of genes upregulated by O4 with clusters 1-4 of functional annotation cluster analysis. Gold squares indicate gene is associated with cluster, black squares indicate no known association as yet between gene and cluster. Genes displayed in order of most upregulated. n = 3.

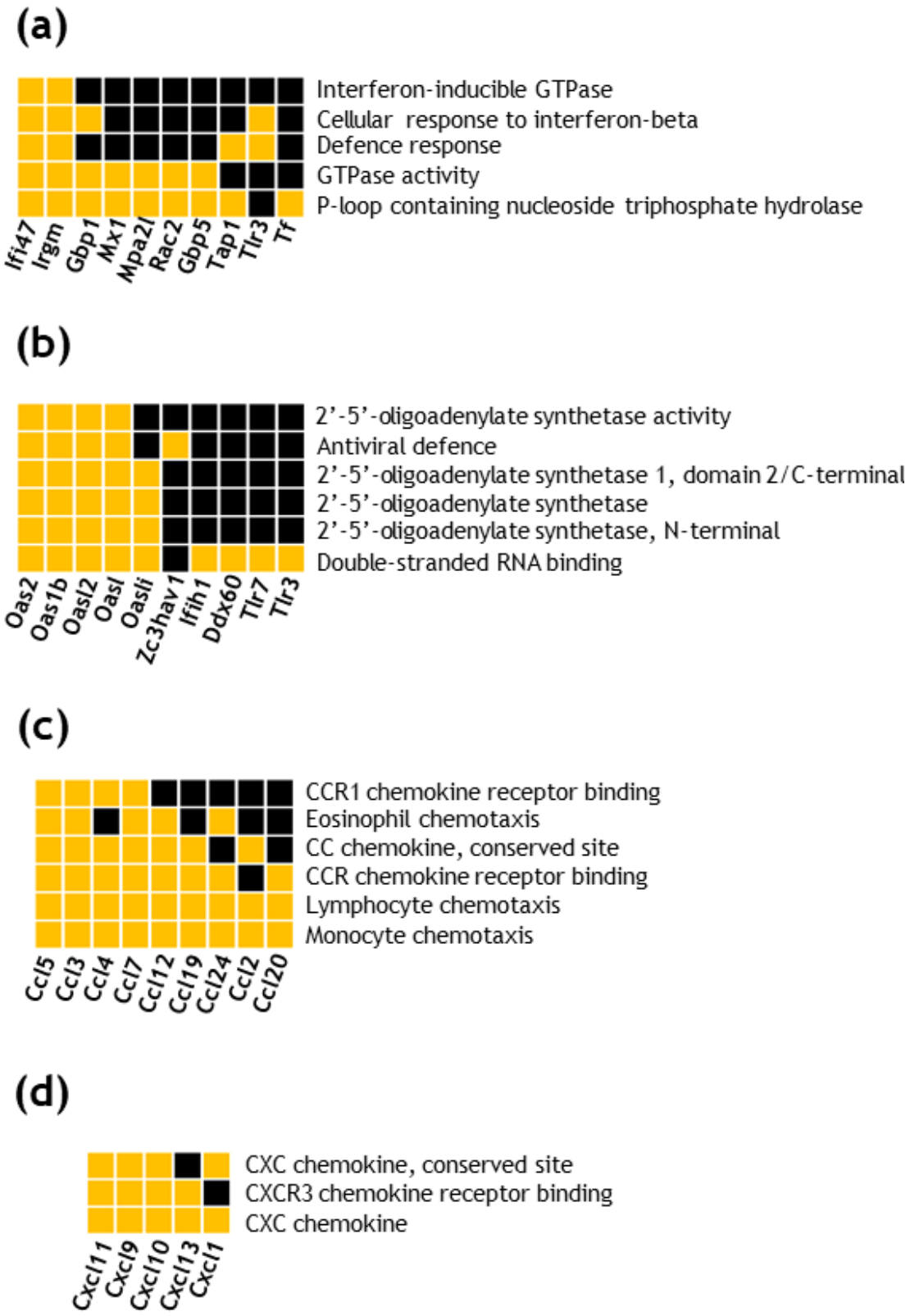

Figure 3.4 Functional annotation clustering of genes differentially expressed by O4, antiviral and chemokine clusters. Heatmaps showing genes and annotation terms associated with (a) "response to interferon-beta" and (b) "double-stranded RNA binding" (c) "CCR" and (d) "CXCR" chemokine families. Gold squares indicate positive association between gene and annotation term. Black squares indicate no association reported as yet. Annotation terms show were enriched by a Bonferroni adjusted *p*-value of < 0.05. n = 3.

3.3 O4 transcriptional signature associated with IFN signalling

As our original hypothesis was that lipid-reactive IgMs induce antiviral activity within the CNS, we investigated the virus-specific aspect of this transcriptional response. Considering the most enriched antiviral cluster in our dataset after "response to virus" was "cellular response to IFN-ß", and remaining enriched antiviral clusters are known to be upregulated by IFN-ß (Cheng, Colonno, and Yin 1983; Rutherford, Hannigan, and Williams 1988), we decided to analyse our data using the Interferome v2.01 database (Rusinova et al. 2013).

3.3.1 Interferome analysis

Interferome is a database containing genes up- and down- regulated by type-I, -II, and -III IFN's, reliably identifying genes or gene signatures in a dataset that are regulated by these IFN's. As IFN responses can vary depending on tissue type, we compared our DEGs to Interferome data derived from murine nervous system tissue only.

A total of 155 genes from our dataset were identified as IFN-regulated, accounting for ~62 % of DEGs in O4-treated cultures (Appendix 8.3). Of these 155 transcripts, 108 were specific to the IFN-I response whilst 46 had a shared association with the IFN-II pathway (Fig 3.5 a). Only one transcript (*Apol9a*) was specific to the IFN-II response (Appendix 8.3), whilst no genes relating to IFN-III were identified (Fig 3.5 a). The proportion of ISGs increases dramatically if we focus on the 20 transcripts most highly upregulated by O4, 18 of which (90 %) were identified as IFN-regulated (Fig 3.5 b).

These data suggest that the co-ordinated immune signature observed in O4-treated cultures could involve, or even be mediated by, IFN signalling. The IFN response is a well-known innate antiviral immune pathway, further supporting the idea that lipid-specific IgM may have antiviral properties in the CNS (Friedman 1970).

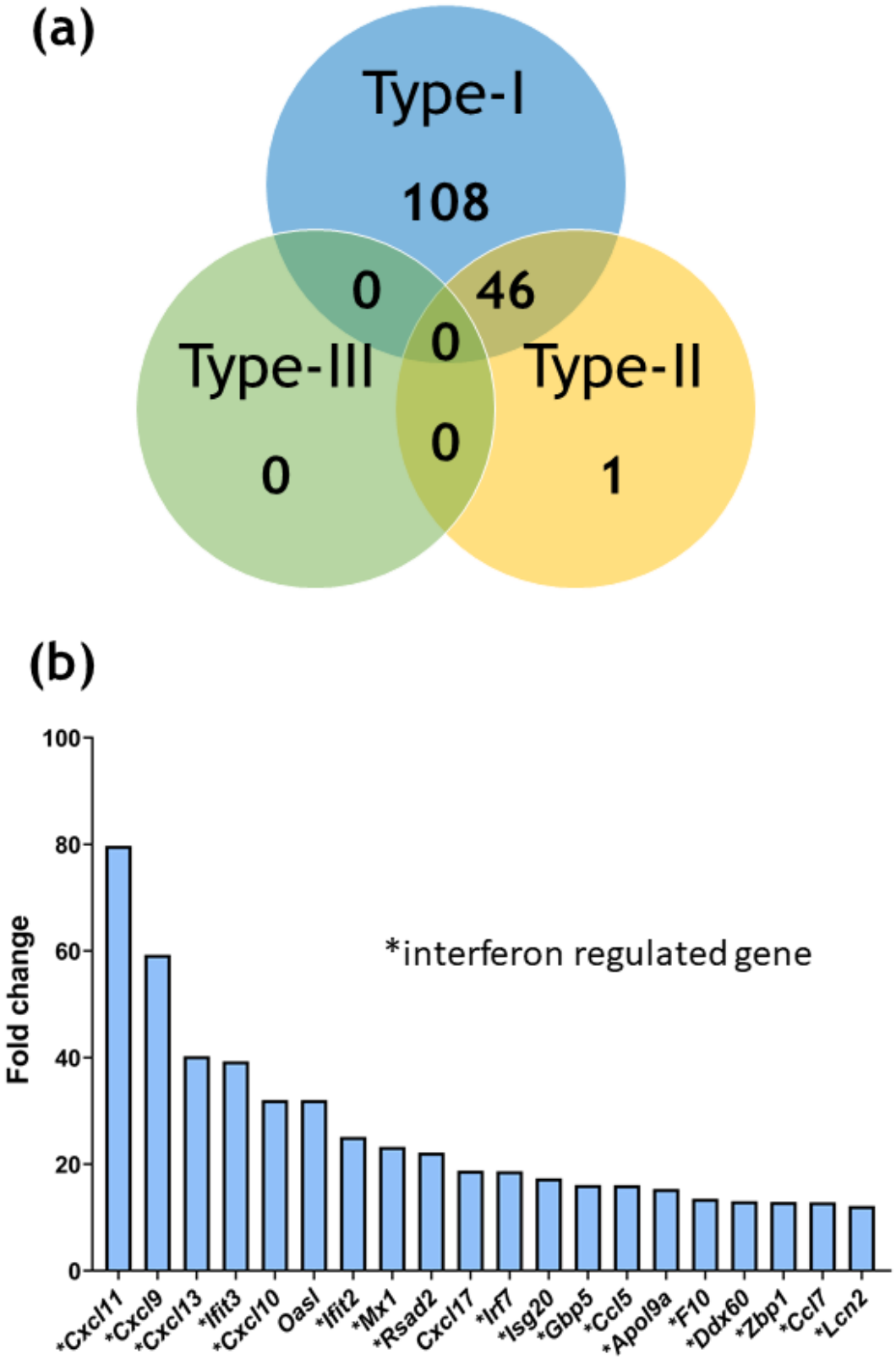

Figure 3.5 Interferome analysis of genes differentially expressed by O4. (a) Venn diagram showing number of genes differentially expressed by O4 identified as interferon regulated genes. Numbers within areas in Venn diagram represent number of genes specific to each interferon type or those which overlap between interferons. (b) Graph showing genes most upregulated by O4. Data presented as fold change. * denotes interferon regulated gene. n = 3.

3.4 Antibody-mediated demyelination attenuates O4-induced ISG signature

Myelinated cultures maintained in serum-free media model the CNS milieu under homeostatic conditions, where the BBB is intact and serum protein leakage into the parenchyma is limited. In MS, the BBB is more permissive to serum protein leakage and immune cell infiltration. Although lipid-reactive IgM might elicit an antiviral response under homeostatic conditions, the presence of serum proteins such as complement could alter this mechanism, leading to complement-dependent antibody-mediated demyelination. Therefore, to model the effect of BBB leakage on cells of the CNS, rat myelinated cultures were treated for 24 hrs with 2 % rat serum in the presence or absence of O4, and transcription analysed by microarray (Hayden et al. 2020; Semenoff 2014).

3.4.1 Serum induces inflammatory signature in myelinated cultures

Although serum alone causes no overt demyelination or axonal loss in myelinated cultures (Elliott et al. 2012; Semenoff 2014), 282 genes were differentially expressed in serum-treated cultures compared to untreated controls (221 upregulated, 61 downregulated; analysed by one-way ANOVA; fold-change ≥ ±2.0; FDR-adjusted $p \leq 0.05$; Appendix 8.4).

Pathway analysis identified multiple GO biological processes related to inflammation including cellular responses to interleukin-1, TNF, IFN-γ, lipopolysaccharide, and organic cyclic compounds, as well as pathways related to migration and recruitment of lymphocytes, monocytes, and neutrophils (Table 3.3). This association with cytokines was repeatedly observed throughout the analysis, with chemokine receptor signalling represented in GO molecular function, KEGG, and Reactome analyses, and cytokine/TNF signalling observed in KEGG analysis (Table 3.3).

The only significantly enriched cellular component was “extracellular space”, reiterating the robust upregulation of cytokines and chemokines with serum treatment (Table 3.3). Compared to the transcriptional signature observed in O4-treated cultures, there was a lack of antiviral processes and pathways such as

Table 3.3: GO, KEGG and Reactome analysis of serum-treated myelinated cultures

BIOLOGICAL PROCESSES			
GO term	**Count**	***q*-value**	**Enrichment**
Response to lipopolysaccharide	35	1.4E-18	8.6
Inflammatory response	33	9.0E-16	7.7
Response to virus	19	2.0E-13	16.0
Cellular response to interleukin-1	19	5.4E-12	13.4
Cellular response to tumor necrosis factor	21	8.3E-12	10.9
Chemokine-mediated signalling pathway	15	9.4E-11	18.2
Neutrophil chemotaxis	15	1.2E-10	17.9
Cellular response to interferon-gamma	14	5.5E-9	15.8
Cellular response to lipopolysaccharide	20	7.0E-9	8.3
Monocyte chemotaxis	11	2.9E-8	23.7
Defense response to virus	17	8.7E-8	9.2
Positive regulation of ERK1 and ERK2 cascade	19	3.9E-7	7.1
Lymphocyte chemotaxis	9	8.1E-7	28.2
Innate immune response	21	2.5E-6	5.6
Immune response	21	3.6E-6	5.4
Cellular response to organic cyclic compound	15	4.5E-6	41.4

CELLULAR COMPONENT			
GO term	**Count**	***q*-value**	**Enrichment**
Extracellular space	66	2.5E-17	3.5

MOLECULAR FUNCTION			
GO term	**Count**	***q*-value**	**Enrichment**
Chemokine activity	16	1.6E-16	31.9
CCR chemokine receptor binding	8	1.8E-6	30.2

KEGG PATHWAYS			
KEGG term	**Count**	***q*-value**	**Enrichment**
Cytokine-cytokine receptor interaction	24	1.3E-10	6.6
TNF signalling pathway	18	1.3E-9	9.1
Chemokine signalling pathway	19	4.1E-7	5.9

REACTOME PATHWAYS			
Reactome term	**Count**	***q*-value**	**Enrichment**
Chemokine receptors bind chemokines	13	1.3E-8	13.9
G alpha (i) signalling events	20	6.9E-7	5.4

Table 3.3 GO, KEGG and Reactome analysis of serum-treated myelinated cultures. Table showing GO, KEGG and Reactome analysis of genes differentially expressed in serum-treated myelinated cultures compared to untreated controls. Count = number genes in dataset associated with that term, *q* – value = Bonferroni adjusted *p* – value.

cellular response to IFN-β (GO biological processes), dsRNA binding (GO molecular function), and viral disease pathways (KEGG).

These data indicate that exposure of myelinated cultures to serum, modelling BBB permeability, induces a robust inflammatory signature without causing overt cellular damage. Unlike the broad, multifaceted immune signature induced by O4, the serum-induced biological response was dominated by cytokines.

3.4.2 Combination of serum and O4 leads to downregulation of homeostatic myelin-associated genes

Cultures which undergo demyelination due to treatment with O4 and serum have only 15 DEGs compared to cultures treated with serum alone (4 upregulated, 11 downregulated; analysed by one-way ANOVA; fold-change ≥ ±2.0; FDR-adjusted $p \leq 0.05$; Table 3.4). Analysis of these DEGs using DAVID identified one functional annotation term that was significantly enriched, the GO cellular component term "myelin sheath" ($p < 0.05$). This indicates that the inflammatory signature observed in cultures treated with serum alone persists in cultures treated with O4 and serum. In other words, the same inflammatory genes were expressed in both the serum only cultures and cultures treated with O4 and serum. The only difference between serum-treated cultures and those treated with O4 and serum, is that the lipid-specific IgM now binds to the myelin sheath in combination with serum complement, leading to antibody-mediated demyelination.

The genes downregulated in cultures treated with O4 in combination with serum are known for their involvement in myelination (*Fa2h*, *Myrf*, *Mag*, *Mog*), oligodendrocyte maturation (*Zfp488*), neurite outgrowth (*Plxnb3*) and cell proliferation (*Tgm1*) (Table 3.4), suggesting that the destruction of myelin leads to a decrease in expression of genes relating to myelin integrity. It can therefore be postulated that in the context of BBB permeability, leakage of serum complement into the parenchyma facilitates antibody-mediated demyelination. This provides evidence for the more aggressive MS disease course associated with intrathecal lipid-specific IgM.

Table 3.4: Genes differentially regulated by O4 in the presence of serum.

Gene name	Gene Symbol	*q*-value	Fold change
Sialic acid binding Ig-like lectin 5	*Siglec5*	0.0116	5.46
C-type lectin domain family 4, member A2	*Clec4a2*	0.0448	2.92
Toll-like receptor 5	*Tlr5*	0.0473	2.13
Immunoresponsive gene 1	*Irg1*	0.0397	2.05
MAP6 domain containing 1	*Map6d1*	0.0005	-2.02
Zinc finger protein 488	*Zfp488*	0.0412	-2.12
Fatty acid 2-hydroxylase	*Fa2h*	0.0001	-2.25
Myelin regulatory factor	*Myrf*	0.0448	-2.26
UDP glycosyltransferase 8	*Ugt8*	0.0006	-2.33
Plexin B3	*Plxnb3*	0.0003	-2.34
Claudin 11	*Cldn11*	0.0363	-2.42
MicroRNA mir-2964	*Mir2964*	0.0192	-2.71
Myelin-associated glycoprotein	*Mag*	0.0002	-3.00
Myelin oligodendrocyte glycoprotein	*Mog*	0.0090	-3.17
Transglutaminase 1	*Tgm1*	0.0377	-3.24

Table 3.4 Genes differentially regulated by O4 in the presence of serum. Table showing genes differentially expressed in myelinated cultures treated with O4 and serum compared to serum only control. Data analysed by one-way ANOVA, p – value adjusted by FDR to account for multiple comparisons (q – value). Showing all genes differentially expressed by fold change ≥ ±2, $q < 0.05$, n = 3.

3.4.3 O4-induced IFN signature is attenuated in the presence of serum

To determine whether the O4-induced IFN signature is retained or altered in the presence of serum, genes differentially expressed in cultures treated with O4 and serum compared to untreated controls were analysed using Interferome. As the original microarray did not directly compare cultures treated with O4 and serum to untreated controls, DEGs from serum-treated cultures were combined with DEGs from cultures treated with O4 and serum to make a complete gene list.

Of the 289 DEGs, 107 (~37 %) were identified as IFN-regulated, almost half that was observed in O4-treated cultures (Appendix 8.5). This indicates that O4-induced ISG expression is attenuated when the IgM is combined with serum. Of the 107 transcripts, 75 were specific to the IFN-I response and 29 were regulated by IFN-I and IFN-II. Three transcripts were specific to the IFN-II response whilst no transcripts were associated with IFN-III (Appendix 8.5).

3.5 Discussion

The data presented in this chapter provides an updated *in silico* analysis of the transcriptional response observed in rat myelinated cultures treated with O4 in the presence and absence of serum. Treatment with O4 alone induced a broad immune transcriptional signature with a significant antiviral component and upregulation of ISGs. In contrast, serum treatment induced an inflammatory signature dominated by cytokines, and in combination with O4, led to phenotypic demyelination and downregulation of myelin-specific genes. Furthermore, the O4-induced IFN signature is attenuated in the presence of serum, indicating that the antiviral effects of lipid-specific IgM might be lost in the event of BBB breakdown. These data provide *in silico* evidence for the clinical observation that MS patients positive for intrathecal lipid-specific IgM have reduced risk of developing PML but a more aggressive disease course.

Although *in silico* analysis had been performed on this dataset previously, pathway analysis tools have become more advanced in the last 7 years

(Semenoff 2014). Previous analysis produced vast lists of genes with their associated KEGG and GO annotation terms. The sheer volume of data could make interpretation of results difficult and could lead to bias with researchers often focusing on genes that they believe to be most relevant to their hypothesis. The analysis presented in the current thesis utilised functional annotation clustering whereby the numerous lists of genes and annotation terms, created by multiple different pathway analysis software, were combined to produce a concise list of key pathways that were upregulated in this dataset. This condensation of results highlighted the multifaceted nature of the lipid-reactive IgM response. This contrasts with the original analysis which focused predominantly on the antiviral component of the response with little mention of other key processes including innate immunity, inflammatory response, and antigen presentation by MHC class I (Semenoff 2014). That being said, it is evident from the current analysis that antiviral immunity is a strong theme across the dataset.

All functional annotation clusters identified in O4-treated cultures contained genes regulated by IFN's, the principle antiviral cytokines of the innate immune system. Cellular response to IFN-β (Isaacs and Lindenmann 1957) and dsRNA binding (Baltimore 1971) are classical antiviral pathways, with associated genes encoding proteins that directly inhibit viral replication/transmission within the infected cell. These include genes involved in dsRNA binding (*Ddx60*), viral RNA degradation (*Zc3hav1*), inhibition of viral genome transcription (*Mx1*, *Ifi47*, *Irgm*, *Gbp1*, *Rac2*), and numerous members of the OAS family which activate RNASEL to prevent the translation of viral protein (*Oas2*, *Oas1b*, *Oasl2*, *Oasli*) (Miyashita et al. 2011; Guo et al. 2007; Horisberger et al. 1990; Gilly, Damore, and Wall 1996; Henry et al. 2009; Staeheli et al. 1984; Castelli, Wood, and Youle 1998).

Chemotactic cytokines are known to recruit peripheral immune cells to the site of inflammation (Oppenheim et al. 1991). CCR and CXCR chemokine families were identified in cluster analysis, with specific enrichment of genes encoding chemokine ligands for CCR1 and CXCR3.

CXCR3 is expressed on natural killer (NK) cells (S. Qin, Rottman, et al. 1998), B cells (Muehlinghaus et al. 2005), and $CD4^+$/$CD8^+$ T-cells (Loetscher et al. 1996), all of which migrate to the CNS during virus infection (Thapa et al. 2008; Marques et al. 2011; Hsieh et al. 2006; B. Zhang et al. 2008; Lokensgard et al.

2016; Mirones et al. 2013; M.T. Liu et al. 2000; Phares et al. 2013). CCR1 is expressed by neutrophils (Combadiere, Ahuja, and Murphy 1995), DCs (Rose et al. 2010), eosinophils (Post et al. 1995), and basophils (Uguccioni et al. 1997), but there are few reports on CCR1-dependent leukocyte chemotaxis to the CNS during viral infection. Chemokine ligands are notoriously promiscuous, with CCR1 ligands CCL3, 5 and 7 also known to interact with CCR3, 4 and 5. Therefore, it is difficult to postulate the role of upregulated CC ligands without *in vivo* experimentation.

Chemokines also have local functions within the CNS. CCR1 and its ligands have undetectable levels of mRNA and protein in healthy homeostatic mouse and human brains (Halks-Miller et al. 2003; Eltayeb et al. 2007), but both receptor and ligands are increased in the CNS during neurological disease including virus infection (Rottman et al. 2000; Sunnemark et al. 2003). *Ccr1*$^{-/-}$ mice were more susceptible to neurotropic coronavirus infection, and CCL5 offered protection to neurons during HIV-1 infection (Dedoni et al. 2018; Hickey et al. 2007). The mechanism of this protection is not well understood but could involve T cell recruitment (Dedoni et al. 2018).

CXCR3 is expressed on mouse and human astrocytes, neurons, oligodendrocytes, and microglia (Biber et al. 2002; Xia et al. 2000; Bhangoo et al. 2007; Omari et al. 2005; Goldberg et al. 2001). Its main ligands are CXCL9 and 10, for which protein expression is increased in the CNS during virus infection, with astrocytes identified as the dominant producers of CXCL10 and microglia upregulating CXCL9 (van Marle et al. 2004; Mehla et al. 2012; Hofer et al. 2008). However, whether the production of CXC chemokine ligands is beneficial or detrimental most likely depends on the virus in question. *Cxcr3* deficiency had no effect on lymphocytic choriomeningitis virus (LCMV) or Borna virus infection, nor did it affect neurological sequalae. In contrast, *Cxcr3*$^{-/-}$ mice cleared HSV infection more rapidly than WT, with improved clinical course and reduced microglial activation (Hausmann et al. 2004; Hofer et al. 2008; Zimmermann et al. 2017). Additionally, during HIV-1 infection astrocytic CXCL10 acts synergistically with HIV-1 protein Nef to induce neurotoxicity (van Marle et al. 2004; Mehla et al. 2012). Therefore, although CXCR3 signalling is associated with viral infection, its requirement for proposed O4-mediated viral protection is unclear.

Innate immune signalling pathways were also enriched in cultures treated with O4, including response to organic cyclic compound, NOD-like receptor signalling, and cellular response to interleukin-6 (IL-6). The term “organic cyclic compound” is broad, but contained within this group are terms such as cellular response to dsDNA, RNA, and other purine-containing compounds, all of which are upregulated in response to virus (Baltimore 1971). NOD-like receptors are upregulated by cytokines such as IFN-γ and TNF-α (Hisamatsu, Suzuki, and Podolsky 2003; Rosenstiel et al. 2003), and stimulate NFκB and IRF-dependent signalling or induce inflammasome formation, aligning with the IFN signature of O4 (D.W. Abbott et al. 2004; Sabbah et al. 2009; Martinon, Burns, and Tschopp 2002). IL-6 is linked to inflammation in human disease and is upregulated in response to pathogens, including viruses (Sehgal et al. 1988).

MHC class I molecules present endogenous antigen to $CD8^+$ T cells during both virus infection and autoimmunity (Burgert and Kvist 1985; Grumet et al. 1971). Genes common to almost all GO/KEGG terms in this cluster were MHC class I loci including *RT1-T24-3*, *RT1-CE1*, *RT1-Ba*, *RT1-Da*, *RT1-M3-1* and *RT1-N2*. Other genes in this cluster were related to virus-mediated diseases rather than diseases associated with autoimmunity e.g. *Irf7*, *Relb* and *Nfkb2* (Nonkwelo, Ruf, and Sample 1997; Ning, Pagano, and Barber 2011; Weih et al. 1997; Roulston et al. 1993; Wirasinha et al. 2021).

This combination of functional annotation clusters enriched in cultures treated with O4 alone depict a broad, multifaceted immune signature with a clear antiviral component. In contrast, cultures treated with O4 in presence of serum lose this antiviral component, with the dominant transcriptional feature being the inflammatory response upregulated by serum proteins.

As serum leakage across the BBB is usually accompanied by immune cell infiltration and pre-existing damage within the CNS, there have been few studies on the effect of serum complement alone on naïve cells of the CNS (Cyong et al. 1982; Vanguri and Shin 1986; Scolding et al. 1989; Wren and Noble 1989). That said, studies have shown that both purified myelin and primary myelinating oligodendrocytes can activate the complement system in a C1-dependent manner (Cyong et al. 1982; Vanguri and Shin 1986; Scolding et al. 1989). This complement activation did not require myelin-specific antibody (Cyong et al.

1982; Scolding et al. 1989) and led to the cleavage of C3 and C5, producing smaller peptides with proinflammatory properties (Vanguri and Shin 1986; Wren and Noble 1989).

Cleavage products C3a and C5a have been shown to alter microglial and astrocytic signalling, upregulating proinflammatory molecules including IL-6, IL-8 and prostaglandins, and polarising microglia towards a reactive phenotype (Möller et al. 1997; Sayah et al. 1999; Jauneau et al. 2003; Blatteis et al. 2004; J. Li et al. 2020; L.Y. Zhang et al. 2020). *C3ar* deficiency has been shown to limit CNS damage in the context of several models of neurological disease including EAE (Boos et al. 2004), experimental lupus (Jacob et al. 2010), and chronic cerebral hypoperfusion (L.Y. Zhang et al. 2020).

Given the lack of damage observed in cultures treated with O4 alone and the evidence of complement contributing to CNS damage, it can be postulated that serum proteins facilitate O4-mediated demyelination by complement-dependent cytotoxicity. This is of particular importance as IFN's can also be upregulated in response to cell damage. However, in the context of O4-treatment, IFN expression does not correlate with cell damage, indicating that IFN expression in cultures treated with O4 alone is not due to a damage response, but a separate antiviral mechanism.

As there is clinical evidence for both the antiviral properties and demyelinating effects of lipid-specific IgM, it is likely that the situation in MS patients is a balancing act between the two functions of these antibodies. MS patients with no active demyelinating lesions, such as those in remission or with progressive forms of disease, have improved BBB integrity compared to those undergoing a relapsing event (Silver et al. 2001). Therefore, it is possible that during relapse the presence of lipid-specific IgM exacerbates damage in the CNS, but when the patient is in remission or in progressive stage of disease, the IgM provides protection against neurotropic viruses such as JCV.

The conditions used in this study might represent two extreme examples of the CNS milieu, one with absolute BBB integrity, and one with a sudden massive influx of serum protein, modelling acute disease such as traumatic brain injury or stroke. Although the current study, and those conducted previously by other research groups, have shown very different functions of lipid-reactive IgM, a

logical explanation can be made for both the antiviral and demyelinating effects of lipid-reactive IgM from this *in silico* data.

The remainder of this thesis will focus on the antiviral properties of lipid-reactive IgM. First and foremost, the validity of the above *in silico* data will be examined using RT-qPCR and the dependence of this antiviral response on the IFN-I pathway will be assessed. Depending on RT-qPCR validation, this thesis will proceed to explore the mechanism of action of this response and its efficacy during neurotropic virus infection *in vitro*.

Chapter 4

O4 induces IFN-β-dependent ISG expression in all major cell-types of the CNS

4 O4 induces IFN-β-dependent ISG expression in all major cell-types of the CNS

4.1 Introduction

Transcriptomic analysis suggested that the lipid-reactive IgM O4 induces an antiviral response with characteristics of an IFN signature. The aims of the current chapter are to:

1. determine which IFN's mediate this response
2. characterise ISG upregulation by RT-qPCR and
3. identify the cell-types upregulating ISGs in response to O4 in myelinated cultures.

4.2 O4 upregulates *Ifnb1* in myelinated cultures

To determine the most appropriate endpoints for this analysis, rat myelinated cultures were treated with O4 for various durations over a period of 18 hrs and *Ifna4*, *Ifnb1*, and *Ifng* expression examined by RT-qPCR. At 4 hrs post-treatment, *Ifnb1* was upregulated ~ 100-fold compared to 0 hr control, increasing to ~ 200-fold by 8 hrs (Fig 4.1 a). *Ifng* and *Ifna4* expression remained close to baseline at all time-points suggesting that IFN-β is selectively upregulated by O4 (Fig 4.1 a).

Having established appropriate time-points to analyse IFN expression, the experiment was repeated to include untreated and IgM controls. *Ifnb1* expression was significantly increased at 4 ($p < 0.01$) and 8 hrs ($p < 0.0001$) post O4-treatment when compared to IgM and A4CD controls (Figure 4.1 b). *Ifnb1* expression was specific to O4, with no increase in *Ifnb1* expression in IgM- or A4CD-treated controls compared to untreated cultures. As A4CD was purified in the same manner as O4 and had no effect on IFN expression, all remaining experiments presented in this thesis used A4CD as the isotype control.

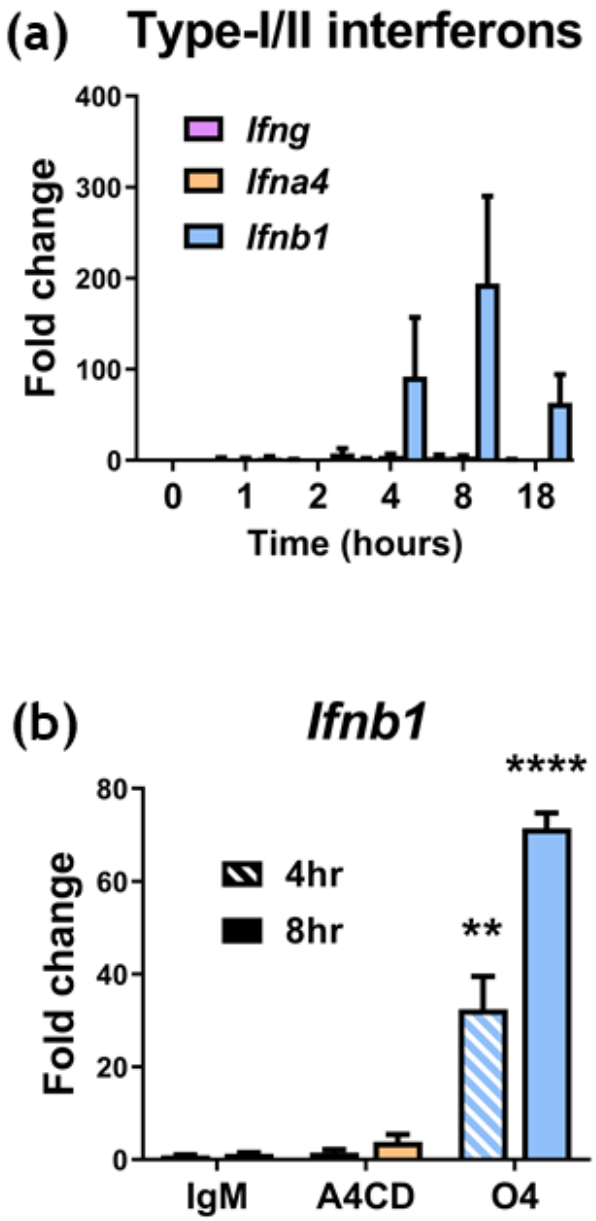

Figure 4.1 O4 upregulates *Ifnb1*, but not *Ifna4* or *Ifng*. Rat myelinated cultures treated for 0, 1, 2, 4, 8 or 18 hrs with O4 and analysed by RT-qPCR. **(a)** type-I and type-II interferon expression **(b)** *Ifnb1* expression at 4 and 8 hrs with IgM controls. Data expressed as mean fold change control ± SEM, all time-points and conditions (n=3).

4.3 ISGs are upregulated by O4 following *Ifnb1* induction

4.3.1 Time-course analysis of ISG expression in response to O4

If O4-induced IFN-ß expression leads to ISG production, one would expect to see ISG upregulation at a time-point after *Ifnb1* induction (Fig. 4.1 a). Using the same time-course samples described in Section 4.2, RT-qPCR was performed on a panel of ISG transcripts.

Eight genes were selected for an initial screen due to being highly upregulated in the aforementioned microarray analysis and for their variety of functions. Representing cytokines and chemokines were *Ccl5* and *Cxcl10*. *Mx1*, *Rsad2*, and *Ifit2* were selected as intracellular antiviral genes, each encoding proteins with different functions including degradation of viral genetic material (*Mx1*), perturbation of lipid rafts to prevent viral budding (*Rsad2*), and inhibition of viral mRNA transcription (*Ifit2*). *Isg15* and *Isg20* are antiviral enzymes which have been reported to be critical in BUNV and SFV infection respectively. ISG15 protein is involved in ubiquitination of other antiviral proteins whilst ISG20 is an exonuclease. No downregulated genes were selected as none were directly involved in antiviral immunity and the fold change observed in downregulated genes was relatively minor compared to the fold change observed in upregulated genes. The fold increase observed in upregulated genes examined ranged from ~ 12-fold to ~80-fold. Downregulated genes ranged in fold decrease from ~ 2 to ~3-fold.

Due to variability of the dataset, significance could not be determined from these data. As this experiment was one of the first performed by the author during this PhD project, variability is most likely due to inexperience with the techniques used combined with the natural biological variability of the myelinated culture system. That being said, a trend could still be observed in the dataset. To aid interpretation of the data, an arbitrary threshold of 20-fold increase compared to control was used to describe the dynamics of O4-induced ISG expression.

Of the 8 ISGs examined, two transcripts, *Rsad2* and *Cxcl10*, were upregulated by > 20-fold at 4 hrs post-treatment (Fig 4.2 b & h). *Mx1*, *Ifit2*, *Oasl*, *Isg15*, and *Ccl5* surpassed this threshold at 8 hrs post-treatment whilst *Isg20* was

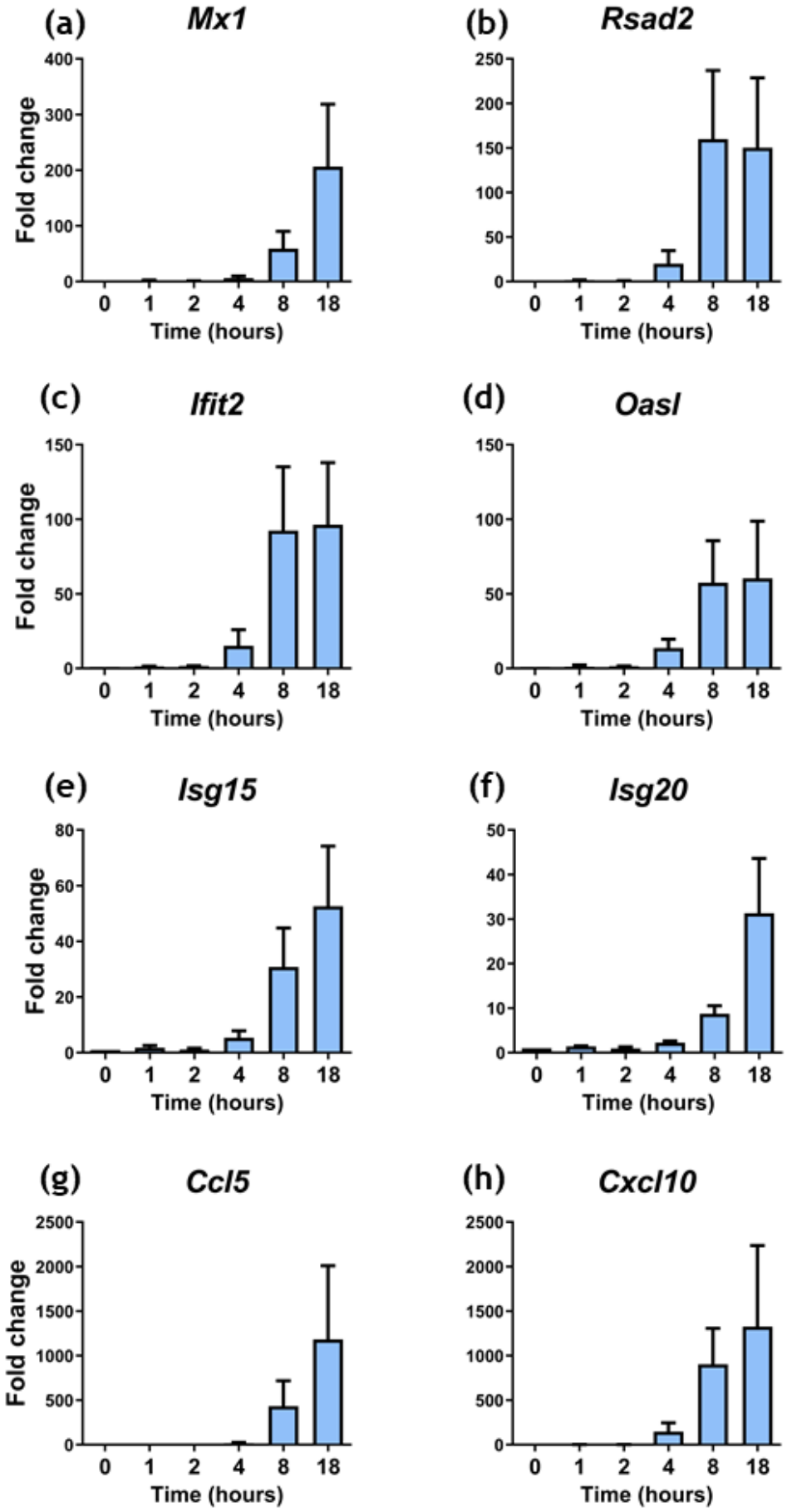

Figure 4.2 Transcriptional time-course of O4-induced ISG expression. Rat myelinated cultures treated 0, 1, 2, 4, 8, and 18 hrs with O4. Data expressed as mean fold change compared to 0 hr control ± SEM, all time-points (n=3).

upregulated relatively late in the time-course at 18 hrs post-treatment (Fig 4.2 a, c, d, e, f, g). Peak expression of all genes examined occurred 8-18 hrs post-treatment.

These data enforce the idea that O4-induced IFN-β expression stimulates downstream ISG expression and provides insight into how different ISGs respond to IFN-β, contributing to our understanding of innate antiviral defence in the CNS.

4.3.2 Significant upregulation of ISGs 24 hrs post O4-treatment

Due to variability in the above dataset, the experiment was repeated using a 24-hr time-point in combination with the previously mentioned IgM and A4CD controls. Of the 8 ISG's examined, 7 were significantly upregulated in response to O4 (*Mx1* ($p < 0.01$), *Rsad2* ($p < 0.05$), *Oasl* ($p < 0.0001$), *Ccl5* ($p < 0.05$), *Ifit2* ($p < 0.01$), *Isg15* ($p = 0.01$), *Isg20* ($p = 0.05$)) (Fig 4.3 a-g). *Cxc10* was upregulated by ~ 400-fold in O4-treated cultures compared to IgM control, but due to variability in the dataset, the *p*-value for this fold-change did not reach significance ($p = 0.0552$) (Figure 4.3 h). Collectively, these data confirm that O4 significantly upregulates ISG expression in rat myelinated cultures.

4.4 O4-induced ISG expression is dependent on IFN-β and IFNAR1

Although the ISGs investigated can indeed be upregulated by IFN-β, many of the genes in question can also be upregulated by other cytokines and transcription factors. Therefore, to determine if O4-induced ISG expression is dependent on IFN-β signalling through IFNAR, we investigated the effect of IFN-β neutralisation and *Ifnar1* knock-out on O4-induced ISG expression.

4.4.1 Neutralisation of IFN-β attenuates downstream ISG expression

To determine whether O4-induced ISG expression was dependent on IFN-β, rat myelinated cultures were treated 24 hrs with A4CD or O4 in the presence of a rabbit anti-rat IFN-β neutralising antibody or control rabbit IgG. Neutralisation of IFN-β significantly attenuated ISG expression in O4-treated cultures whilst having no effect on A4CD-treated cultures.

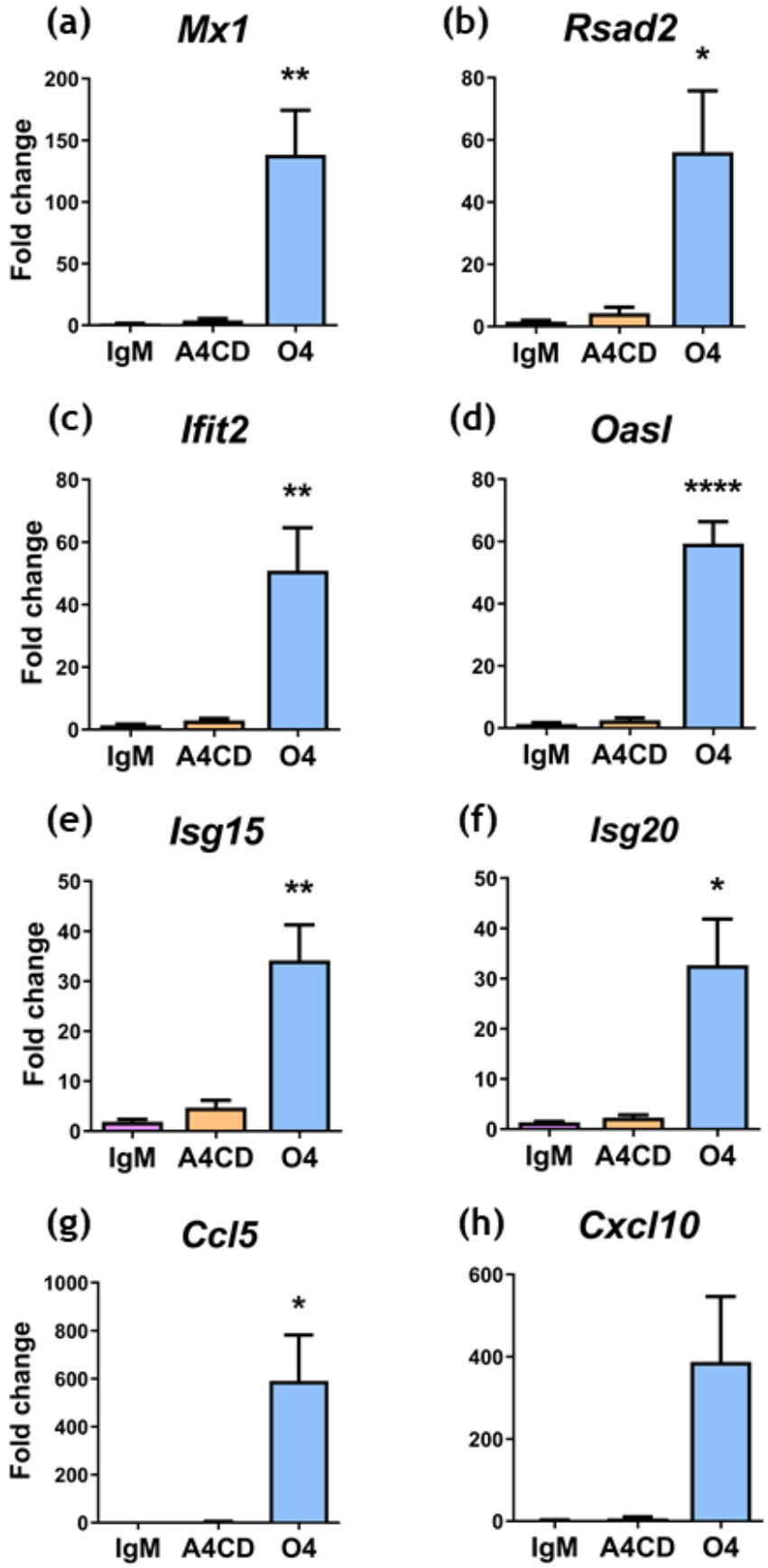

Figure 4.3 ISG expression in rat myelinated cultures treated 24 hrs with IgM, A4CD and O4. Data expressed as mean fold change compared to untreated control ± SEM, analysed by one-way ANOVA and significance determined by Tukey's *post hoc* test, *p*-values adjusted for multiple comparisons. IgM (n=4), A4CD (n=3) and O4 (n=4). *p < 0.05, **p < 0.01 and ****p < 0.0001.

Analysis by two-way ANOVA showed a significant interaction between O4 treatment and IFN-β neutralisation in 3 of 4 ISG's analysed (*Cxcl10*, *Mx1* and *Rsad2* (all $p < 0.05$)) (Figure 4.4 a-c). This highlights that IFN-β neutralisation selectively affects cultures treated with O4 by attenuating O4-induced ISG expression. This effect is not observed in A4CD-treated cultures due to lack of ISG expression. The interaction of these variables was not significant for *Oasl;* however, neutralisation resulted in a 60% decrease in *Oasl* expression in O4-treated cultures ($F = 3.298$, $df_{1,8}$, $p = 0.1069$) (Figure 4.4 d).

Therefore, it can be concluded that induction of these ISGs is largely dependent on IFN-β. Residual ISG expression in neutralising antibody-treated cultures could be due to limitations of IFN-β neutralisation or could indicate involvement of other IFN's or IFN-independent factors.

4.4.2 O4-mediated ISG expression is ablated in the absence of IFNAR1

To test if ISG induction is dependent on IFNAR, WT and *Ifnar1*$^{-/-}$ mouse myelinated cultures were treated 24 hrs with A4CD or O4 and analysed by RT-qPCR. ISG expression was almost completely ablated in O4-treated *Ifnar1*$^{-/-}$ cultures, with significant interactions between O4 treatment and genotype observed in all four genes analysed (*Cxcl10* ($p < 0.0001$), *Rsad2* ($p < 0.001$), *Mx1* ($p < 0.01$), *Oasl* ($p < 0.001$)) (Figure 4.5 a-d). Again, these interactions show that knock-out of *Ifnar1* selectively affects O4-treated cultures by way of attenuated ISG expression. Thus, *Ifnar1* is critical for robust ISG signalling in response to O4 treatment, although residual ISG expression suggests that *Ifnar1*-independent factors contribute to ISG expression but play a minor role. In summary, these data show that O4 upregulates an antiviral response that is predominantly dependent on IFN-β signalling through IFNAR1.

4.5 All major cell types of the CNS express ISGs in response to O4

To determine which cell types of the CNS upregulate ISGs in response to O4, we performed fluorescence *in situ* hybridisation (F*is*H) coupled with immunocytochemistry. Four candidate ISGs were selected (*Cxcl10*, *Rsad2*, *Mx1*

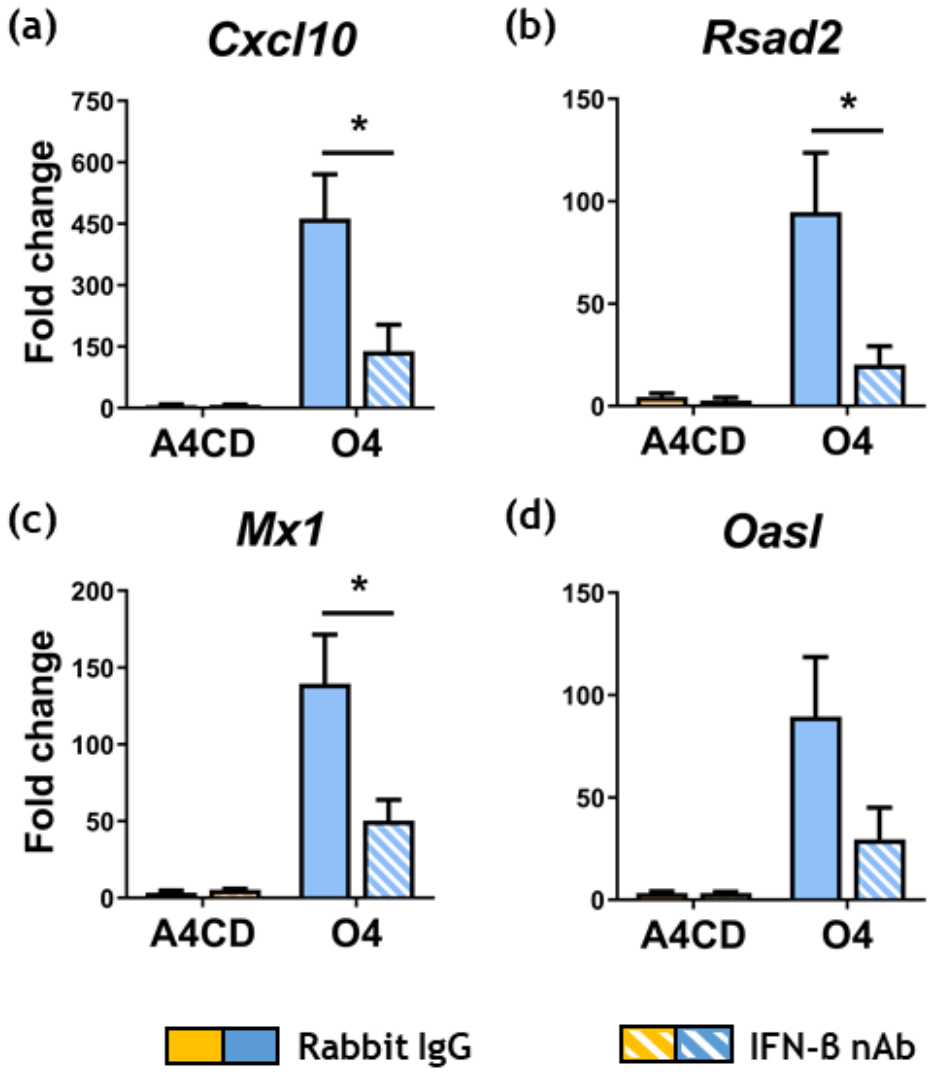

Figure 4.4 Neutralisation of IFN-β attenuates downstream ISG expression. RT-qPCR analysis of rat myelinated cultures treated 24 hrs with A4CD or O4 in combination with rabbit IgG or rabbit anti-rat IFN-β neutralising antibody. Data presented as mean fold change compared to untreated control ± SEM and analysed by two-way ANOVA. Significant interaction between treatment and neutralisation denoted as $*p < 0.05$. All conditions (n=3).

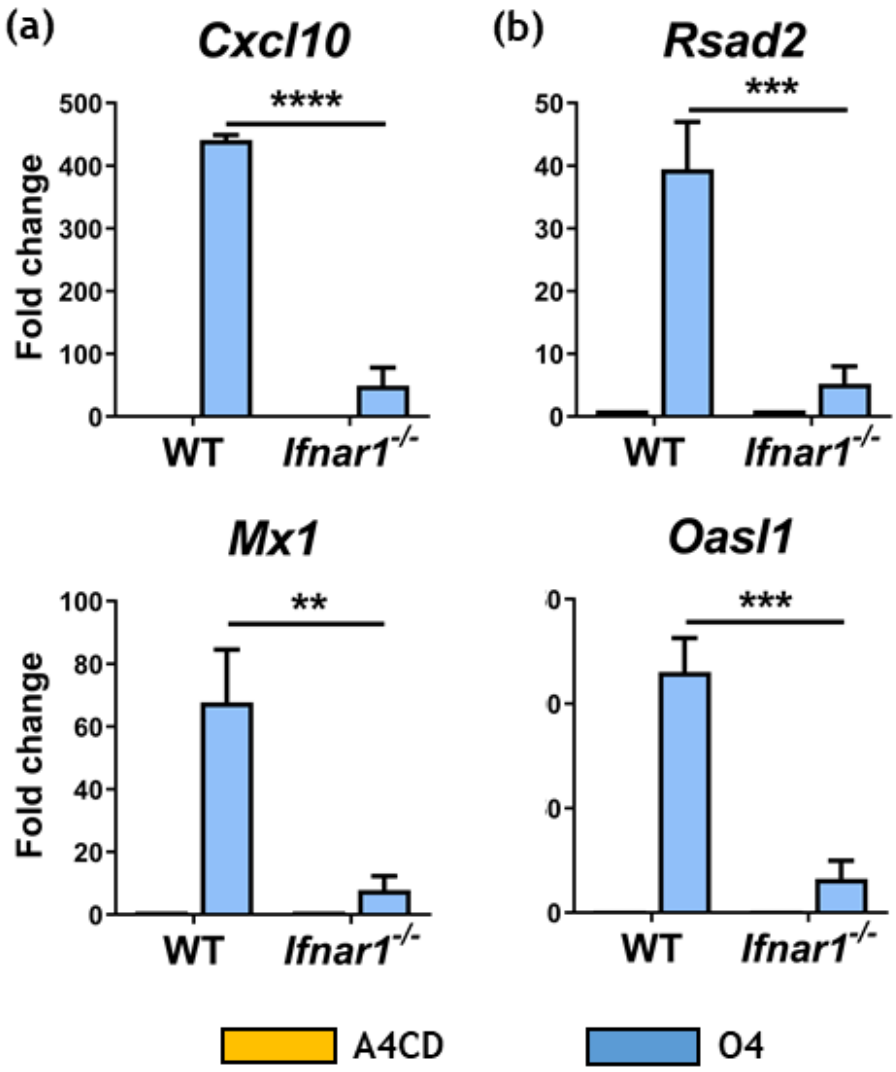

Figure 4.5 O4-mediated ISG expression is ablated in the absence of IFNAR1. RT-qPCR analysis of WT and *Ifnar1*$^{-/-}$ myelinated cultures treated 24 hrs with A4CD or O4. Data presented as mean fold change compared to untreated control ± SEM and analysed by two-way ANOVA. Significant interaction between genotype and treatment denoted as $^{**}p < 0.01$, $^{***}p < 0.001$ and $^{****}p < 0.0001$. WT (n = 2), *Ifnar1*$^{-/-}$ (n = 4).

and *Oasl*) and their expression determined in the four major cell-types of the CNS (astrocytes, neurons, oligodendrocytes, and microglia).

Rat myelinated cultures were treated 24 hrs with A4CD or O4, processed for F*is*H, imaged, and quantified blind. All results were expressed as ISG^+ cells per field of view with raw DAPI counts found in Appendix 8.6 to show no difference between cell numbers for each treatment condition and gene of interest. Figure 4.6 shows ISG^+ cells per field of view for each cell-type and for $DAPI^+$ nuclei.

To ensure that the gene expression patterns observed in 4.3.2 could be replicated using F*is*H, ISG^+ $DAPI^+$ nuclei were quantified in A4CD and O4-treated cultures. A significant increase in ISG^+ $DAPI^+$ nuclei was observed in O4-treated cultures compared to A4CD control for each gene analysed (*Cxcl10* ($p < 0.001$), *Rsad2* ($p < 0.001$), *Mx1* ($p < 0.0001$), *Oasl* ($p < 0.01$)) (Fig 4.6 and 4.7). These data show that F*is*H can reliably detect mRNA, replicating transcript quantification by RT-qPCR.

In terms of cell-type specific expression, all cell-types analysed upregulated at least one of the selected ISGs in response to O4 (Fig 4.6). Astrocytes significantly upregulated all ISGs in response to O4 (Fig 4.6, Fig 4.8). Oligodendrocytes and neurons significantly upregulated *Cxcl10* and *Mx1*, with neurons also upregulating *Rsad2* (Fig 4.6, Fig 4.9, Fig 4.10). Microglia, the immune cells of the CNS, upregulated only the negative regulator of IFN signalling, *Oasl,* suggesting that at this time-point, microglia begin to downregulate the IFN response by a negative feedback mechanism (Fig 4.6, Fig 4.11). These data show that O4 induces ISG expression in the four main cell-types of the CNS and that the ISGs upregulated is cell-type specific.

4.5 Discussion

The data presented in this chapter shows that O4 upregulates IFN-β in murine myelinated cultures and that IFN-β signalling through IFNAR1 is required for ISG expression. All major cell-types of CNS upregulate ISGs in response to O4, indicating that these cells could be protected in the event of virus infection.

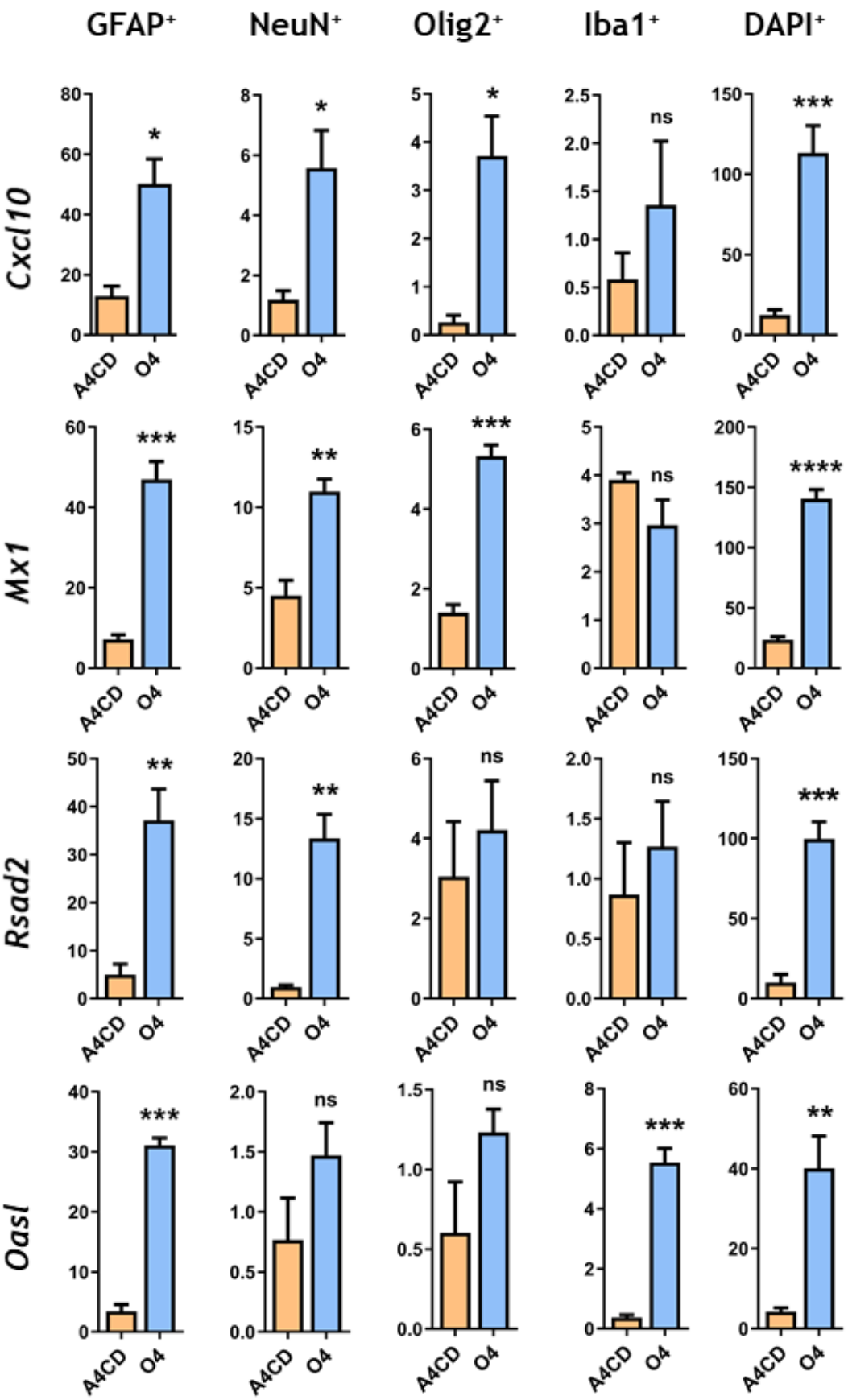

Figure 4.6 ISG expression in astrocytes, neurons, oligodendrocytes, microglia, and DAPI+ nuclei in A4CD- and O4-treated cultures as determined by fluorescence in situ hybridisation. Data presented as mean ISG+ cell per field of view ± SEM, analysed by paired two-tailed t-test, significant difference denoted by *p < 0.5, **p < 0.1, ***p < 0.001 and ****p < 0.0001. n = 3 for GFAP+, NeuN+, Olig2+, and Iba1+ counts. n = 6 for DAPI+ counts.

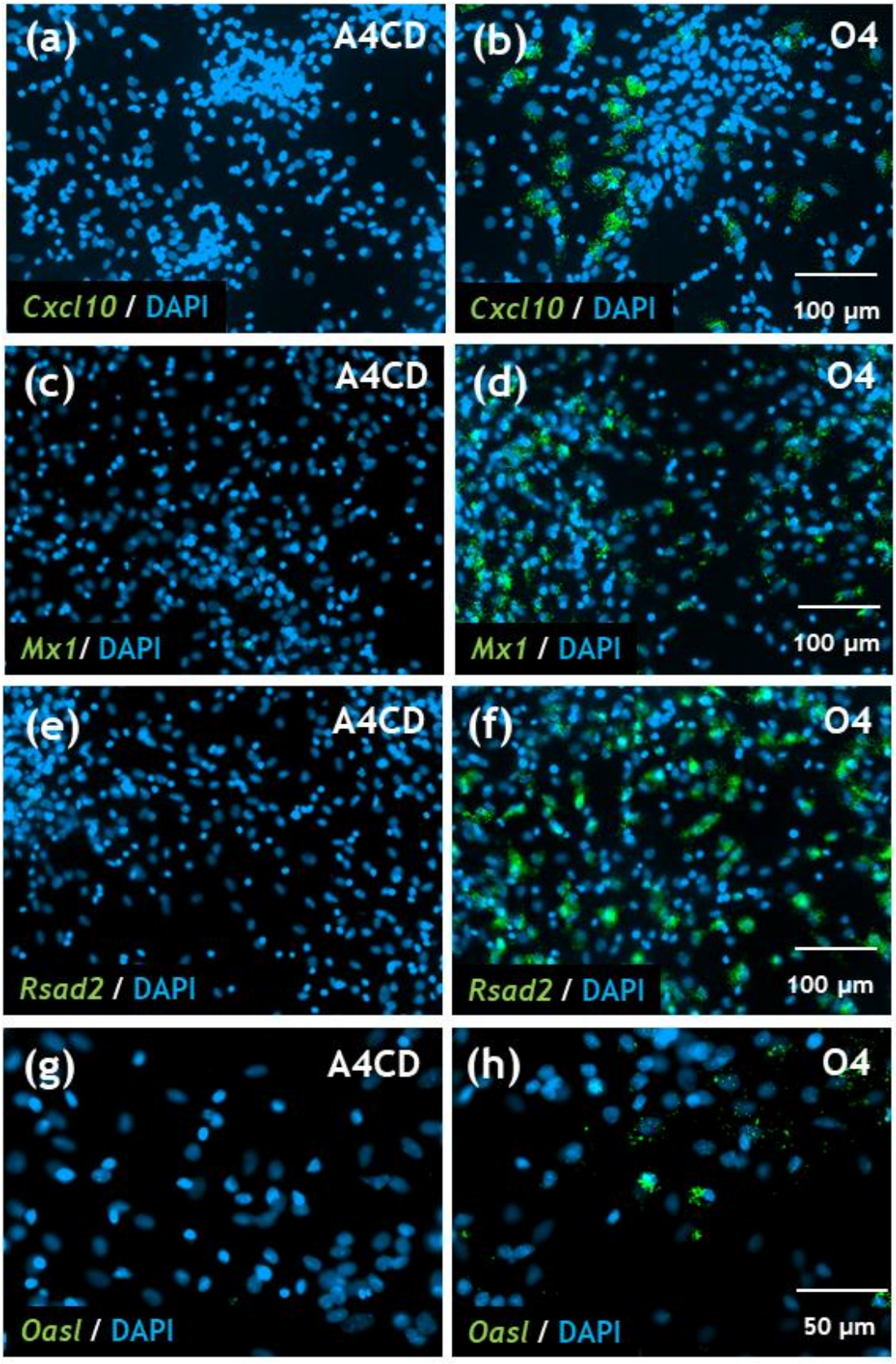

Figure 4.7 Visualisation of O4-induced ISG expression using fluorescence *in situ* hybridisation. Representative images of (a,b) *Cxcl10* (c,d) *Mx1* (e,f) *Rsad2* and (g,h) *Oasl* expression in rat myelinated cultures treated 24 hrs with A4CD or O4.

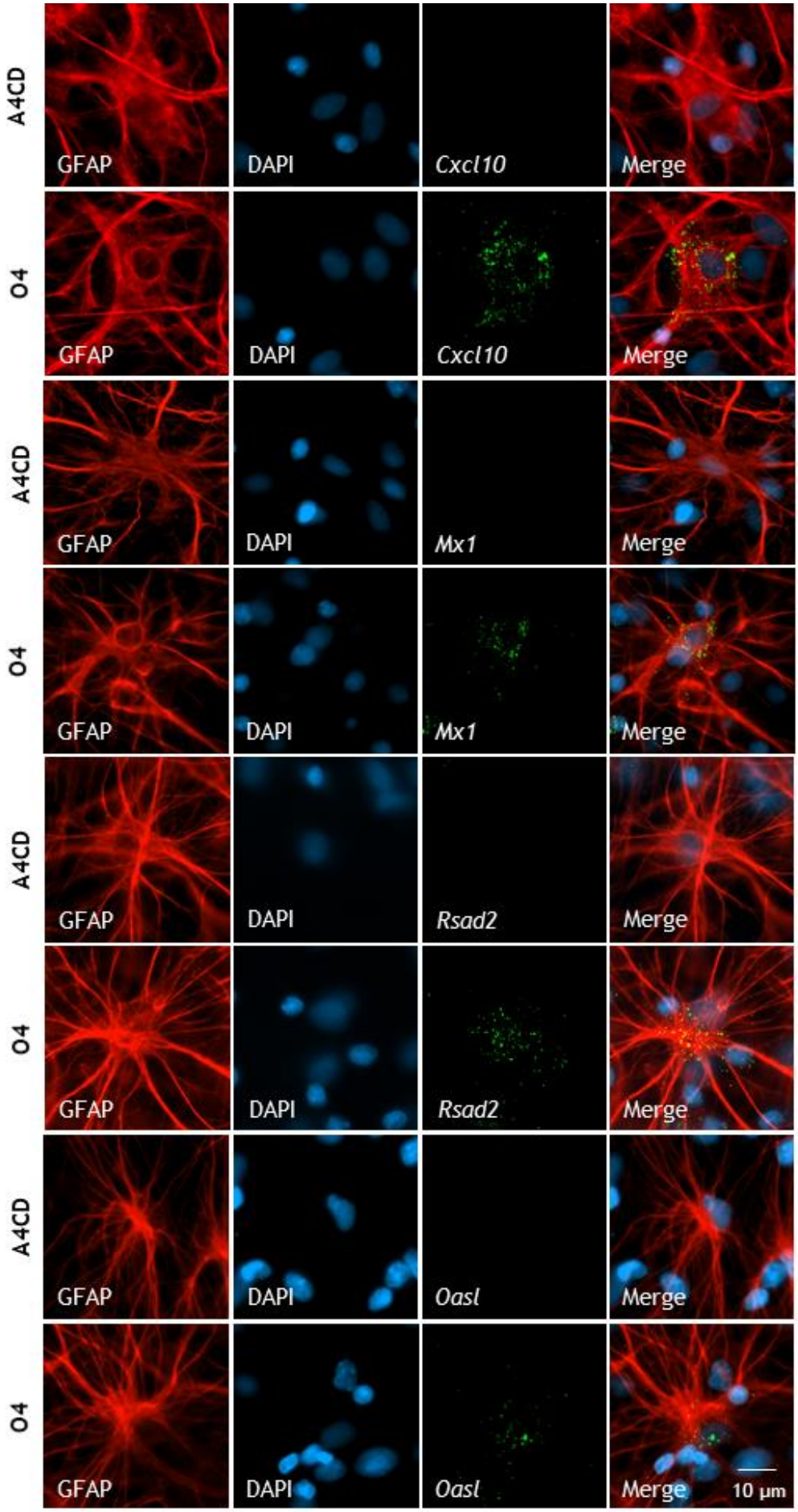

Figure 4.8 ISG expression in GFAP$^+$ astrocytes. Representative images of astrocytic ISG expression in cultures treated 24 hrs with A4CD or O4.

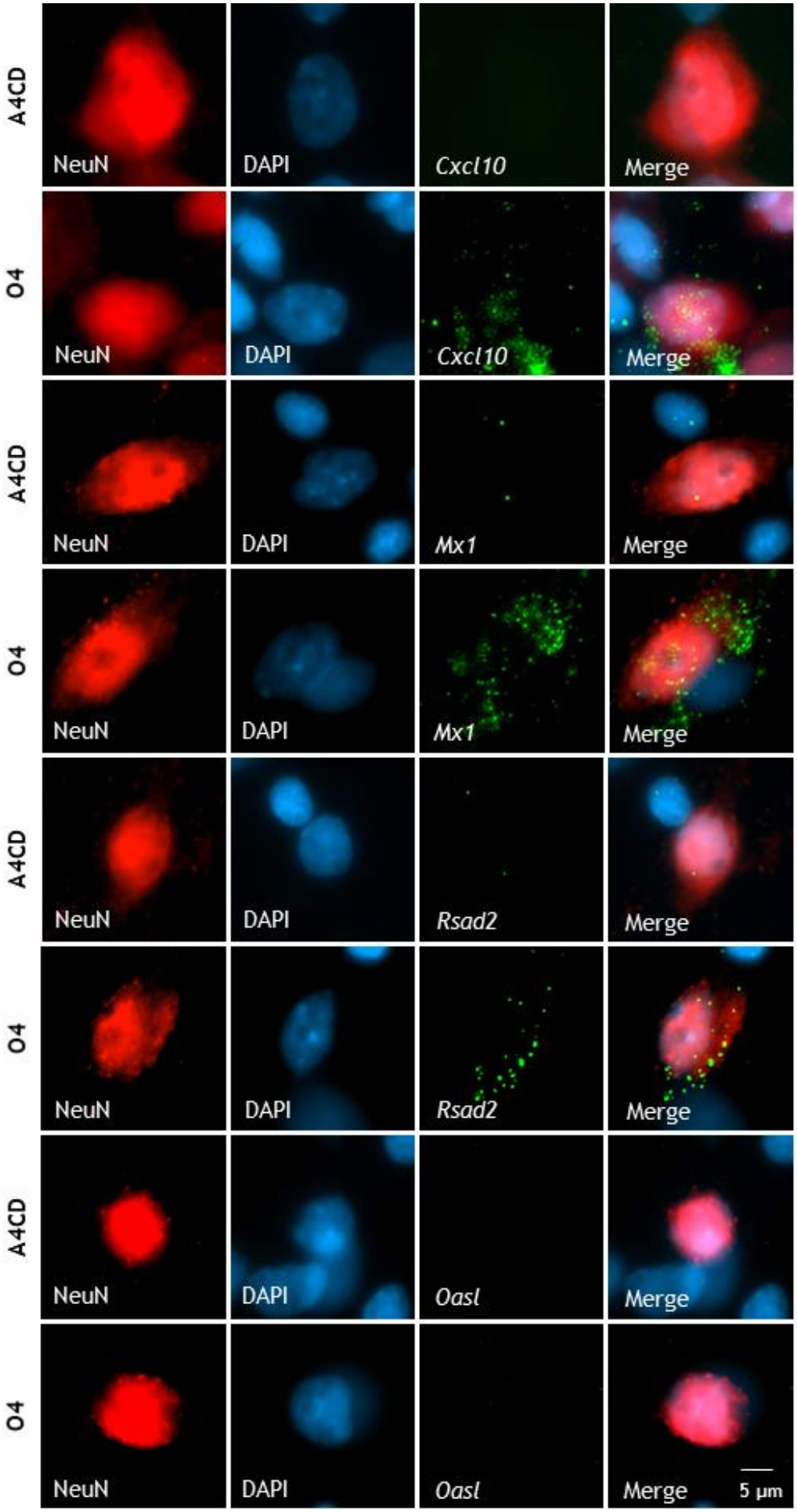

Figure 4.9 ISG expression in NeuN$^+$ neurons. Representative images of neuronal ISG expression in cultures treated 24 hrs with A4CD or O4.

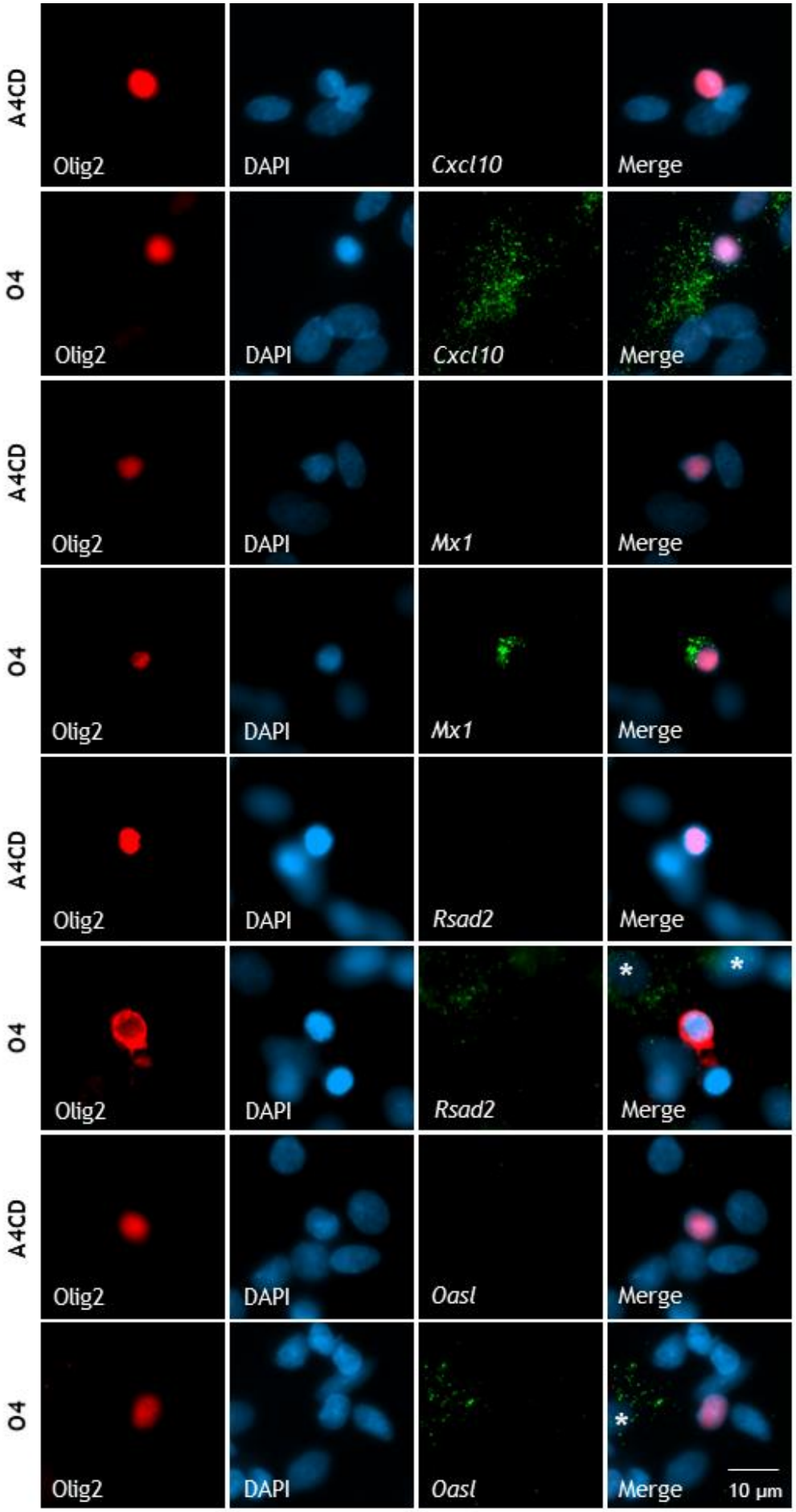

Figure 4.10 ISG expression in Olig2^{+} oligodendrocytes. Representative images of oligodendroglial ISG expression in cultures treated 24 hrs with A4CD or O4. ***** denotes ISG expression in Olig2^{-} cell.

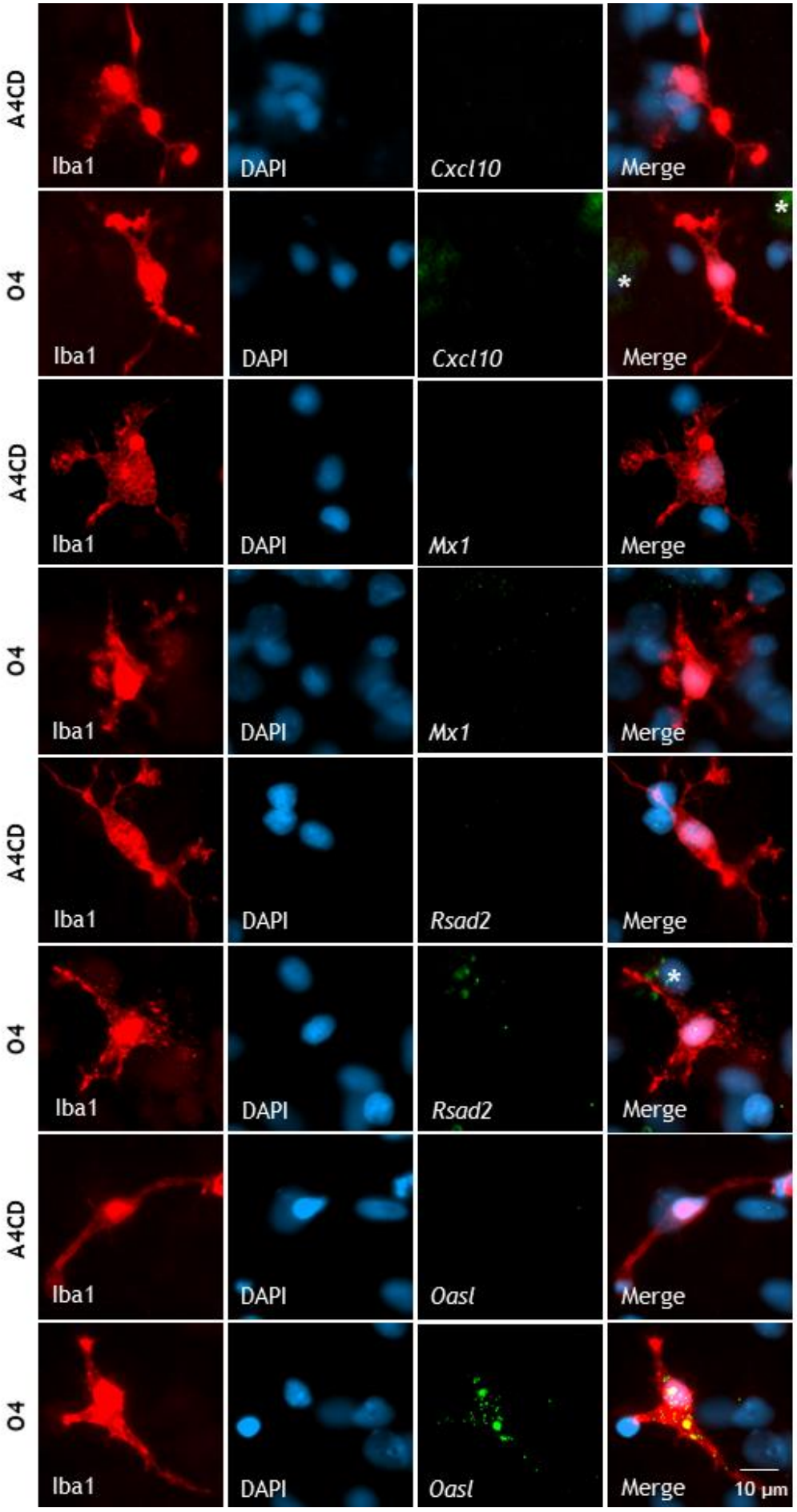

Figure 4.11 ISG expression in Iba1^{+} microglia. Representative images of microglial ISG expression in cultures treated 24 hrs with A4CD or O4.

***** denotes ISG expression in Iba1^{-} cell.

IFN-β expression by cells of the CNS is well documented in the context of both viral infection and inflammatory disease (Khorooshi et al. 2015; Kocur et al. 2015; Delhaye et al. 2006; Pfefferkorn et al. 2016; Vitner et al. 2016). In contrast, IFN-γ is predominantly expressed by activated NK cells (Anegon et al. 1988), $CD4^+$ (Mosmann and Coffman 1989) and, $CD8^+$ T cells (Sad, Marcotte, and Mosmann 1995), with little evidence of IFN-γ expression in cells resident to the CNS.

IFN-λ was not investigated in this study as the true sequence of rat IFN-λ has not been determined. However, current literature states that IFN-III expression is limited to epithelial cells and subsets of myeloid cells at "barrier" interfaces such as the gastrointestinal tract and respiratory tract. Although neuronal IFN-λ receptor (IFNλR) expression has been reported (L. Zhou et al. 2009) and IFN-λ has been shown to prevent West Nile virus migration to the CNS by BBB tightening (D. Ma et al. 2009), once virus gains access to the CNS, IFN-I's are the dominant cytokine in the brain, with negligible IFN-λ expression (Sommereyns et al. 2008). Therefore, the observation in the current study that IFN-β is the mediating cytokine of this antiviral response corresponds with our current understanding of antiviral defences in the CNS. Residual ISG expression observed in *Ifnar1*$^{-/-}$ cultures could be explained by low-level epithelial or endothelial cell contamination, or IFNAR1-independent signalling through IFNAR2. Little is known about the dynamics of IFN-β-dependent ISG expression in cells of the CNS, however, IFN-β-treated microglia secrete CXCL10 and CCL5 protein, peaking 24 hrs post treatment (McDonough et al. 2017). This aligns with the time-course data presented in this chapter, with the ISG panel used in the current study improving our understanding of IFN-β-induced ISG expression in a heterogenous CNS cell culture system.

All cells of the CNS express IFNAR, therefore in principle, all cells could respond to O4-mediated IFN-β expression. However, not all cell-types of the CNS respond to IFN signalling in the same manner. This depends on basal levels of proteins involved in downstream IFN signalling and the internal thresholds for initiating ISG transcription (Cavanaugh, Holmgren, and Rall 2015; Kapil et al. 2012).

The ISGs selected for this experiment were chosen due to being highly upregulated in microarray analysis, the diversity of their functions, and their

role in CNS viral infection. The contributions of CXCL10 during CNS viral infection have been discussed in Chapter 3, with its dominant role in the recruitment of NK cells, antibody secreting cells, and virus specific $CD4^+$ and $CD8^+$ T cells. Examples of CNS virus infections where CXCL10 has been shown to have a role include LCMV, HSV1, and coronavirus infection (Christensen et al. 2006; Thapa et al. 2008; Stiles et al. 2009; Phares et al. 2013).

RSAD2 prevents viral budding by perturbing lipid-rafts of the host cell, and its importance has been demonstrated against BUNV and several members of the *Flavivirus* genus including West Nile virus, Zika virus, and tick-borne encephalitis virus (TBEV) (X. Wang, Hinson, and Cresswell 2007; Carlton-Smith and Elliott 2012; Szretter et al. 2011; Lindqvist, Kurhade, Gilthorpe, and Överby 2018; Panayiotou et al. 2018). Indeed, RSAD2 has additional antiviral viral functions specific to Zika and TBEV, where the NS3 protein of both viruses are targeted by RSAD2 for proteasomal degradation, inhibiting replication (Panayiotou et al. 2018).

MX1 is a GTPase that interferes with viral genome replication and has been shown to prevent influenza virus dissemination into the CNS and reduce mortality rate in infected mice (Horisberger et al. 1990; Hodgson et al. 2012). As mentioned previously, OASL is a negative regulator of IFN signalling and its absence is associated with increased mortality during West Nile virus infection (Ghosh et al. 2019; Tag-El-Din-Hassan et al. 2012).

Astrocytes were highly efficient in responding to O4, with all genes analysed being significantly upregulated. Astrocytes are the major glial cell-type in the CNS and are found adjacent to the BBB as well as throughout the parenchyma. Given their location at the BBB, once virus enters the CNS these cells are the first cell-type that the virus will encounter. Therefore, it seems logical that astrocytes mount a robust antiviral response when exposed to IFN-β. Astrocytic *Cxcl10* (Khorooshi et al. 2015), *Mx1* (Delhaye et al. 2006) and *Rsad2* (Lindqvist, Kurhade, Gilthorpe, and Overby 2018) transcription has been reported, but *Oasl* expression has not been previously documented. The upregulation of *Oasl* provides evidence for a negative feedback loop in astrocytes during the IFN response, possibly to limit astrocyte reactivity.

Oligodendrocytes and neurons upregulated two/three of the genes analysed respectively. Both cell-types have low basal expression of proteins involved in downstream IFN signalling, however, *in vivo* studies have shown that neurons can mount a rapid, robust, and prolonged response to viral infection (Cavanaugh, Holmgren, and Rall 2015), including the expression of *Cxcl10*, *Mx1*, and *Rsad2* (Reinert et al. 2016; Delhaye et al. 2006; Lindqvist, Kurhade, Gilthorpe, and Overby 2018). In contrast, oligodendrocytes tend to be poorer responders to IFN-I, with *in vivo* studies reporting a modest and delayed ISG response in these cells when challenged with virus (Kapil et al. 2012). However, ISG expression can be induced and there have been reports of oligodendrocyte expression of CXCL10 and MX protein (Darbinyan et al. 2013; Szuchet, Plachetzki, and Karialukas 2002).

Despite an abundance of literature citing microglial ISG expression in response to virus, microglia exposed to O4 upregulated only one of the four genes analysed at this 24-hr time-point. OASL has alternate functions depending on the type and stage of virus infection. During DNA virus infection, OASL binds to cGAS leading to STING-dependent termination of IFN signalling (de Toledo-Pinto et al. 2016; Ghosh et al. 2019), whereas during RNA virus infection, OASL activates RIG-I to enhance IFN signalling (Zhu et al. 2014; Ibsen et al. 2015; J.S. Kang et al. 2018; Chen et al. 2021). In later stages of RNA virus infection, OASL binds to *Irf7* mRNA transcripts and inhibits their translation, downregulating IFN production (J.S. Kang et al. 2018).

Therefore, OASL has a clear role in negative regulation of the IFN response and its expression has been previously reported in myeloid cells (Zhu et al. 2014; de Toledo-Pinto et al. 2016). This suggests that microglia express *Oasl* to terminate the IFN response once evidence of a viral threat has been eliminated.

In summary, the data presented in this chapter shows that O4 selectively upregulates IFN-β resulting in IFNAR1-dependent ISG expression in all major cell-types of the CNS. This is a major advancement in understanding the mechanism of this antiviral response and provides us with a foundation to further explore this novel antibody-mediated antiviral pathway. Indeed, numerous hypotheses regarding the mechanism of action of this response can be generated from the results presented in this chapter.

Given that O4 reacts with sulfatide, one might hypothesise that the IgM binds to the oligodendrocyte surface initiating a cascade of events leading to interferon signalling. If this hypothesis is indeed true, one would suspect that the antibody is causing some sort of oligodendroglial injury, leading to the release of damage associated molecular patterns and inducing a global interferon response. However, the idea that O4 induces a damage response in the absence of serum contradicts with results shown in section 3.4. Therefore, other mechanistic avenues should also be investigated including the impact of O4 on the immune cells of the CNS, microglia.

Chapter 5

Exploring the mechanism of action of lipid-reactive IgMs

5 Exploring the mechanism of action of lipid-reactive IgMs

5.1 Introduction

After demonstrating that O4 induces global ISG expression in cells of the CNS and that this response is largely dependent on IFN-β, we sought to determine how lipid-reactive IgM antibodies could elicit such a response. To this end, we proposed a number of hypotheses surrounding O4-induced IFN signalling. The following hypotheses, which are not mutually exclusive, were explored:

1. O4-induced IFN signalling is caused by low molecular weight (LMW) DAMPs.
2. Sulfatide binding is required for IFN-β upregulation.
3. Microglia upregulate IFN-β in response to O4.

After gaining some insight into the mechanism of action, a panel of human-derived IgM antibodies were screened for antiviral properties.

5.2 O4-induced IFN response not caused by DAMPs

Although results from our *in silico* analysis in Chapter 3 suggested that O4-induced IFN signalling was not due to an IgM-mediated damage response, we felt it necessary to explore this possibility further. To this end, we determined whether O4-treatment led to the production of LMW DAMPs, which in turn induced an IFN response in myelinated cultures.

5.2.1 Failure to identify IFN-inducing DAMPs in O4 supernatant

Many DAMPs that contribute to IFN signalling have a molecular weight of less than 50 kDa. Examples include S100 proteins (12 kDa) (Pouliot et al. 2008; Endoh et al. 2009; Fritz et al. 2010), adenosine triphosphate (ATP) (Wilhelm et al. 2010), high mobility group box protein 1 (HMGB1, 25 kDa) (Zetterström et al. 2002; J.S. Park et al. 2006; Tian et al. 2007), and nuclear / mitochondrial DNA (Ries et al. 2013; Kumar et al. 2019; Moriyama et al. 2020).

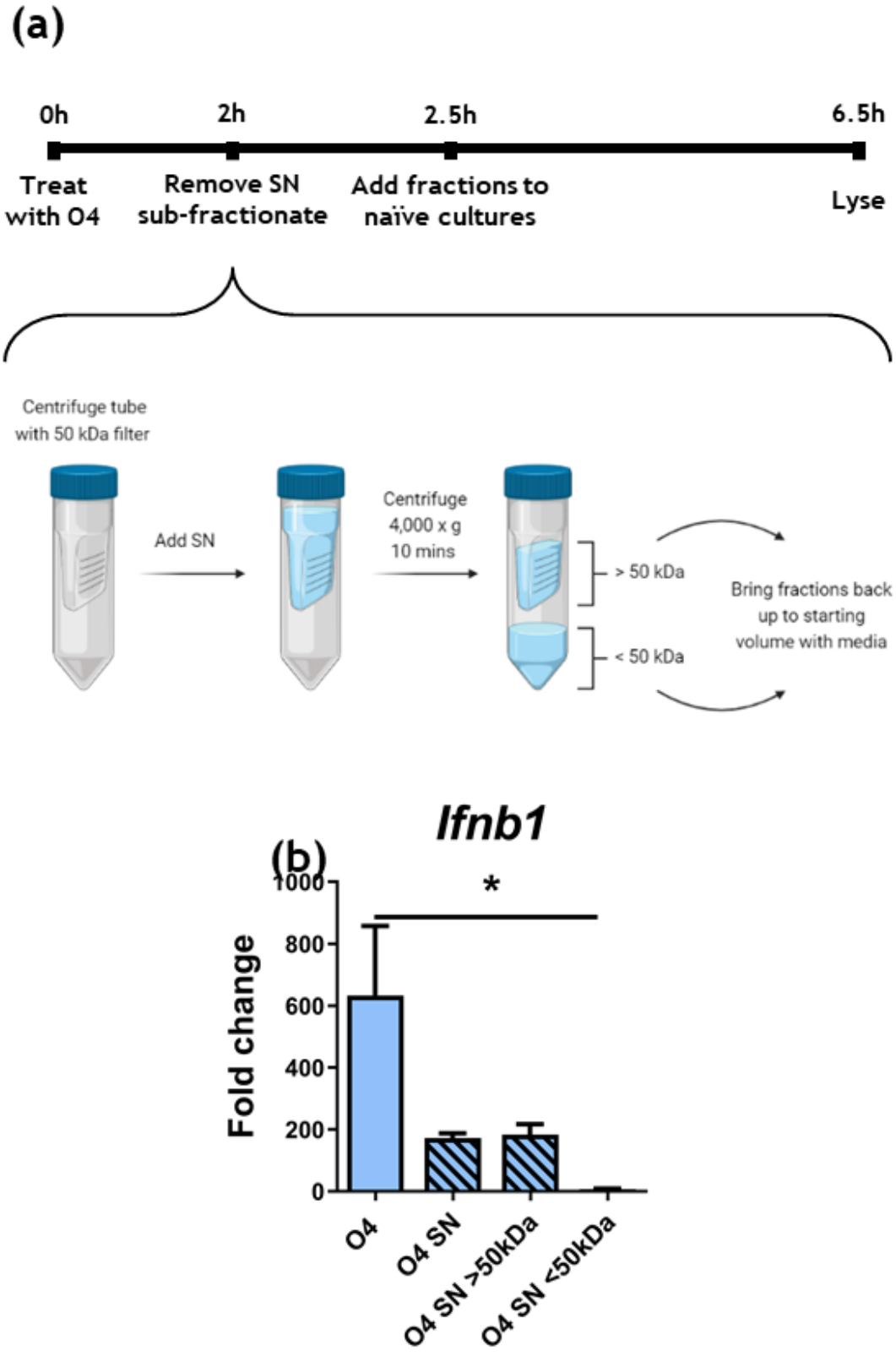

Figure 5.1 Sub-fractionation of supernatants from O4-treated cultures show *Ifnb1* expression is not due to a low molecular weight DAMP. (a) Schematic showing experimental time-course. (b) *Ifnb1* expression in cultures treated with O4 (6hrs, no interruption), O4 supernatant (4hrs, supernatant not sub-fractionated), O4 supernatant > 50 kDa fraction (4hrs) and O4 supernatant < 50 kDa fraction (4hrs). Data presented as mean ± SEM and analysed by one-way ANOVA with Tukey's post *hoc* test. n = 3. *p < 0.05.

To this end, rat myelinated cultures were treated for 2 hrs with O4, supernatants harvested and passed through a sterile 50 kDa molecular weight cut-off filter. The > 50 kDa fraction and < 50 kDa fraction were brought back up to original supernatant volume and added to naïve cells for 4 hrs, with the hypothesis that if LMW DAMPs were present, the < 50 kDa fraction would induce an IFN response. As additional controls, cultures were treated 6 hrs straight with O4 or treated for 4 hrs with non-fractionated supernatant that was kept at 4°C during sub-fractionation process. A schematic showing the experimental procedure is found in Figure 5.1 a.

Cultures treated with O4, or the non-fractionated supernatant displayed an increase in *Ifnb1* expression compared to untreated controls (Fig 5.1 b). *Ifnb1* induction was retained in cultures treated with the > 50 kDa fraction but was lost in the < 50 kDa fraction (Fig 5.1 b). This experiment suggests that O4-mediated *Ifnb1* induction is not mediated by LMW DAMPs.

5.2.2 DAMPs ATP and HMGB1 fail to mimic O4-induced IFN response

Although sub-fractionation was rapid (10-minute centrifugation followed by resuspension in cell culture media) and performed at 4°C, it is possible any LMW DAMPs generated in response to O4 might have degraded and therefore had no effect on naïve cultures. Consequently, we explored whether two physiologically relevant DAMPs might mimic the IFN response induced by O4 in myelinated cultures.

Prior to selecting "candidate" DAMPs, we investigated whether O4 caused cell death in myelinated cultures as some DAMPs are only released during cell death, whilst others are released when cells undergo stress, autophagy, or sub-lytic injury (Matzinger 2002; Bianchi 2007). Cultures were treated 24 hrs with A4CD or O4 and stained with propidium iodide (PI) to identify dead cells. To provide a positive control, cultures were heat-killed (50°C for 10 mins), then returned to 37°C for 45 mins before staining with PI.

Less than 1 % of cells in A4CD- and O4-treated cultures were PI^+, mirroring the baseline level of cell death observed in untreated myelinated cultures (Fig 5.2 a, b, d). In contrast, robust PI staining was observed in the heat-killed cultures (Fig

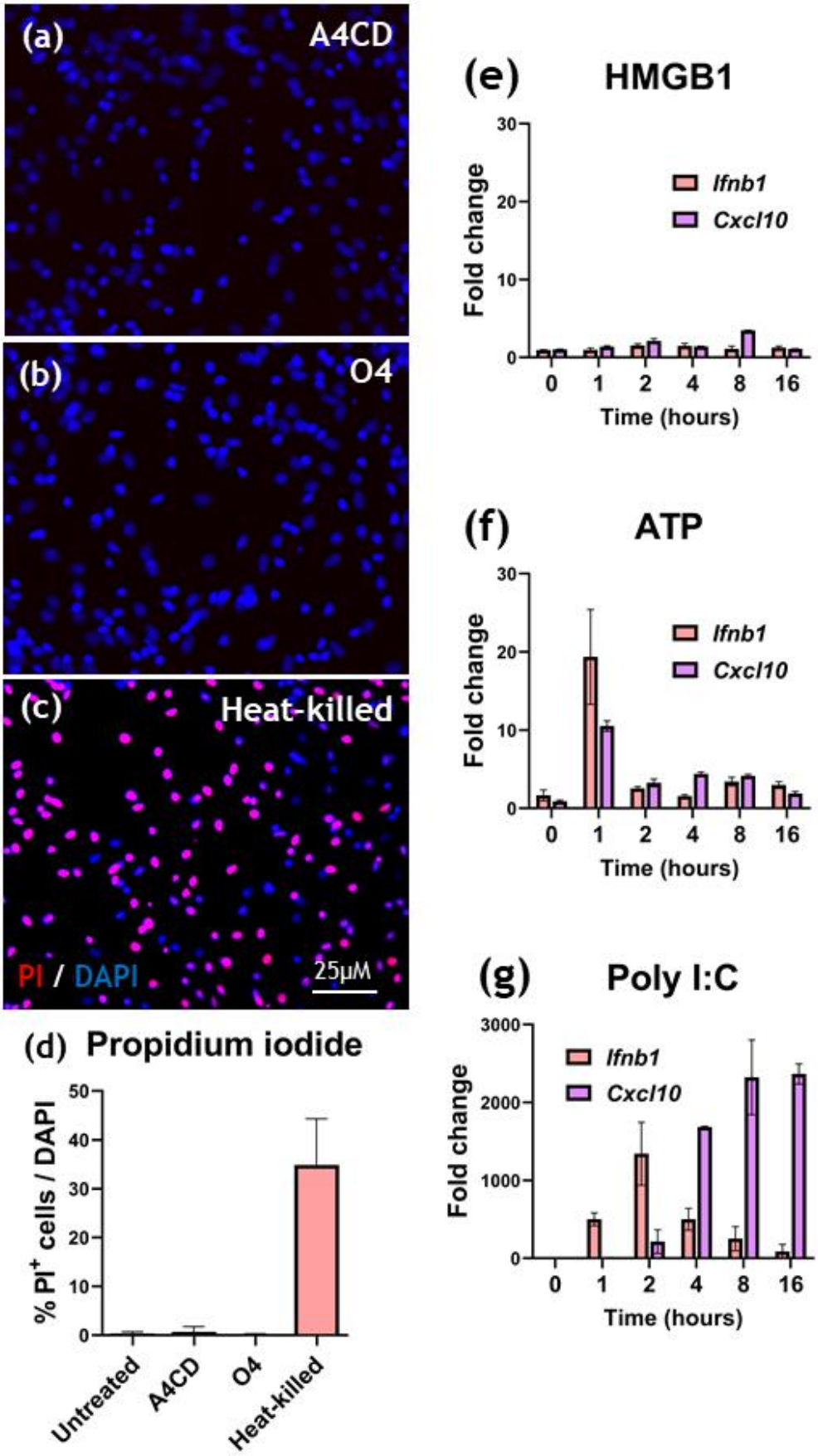

Figure 5.2 DAMPs HMGB1 and ATP fail to mimic O4-induced interferon response (a-c) Representative images of propidium iodide (PI) staining in A4CD/O4 treated and heat-killed cultures (d) Quantification of PI^+ cells. Data presented as mean ± SEM, n = 1, technical triplicates (e-g) *Ifnb1* and *Cxcl10* expression in cultures treated 0, 1, 2, 4, 8, and 16 hrs with (d) HMGB1 (e) ATP or (f) Poly I:C. Data presented as mean ± SEM, biological n = 1, technical triplicates.

5.2 c, d). This experiment indicates that O4 does not induce cell death, therefore our DAMP investigation focused on two molecules released in response to cell stress in the CNS: HMGB1 and ATP (Guazzi et al. 2003; Y. Dong et al. 2013; S.W. Perry et al. 2005; Davalos et al. 2005).

Cultures were treated for 0, 1, 2, 4, 8, and 16 hrs with HMGB1 or ATP, using the viral mimetic poly I:C as a positive control for IFN induction. HMGB1 did not upregulate *Ifnb1* or *Cxcl10* at any time-point (Fig 5.2 e), whereas ATP induced a small, transient increase in *Ifnb1* expression 1 hr post-treatment (~ 20-fold) (Fig 5.2 f). This increase was associated with limited induction of *Cxcl10* (~ 10-fold) (Fig 5.2 f), in contrast to O4-induced *Cxcl10* expression whereby a 200-fold increase in *Ifnb1* expression (Fig 4.1 a) induced a 1,000-fold increase in *Cxcl10* (Fig 4.2 h). Poly I:C induced a 1,000-fold increase in *Ifnb1* expression 2 hrs post-treatment followed by a 2,000-fold increase in *Cxcl10* by 8 hrs, a level maintained until the experiment was terminated at 16 hrs (Fig 5.2 g).

Collectively these data show that O4 does not cause cell death or the release of LMW DAMPs and that the addition of individual DAMPs to myelinated cultures did not mimic the O4-induced IFN response.

5.3 Sulfatide binding is not required for IFN response

5.3.1 Sulfatide is not required for O4-induced *Ifnb1* expression

Although O4 is polyreactive, it is best characterised as an IgM that targets sulfatide, a myelin-ssociated glycosphingolipid abundant in the CNS (Rosenbluth et al. 2003). To determine if sulfatide was required for O4-induced *Ifnb1* expression, myelinated cultures were generated from cerebroside sulfotransferase (CST) wild-type, heterozygous, and homozygous knock-out embryos, then treated with A4CD or O4. CST is an enzyme required for sulfatide synthesis (Fig 5.3 a), and in *Cst* wild-type and heterozygous cultures, O4 recognises sulfatide on oligodendrocyte membranes which can be visualised by live-staining with O4 (Fig 5.3 b & c). In *Cst* knock-out cultures, O4 fails to bind oligodendroglial structures with only non-specific background staining being observed due to autofluorescence.

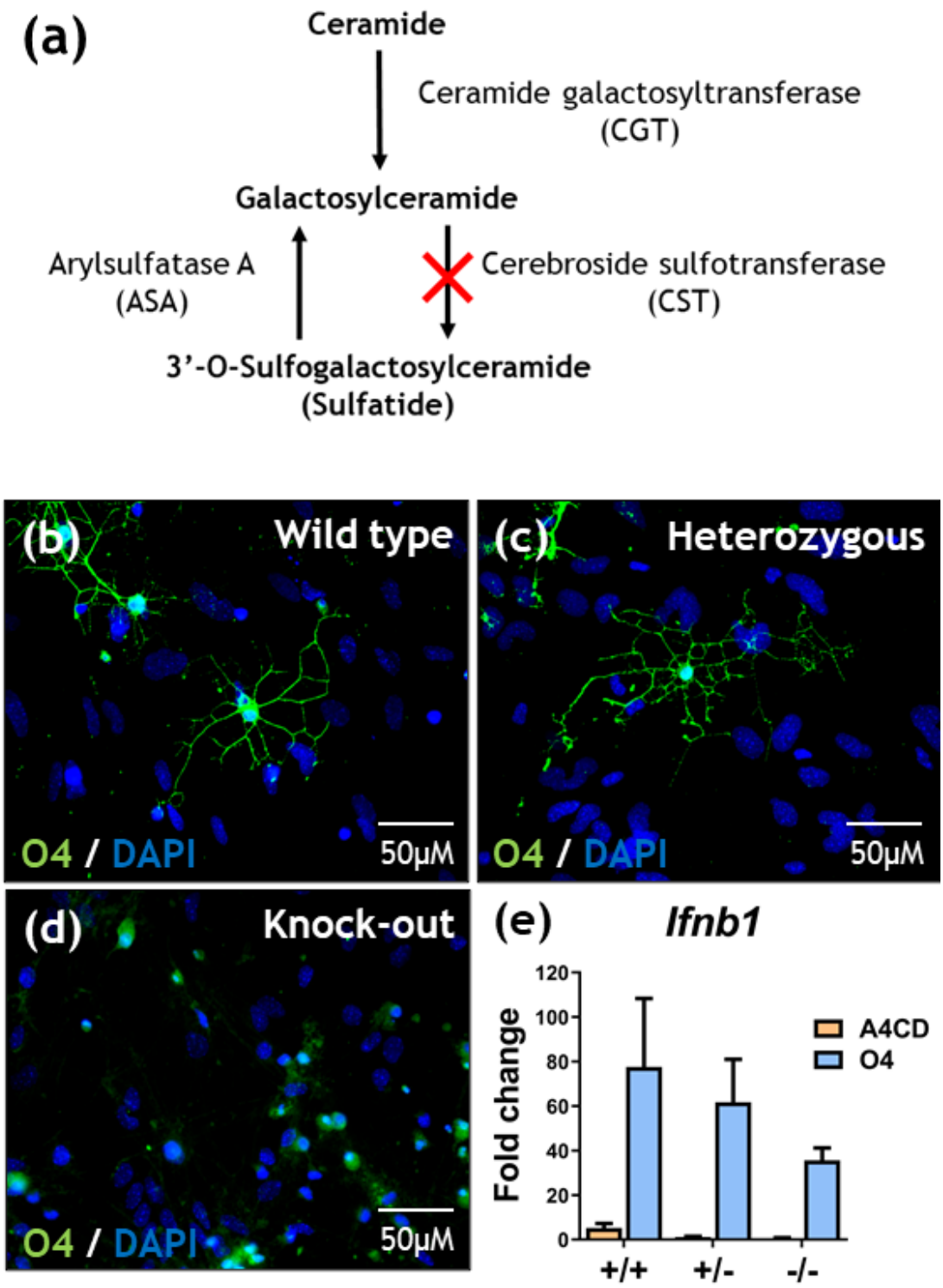

Figure 5.3 Sulfatide not required for O4-induced *Ifnb1* expression (a) Schematic of CST function (b-d) Representative images of sulfatide reactivity in WT, heterozygous and *Cst* knock-out cultures (e) *Ifnb1* expression in WT, heterozygous and *Cst* knock-out cultures treated 6 hrs with O4. Data presented as mean ± SEM, analysed by two-way ANOVA with Bonferroni post *hoc* test, **n** = 3.

In parallel, *Cst* wild-type, heterozygous and knock-out cultures were treated 6 hrs with A4CD or O4 and *Ifnb1* expression quantified. Analysis by two-way ANOVA identified a significant effect of O4 treatment but no effect of genotype (Fig 5.3 e). This shows that O4 recognition of sulfatide on the oligodendrocyte membrane is not required for IFN signalling.

5.3.2 Screening of additional lipid-reactive IgMs for antiviral activity

To determine whether other lipid-reactive IgM antibodies could upregulate an IFN response in myelinated cultures, two additional antibodies were tested. Due to the high cost and time required to obtain additional hybridoma cell lines and produce sufficient antibody under sterile, ultra-low endotoxin conditions, it was decided that we acquire sterile, carrier-free antibody from a commercial source. Commercially available antibodies that met these criteria were the O1 and A2B5 antibody clones. O1 binds to galactosylceramide (GalC) on mature oligodendrocytes and A2B5 recognises multiple c-series gangliosides on neuron and oligodendrocyte progenitor cells (Sommer and Schachner 1981; Saito, Kitamura, and Sugiyama 2001).

As in 5.3.1, live-staining was performed using these additional lipid-reactive IgMs to ascertain their binding patterns in mature DIV24 myelinated cultures. As expected, A4CD demonstrated no immunoreactivity in DIV24 myelinated cultures aside from some minimal background staining (Fig 5.4 a). Both O4 and O1 displayed strong immunoreactivity, with O1 binding specifically to post-myelination oligodendrocytes and O4 binding to both pre-myelinating and myelinating oligodendrocytes (Fig 5.4 b & c). A2B5 displayed poor immunoreactivity, with weak punctate staining on what appear to be oligodendrocytes (Fig 5.4 d). This is most likely due to the maturity of the myelinated cultures and lack of progenitor cells.

After a 24-hr treatment with the above IgMs, the expression of two ISGs was examined: *Cxcl10* and *Mx1*. There was a significant increase in *Cxcl10* and *Mx1* expression in O4-treated cultures whilst neither A4CD nor O1 induced ISG expression (Fig 5.4 e & f). A2B5 produced a similar ISG response to O4, with similar mean fold-increases in ISG expression observed in both conditions. Although the increase in ISG expression did not reach significance in the A2B5 condition, this is most likely due to intra-experimental variability in the dataset.

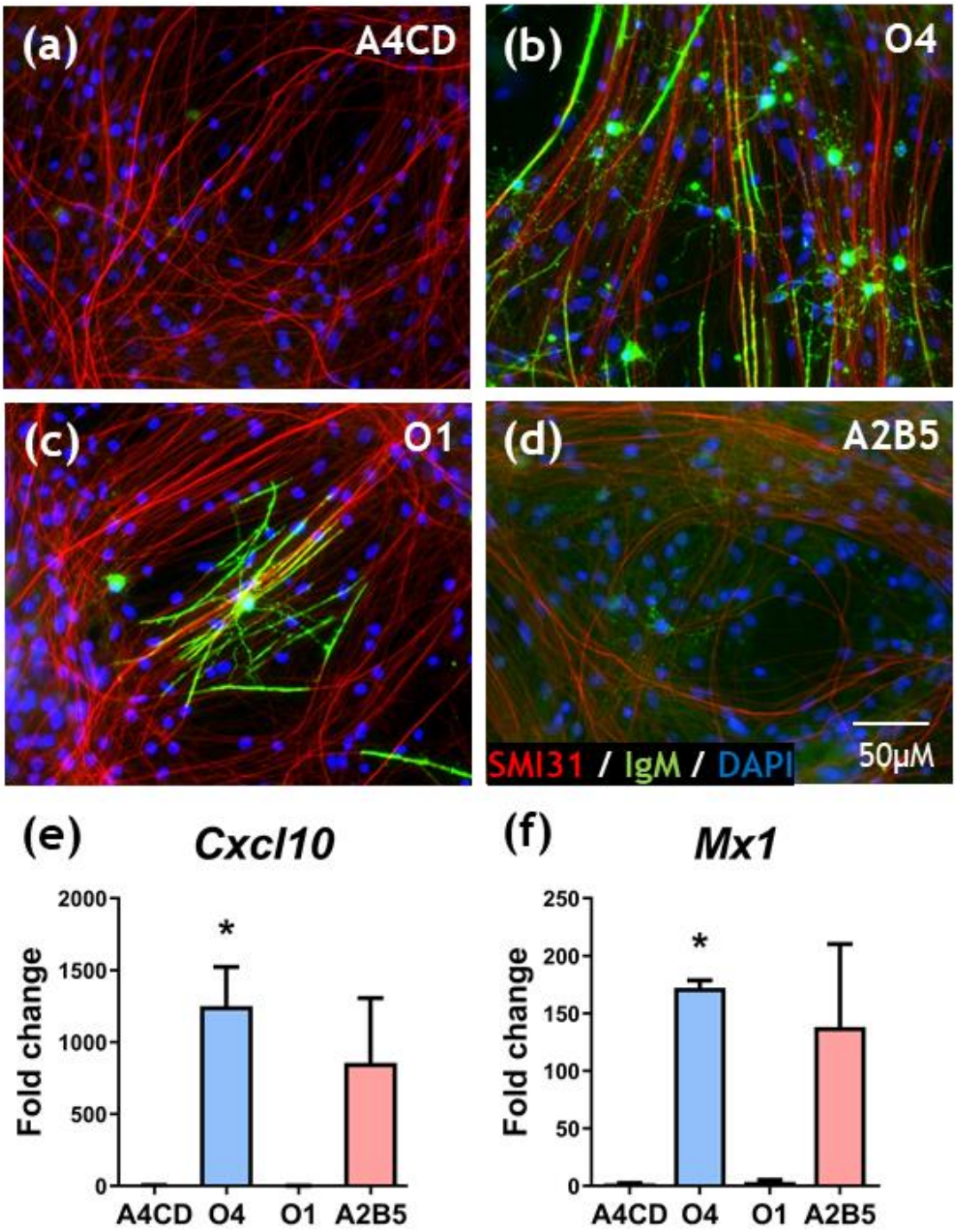

Figure 5.4 Screening panel of mouse lipid-reactive IgMs for ISG induction (a-d) Representative images of (a) A4CD, (b) O4, (c) O1 and (d) A2B5 immunoreactivity in rat myelinated cultures. (e) *Cxcl10* and (f) *Mx1* expression in cultures treated 24 hrs with A4CD, O4, O1 and A2B5. Data presented as mean ± SEM, analysed by one-way ANOVA with Tukey's post *hoc test*. Significance denoted as *$p < 0.05$, n = 3.

Therefore, we propose that A2B5 elicits a similar ISG response to O4, indicating that other lipid-reactive IgMs can induce IFN signalling in cells of the CNS. It is noteworthy that A2B5 could upregulate ISGs despite poor immunoreactivity in the myelinated cultures. This further supports the idea that IgM binding to a target on the oligodendrocyte is not required for ISG expression.

5.4 O4 induces microglial *Ifnb1* expression in a cGAS-STING-dependent manner

With evidence suggesting that oligodendrocyte binding might not be involved in IgM-induced *Ifnb1* upregulation, we focused our attention on identifying the cellular source of IFN-β in O4-treated cultures. Microglia and astrocytes are the dominant producers of *Ifnb1* in the CNS (Roth-Cross, Bender, and Weiss 2008; Kocur et al. 2015; Pfefferkorn et al. 2016). Given the commercial availability of efficient microglia inhibitors, we examined the effect of microglial depletion on O4-induced *Ifnb1* expression.

5.4.1 Microglial depletion attenuates O4-induced *Ifnb1* expression

Rat myelinated cultures were depleted of microglia using the CSF1R inhibitor PLX3397. Vehicle control cultures were treated with an equivalent volume of DMSO. After depletion, cultures were treated with A4CD or O4 for 6 hrs and *Ifnb1* expression quantified.

Treatment with PLX3397 depleted > 99 % of Iba1$^+$ microglia as determined by immunocytochemistry (Fig 5.5 a-c). The CSF1R inhibitor had minimal side effects on non-microglial cells, with the average decrease in DAPI counts with PLX3397 equivalent to the average number of microglia present in DMSO-treated cultures (Fig 5.5 d). O4-induced *Ifnb1* expression was almost completely ablated in microglial-depleted cultures compared to DMSO-control (Fig 5.5 e). There was some residual *Ifnb1* expression in O4-treated microglial depleted cultures, indicating that another cell-type might contribute to *Ifnb1* expression.

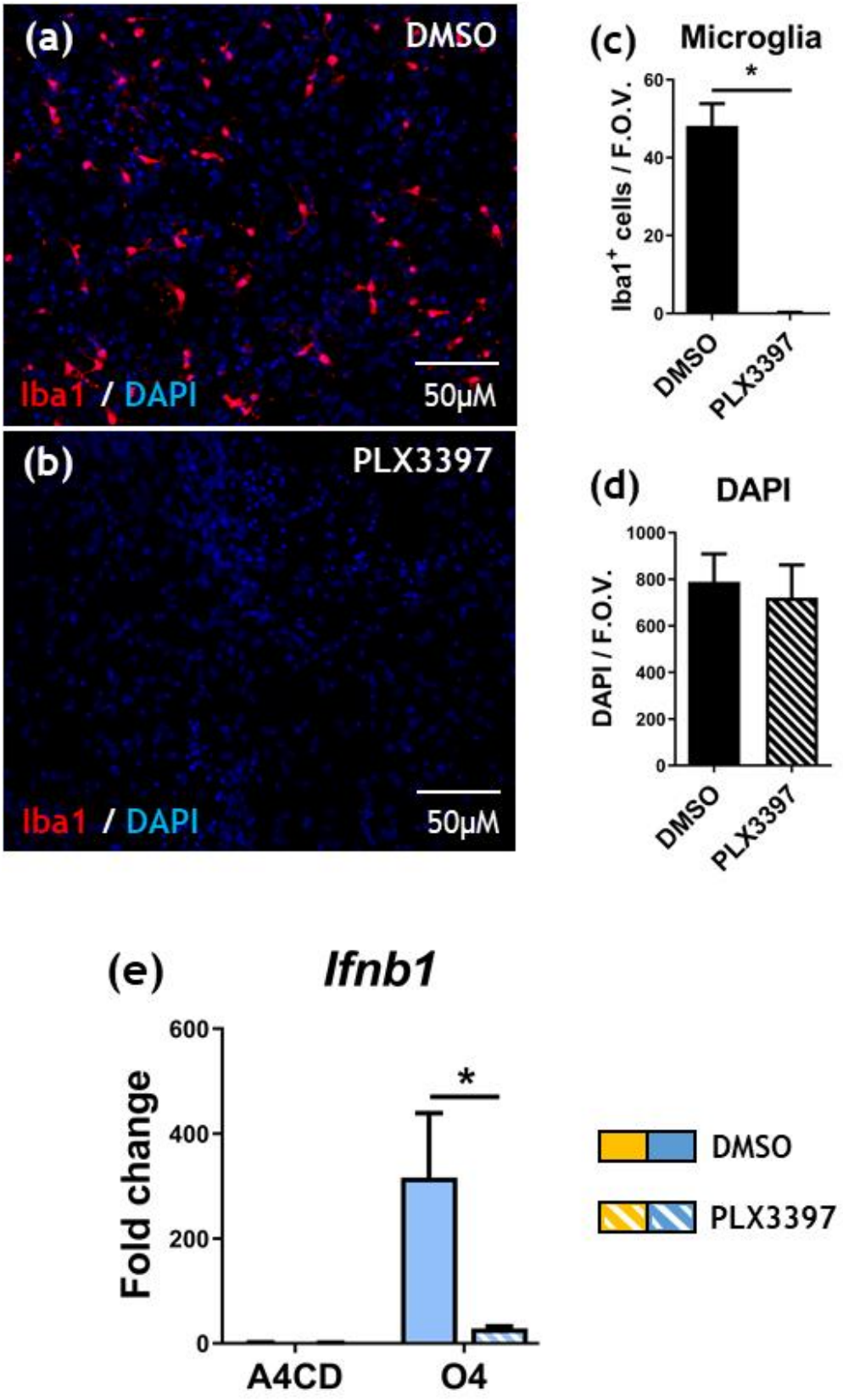

Figure 5.5 Microglial depletion attenuates O4-induced *Ifnb1* expression. (a, b) Representative images of cultures treated from DIV18-28 with (a) DMSO or (b) PLX3397 (c) DAPI and (d) Iba1 counts in cultures treated with DMSO or PLX3397. Analysed by two-tailed paired *t*-test. (e) *Ifnb1* expression in cultures with/without microglia treated 6 hrs with A4CD or O4. Data presented as mean ± SEM and analysed by two-way ANOVA with Bonferroni post *hoc* test. n = 3, Significance denoted as *p < 0.05.

5.4.2 O4-induced *Ifnb1* attenuated by cGAS, STING and TBK1/IKKε inhibition

After demonstrating that microglia are required for robust *Ifnb1* upregulation, we investigated the signalling pathways involved in *Ifnb1* upregulation. Several PRRs can induce *Ifnb1* expression including MyD88- and TRIF-dependent toll-like receptors, and cytosolic DNA/RNA sensors such as cGAS, STING, and RIG-I (Fig 5.6 a). Therefore, we acquired pharmacological inhibitors for proteins involved in these signalling pathways. These included: ST2825 (MyD88), RU.521 (cGAS), C-176 (STING), and BX795 (TBK1/IKKε). MyD88, cGAS, and STING are involved in specific PRR signalling whereas TBK1/IKKε is a protein complex central to several PRR pathways (Fig 5.6 a). Cultures were treated 6 hrs with O4 alone or in combination with one of the inhibitors. DMSO was used as a vehicle control.

O4-induced *Ifnb1* expression was unchanged in the presence of DMSO and the MyD88 inhibitor ST2825 (Fig 5.6 b). cGAS and STING inhibition led to a 90 % decrease in O4-induced *Ifnb1* expression whilst inhibition of TBK1/IKKε completely abolished *Ifnb1* expression. The decrease in O4-induced *Ifnb1* expression was significant for both STING and TBK1/IKKε ($p < 0.05$). Significance could not be determined for the cGAS inhibitor (RU.521) as only an n of 2 was used. However, the level of *Ifnb1* expression with cGAS and STING inhibition is remarkably similar, suggesting that both of these proteins are involved in O4-induced *Ifnb1* expression.

From these data, we propose that O4 induces *Ifnb1* upregulation in a predominantly cGAS-STING-TBK1-dependent manner. The total abolition of *Ifnb1* expression in the TBK1/IKKε condition could suggest that some other pathway provides a minor contribution to *Ifnb1* induction, such as RIG-I or MDA5.

5.5 Identification of antiviral lipid-reactive IgM in humans

Collaborators at the Mayo Clinic provided a panel of IgM antibodies that were either isolated from human patient sera or were recombinant clones of patient-derived antibodies. The patients from which these antibodies were derived were experiencing IgM gammopathy, meaning they produced excess amounts of IgM antibody.

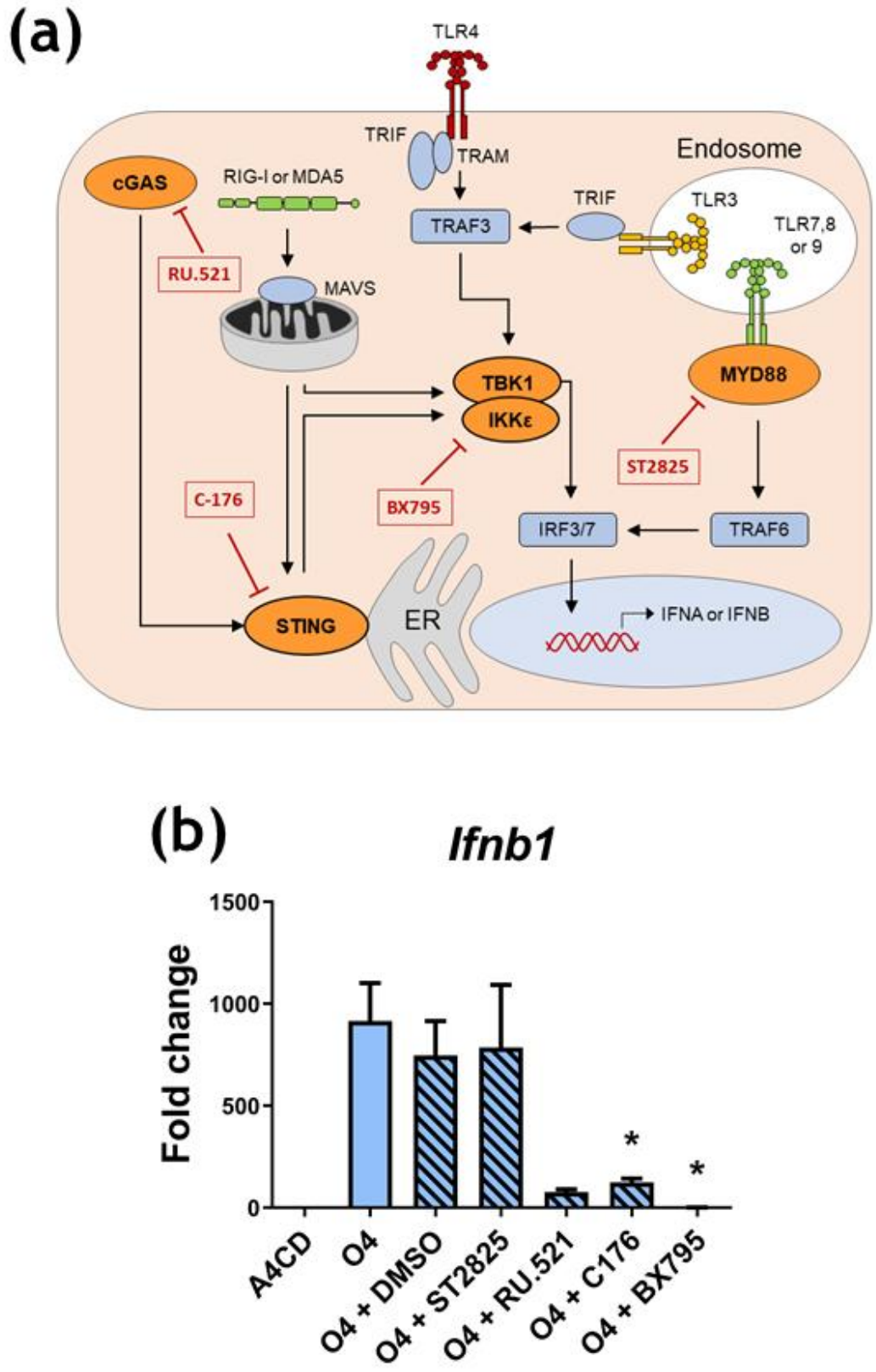

Figure 5.6 O4-induced *Ifnb1* expression attenuated upon cGAS, STING and TBK1/IKKε. (a) Schematic of pathways involved in *Ifnb1* upregulation. (b) *Ifnb1* expression in cultures treated 6 hrs with A4CD, O4 and O4 in the presence of DMSO, ST2825, RU.521, C-176, and BX795. Data presented as mean ± SEM and analysed by one-way ANOVA with Tukey's post *hoc* test. Significance denoted as *p < 0.05, A4CD (n = 6), O4 (n = 6), O4 + DMSO (n = 6), ST2825 (n = 3), RU.521 (n = 2), C-176 (n = 5), BX795 (n = 3).

An initial screen of these antibodies, whereby mouse myelinated cultures were treated for 2 or 24 hrs with the antibodies and analysed by RT-qPCR, identified one antibody clone (IgM22) that upregulated both *Ifnb1* and *Cxcl10*. Details of this experiment can be found in Hayden et al. 2020, a copy of which is located in Appendix 8.7.

The aim of the current section is to determine whether the human recombinant IgM22 (rhIgM22) induced an interferon response by the same mechanism described in section 5.4. For these experiments, rat cultures were treated with rhIgM22 or pentaglobin, a cocktail of human IgM antibody that has been shown to lack IFN-inducing ability in myelinated cultures. Both of these antibodies passed phase I clinical trials and are produced under GMP regulations.

As the following investigation was to be performed in rat cultures, a preliminary experiment was performed whereby rat myelinated cultures were treated 24 hrs with pentaglobin or rhIgM22. A significant increase in *Cxcl10* and *Ccl5* expression was observed in rhIgM22-treated cultures compared to pentaglobin-control ($p < 0.01$) (Fig 5.7 a). This result ensured that the antibodies were effective in rat myelinated cultures and that the specific batch of antibody was functioning as observed previously.

Rat myelinated cultures were then treated for 4 hrs with rhIgM22 in combination with the inhibitors mentioned in 5.4.2. As observed with O4, cGAS and STING inhibitors decreased *Ifnb1* expression by ~ 90 % compared to cultures treated with rhIgM22 only, and the TBK1/IKKε inhibitor completely abolished rhIgM22-indiced *Ifnb1* expression (Fig 5.7 b). As this experiment was performed as an n of 2, there is some variability in the rhIgM22 and rhIgM22 + DMSO conditions. However, the mean of the ST2825 condition lies within the error of the rhIgM22 + DMSO condition, suggesting that MyD88 inhibition remains ineffective. Further n's would be required to reach absolute certainty, however, due to time-constraints this experiment was not repeated.

To determine whether rhIgM22 upregulated *Ifnb1* by a microglial-dependent mechanism, we used pure primary rat microglial cultures. Treatment with rhIgM22 for 4 hrs increased *Ifnb1* expression by ~ 100-fold whilst *Ccl5* was increased by ~ 500-fold compared to untreated control (Fig 5.7 c). These data show that rhIgM22 can induce an IFN response in rat myelinated cultures and

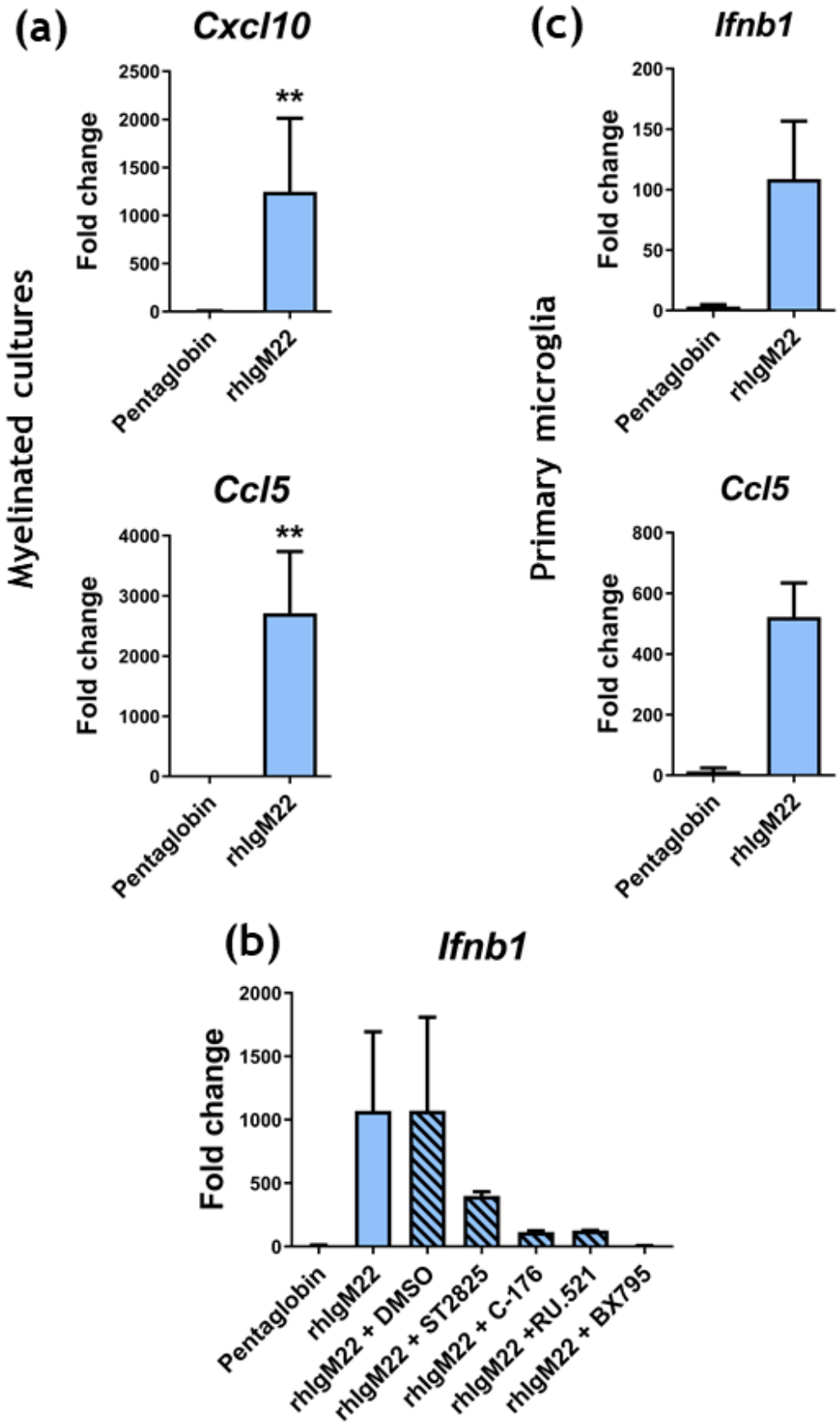

Figure 5.7 Identification of antiviral lipid-reactive IgM in human antibody repertoire. Cultures treated (a) 24 hrs or (b, c) 6 hrs with pentaglobin or rhIgM22 (a) *Cxcl10* and *Ccl5* expression in myelinated cultures (n = 3). Data expressed as mean ± SEM, analysed by two-tailed ratio *t*-test, $^{**}p < 0.01$ (b) *Ifnb1* expression in cultures treated with rhIgM22 in combination with DMSO, ST2825, RU.521, C-176 or BX795 (n = 2) (c) *Ifnb1* and *Cxcl10* expression in primary microglia (n = 2). (b-d) Data presented as mean ± SD.

that rhIgM22 directly stimulates microglia to upregulate *Ifnb1* expression in a cGAS-STING-TBK1 dependent manner.

5.6 Discussion

The data presented in this chapter show that a subset of mouse and human IgM antibodies stimulate microglia to upregulate IFN signalling in a cGAS-STING-TBK1 dependent manner. These data provide a plausible explanation for the association between intrathecal IgM synthesis and reduced risk of MS patients developing PML in response to natalizumab-treatment. Given that oligodendrocyte binding does not appear necessary for this response, it is possible that the mechanism could be manipulated to provide antiviral protection without the demyelinating effect of myelin-reactive antibody.

cGAS and STING are cytosolic PRRs which upregulate IFN in response to DNA. TBK1/IKKε is a protein complex central to multiple IFN-inducing pathways including the cGAS-STING pathway. Given the partial ablation of *Ifnb1* expression with cGAS and STING inhibition (~ 90 % ablation), and total abolition of *Ifnb1* expression with a TBK1/IKKε inhibitor, we concluded that both O4 and rhIgM22 upregulated *Ifnb1* in a predominantly cGAS-STING-TBK1 dependent manner.

The partial ablation of *Ifnb1* expression with cGAS and STING inhibition could be due to limitations of the inhibitors used or due to the inhibitors being added at the same time as the IgM. However, it is possible that another PRR is partially contributing to IFN upregulation in response to O4/rhIgM22. Given the ineffectiveness of the MyD88 inhibitor, a likely candidate for this would be RIG-I which upregulates IFN independent of cGAS and STING, through TBK1/IKKε (Ishii et al. 2006; Ishikawa and Barber 2008; Ishikawa, Ma, and Barber 2009; Sun et al. 2013; Abe et al. 2013; Raicevic et al. 2017). Simultaneous activation of cGAS and RIG-I would explain the partial ablation of IgM-induced IFN signalling in the presence of cGAS and STING inhibitors and the total abolition in the presence of a TBK1/IKKε inhibitor. Furthermore, it has been recently shown that STING degrades IgM in B cells, providing a possible mechanism for IgM-mediated STING activation (Tang et al. 2021).

It is unclear why this subset of IgMs induce IFN signalling whilst other antibodies have no such effect. Indeed, the data presented in this chapter have shown that an IgM being "lipid-reactive" is not the minimum requirement to elicit an IFN response, with O1 failing to induce ISG expression. This could suggest either a shared specificity or structural commonality between IFN-inducing IgMs.

IgM antibodies are known for their poly- and auto-reactivity, which allows them to provide broad protection against pathogens and clear apoptotic and necrotic cells from circulation (Nakamura et al. 1988; Blandino and Baumgarth 2019). They also have six N-linked glycosylation sites, and it has been shown that differential glycosylation patterns can affect their immunological function (Kehry et al. 1979; Fagioli and Sitia 2001; J.F. Wright et al. 1990; Colucci et al. 2015). Therefore, the idea that (a) the IgM antibodies bind to a common alternative target which is phagocytosed by microglia, triggering an IFN response or (b) microglia recognise a specific structural feature of certain lipid-reactive IgMs leading to IFN upregulation, is entirely plausible.

Autoreactive IFN-inducing antibodies have been described in the context of systemic lupus erythematosus (SLE), but the involvement of IgM is a matter of debate. It was first shown in 1986 that IgG and IgM antibodies derived from SLE patients could induce IFN production in normal human peripheral blood mononuclear cells (PBMC's) (Ramirez et al. 1986). A peripheral blood IFN signature is a characteristic of SLE, with ISG levels increasing with the severity of SLE and incomplete SLE (iSLE) (Baechler et al. 2003; Q.Z. Li et al. 2010). A number of studies have identified a positive correlation between autoantibody IgG titres, plasma B cells, and IFN signature in SLE patients (Q.Z. Li et al. 2010; Henning et al. 2020). This is further supported by the observation that both antibody neutralisation and siRNA silencing of Fc gamma receptor IIa attenuates the ISG response of human PBMCs to SLE patient serum (Porat et al. 2018).

Results for IgM autoantibodies have been more conflicting with one report of IgM autoantibody levels being negatively correlated with peripheral blood IFN levels whilst another *in vivo* study showed that the lupus-induced IFN signature was dependent on IgM and complement (Q.Z. Li et al. 2010; Zhuang et al. 2016). The latter study further conflicts with the patient observation that peripheral blood IFN signature negatively correlates with complement levels and the fact that

complement deficiency is a diagnostic indicator of SLE (Q.Z. Li et al. 2010; Sliwinski and Zvaifler 1972). Therefore, the involvement of IgM in the SLE IFN signature remains a matter of debate.

Although the lipid-reactive IgM response of MS patients might not fully resemble the antibody-mediated IFN response observed in SLE patients, it would be wise to use our knowledge of SLE to propose hypotheses as to how lipid-reactive IgMs might elicit an IFN response in cells of the CNS. IFN-inducing autoantibodies in SLE are typically reactive to ds/ssDNA, dsRNA, and chromatin (Q.Z. Li et al. 2010). The idea that IFN-inducing IgMs bind to a common genetic structure would support our finding that IgM-mediated IFN signalling is dependent on the DNA sensors cGAS and STING.

For this hypothesis, IgM complexed with DNA would need to be phagocytosed by microglia and interact with cGAS and/or STING. IgM phagocytosis is mediated by a number of IgM receptors; however, most are not found on myeloid cells. The most likely candidate for microglia-mediated IgM internalisation is the Fcα/μR. Although Fcα/μR expression has not been confirmed in microglia, its expression on peripheral macrophages would support a role in microglia-mediated IgM endocytosis (Shibuya et al. 2000). Upon internalisation, the IgM complex itself could interact with PRRs, or the complex could dissociate, releasing the DNA cargo into the cytosol for cGAS recognition.

It should also be mentioned that an intracellular receptor for virus-bound IgM does exist, the cytosolic Fc receptor tripartite motif containing 21 (TRIM21) (Yang et al. 1999). TRIM21 can bind to IgG, IgM, and IgA when they have coated a non-enveloped virus and have been internalised by the host cell (Mallery et al. 2010). Unlike classical Fc receptors, TRIM21 is expressed by most cell types and possesses E3 ubiquitin ligase activity, which targets antibody-bound virus for proteasomal degradation (Reymond et al. 2001; James et al. 2007). This antiviral defence mechanism is considered a safety net if the extracellular antibody response fails to prevent viral entry to the host cell (Foss et al. 2015).

Although this receptor does indeed bind to IgM, it has been shown that TRIM21 is upregulated by IFN-α, rather than TRIM21 having the ability to induce IFN-I signalling itself. Treatment of HeLa cells with antibody-coated adenovirus has been shown to induce a TRIM21-dependent increase in CXCL10 protein

expression, but this response is not observed in cells treated with antibody alone (McEwan et al. 2013). Therefore, it is possible that in the event of viral infection, TRIM21 contributes to the IgM-induced antiviral response, but the induction of interferon signalling by O4/rhIgM22 in the absence of virus would suggest an alternative mechanism for IFN-I induction.

However, IgM antibodies against DNA, RNA, phosphatidylcholine, and sphingolipids are all found in normal healthy individuals (Nakamura et al. 1988; Hayakawa et al. 1999; D.N. Glass et al. 1973; Mercolino, Arnold, and Haughton 1986; J.C. Lee et al. 1974; M. Kato, Kubo, and Naiki 1978). In fact, IgM antibodies are required to prevent autoimmunity and limit the proportion of autoreactive IgG antibodies in the circulation (Honjo et al. 2012; Ehrenstein, Cook, and Neuberger 2000). Therefore, there must be something else that contributes to the IFN-inducing aspect of these lipid-reactive IgMs. This could simply be the presence of IgM in the CSF and parenchyma of MS patients which is not observed under homeostatic conditions as IgM is too large to extravasate into tissues (Howie, McBride, and James 1982). Additionally, the sheer concentration of IgM in MS patient CSF could push microglia to elicit an IFN response.

Another possibility is that IFN-inducing IgMs have a common structural feature that triggers microglia to upregulate IFN signalling. Given the excessive antibody production observed in MS patients and in patients with IgM gammopathies, it is possible that B cells which secrete these antibodies have a germline mutation causing them to produce IgMs with abnormal IFN-inducing capabilities. A structural anomaly could indeed cause abnormal signalling through TRIM21, leading to IFN-I induction. However, a structural mutation could also lead to an interaction with receptors on the microglial cell-surface. IgM receptors that could facilitate this cell-surface interaction include the FcμR and CD36.

Although the existence of an FcμR had been postulated over the last 40 years, the gene encoding human FcμR was only identified in 2009 (Basten, Warner, and Mandel 1972; Kubagawa et al. 2009). FcμR is the only receptor that exclusively binds to IgM (Kubagawa et al. 2009) and is predominantly expressed on B and T cells. FcμR expression on myeloid cells has been a matter of debate, with Kubagawa and colleagues using PBMCs to show that human myeloid cells do not express the *FCMR* gene and that mouse bone-marrow-derived and splenic

myeloid cells did not express the receptor (Honjo, Kubagawa, and Kubagawa 2013). However, historical papers have described an FcμR on peritoneal macrophages and the presence of FcμR on microglia has not been investigated (Medgyesi et al. 1984; Isaac and Mariano 1988).

Nevertheless, the identification of the *FCMR* gene in humans has rejuvenated interest in the protein and recent studies into FcμR have shown that mice lacking the receptor have poorer IgG responses post-infection/-immunisation and have an increased proportion of autoreactive antibodies (Honjo et al. 2012; Ouchida et al. 2012; Nguyen et al. 2017). The mechanism for these properties has yet to be unravelled and it is possible that there are still functions of the FcμR that remain unknown which could vary depending on cell type and IgM structure.

It was recently discovered that pentameric IgM binds to the serum protein AIM, also known as CD5L (Hiramoto et al. 2018). AIM/CD5L can be released from IgM locally or systemically depending on the disease setting and exerts its function through CD36, a scavenger receptor of the cysteine-rich (SRCR) family expressed on macrophages and microglia cells (Kurokawa et al. 2010; Arai et al. 2016; Joseph et al. 2004; Iannaccone et al. 2017).

The namesake function of AIM/CD5L is to combat insults during infection or injury that would lead to myeloid cell apoptosis (Joseph et al. 2004; Iannaccone et al. 2017). However, AIM/CD5L has also been shown to bind to dying/cancer cells marking them for phagocytosis/degradation, and AIM internalisation inactivates cytoplasmic fatty acid synthase, reducing triacylglycerol deposition (Maehara et al. 2014; Arai et al. 2016; Kurokawa et al. 2010). Although the specific function of AIM/CD5L has not been explored in the CNS, its receptor CD36, has been implicated in a number of neurological diseases including Alzheimer's disease (AD) and MS.

CD36 is required for the clearance of amyloid beta (Aß) in AD and myelin debris in MS, however, CD36 has also been shown to alter microglial phenotype (Ricciarelli et al. 2004; Grajchen et al. 2020). In AD, signalling by CD36 drives microglia towards a proinflammatory phenotype, with CD36 directly contributing to IL-1ß secretion, iNOS upregulation, and NO release. Additionally, stimulation of microglia with Aß or prion protein induces trimer formation between CD36

and TLR's 4 and 6, leading to TLR-dependent NFκB upregulation and TNF-α secretion (Stewart et al. 2010; Kouadir et al. 2012). In contrast, AIM/CD5L and CD36 have protective roles in MS, with the absence of AIM/CD5L leading to an increase in pathogenic Th17 cells whilst a lack of CD36 increases CNS inflammation during EAE and is required for microglial migration (C. Wang et al. 2015; Grajchen et al. 2020; Stuart et al. 2007).

Therefore, it is possible that IgM-mediated IFN induction could be a result of AIM/CD5L release, or indeed be a co-operative feat between IgM structural alterations, cargo, and associated AIM/CD5L. This could be mediated by FcμR/CD36-dependent recruitment of IFN-inducing PRRs or phagocytosis by Fcα/μR, leading to stimulation of intracellular DNA sensors.

Further research needs to be performed to completely unravel this mechanism, but the data presented in this thesis has made a significant step forward in understanding the correlation between lipid-reactive IgMs and reduced risk of PML.

Chapter 6

O4 and rhIgM22 limit virus replication

6 O4 and rhIgM22 limit virus replication

6.1 Introduction

Having identified mouse and human IgMs which induce ISG expression in myelinated cultures, we examined their ability to suppress the replication of model neurotropic viruses. The following aims were addressed in this chapter:

1. To determine whether O4 pre-treatment could suppress neurotropic virus replication *in vitro*.
2. To develop an *in vivo* model to explore the therapeutic potential of IgMs in the context of viral encephalitis.

Previous experiments performed by our laboratory showed that pre-treatment of myelinated cultures with O4 and rhIgM22 reduced SFV A7(74) replication in an IFNAR1-dependent manner (Hayden et al. 2020). The paper detailing these experiments can be found in Appendix 8.7. SFV A7(74) is a mouse-adapted positive-sense ssRNA virus with similar pathogenesis to JCV (Fazakerley and Webb 1987). This chapter will examine the effect of O4 on BUNV replication *in vitro* to determine the IgM's efficacy against a human relevant pathogen of an alternative genetic lineage (Hughes et al. 2020; Tauro et al. 2015). Subsequent *in vivo* experiments will utilise SFV A7(74) as its pathogenesis *in vivo* has been well described.

6.2 BUNV exhibits neuronal cell tropism

Although BUNV is encephalitogenic, its cellular tropism within the CNS is unknown. Thus, BUNV tropism was investigated in naïve rat myelinated cultures using immunocytochemistry. Antibody targeting BUNV protein (herein termed "BUN" (Lappin et al. 1994)) predominantly co-localised with $NeuN^+$ mature neurons and $Nestin^+$ neuronal progenitors (Fig 6.1 a, b & f). Less than five percent of total BUN^+ cells co-localised with Olig2 or GFAP, markers for oligodendrocytes and astrocytes respectively (Fig 6.1 c, d & f). The percent of

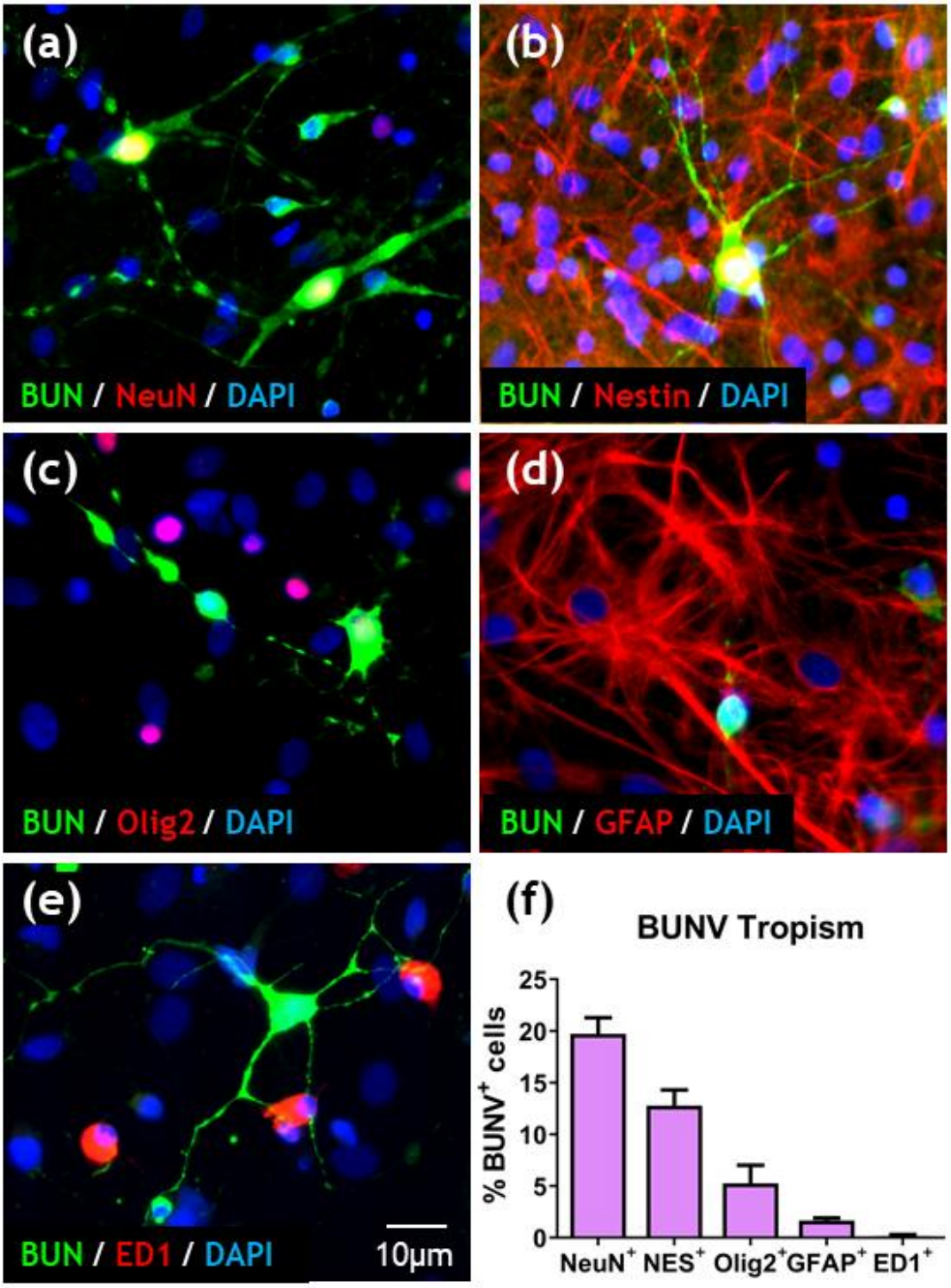

Figure 6.1 BUNV exhibits neuronal cell tropism. (a-e) Representative images of BUNV-infected cultures co-stained with (a) NeuN (b) Nestin (c) Olig2 (d) GFAP and (e) ED1. (f) Graph showing % BUN^+ cells that co-localised with each cell-marker. Data presented as mean ± SEM. n = 3.

BUN$^+$ cells that co-localised with ED1 (CD68), a marker for microglia, was negligible with values close to zero (Fig 6.1 e & f). Therefore, we can conclude that BUNV preferentially infects cells of neuronal lineage *in vitro*.

6.3 O4 limits BUNV replication in IFNAR1-dependent manner

6.3.1 O4 limits BUNV replication in rat myelinated cultures

To determine whether O4 could protect against virus infection, rat myelinated cultures were pre-treated with IgM, A4CD, O4, or poly I:C and infected for 24 hrs with BUNV (MOI = 1). Pre-treatment with O4 and poly I:C significantly reduced the number of BUN$^+$ cells compared to IgM and A4CD controls as determined by immunocytochemistry (Fig 6.2 a-e) (all $p < 0.01$ except IgM-poly I:C ($p < 0.001$)). No difference was observed between IgM and A4CD controls (Fig 6.2 a, b & e).

RT-qPCR analysis showed a log fold decrease in the expression of the BUNV M genome (*BUNM*) in O4 and poly I:C-treated cultures compared to IgM and A4CD (Fig 6.2 f). However, this decrease was not statistically significant by one-way ANOVA, possibly due inter-experimental variability. To determine whether these effects were associated with a decreased production of infectious virus particles, our collaborator Xiaohong Shi (Centre for Virus Research, Glasgow) kindly performed plaque assays on supernatants harvested from A4CD and O4 pre-treated cultures. The number of infectious BUNV particles in O4-treated culture supernatants was dramatically reduced compared to A4CD-treated controls in two separate experiments (Fig 6.2 g).

Collectively, these data show that pre-treatment with O4 reduced BUNV replication in rat myelinated cultures.

6.3.2 O4-mediated antiviral protection dependent on IFNAR1

To determine if this protective response was IFN-dependent, WT and *Ifnar1*$^{-/-}$ myelinated cultures were pre-treated with A4CD or O4 and infected with BUNV. O4 pre-treatment significantly decreased number of BUN$^+$ cells and infectious virus particles in WT cultures but had no effect on *Ifnar1*$^{-/-}$ cultures (Fig 6.3 a-e).

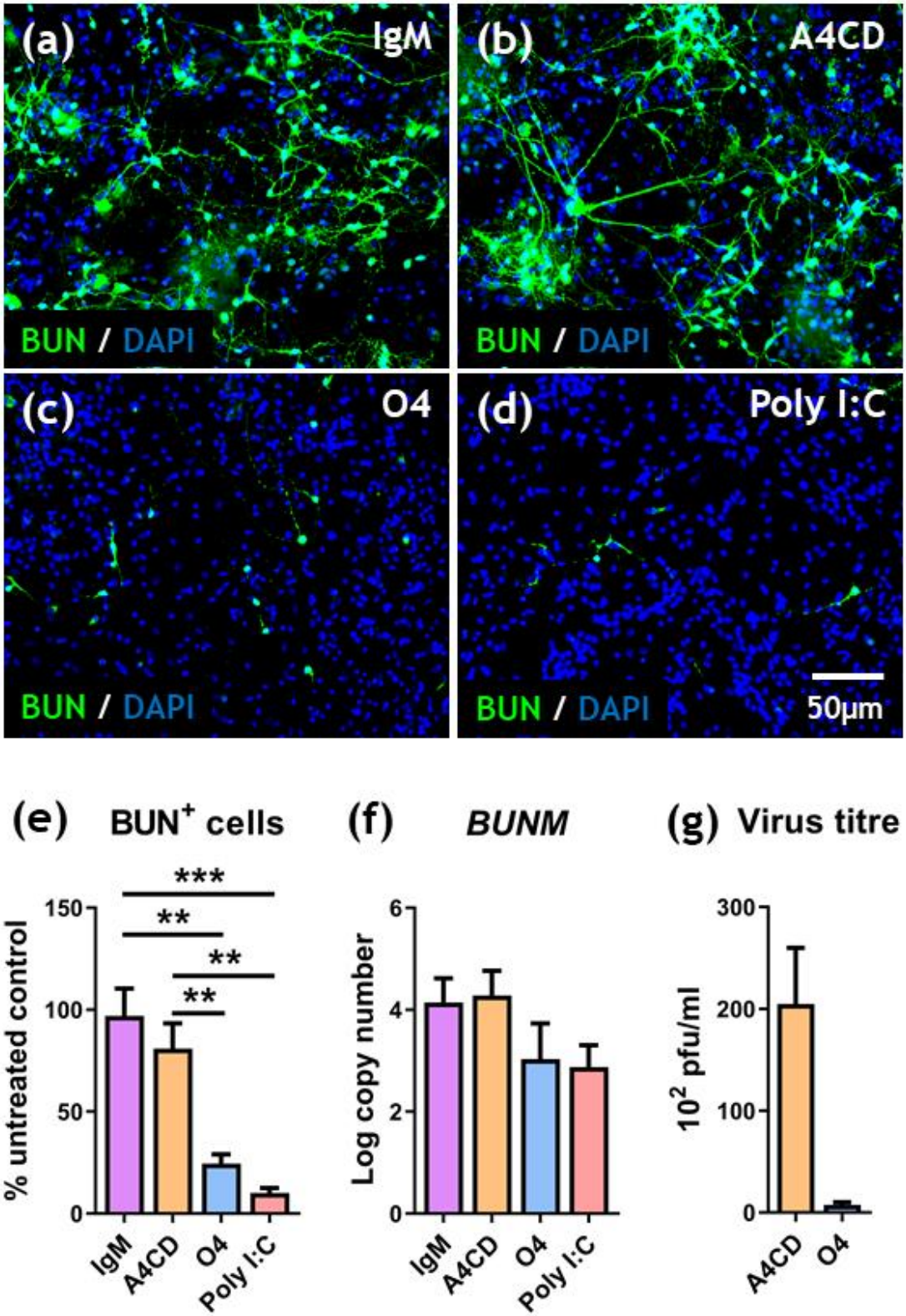

Figure 6.2 Pre-treatment with O4 limits BUNV infection. DIV24 rat myelinated cultures treated 24 hrs with IgM, A4CD, O4, or poly I:C and infected with BUNV. (a-d) Representative images of BUNV-infected cultures pre-treated with (a) IgM (b) A4CD (c) O4 and (d) poly I:C. (e) Immunocytochemical analysis of BUN^+ cells (f) RT-qPCR analysis of *BUNM* gene expression. Data presented as mean (e) % untreated control and (f) log copy number ± SEM. Analysed by one-way ANOVA and significance determined by Tukey's post *hoc* test. Significant difference denoted as $^{**}p < 0.01$ and $^{***}p < 0.001$. (e) n = 4, (f) n = 3. (g) graph showing plaque assay analysis, data expressed as 10^2 pfu/ml, n = 2.

These data show that the antiviral protection provided by O4 is mediated by IFN signalling through IFNAR1, supporting results presented in 4.4.2.

6.4 Establishing an *in vivo* model to study antiviral IgMs

Although the data presented above demonstrates the efficacy of O4 against BUNV, a human-relevant encephalitogenic virus, there are limited prior *in vivo* studies performed on this virus due to poor dissemination in mice (Dutuze et al. 2018). In contrast, SFV strain A7(74) has been used extensively to study both encephalitis and virus-induced demyelination *in* vivo (Smith et al. 2000; Fazakerley et al. 2006).

Thus, to establish an appropriate *in vivo* model for the of study IgM-mediated antiviral protection, we used SFV A7(74) as a model neurotropic virus. This model would have relevance to both PML and viral encephalitis, with SFV causing infection of oligodendroglia and symptoms of encephalitis (Seamer, Boulter, and Zlotnik 1971; Fazakerley et al. 2006). JCV, the causative agent of PML, could not be used in this study as it is an obligate human pathogen (Tan and Koralnik 2010).

For the IFN-inducing IgM, rhIgM22 was selected for this model as it is more clinically relevant, can be identified easily in mouse tissue due to different species origin, and has been through phase one clinical trials demonstrating its safety in humans. To facilitate IgM entry to the CNS with minimal injury to the animal, we trialled an intranasal (i.n.) method of antibody administration. This method has been shown to yield increased protein entry to the CNS compared to intraperitoneal (i.p.) injection (Chauhan and Chauhan 2015), without the need of injecting antibody straight into the brain by intracerebral injection.

6.4.1 rhIgM22 induces *Ifnb1* and *Cxcl10* expression in the CNS *in vivo*

In our first pilot study, nine-week-old male C57Bl/6 mice (two per group) were anaesthetised with isoflurane and treated i.n. with 20 µg/ml rhIgM22 or human IgM control in 20 µl PBSA [0.75% bovine serum albumin in PBS]. After 24 hrs,

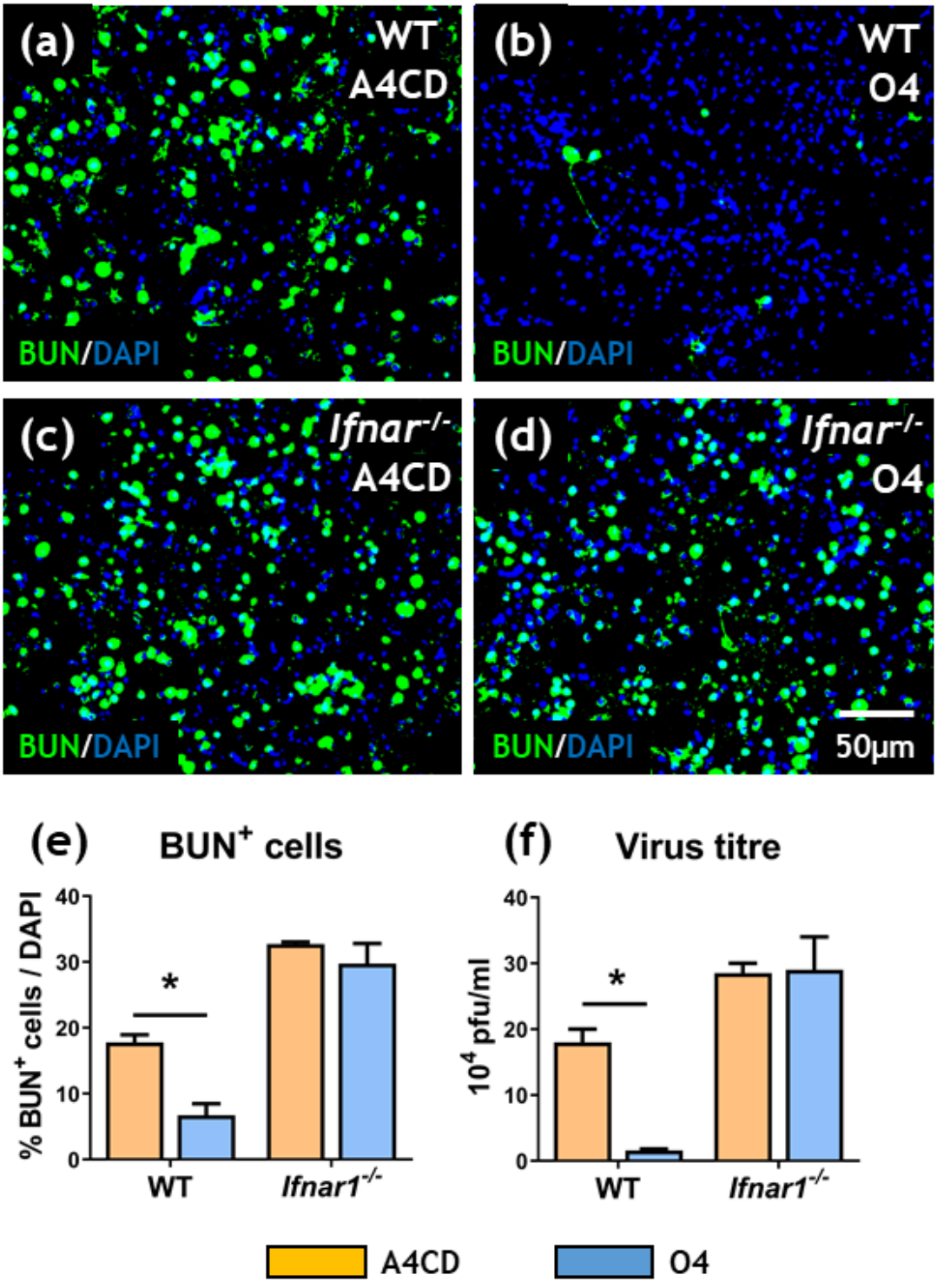

Figure 6.3 O4-mediated viral protection ablated in *Ifnar1*$^{-/-}$ cultures. DIV24 wild-type and *Ifnar1*$^{-/-}$ myelinated cultures pre-treated for 24 hrs with A4CD or O4 then infected with BUNV (a-d) Representative images of BUNV-infected (a, b) wild-type and (c, d) *Ifnar1*$^{-/-}$ cultures pre-treated with A4CD or O4. (e) Immunocytochemical analysis of BUN^{+} cells and (f) plaque assay analysis of supernatant virus titre. Data presented as mean (e) % BUN^{+} cells / DAPI (f) 10^{4} pfu/ml ± SEM. Analysed by two-way ANOVA and significance determined by Sidak's post *hoc* test. Significant difference denoted as *p < 0.05 (e) WT (n = 2). *Ifnar1*$^{-/-}$ (n = 3), (f) n = 2 all conditions.

mice were euthanised and the following tissues processed for RT-qPCR: olfactory bulb (OFB), cortex (CX), cerebellum (CB), and spleen (SP).

Ifnb1 and *Cxcl10* expression was increased in the OFB of rhIgM22-treated mice compared to PBSA and human IgM control (Fig 6.4 a & e). Due to the n-value of this pilot study, statistical significance could not be determined. No apparent difference was observed in *Ifnb1* or *Cxcl10* expression in CX, CB or SP (Fig 6.4 b-d, f-h).

These data provide a strong indication that rhIgM22 can induce a localised IFN response *in vivo* which could restrict SFV A7(74) replication. Future experiments could utilise a pharmacological agent to permeabilise OFB tight junctions to allow the antibody access to the brain parenchyma (Lochhead et al. 2015). However, if virus is also administered intranasally, the increase in OFB IFN-ß and ISGs might be sufficient to prevent virus spread to the brain parenchyma.

6.4.2 SFV successfully infects brain after intranasal administration

A second pilot experiment was performed to investigate the efficiency of intranasal administration of SFV A7(74) as this method has not been used by our laboratory previously. Nine-week-old male C57Bl/6 mice were infected i.n. for 24, 48 and 72 hrs with 1 x 10^5 pfu SFV. The suitability of this method was assessed by performing RT-qPCR for SFV *NSP3* expression, plaque assay on peripheral blood, and monitoring mouse health by weight change for the duration of the experiment.

No significant decrease in weight was observed for the duration of the experiment as determined by one-way ANOVA with Tukey's post *hoc* test (Fig 6.5 a & b). From analysis of OFB, CX and CB, *nsP3* expression appears to peak at 48 hrs and then plateau, with little apparent difference between 48 and 72 hrs (Fig 6.5 c-e). Viral gene expression is more robust in the OFB, with a log-fold difference observed in OFB *nsP3* expression compared to CX and CB (Fig 6.5 c-e). A similar trend was observed in plasma virus titres, where titres increase between 24 and 48 hrs and remain consistent between 48 and 72 hrs (Fig 6.5 f). These data show that i.n. administration of SFV leads to successful infection of the mouse CNS without causing measurable negative impact to animal health within 72 hrs of infection.

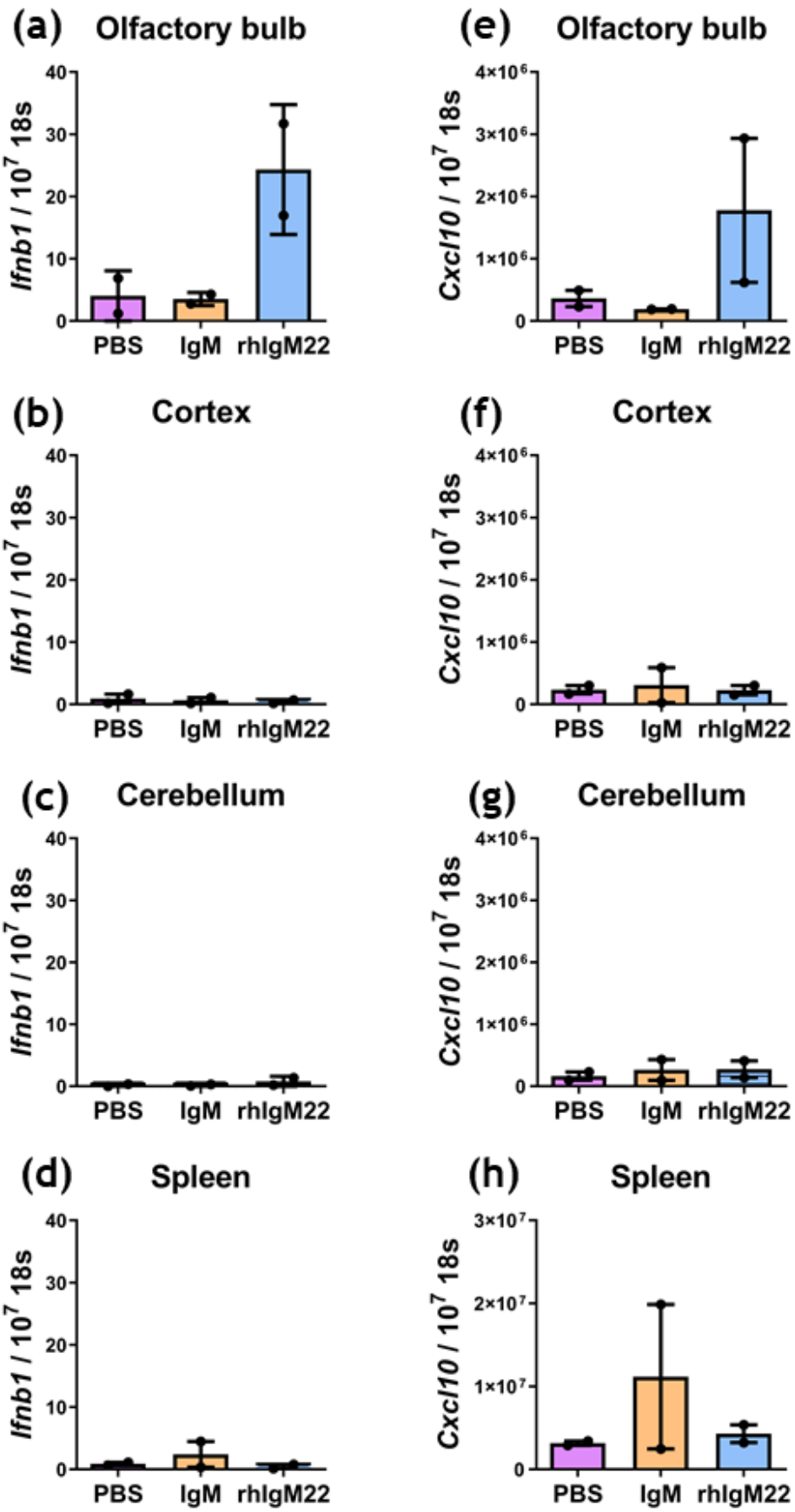

Figure 6.4 rhIgM22 induces interferon response in vivo. RT-qPCR analysis of (a-d) *Ifnb1* and (e-h) *Cxcl10* expression in olfactory bulb, cortex, cerebellum and spleen of nine-week-old male C57Bl/6 mice treated intranasally with PBS, IgM control or rhIgM22 for 24 hrs. Data expressed as mean copy number ± SD, n = 2.

6.5 Discussion

The data presented in this chapter show that O4 offers protection against a neurotropic virus *in vitro* and has made progress in the development of an *in vivo* model to study the functional antiviral properties of rhIgM22. Data presented in the current study alongside investigations by other colleagues show that these antibodies can protect against genetically unrelated viruses in an *Ifnar1*-dependent manner, and that protection is not specific to one cell-type, with neurons and oligodendrocytes protected from infection. Although *in vitro* data for SFV A7(74) was not presented in this thesis, these data have been published in Hayden et al. 2020 and the full paper can be found in Appendix 8.7.

Collectively, these data provide functional evidence for the observation that MS patients positive for lipid-reactive IgM have reduced risk of developing PML and could have wider implications for the treatment of viral encephalitis, a disease with limited treatment options due to the vast array of viruses that can cause encephalitis.

In vitro experiments were repeated with BUNV to determine whether this antibody-mediated IFN response was effective against multiple viruses, or if the effect was SFV-specific. Although BUNV tropism had not been determined previously, other members of the *Orthobunya* genus infect neurons, such as Akabane and La Crosse viruses (Kitani, Yamakawa, and Ikeda 2000; Blakqori et al. 2007). Our BUNV experiments showed that O4 is effective against two genetically unrelated viruses and that protection is not cell-type specific, with neurons and oligodendrocytes protected from viral infection.

An additional advantage of using BUNV is the human relevance of the pathogen, with many members of the *Orthobunyavirus* genus causing encephalitis in humans, and BUNV itself causing encephalitis in domestic animals (Balfour et al. 1973; Tauro et al. 2015). The *Orthobunyavirus* genus is of particular concern in terms of emerging and resurging viruses as they are vector borne and have a segmented genome. These two factors allow for migration to new geographic regions where the population might not have immunity and allows for genome reorganisation between different species of the genus, forming new viruses with altered pathogenicity (Hover et al. 2016). Both scenarios can lead to a pandemic

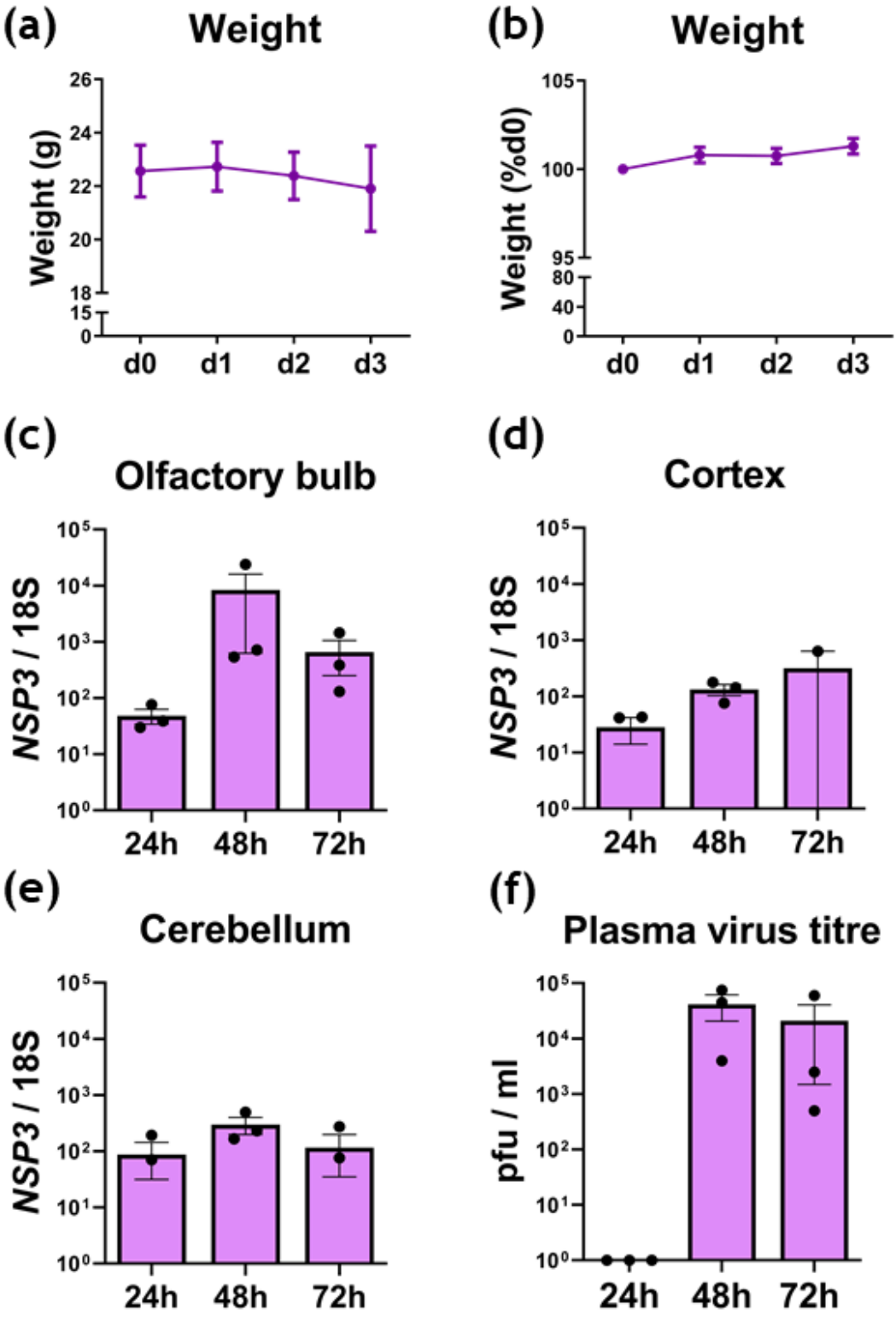

Figure 6.5: SFV successfully infects brain after intranasal administration. Nine-week-old male C57Bl/6 mice were infected intranasally with 10^5 pfu of SFV A7(74) mCherry for 24, 48 or 72 hrs. (a, b) weight of mice for duration of experiment presented as (a) grams and (b) % original weight ± SEM. Significant difference over time determined by Tukey's post *hoc* test. d0 (n = 9), d1 (n = 9), d2 (n = 6), d3 (n = 3) for each titre. (c-e) RT-qPCR for *NSP3* gene expression in olfactory bulb, cortex and cerebellum of infected mice. (f) Plasma virus titre as measured by plaque assay. Data presented as mean ± SEM. n = 3 all conditions.

where the risk of encephalitis is significant given the propensity of this virus family to migrate to the brain.

However, the *Orthobunyavirus* genus is not the only group of viruses that can cause encephalitis. In the *Alphavirus* family, from which SFV derives, there are a plethora of encephalitogenic viruses including Western, Eastern and Venezuelan equine viruses, Chikungunya virus, and Ross River virus (White et al. 2001; Julander et al. 2007; Gall et al. 2018). Again, *Alphaviruses* are vector-borne, and due to modern day factors such as climate change, urbanisation of tropical regions and, increased national and international transportation, these vector-borne viruses are more likely to cause pandemics from emergence or resurgence (Go, Balasuriya, and Lee 2014).

For IgM-mediated IFN-induction to be used as a prophylactic therapy for viral encephalitis, the virus in question must be IFN-sensitive. Viruses have different degrees of susceptibility to IFN, for example, *Alphaviruses* are particularly sensitive to IFN whilst IFN sensitivity can vary in other genera such as the *Flaviviruses* (Reynaud et al. 2015; Sooryanarain, Sapkal, and Gore 2012; Lin et al. 2004).

One factor that contributes to differential IFN susceptibility is the production of IFN antagonists by viruses. BUNV produces the non-structural protein NSs which inhibits RNA polymerase-II driven transcription, preventing IFN mRNA synthesis (Léonard et al. 2006). Despite this antagonistic property, the IFN response induced by O4 was sufficient to limit BUNV infection.

Other encephalitogenic viruses that are IFN-sensitive include Western and Venezuelan equine viruses, HSV1, Sindbis virus, pseudorabies virus, poliovirus, influenza A, Zika, West Nile and the newly emerged Tembusu virus (Wei et al. 2017; D.J. Carr and Campbell 2006; Lucas et al. 2003; Lancaster and Pfeiffer 2010; Gao et al. 2018; Julander et al. 2007; White et al. 2001; X. Wang et al. 2016). Therefore, a therapeutic that enhances endogenous IFN signalling could have broad protection against multiple viruses.

One possible limitation of this mechanism in the treatment of viral encephalitis is that induction of IFN's might not be effective after infection of the CNS. *In vitro* experiments using BUNV have shown that pre-treatment with IFN-β 24 hrs

prior to infection attenuated virus replication but administration of IFN 0, 6 or 24 hrs post-infection had no effect (Carlton-Smith and Elliott 2012). Similar *in vitro* experiments were performed on Japanese encephalitis virus, where IFN treatment limited virus infection when administered between 18 hrs prior to infection, up to 1 hr post-infection. After 1 hr post-infection, IFN had no effect on virus replication (Sooryanarain, Sapkal, and Gore 2012).

However, in the event of a pandemic where an outbreak of an encephalitogenic virus is apparent, there could be sufficient opportunity to administer the prophylactic treatment to unaffected individuals prior to infection. Similarly, viruses do not immediately infect the brain as they must first migrate through the periphery from the site of infection. *In vitro* experiments do not consider migration of the virus to the CNS or extravasation across the BBB. Instead, high quantities of virus are incubated with cells, often in the absence of innate or adaptive immune cells, making these models less physiologically relevant. Thus, prompt administration of a CNS-specific IFN-inducing therapy could be invaluable in preventing long-term neurological sequalae associated with viral encephalitis.

Although the prospect of a new treatment for viral encephalitis is exciting, the primary aim of this investigation was to explore the impact of lipid-reactive IgMs on JCV-mediated PML in the context of MS. JCV is an obligate human pathogen and therefore could not be used in our murine myelinated culture system or in our *in vivo* model (Tan and Koralnik 2010). Instead we used SFV strain A7(74) which, although genetically unrelated to JCV, causes demyelination *in vivo* making its pathogenesis functionally similar to JCV (Fazakerley and Webb 1987).

Prior research undertaken by colleagues in our laboratory showed that O4 and rhIgM22 could limit SFV A7(74) replication *in vitro* in an IFNAR1-dependent manner (Hayden et al. 2020). The next step in confirming IgM-mediated antiviral protection was to establish an *in vivo* model. Previous work undertaken by Clive McKimmie and Daniel McElroy failed to see antibody infiltration or antiviral activity in the CNS following i.p. or subcutaneous administration of lipid-reactive IgM. This was most likely due to the size of the IgM (~ 970 kDa) which fails to cross the BBB unless the BBB is compromised (Nilaratanakul et al. 2018).

Several alternative approaches were considered including intracerebral injection and co-administration of an adjuvant that would permeabilise the BBB, allowing IgM entry to the CNS. However, with the knowledge that puncture wounds and proinflammatory molecules could skew our results, we opted for the minimally invasive i.n. approach which was supported by studies showing improved transport across the BBB compared to i.p. (Chauhan and Chauhan 2015).

The data presented in this chapter show encouraging preliminary results regarding the efficacy of i.n. administration of rhIgM22, with IFN and ISG expression being observed in the OFB. Furthermore, the successful administration of SFV A7(74) intranasally lays the groundwork for future experiments exploring the functional antiviral activity of IFN-inducing IgM *in vivo*. Unfortunately, due to time constraints and the COVID-19 pandemic, a full *in vivo* experiment could not be performed combining both IgM administration and SFV A7(74) infection. However, results from both *in vitro* and preliminary *in vivo* experiments provide exciting functional data regarding the efficacy of lipid-reactive IgM antibodies against neurotropic virus infection.

Chapter 7

Discussion

7. Discussion

The data presented in this thesis demonstrate that a subset of human and mouse lipid-reactive IgM antibodies induce microglial IFN-β expression in a cGAS-STING-dependent manner, thereby triggering IFNAR1-dependent ISG expression in all major cell-types of the CNS. This antibody-mediated ISG response effectively limits the replication two genetically unrelated neurotropic viruses with different cellular tropisms, highlighting the broad efficacy of this antiviral response. Additionally, this thesis provides pilot data supporting the IFN-inducing properties of the recombinant human IgM22 *in vivo*.

These data provide a plausible explanation for the reduced incidence of natalizumab-induced PML in MS patients positive for intrathecal lipid-reactive IgM antibodies and achieves the aims set out at the beginning of this thesis (Villar et al. 2015). The data generated in this thesis has could provide the basis for a patient risk stratification system, allowing those positive for intrathecal lipid-reactive IgM to avail of high efficacy therapeutics earlier in their disease course. Confirmation of these data *in vivo* and/or with human-derived neural cells, as well as further understanding of this antiviral mechanism would be required to take this research to the stage of clinical application.

Although a plethora of highly effective drugs have been approved for the treatment of MS over the last 20 years, many of these come with serious side effects that are not associated with less effective therapeutics such as IFN-β or GA (Rae-Grant et al. 2018). The most serious of these side-effects is PML, with many MS drugs positively associated with this side effect (Berger 2017). The typical treatment strategy for MS is to prescribe lower risk first-line therapies initially, and then move on to higher risk therapies if the patient does not respond or if the disease course is aggressive (K.P. Johnson et al. 1995; Jacobs et al. 1996). Being able to identify patients with low risk of developing PML could allow patients early, safe access to higher efficacy drugs, thereby improving quality of life and life expectancy.

The data presented in this thesis advocates that intrathecal lipid-reactive IgM bands could be used as a risk stratification tool in the treatment of MS.

However, the experiments presented in this thesis investigate the acute effects of lipid-reactive IgM, with antibody being added to cultures no longer than 24 hrs before analysis or virus infection. Microglial have been shown to display exhaustion or senescence in the event of constant stimulation (Izzy et al. 2019; Angelova and Brown 2019). This begs the question as to whether lipid-reactive IgMs in MS patients offer protection if they are in constant contact with the CNS parenchyma. Given the human association between CSF IgM and reduced risk of PML, it is likely that antiviral protection occurs despite constant exposure. Whether this is due to a constant raised IFN-response or due to priming of microglia leading to a robust, prompt response in the event of virus infection remains to be seen and warrants further research (V.H. Perry and Holmes 2014).

Other MS phenotypes are associated with intrathecal lipid-reactive IgM bands, including a more aggressive disease course (Villar, Sadaba, et al. 2005). The data presented in Chapter 3 of this thesis has proposed that transient BBB permeability could allow serum protein entry to the CNS, leading to antibody-mediated demyelination. Demyelination could certainly contribute to a more aggressive disease course; however, this concept was not addressed *in vivo* with a physiologically relevant serum protein influx. Indeed, studies have shown that depletion of B cells, but not CSF antibody, leads to a reduction in relapse rates and new expanding lesions, adding further complexity to the role of lipid-reactive IgM in exacerbating MS disease course (Montalban et al. 2017).

The data presented in Chapter 3 could be considered two extreme examples of the CNS parenchyma, one with no BBB permeability and one with a massive influx of serum protein. To truly address the detrimental aspects of lipid-reactive IgM, one could consider using a BBB permeabilising agent at physiologically relevant concentrations such as a cytokine (e.g. TNF-α), or a systemic pathogen which causes BBB disturbances (Kido, Wright, and Merchant 1991; Tsao et al. 2001). The latter option could be particularly interesting as patients with RRMS often present with a relapse after experiencing an infection (Tarlinton et al. 2020).

Another aspect of the lipid-reactive IgM response that was not addressed fully in this thesis was the contribution of cytokines, chemokines, and peripheral immune cells post-IFN induction. In both MS and viral encephalitis, peripheral

immune cells can do more harm than good indicating that their role in this IgM response should be investigated (van Marle et al. 2004; Hausmann et al. 2004). Infiltrating leukocytes could exacerbate MS pathology, contributing to the associated aggressive disease course (Yamasaki and Kira 2019). Alternatively, the recruitment of immune cells could enhance the antiviral effect of these IFN-inducing IgMs (Hickey et al. 2007; Dedoni et al. 2018).

The potential of lipid-reactive IgMs to recruit peripheral immune cells could be investigated *in vivo* or *in vitro*. An *in vivo* investigation could characterise infiltrating immune cells to the CNS by fluorescence activated cell sorting, whilst *in vitro* migration experiments could be performed using a compartmentalised platform. In the latter example, CNS cells could be contained in one compartment, and peripheral immune cells in another. Using a transwell system or microfluidic device, the migration of immune cells could be examined upon IgM treatment of the CNS compartment. This experiment could be further enhanced by using peripheral immune cells derived from MS patients. The theory behind this being that MS is thought to be mediated by autoreactive T cells (Yamasaki and Kira 2019). It is uncertain whether T cells of a naïve mouse or healthy human would migrate to the CNS in response to lipid-reactive IgM. If migration occurred, these cells may not cause damage if not autoreactive. Thus, using MS patient-derived peripheral blood cells could provide a critical insight into the effect of lipid-reactive IgM of immune cell recruitment in the context of MS.

Although deciphering the peripheral immune cell response to IFN-inducing IgM is important, there are many mechanistic questions regarding this IgM response that remain to be answered. As detailed in Chapter 5, we hypothesised that IFN-inducing IgMs may either have a common structural feature that stimulates microglia IFN production, or that they have a common target which, upon phagocytosis, interacts with cGAS to upregulate IFN-β expression. The discussion of Chapter 5 detailed several hypotheses including receptors that could be involved. These hypotheses generate a plethora of future experiments that could be performed to deduce the mechanism of the IgM-mediated response.

The first of these would be determining whether lipid-reactive IgM is phagocytosed by microglia, and subsequently whether IFN-β expression is

dependent on IgM internalisation. IgM could be labelled with a pH-rhodo dye which would fluoresce only when internalised. If the IgM is internalised, inhibitors of phagocytosis could be used to assess its role in IFN upregulation. If phagocytosis was not involved in IFN induction, one could screen all known IFN-inducing IgMs using mass spectrometry to ascertain whether these IgMs have a common structural feature.

Elucidation of this mechanism could not only provide confirmation of the role of lipid-reactive IgM in reducing the risk pf PML but could be adapted as a broad-spectrum antiviral therapy that protects the CNS from encephalitogenic virus infection. We have demonstrated that oligodendrocyte binding is not required for this IFN response, with cultures lacking sulfatide capable of upregulating *Ifnb1* in the presence of the sulfatide-reactive IgM O4 (Fig 5.3). This was further supported by the fact that primary purified microglia could upregulate *Ifnb1* in response to rhIgM22 in the absence of oligodendroglial cells (< 1 %) (Fig 5.7). Therefore, understanding the downstream mechanism of this IgM-response could lead to the development of a small molecule agonist which induces IFN signalling without the need for a myelin-reactive IgM which can cause demyelination (Storch et al. 1998). Such an agonist could be used as a co-treatment with MS therapies or could be utilised as a stand-alone therapy in the treatment of viral encephalitis.

Viral encephalitis is a severe, life-threatening condition affecting those with weak or underdeveloped immune systems, particularly infants, the elderly, and the immunosuppressed (Rozenberg 2013). The incidence of viral encephalitis in the UK during the first three months of life is estimated at 80/100,000 live-births, a figure likely to increase due to failing vaccination rates and the continuous emergence of new viruses which can infect the CNS (Venkatesan and Murphy 2018; Afrough, Dowall, and Hewson 2019). Onset of neurological symptoms is rapid and severe, meaning fast effective treatment is vital to prevent permanent damage to the brain. Currently, antiviral therapies exist only for herpes viruses, meaning > 50% of cases are treated using generally supportive therapies (Chaudhuri and Kennedy 2002). The lack of antivirals is a major contributor to the high mortality rate and risk of chronic disability associated with viral encephalitis, highlighting a pressing need to develop broad-spectrum treatments.

A small molecule agonist of the interferon response could prime the CNS in advance of virus entering the CNS. This form of treatment could be administered on suspicion of sepsis in a patient, which poses substantial risk to virus entering the CNS from the blood stream. Furthermore, in the event of a pandemic where the virus can infect the brain leading to encephalitis, a prophylactic regiment could be employed.

If using the IgM mechanism as a prophylactic, the long-term dynamics of this IgM response should be investigated using low MOI of a clinically relevant neurotropic virus to ascertain how long a single dose of IgM could suppress CNS viral replication. This is of particular importance as BUNV-infected cells were still present in O4-treated cultures despite a significant reduction compared to IgM controls (Fig 6.2). It is possible that a virus could eventually overcome the IFN response and productively infect cells of the CNS. Many factors could affect this outcome including recruitment of peripheral immune cells and additional IgM doses post-infection.

Although two genetically unrelated viruses were used in this study, neither of these viruses are related to JCV, making direct comparison to PML difficult. Both BUNV and SFV are ssRNA viruses whilst JCV is a dsDNA virus. This is an important point as considerable differences have been documented regarding CNS responses to DNA and RNA viruses (Zhu et al. 2014; Ghosh et al. 2019).

JCV is an obligate human pathogen but experiments in this thesis have identified the cell types involved in this antiviral response (Tan and Koralnik 2010). Using this knowledge, hiPSC-derived microglia and oligodendrocytes could be co-cultured, treated with rhIgM22, and infected with JCV to investigate the IgMs antiviral potential in the context of PML. In the absence of a human-derived culture system, other human-relevant encephalitogenic viruses such as HSV1 and rabies virus could be studied using our murine myelinated culture model.

Although this thesis did not look directly at dsDNA viruses, many viruses including dsDNA viruses are susceptible to IFN as outlined in the discussion in Chapter 6. With the number of encephalitogenic viruses increasing due to increasing rates of virus emergence and resurgence, developing a safe, broad-spectrum therapeutic could prove invaluable should there be a pandemic

involving an encephalitogenic virus (Venkatesan and Murphy 2018; Afrough, Dowall, and Hewson 2019).

The results presented in this thesis make exciting progress in understanding the role of lipid-reactive IgM antibodies in controlling JCV in the context of iatrogenic PML. Although many questions remain, a fundamental understanding of this response has been established and the foundation has been laid to explore this phenomenon in detail both *in vitro* and *in vivo,* facilitating future research questions for years to come.

Chapter 8

Appendices

8 Appendices

8.1 List of genes differentially regulated by O4 compared to control IgM

Table 8.1: Genes differentially expressed by O4 compared to IgM control.

Gene_assignment	Symbol	Fold change
Chemokine (C-X-C motif) ligand 11	*Cxcl11*	79.7362
Chemokine (C-X-C motif) ligand 9	*Cxcl9*	59.2941
Chemokine (C-X-C motif) ligand 13	*Cxcl13*	40.2532
Interferon-induced protein with tetratricopeptide repeats 3	*Ifit3*	39.2844
Chemokine (C-X-C motif) ligand 10	*Cxcl10*	34.8727
2'-5'-oligoadenylate synthetase-like	*Oasl*	32.0291
Interferon-induced protein with tetratricopeptide repeats 2	*Ifit2*	25.1158
Myxovirus (influenza virus) resistance 1	*Mx1*	23.2507
Radical S-adenosyl methionine domain containing 2	*Rsad2*	22.189
Chemokine (C-X-C motif) ligand 17	*Cxcl17*	18.8138
Interferon regulatory factor 7	*Irf7*	18.6748
Interferon stimulated exonuclease gene 20	*Isg20*	17.3376
Guanylate binding protein 5	*Gbp5*	16.1022
Chemokine (C-C motif) ligand 5	*Ccl5*	16.0463
Apolipoprotein L 9a	*Apol9a*	15.3545
Coagulation factor X	*F10*	13.5068
DEAD (Asp-Glu-Ala-Asp) box polypeptide 60	*Ddx60*	13.0554
Z-DNA binding protein 1	*Zbp1*	12.9286
Chemokine (C-C motif) ligand 7	*Ccl7*	12.8555
Lipocalin 2	*Lcn2*	12.1514
ISG15 ubiquitin-like modifier	*Isg15*	12.0388
Ubiquitin specific peptidase 18	*Usp18*	11.6987
2'-5' oligoadenylate synthetase 2	*Oas2*	9.82098
Lectin, galactoside-binding, soluble, 9	*Lgals9*	9.59523
RT1 class I, locus T24, gene 3	*RT1-T24-3*	9.56269
2-5 oligoadenylate synthetase 1B	*Oas1b*	9.4805
Chemokine (C-C motif) ligand 19	*Ccl19*	9.15446
Serpin peptidase inhibitor, clade E	*Serpine1*	8.99302
Cd72 molecule	*Cd72*	8.88603
Chemokine (C-C motif) ligand 12	*Ccl12*	8.69854
C-type lectin domain family 4, member A2	*Clec4a2*	8.15189
Interferon, alpha-inducible protein 27 like 2B	*Ifi27l2b*	8.05335
Macrophage activation 2 like	*Mpa2l*	7.98949
Interleukin 1 beta	*Il1b*	7.81047

Continued overleaf

DEXH (Asp-Glu-X-His) box polypeptide 58	*Dhx58*	7.62494
Complement component 3	*C3*	7.5046
ATP-binding cassette, sub-family B	*Tap1*	7.4345
Sialic acid binding Ig-like lectin 1	*Siglec1*	7.3837
SLAM family member 9	*Slamf9*	7.38286
2 ' -5 ' oligoadenylate synthetase 1l	*Oas1i*	7.10639
similar to CDNA sequence BC023105	*RGD1305184*	6.93611
Ubiquitin-like modifier activating enzyme 7	*Uba7*	6.80602
Sialic acid binding Ig-like lectin 5	*Siglec5*	6.58333
RT1 class I, locus CE4	*RT1-CE4*	6.37515
Cytidine monophosphate (UMP-CMP) kinase 2	*Cmpk2*	6.31348
Interleukin 18 binding protein	*Il18bp*	6.31101
Proteasome (prosome, macropain) subunit, beta type, 9	*Psmb9*	6.2268
Schlafen 3	*Slfn3*	6.17622
similar to interferon-inducible GTPase	*RGD1309362*	6.08175
CD14 molecule	*Cd14*	5.94211
Schlafen 1	*Slfn1*	5.86435
Baculoviral IAP repeat-containing 3	*Birc3*	5.84982
EGF-like module containing, mucin-like, hormone receptor-like 1	*Emr1*	5.82108
RT1 class I, locus CE12	*RT1-CE12*	5.72942
Epstein-Barr virus induced 3	*Ebi3*	5.66954
Apolipoprotein L, 3	*Apol3*	5.66729
RT1 class Ib, locus S3	*RT1-S3*	5.6581
Interleukin 1 alpha	*Il1a*	5.65014
RT1 class Ib, locus N3	*RT1-N3*	5.5771
Proteasome (prosome, macropain) subunit, beta type, 8	*Psmb8*	5.5665
Transmembrane protein 106A	*Tmem106a*	5.55969
SP100 nuclear antigen	*Sp100*	5.49596
Cholesterol 25-hydroxylase	*Ch25h*	5.49127
Integrin, alpha L	*Itgal*	5.44722
TAP binding protein (tapasin)	*Tapbp*	5.42862
Solute carrier family 11	*Slc11a1*	5.37202
Apolipoprotein L, 3	*Apol3*	5.30033
Secretory leukocyte peptidase inhibitor	*Slpi*	5.1551
Tumor necrosis factor, alpha-induced protein 2	*Tnfaip2*	5.12828
Interferon gamma inducible protein 47	*Ifi47*	5.10619
Ras-related C3 botulinum toxin substrate 2	*Rac2*	4.98633
Placenta-specific 8 2	*Plac8*	4.95667
Vascular cell adhesion molecule 1	*Vcam1*	4.89255
Interferon induced with helicase C domain 1	*Ifih1*	4.87846
G protein-coupled receptor 31	*Gpr31*	4.81717
Chemokine (C-C motif) ligand 4	*Ccl4*	4.75997
Triggering receptor expressed on myeloid cells 1	*Trem1*	4.63838
SLP adaptor and CSK interacting membrane protein	*Scimp*	4.60533
Torsin family 3, member A	*Tor3a*	4.41821
Membrane-spanning 4-domains, subfamily A, member 11	*Ms4a11*	4.34413
Peroxisomal proliferator-activated receptor A	*Pric285*	4.32606

Continued overleaf

2'-5' oligoadenylate synthetase-like 2	*Oasl2*	4.30435
Suppressor of cytokine signaling 1	*Socs1*	4.29259
Receptor (chemosensory) transporter protein 4	*Rtp4*	4.28647
Integrin, alpha M	*Itgam*	4.27776
Caspase 12	*Casp12*	4.27644
Poly (ADP-ribose) polymerase family, member 12	*Parp12*	4.27329
Lymphocyte antigen 6 complex, locus E	*Ly6e*	4.23903
Schlafen family member 13	*Slfn13*	4.19856
Immunity-related GTPase family, M	*Irgm*	4.09964
Similar to cDNA sequence BC023105	*MGC105567*	4.09651
Hemopoietic cell kinase	*Hck*	4.09429
Proteasome (prosome, macropain) subunit, beta type 10	*Psmb10*	4.08229
Chemokine (C-X-C motif) ligand 16	*Cxcl16*	3.97104
Transporter 2, ATP-binding cassette, sub-family B	*Tap2*	3.95693
Protein phosphatase, Mg2+/Mn2+ dependent, 1N	*Ppm1n*	3.9428
CD274 molecule	*Cd274*	3.91386
Macrophage scavenger receptor 1	*Msr1*	3.91039
ATP-binding cassette, subfamily B, member 1B	*Abcb1b*	3.90055
Schlafen family member 5	*Slfn5*	3.87482
Gardner-Rasheed feline sarcoma viral oncogene homolog	*Fgr*	3.83537
Copine II	*Cpne2*	3.82874
Toll-like receptor 3	*Tlr3*	3.82344
PML-RARA regulated adaptor molecule 1	*Pram1*	3.79098
Similar to interferon-inducible GTPase	*MGC108823*	3.76991
SP140 nuclear body protein	*Sp140*	3.75265
Ubiquitin-conjugating enzyme E2L 6	*Ube2l6*	3.73676
Fc fragment of IgG, low affinity IIIa, receptor	*Fcgr3a*	3.71977
solute carrier family 4 (anion exchanger), member 1	*Slc4a1*	3.68246
Caspase 1	*Casp1*	3.6349
Lectin, galactose binding, soluble 5	*Lgals5*	3.62343
Chemokine (C-C motif) ligand 3	*Ccl3*	3.61866
Sterile alpha motif domain containing 9-like	*Samd9l*	3.5876
Interferon-induced protein 44	*Ifi44*	3.56483
Lymphocyte antigen 86	*Ly86*	3.54101
Solute carrier family 6	*Slc6a12*	3.53763
Cd74 molecule	*Cd74*	3.51855
Guanylate binding protein 1, interferon-inducible	*Gbp1*	3.5101
Proline-serine-threonine phosphatase-interacting protein 1	*Pstpip1*	3.47141
Chemokine (C-X-C motif) ligand 1	*Cxcl1*	3.45088
B-cell CLL/lymphoma 3	*Bcl3*	3.35497
Neutrophil cytosolic factor 1	*Ncf1*	3.35132
Cd69 molecule	*Cd69*	3.32274
Signal transducer and activator of transcription 2	*Stat2*	3.31276
Intercellular adhesion molecule 1	*Icam1*	3.27673
Leucine rich repeat containing 25	*Lrrc25*	3.2755
Interleukin 1 receptor antagonist	*Il1rn*	3.24795
RT1 class I, locus1	*RT1-CE1*	3.1983

Continued overleaf

Family with sequence similarity 46, member A	*Fam46a*	3.18129
Hyaluronan synthase 2	*Has2*	3.17919
Serpin peptidase inhibitor, clade G (C1 inhibitor), member 1	*Serping1*	3.17837
RAS p21 protein activator 4	*Rasa4*	3.16678
G protein-coupled receptor 114	*Gpr114*	3.15438
Pleckstrin	*Plek*	3.14351
Tripartite motif-containing 21	*Trim21*	3.13756
Receptor-interacting serine-threonine kinase 3	*Ripk3*	3.12414
Carbonic anhydrase 13	*Car13*	3.12011
Integrin, beta 2	*Itgb2*	3.10169
Indoleamine 2,3-dioxygenase 2	*Ido2*	3.08277
Nuclear factor of kappa light polypeptide gene enhancer in B-cells inhibitor epsilon	*Nfkbie*	3.07715
Interferon regulatory factor 9	*Irf9*	3.07097
RT1 class II, locus Da	*RT1-Da*	3.06181
Nuclear factor of kappa light polypeptide gene enhancer in B-cells	*Nfkb2*	3.0414
Gamma-secretase activating protein	*Gsap*	3.03608
Uridine phosphorylase 1	*Upp1*	3.03137
Lectin, galactoside-binding, soluble, 3 binding protein	*Lgals3bp*	3.02969
Interferon-induced protein 35	*Ifi35*	3.0272
Moloney leukemia virus 10	*Mov10*	3.02089
Three prime repair exonuclease 1	*Trex1*	3.00062
RT1 class Ib, locus N2	*RT1-N2*	2.98428
Tripartite motif-containing 30	*Trim30*	2.97097
Retinol binding protein 1, cellular	*Rbp1*	2.9326
Zinc finger, NFX1-type containing 1	*Znfx1*	2.93148
Tubulin, alpha 1C	*Tuba1c*	2.92612
Tripartite motif-containing 25	*Trim25*	2.92547
PYD and CARD domain containing	*Pycard*	2.90794
C-type lectin domain family 4, member A1	*Clec4a1*	2.87707
Tumor necrosis factor (ligand) superfamily, member 10	*Tnfsf10*	2.86467
Major vault protein	*Mvp*	2.84297
Chemokine (C-C motif) ligand 20	*Ccl20*	2.81924
Schlafen 2	*Slfn2*	2.8115
Toll-like receptor 7	*Tlr7*	2.80452
Complement component 1, r subcomponent	*C1r*	2.79381
Pyrimidinergic receptor P2Y, G-protein coupled, 6	*P2ry6*	2.79159
Immunoresponsive gene 1	*Irg1*	2.7901
Leukocyte immunoglobulin-like receptor, subfamily B, member 4	*Lilrb4*	2.78747
Sterile alpha motif domain containing 9-like	*Samd9l*	2.78526
C-type lectin domain family 4, member D	*Clec4d*	2.78414
N-myc (and STAT) interactor	*Nmi*	2.78359
Hematopoietic cell specific Lyn substrate 1	*Hcls1*	2.72859
Receptor-interacting serine-threonine kinase 2	*Ripk2*	2.71916
Chemokine (C-C motif) ligand 2	*Ccl2*	2.70529

Continued overleaf

Superoxide dismutase 2, mitochondrial	*Sod2*	2.70316
TAP binding protein-like	*Tapbpl*	2.69982
RT1 class II, locus Ba	*RT1-Ba*	2.6907
v-rel reticuloendotheliosis viral oncogene homolog B	*Relb*	2.68848
Discoidin domain receptor tyrosine kinase 2	*Ddr2*	2.68667
similar to cell surface receptor FDFACT	*RGD1561730*	2.65378
v-yes-1 Yamaguchi sarcoma viral related oncogene homolog	*Lyn*	2.62031
RT1 class Ib, locus M3, gene 1	*RT1-M3-1*	2.61471
RT1 class I, locus CE5	*RT1-CE5*	2.61365
C3ar1	*C3ar1*	2.60414
Interleukin 18	*Il18*	2.59538
Proteasome (prosome, macropain) activator subunit 2	*Psme2*	2.58634
Mucin 15, cell surface associated	*Muc15*	2.58626
Zinc finger CCCH type containing 12A	*Zc3h12a*	2.58331
SEC14-like 4 (S. cerevisiae)	*Sec14l4*	2.57117
FYN binding protein	*Fyb*	2.55272
Src-like adaptor	*Sla*	2.54628
Integrin, alpha X	*Itgax*	2.54169
Oncostatin M receptor	*Osmr*	2.47349
C-type lectin domain family 2, member G	*Clec2g*	2.47247
Piezo-type mechanosensitive ion channel component 1	*Piezo1*	2.46581
Interferon induced transmembrane protein 3	*Ifitm3*	2.4526
C-type lectin domain family 4, member E	*Clec4e*	2.43917
Caspase 7	*Casp7*	2.42174
Retinoic acid receptor responder (tazarotene induced) 2	*Rarres2*	2.40935
Epithelial stromal interaction 1 (breast)	*Epsti1*	2.39924
SLAM family member 8	*Slamf8*	2.39503
Allograft inflammatory factor 1	*Aif1*	2.39266
Cd80 molecule	*Cd80*	2.37727
Transferrin	*Tf*	2.37088
Tripartite motif-containing 34	*Trim34*	2.3646
Zinc finger CCCH type, antiviral 1	*Zc3hav1*	2.36084
Triggering receptor expressed on myeloid cells 3	*Trem3*	2.32497
Lymphocyte-specific protein 1	*Lsp1*	2.3206
Ras homolog family member H	*Rhoh*	2.31907
Interferon induced transmembrane protein 2	*Ifitm2*	2.31363
Toll-like receptor 2	*Tlr2*	2.31292
Acyloxyacyl hydrolase (neutrophil)	*Aoah*	2.30512
Immunoglobulin superfamily, member 6	*Igsf6*	2.2879
Cystatin F (leukocystatin)	*Cst7*	2.27646
Cytochrome b-245, alpha polypeptide	*Cyba*	2.25658
Capping protein (actin filament), gelsolin-like	*Capg*	2.25582
Solute carrier family 12	*Slc12a7*	2.25377
Mannose receptor, C type 2	*Mrc2*	2.25062
Selectin P ligand	*Selplg*	2.24831
Torsin family 1, member B	*Tor1b*	2.23279
SH2 domain containing 1B	*Sh2d1b*	2.22549

Continued overleaf

Phospholipase A2, group XVI	*Pla2g16*	2.22289
Annexin A4	*Anxa4*	2.21913
Exocyst complex component 3-like 4	*Exoc3l4*	2.21291
Nuclear factor of kappa light polypeptide gene enhancer in B-cells inhibitor alpha	*Nfkbia*	2.21147
NLR family, pyrin domain containing 1A	*Nlrp1a*	2.20792
Tumor necrosis factor receptor superfamily, member 1b	*Tnfrsf1b*	2.20223
Myosin binding protein H-like	*Mybphl*	2.17914
Basic leucine zipper transcription factor, ATF-like 2	*Batf2*	2.17879
Interferon, alpha-inducible protein 27	*Ifi27*	2.1619
Interleukin 13 receptor, alpha 1	*Il13ra1*	2.15777
F-box and WD-40 domain protein 17	*Fbxw17*	2.15127
Poly (ADP-ribose) polymerase family, member 10	*Parp10*	2.14615
Proteasome (prosome, macropain) activator subunit 1	*Psme1*	2.14468
Xanthine dehydrogenase	*Xdh*	2.13267
Cytochrome P450, family 4, subfamily v, polypeptide 3	*Cyp4v3*	2.10944
solute carrier family 7	*Slc7a7*	2.10607
Transient receptor potential cation channel, subfamily M	*Trpm2*	2.08065
Interleukin 7	*Il7*	2.05692
Leukocyte specific transcript 1	*Lst1*	2.03649
Translocator protein	*Tspo*	2.03026
Interleukin 13 receptor, alpha 1	*Il13ra1*	2.01715
Chitinase 3-like 1 (cartilage glycoprotein-39)	*Chi3l1*	2.01468
CDC42 effector protein (Rho GTPase binding) 5	*Cdc42ep5*	2.00798
Vesicle-associated membrane protein 5	*Vamp5*	2.00585
BCL2-related protein A1	*Bcl2a1*	2.005
Transmembrane protein 140	*Tmem140*	2.00013
Leucine rich repeat containing 2	*Lrrc2*	-2.07519
Na+/K+ transporting ATPase interacting 4	*Nkain4*	-2.10143
Glutamate receptor, ionotropic, N-methyl D-aspartate 2C	*Grin2c*	-2.11196
Galanin-like peptide	*Galp*	-2.11757
Claudin 19	*Cldn19*	-2.15078
Chemokine (C-C motif) ligand 24	*Ccl24*	-2.17139
Flavin containing monooxygenase 1	*Fmo1*	-2.24302
Double C2-like domains, gamma	*Doc2g*	-2.32026
Toll-like receptor 5	*Tlr5*	-2.4412
Protein phosphatase 1, regulatory (inhibitor) subunit 1B	*Ppp1r1b*	-2.55688
3'-phosphoadenosine 5'-phosphosulfate synthase 2	*Papss2*	-2.84374
Stabilin 1	*Stab1*	-3.07842
Solute carrier family 40 (iron-regulated transporter), member 1	*Slc40a1*	-3.19828
Succinate receptor 1	*Sucnr1*	-3.29219

Table 8.1: Genes differentially regulated by O4 compared to IgM control. Table showing genes differentially regulated by O4, fold change ≥ 2, FDR adjusted $p < 0.05$.

8.2 List of genes and annotation terms associated with each cluster identified in functional annotation cluster analysis

Table 8.2: Functional annotation cluster analysis, cluster 1, innate immunity

CLUSTER 1			
Database	**Annotation Term**	**Count**	***q*-value**
UP_KEYWORDS	Immunity	36	4.50E-27
UP_KEYWORDS	Innate immunity	21	3.50E-15
GOTERM_BP_DIRECT	innate immune response	28	3.10E-14

Gene Symbol	**Gene Name**
Oas2	2'-5' oligoadenylate synthetase 2(Oas2)
Oasl2	2'-5' oligoadenylate synthetase-like 2(Oasl2)
Oasl	2'-5'-oligoadenylate synthetase-like(Oasl)
Oas1b	2-5 oligoadenylate synthetase 1B(Oas1b)
Clec4d	C-type lectin domain family 4, member D(Clec4d)
Clec4e	C-type lectin domain family 4, member E(Clec4e)
Cd14	CD14 molecule(Cd14)
Cd74	CD74 molecule(Cd74)
Fgr	FGR proto-oncogene, Src family tyrosine kinase(Fgr)
Hck	HCK proto-oncogene, Src family tyrosine kinase(Hck)
Lyn	LYN proto-oncogene, Src family tyrosine kinase(Lyn)
Nlrp1a	NLR family, pyrin domain containing 1A(Nlrp1a)
Relb	RELB proto-oncogene, NF-kB subunit(Relb)
RT1-CE12	RT1 class I, locus CE12(RT1-CE12)
RT1-CE4	RT1 class I, locus CE4(RT1-CE4)
RT1-CE5	RT1 class I, locus CE5(RT1-CE5)
RT1-CE1	RT1 class I, locus1(RT1-CE1)
RT1-Ba	RT1 class II, locus Ba(RT1-Ba)
RT1-Da	RT1 class II, locus Da(RT1-Da)
C3	complement C3(C3)
Cyba	cytochrome b-245 alpha chain(Cyba)
Lgals9	galectin 9(Lgals9)
Irgm	immunity-related GTPase M(Irgm)
Ido2	indoleamine 2,3-dioxygenase 2(Ido2)
Ifih1	interferon induced with helicase C domain 1(Ifih1)
Lcn2	lipocalin 2(Lcn2)
Mx1	myxovirus (influenza virus) resistance 1(Mx1)
Nfkb2	nuclear factor kappa B subunit 2(Nfkb2)
Psmb8	proteasome subunit beta 8(Psmb8)
Psmb9	proteasome subunit beta 9(Psmb9)
Rsad2	radical S-adenosyl methionine domain containing 2(Rsad2)
Ripk2	receptor-interacting serine-threonine kinase 2(Ripk2)
Slpi	secretory leukocyte peptidase inhibitor(Slpi)

Continued overleaf

Serping1	serpin family G member 1(Serping1)
Tlr2	toll-like receptor 2(Tlr2)
Tlr3	toll-like receptor 3(Tlr3)
Tlr5	toll-like receptor 5(Tlr5)
Tlr7	toll-like receptor 7(Tlr7)
Tap1	transporter 1, ATP binding cassette subfamily B member(Tap1)
Tap2	transporter 2, ATP binding cassette subfamily B member(Tap2)
Trim21	tripartite motif-containing 21(Trim21)
Trim25	tripartite motif-containing 25(Trim25)
Zc3h12a	zinc finger CCCH type containing 12A(Zc3h12a)
Zc3hav1	zinc finger CCCH-type containing, antiviral 1(Zc3hav1)

Table 8.2: Functional annotation cluster analysis, cluster 1, innate immunity. Table showing genes and annotation terms in cluster 1. “Database” indicates where the annotation term was derived, “Count” is the number of genes associated with the annotation term and *q*-value is the Bonferroni adjusted *p*-value.

Table 8.3: Functional annotation cluster analysis, cluster 2, viral defence

CLUSTER 2			
Database	**Annotation Term**	**Count**	***q*-value**
GOTERM_BP_DIRECT	response to virus	19	1.00E-14
GOTERM_BP_DIRECT	negative regulation of viral genome	11	2.60E-09
UP_KEYWORDS	Antiviral defense	8	1.10E-04

Gene Symbol	**Gene Name**
Oas2	2'-5' oligoadenylate synthetase 2(Oas2)
Oasl2	2'-5' oligoadenylate synthetase-like 2(Oasl2)
Oasl	2'-5'-oligoadenylate synthetase-like(Oasl)
Oas1b	2-5 oligoadenylate synthetase 1B(Oas1b)
Bcl3	B-cell CLL/lymphoma 3(Bcl3)
Ccl5	C-C motif chemokine ligand 5(Ccl5)
Cxcl10	C-X-C motif chemokine ligand 10(Cxcl10)
Dhx58	DEXH-box helicase 58(Dhx58)
Isg15	ISG15 ubiquitin-like modifier(Isg15)
Ifitm2	interferon induced transmembrane protein 2(Ifitm2)
Ifitm3	interferon induced transmembrane protein 3(Ifitm3)
Ifih1	interferon induced with helicase C domain 1(Ifih1)
Isg20	interferon stimulated exonuclease gene 20(Isg20)
Ifit2	interferon-induced protein with tetratricopeptide repeats 2(Ifit2)
Ifit3	interferon-induced protein with tetratricopeptide repeats 3(Ifit3)
Lcn2	lipocalin 2(Lcn2)
Mx1	myxovirus (influenza virus) resistance 1(Mx1)
Parp10	poly (ADP-ribose) polymerase family, member 10(Parp10)
Rsad2	radical S-adenosyl methionine domain containing 2(Rsad2)
Slpi	secretory leukocyte peptidase inhibitor(Slpi)
Tlr3	toll-like receptor 3(Tlr3)
Zc3hav1	zinc finger CCCH-type containing, antiviral 1(Zc3hav1)

Table 8.3: Functional annotation cluster analysis, cluster 2, viral defence. Table showing genes and annotation terms in cluster 2. “Database” indicates where the annotation term was derived, “Count” is the number of genes associated with the annotation term and *q*-value is the Bonferroni adjusted *p*-value.

Table 8.4: Functional annotation cluster analysis, cluster 3, inflammatory response

CLUSTER 3			
Database	**Annotation Term**	**Count**	***q*-value**
GOTERM_BP_DIRECT	inflammatory response	38	2.70E-23
UP_KEYWORDS	Inflammatory response	20	1.40E-17
GOTERM_MF_DIRECT	chemokine activity	15	1.50E-15
INTERPRO	Chemokine interleukin-8-like domain	14	5.10E-14
SMART	SCY	14	2.50E-14
GOTERM_BP_DIRECT	cellular response to tumor necrosis factor	21	3.30E-13
UP_KEYWORDS	Chemotaxis	15	8.50E-14
GOTERM_BP_DIRECT	cellular response to interferon-gamma	16	9.80E-13
GOTERM_BP_DIRECT	neutrophil chemotaxis	15	1.30E-11
UP_KEYWORDS	Cytokine	18	2.40E-12
GOTERM_BP_DIRECT	cellular response to interleukin-1	17	1.10E-10
GOTERM_BP_DIRECT	chemokine-mediated signaling pathway	14	2.60E-10
GOTERM_BP_DIRECT	positive regulation of ERK1 and ERK2 cascade	20	2.80E-09
KEGG_PATHWAY	Chemokine signaling pathway	22	5.60E-10
GOTERM_BP_DIRECT	lymphocyte chemotaxis	9	2.00E-07
KEGG_PATHWAY	Cytokine-cytokine receptor interaction	21	4.00E-08
GOTERM_MF_DIRECT	CCR chemokine receptor binding	8	6.80E-07
GOTERM_BP_DIRECT	monocyte chemotaxis	9	6.00E-06
INTERPRO	CC chemokine, conserved site	7	2.60E-06
GOTERM_BP_DIRECT	chemotaxis	11	8.90E-06
GOTERM_CC_DIRECT	extracellular space	39	1.60E-04
GOTERM_BP_DIRECT	positive regulation of inflammatory response	9	1.60E-03
GOTERM_BP_DIRECT	eosinophil chemotaxis	5	6.80E-03
UP_KEYWORDS	Secreted	31	1.30E-03

Gene Symbol	**Gene Name**
Abcb1b	ATP-binding cassette, subfamily B (MDR/TAP), member 1B(Abcb1b)
Ccl19	C-C motif chemokine ligand 19(Ccl19)
Ccl2	C-C motif chemokine ligand 2(Ccl2)
Ccl20	C-C motif chemokine ligand 20(Ccl20)
Ccl24	C-C motif chemokine ligand 24(Ccl24)
Ccl3	C-C motif chemokine ligand 3(Ccl3)
Ccl4	C-C motif chemokine ligand 4(Ccl4)
Ccl5	C-C motif chemokine ligand 5(Ccl5)
Ccl7	C-C motif chemokine ligand 7(Ccl7)
Cxcl1	C-X-C motif chemokine ligand 1(Cxcl1)
Cxcl10	C-X-C motif chemokine ligand 10(Cxcl10)
Cxcl11	C-X-C motif chemokine ligand 11(Cxcl11)
Cxcl13	C-X-C motif chemokine ligand 13(Cxcl13)
Cxcl16	C-X-C motif chemokine ligand 16(Cxcl16)
Cxcl17	C-X-C motif chemokine ligand 17(Cxcl17)

Continued overleaf

Cxcl9	C-X-C motif chemokine ligand 9(Cxcl9)
Cd14	CD14 molecule(Cd14)
Cd74	CD74 molecule(Cd74)
Fgr	FGR proto-oncogene, Src family tyrosine kinase(Fgr)
Hck	HCK proto-oncogene, Src family tyrosine kinase(Hck)
Lyn	LYN proto-oncogene, Src family tyrosine kinase(Lyn)
Mov10	Mov10 RISC complex RNA helicase(Mov10)
Nfkbia	NFKB inhibitor alpha(Nfkbia)
Nlrp1a	NLR family, pyrin domain containing 1A(Nlrp1a)
Pycard	PYD and CARD domain containing(Pycard)
Relb	RELB proto-oncogene, NF-kB subunit(Relb)
Scimp	SLP adaptor and CSK interacting membrane protein(Scimp)
Tnfrsf1b	TNF receptor superfamily member 1B(Tnfrsf1b)
Aif1	allograft inflammatory factor 1(Aif1)
Birc3	baculoviral IAP repeat-containing 3(Birc3)
Capg	capping actin protein, gelsolin like(Capg)
Ccl12	chemokine (C-C motif) ligand 12(Ccl12)
Chi3l1	chitinase 3 like 1(Chi3l1)
F10	coagulation factor X(F10)
C3	complement C3(C3)
C3ar1	complement C3a receptor 1(C3ar1)
Cst7	cystatin F(Cst7)
Cyba	cytochrome b-245 alpha chain(Cyba)
Galp	galanin-like peptide(Galp)
Lgals3bp	galectin 3 binding protein(Lgals3bp)
Lgals9	galectin 9(Lgals9)
Gbp1	guanylate binding protein 1(Gbp1)
Gbp5	guanylate binding protein 5(Gbp5)
Has2	hyaluronan synthase 2(Has2)
Itgam	integrin subunit alpha M(Itgam)
Itgb2	integrin subunit beta 2(Itgb2)
Icam1	intercellular adhesion molecule 1(Icam1)
Il1a	interleukin 1 alpha(Il1a)
Il1b	interleukin 1 beta(Il1b)
Il1rn	interleukin 1 receptor antagonist(Il1rn)
Il13ra1	interleukin 13 receptor subunit alpha 1(Il13ra1)
Il18bp	interleukin 18 binding protein(Il18bp)
Il18	interleukin 18(Il18)
Il7	interleukin 7(Il7)
Lcn2	lipocalin 2(Lcn2)
Lsp1	lymphocyte-specific protein 1(Lsp1)
Ncf1	neutrophil cytosolic factor 1(Ncf1)
Nfkb2	nuclear factor kappa B subunit 2(Nfkb2)
Osmr	oncostatin M receptor(Osmr)
Psmb9	proteasome subunit beta 9(Psmb9)
Rac2	ras-related C3 botulinum toxin substrate 2 (rho family, small GTP binding protein Rac2)(Rac2)
Ripk2	receptor-interacting serine-threonine kinase 2(Ripk2)

Continued overleaf

Rarres2	retinoic acid receptor responder 2(Rarres2)
Slpi	secretory leukocyte peptidase inhibitor(Slpi)
Serpine1	serpin family E member 1(Serpine1)
Serping1	serpin family G member 1(Serping1)
Stat2	signal transducer and activator of transcription 2(Stat2)
Slc11a1	solute carrier family 11 member 1(Slc11a1)
Tlr2	toll-like receptor 2(Tlr2)
Tlr3	toll-like receptor 3(Tlr3)
Tlr5	toll-like receptor 5(Tlr5)
Tlr7	toll-like receptor 7(Tlr7)
Tf	transferrin(Tf)
Trem1	triggering receptor expressed on myeloid cells 1(Trem1)
Trem3	triggering receptor expressed on myeloid cells 3(Trem3)
Tnfsf10	tumor necrosis factor superfamily member 10(Tnfsf10)
Vcam1	vascular cell adhesion molecule 1(Vcam1)
Xdh	xanthine dehydrogenase(Xdh)
Zc3h12a	zinc finger CCCH type containing 12A(Zc3h12a)

Table 8.4: Functional annotation cluster analysis, cluster 3, inflammatory response. Table showing genes and annotation terms in cluster 3. “Database” indicates where the annotation term was derived, “Count” is the number of genes associated with the annotation term and *q*-value is the Bonferroni adjusted *p*-value.

Table 8.5: Functional annotation cluster analysis, cluster 4, MHC class I

CLUSTER 4			
Database	**Annotation Term**	**Count**	***q*-value**
KEGG_PATHWAY	Herpes simplex infection	28	9.10E-14
KEGG_PATHWAY	Phagosome	25	4.70E-12
KEGG_PATHWAY	Antigen processing and presentation	17	1.50E-09
KEGG_PATHWAY	Cell adhesion molecules (CAMs)	21	2.80E-09
KEGG_PATHWAY	Viral myocarditis	16	6.00E-09
KEGG_PATHWAY	Graft-versus-host disease	14	1.40E-08
INTERPRO	Immunoglobulin-like domain	29	1.60E-07
INTERPRO	Immunoglobulin C1-set	13	1.80E-07
KEGG_PATHWAY	Type I diabetes mellitus	14	9.00E-08
INTERPRO	Immunoglobulin-like fold	33	3.50E-07
SMART	IGc1	13	2.40E-07
INTERPRO	Immunoglobulin/major histocompatibility complex, conserved site	12	1.70E-06
GOTERM_MF_DIRECT	peptide antigen binding	9	5.20E-06
INTERPRO	MHC classes I/II-like antigen recognition protein	11	7.00E-06
KEGG_PATHWAY	Allograft rejection	12	5.00E-06
KEGG_PATHWAY	Epstein-Barr virus infection	16	7.10E-06
INTERPRO	MHC class I, alpha chain, alpha1/alpha2	9	3.40E-05
KEGG_PATHWAY	Autoimmune thyroid disease	12	1.40E-05
GOTERM_BP_DIRECT	antigen processing and presentation of peptide antigen via MHC class I	8	3.80E-04
INTERPRO	MHC class I-like antigen recognition	9	2.60E-04
KEGG_PATHWAY	HTLV-I infection	19	4.90E-04
KEGG_PATHWAY	Viral carcinogenesis	15	1.00E-02
GOTERM_CC_DIRECT	MHC class I protein complex	5	3.20E-02

Gene Symbol	**Gene Name**
Oas2	2'-5' oligoadenylate synthetase 2(Oas2)
Oas1b	2-5 oligoadenylate synthetase 1B(Oas1b)
Ccl2	C-C motif chemokine ligand 2(Ccl2)
Ccl5	C-C motif chemokine ligand 5(Ccl5)
Cd14	CD14 molecule(Cd14)
Cd274	CD274 molecule(Cd274)
Cd74	CD74 molecule(Cd74)
Cd80	Cd80 molecule(Cd80)
Ebi3	Epstein-Barr virus induced 3(Ebi3)
Fcgr3a	Fc fragment of IgG, low affinity IIIa, receptor(Fcgr3a)
Lyn	LYN proto-oncogene, Src family tyrosine kinase(Lyn)
Nfkbia	NFKB inhibitor alpha(Nfkbia)
Nfkbie	NFKB inhibitor epsilon(Nfkbie)
Relb	RELB proto-oncogene, NF-kB subunit(Relb)
RT1-CE12	RT1 class I, locus CE12(RT1-CE12)
RT1-CE4	RT1 class I, locus CE4(RT1-CE4)

Continued overleaf

RT1-CE5	RT1 class I, locus CE5(RT1-CE5)
RT1-T24-3	RT1 class I, locus T24, gene 3(RT1-T24-3)
RT1-CE1	RT1 class I, locus1(RT1-CE1)
RT1-Ba	RT1 class II, locus Ba(RT1-Ba)
RT1-Da	RT1 class II, locus Da(RT1-Da)
RT1-M3-1	RT1 class Ib, locus M3, gene 1(RT1-M3-1)
RT1-N2	RT1 class Ib, locus N2(RT1-N2)
RT1-N3	RT1 class Ib, locus N3(RT1-N3)
RT1-S3	RT1 class Ib, locus S3(RT1-S3)
Slamf8	SLAM family member 8(Slamf8)
Slamf9	SLAM family member 9(Slamf9)
Tapbp	TAP binding protein(Tapbp)
Tapbpl	TAP binding protein-like(Tapbpl)
Ccl12	chemokine (C-C motif) ligand 12(Ccl12)
Cldn19	claudin 19(Cldn19)
C1r	complement C1r(C1r)
C3	complement C3(C3)
Cyba	cytochrome b-245 alpha chain(Cyba)
Igsf6	immunoglobulin superfamily, member 6(Igsf6)
Itgal	integrin subunit alpha L(Itgal)
Itgam	integrin subunit alpha M(Itgam)
Itgb2	integrin subunit beta 2(Itgb2)
Icam1	intercellular adhesion molecule 1(Icam1)
Ifih1	interferon induced with helicase C domain 1(Ifih1)
Irf7	interferon regulatory factor 7(Irf7)
Irf9	interferon regulatory factor 9(Irf9)
Il1a	interleukin 1 alpha(Il1a)
Il1b	interleukin 1 beta(Il1b)
Il13ra1	interleukin 13 receptor subunit alpha 1(Il13ra1)
Il18bp	interleukin 18 binding protein(Il18bp)
Lilrb4	leukocyte immunoglobulin like receptor B4(Lilrb4)
Msr1	macrophage scavenger receptor 1(Msr1)
Mrc2	mannose receptor, C type 2(Mrc2)
Mybphl	myosin binding protein H-like(Mybphl)
Ncf1	neutrophil cytosolic factor 1(Ncf1)
Nfkb2	nuclear factor kappa B subunit 2(Nfkb2)
Osmr	oncostatin M receptor(Osmr)
Psme1	proteasome activator subunit 1(Psme1)
Psme2	proteasome activator subunit 2(Psme2)
Rac2	ras-related C3 botulinum toxin substrate 2 (rho family, small GTP binding protein Rac2)(Rac2)
Selplg	selectin P ligand(Selplg)
Siglec1	sialic acid binding Ig like lectin 1(Siglec1)
Siglec5	sialic acid binding Ig-like lectin 5(Siglec5)
Stat2	signal transducer and activator of transcription 2(Stat2)
Tlr2	toll-like receptor 2(Tlr2)
Tlr3	toll-like receptor 3(Tlr3)
Tspo	translocator protein(Tspo)

Continued overleaf

Tap1	transporter 1, ATP binding cassette subfamily B member(Tap1)
Tap2	transporter 2, ATP binding cassette subfamily B member(Tap2)
Trem1	triggering receptor expressed on myeloid cells 1(Trem1)
Trem3	triggering receptor expressed on myeloid cells 3(Trem3)
Tuba1c	tubulin, alpha 1C(Tuba1c)
Vcam1	vascular cell adhesion molecule 1(Vcam1)

Table 8.5: Functional annotation cluster analysis, cluster 4, MHC class I. Table showing genes and annotation terms in cluster 4. "Database" indicates where the annotation term was derived, "Count" is the number of genes associated with the annotation term and *q*-value is the Bonferroni adjusted *p*-value.

Table 8.6: Functional annotation cluster analysis, cluster 5, cellular response to IFN-β

CLUSTER 5			
Database	**Annotation Term**	**Count**	***q*-value**
GOTERM_BP_DIRECT	defense response	12	1.9E-08
GOTERM_BP_DIRECT	cellular response to interferon-beta	10	4.7E-07
INTERPRO	Interferon-inducible GTPase	6	1.6E-04
INTERPRO	P-loop containing nucleoside triphosphate hydrolase	29	3.2E-03
GOTERM_MF_DIRECT	GTPase activity	12	1.4E-02

Gene Symbol	**Gene Name**
Papss2	3'-phosphoadenosine 5'-phosphosulfate synthase 2(Papss2)
Abcb1b	ATP-binding cassette, subfamily B (MDR/TAP), member 1B(Abcb1b)
Cxcl1	C-X-C motif chemokine ligand 1(Cxcl1)
Cd74	CD74 molecule(Cd74)
Ddx60	DEXD/H-box helicase 60(Ddx60)
Dhx58	DEXH-box helicase 58(Dhx58)
Mov10	Mov10 RISC complex RNA helicase(Mov10)
Nlrp1a	NLR family, pyrin domain containing 1A(Nlrp1a)
Tapbp	TAP binding protein(Tapbp)
Cmpk2	cytidine/uridine monophosphate kinase 2(Cmpk2)
Gbp1	guanylate binding protein 1(Gbp1)
Gbp5	guanylate binding protein 5(Gbp5)
Irgm	immunity-related GTPase M(Irgm)
Ifi47	interferon gamma inducible protein 47(Ifi47)
Ifih1	interferon induced with helicase C domain 1(Ifih1)
Ifi44	interferon-induced protein 44(Ifi44)
Ifit3	interferon-induced protein with tetratricopeptide repeats 3(Ifit3)
Lsp1	lymphocyte-specific protein 1(Lsp1)
Mpa2l	macrophage activation 2 like(Mpa2l)
Mx1	myxovirus (influenza virus) resistance 1(Mx1)
Rhoh	ras homolog family member H(Rhoh)
Rac2	ras-related C3 botulinum toxin substrate 2 (rho family, small GTP binding protein Rac2)(Rac2)
Slfn13	schlafen family member 13(Slfn13)
Slfn5	schlafen family member 5(Slfn5)
RGD1305184	similar to CDNA sequence BC023105(RGD1305184)
MGC105567	similar to cDNA sequence BC023105(MGC105567)
MGC108823	similar to interferon-inducible GTPase(MGC108823)
RGD1309362	similar to interferon-inducible GTPase(RGD1309362)
Trex1	three prime repair exonuclease 1(Trex1)
Tlr3	toll-like receptor 3(Tlr3)
Tor1b	torsin family 1, member B(Tor1b)
Tor3a	torsin family 3, member A(Tor3a)

Continued overleaf

Tf	transferrin(Tf)
Tap1	transporter 1, ATP binding cassette subfamily B member(Tap1)
Tap2	transporter 2, ATP binding cassette subfamily B member(Tap2)
Tuba1c	tubulin, alpha 1C(Tuba1c)
Znfx1	zinc finger, NFX1-type containing 1(Znfx1)

Table 8.6: Functional annotation cluster analysis, cluster 5, cellular response to IFN-β. Table showing genes and annotation terms in cluster 5. "Database" indicates where the annotation term was derived, "Count" is the number of genes associated with the annotation term and *q*-value is the Bonferroni adjusted *p*-value

Table 8.7: Functional annotation cluster analysis, cluster 6, CCR chemokine family

CLUSTER 6			
Database	**Annotation Term**	**Count**	***q*-value**
GOTERM_BP_DIRECT	lymphocyte chemotaxis	9	2.00E-07
GOTERM_MF_DIRECT	CCR chemokine receptor binding	8	6.80E-07
GOTERM_BP_DIRECT	monocyte chemotaxis	9	6.00E-06
INTERPRO	CC chemokine, conserved site	7	2.60E-06
GOTERM_BP_DIRECT	eosinophil chemotaxis	5	6.80E-03
GOTERM_MF_DIRECT	CCR1 chemokine receptor binding	4	1.40E-02
GOTERM_BP_DIRECT	positive regulation of natural killer cell chemotaxis	4	5.30E-02

Gene Symbol	**Gene Name**
Ccl19	C-C motif chemokine ligand 19(Ccl19)
Ccl2	C-C motif chemokine ligand 2(Ccl2)
Ccl20	C-C motif chemokine ligand 20(Ccl20)
Ccl24	C-C motif chemokine ligand 24(Ccl24)
Ccl3	C-C motif chemokine ligand 3(Ccl3)
Ccl4	C-C motif chemokine ligand 4(Ccl4)
Ccl5	C-C motif chemokine ligand 5(Ccl5)
Ccl7	C-C motif chemokine ligand 7(Ccl7)
Ccl12	chemokine (C-C motif) ligand 12(Ccl12)

Table 8.7: Functional annotation cluster analysis, cluster 6, CCR chemokine family. Table showing genes and annotation terms in cluster 6. “Database” indicates where the annotation term was derived, “Count” is the number of genes associated with the annotation term and *q*-value is the Bonferroni adjusted *p*-value.

Table 8.8: Functional annotation cluster analysis, cluster 7, disulfide bond

CLUSTER 7			
Database	**Annotation Term**	**Count**	***q*-value**
UP_KEYWORDS	Disulfide bond	55	2.70E-05

Gene Symbol	**Gene Name**
Ccl2	C-C motif chemokine ligand 2(Ccl2)
Ccl20	C-C motif chemokine ligand 20(Ccl20)
Ccl3	C-C motif chemokine ligand 3(Ccl3)
Ccl4	C-C motif chemokine ligand 4(Ccl4)
Ccl5	C-C motif chemokine ligand 5(Ccl5)
Ccl7	C-C motif chemokine ligand 7(Ccl7)
Cxcl1	C-X-C motif chemokine ligand 1(Cxcl1)
Cxcl10	C-X-C motif chemokine ligand 10(Cxcl10)
Cxcl11	C-X-C motif chemokine ligand 11(Cxcl11)
Cxcl16	C-X-C motif chemokine ligand 16(Cxcl16)
Cxcl9	C-X-C motif chemokine ligand 9(Cxcl9)
Clec4a2	C-type lectin domain family 4, member A2(Clec4a2)
Clec4d	C-type lectin domain family 4, member D(Clec4d)
Clec4e	C-type lectin domain family 4, member E(Clec4e)
Cd14	CD14 molecule(Cd14)
Cd274	CD274 molecule(Cd274)
Cd74	CD74 molecule(Cd74)
Cd80	Cd80 molecule(Cd80)
RT1-CE12	RT1 class I, locus CE12(RT1-CE12)
RT1-CE4	RT1 class I, locus CE4(RT1-CE4)
RT1-CE5	RT1 class I, locus CE5(RT1-CE5)
RT1-T24-3	RT1 class I, locus T24, gene 3(RT1-T24-3)
RT1-Ba	RT1 class II, locus Ba(RT1-Ba)
RT1-Da	RT1 class II, locus Da(RT1-Da)
RT1-M3-1	RT1 class Ib, locus M3, gene 1(RT1-M3-1)
RT1-N2	RT1 class Ib, locus N2(RT1-N2)
RT1-N3	RT1 class Ib, locus N3(RT1-N3)
RT1-S3	RT1 class Ib, locus S3(RT1-S3)
Tnfrsf1b	TNF receptor superfamily member 1B(Tnfrsf1b)
Aoah	acyloxyacyl hydrolase(Aoah)
Chi3l1	chitinase 3 like 1(Chi3l1)
F10	coagulation factor X(F10)
C1r	complement C1r(C1r)
C3	complement C3(C3)
C3ar1	complement C3a receptor 1(C3ar1)
Lgals3bp	galectin 3 binding protein(Lgals3bp)
Igsf6	immunoglobulin superfamily, member 6(Igsf6)
Icam1	intercellular adhesion molecule 1(Icam1)
Il1rn	interleukin 1 receptor antagonist(Il1rn)
Il7	interleukin 7(Il7)

Continued overleaf

Lcn2	lipocalin 2(Lcn2)
Msr1	macrophage scavenger receptor 1(Msr1)
Mrc2	mannose receptor, C type 2(Mrc2)
Mybphl	myosin binding protein H-like(Mybphl)
Osmr	oncostatin M receptor(Osmr)
Piezo1	piezo-type mechanosensitive ion channel component 1(Piezo1)
P2ry6	pyrimidinergic receptor P2Y6(P2ry6)
Siglec1	sialic acid binding Ig like lectin 1(Siglec1)
Slc7a7	solute carrier family 7 member 7(Slc7a7)
Stab1	stabilin 1(Stab1)
Sucnr1	succinate receptor 1(Sucnr1)
Tlr2	toll-like receptor 2(Tlr2)
Tf	transferrin(Tf)
Vcam1	vascular cell adhesion molecule 1(Vcam1)
Xdh	xanthine dehydrogenase(Xdh)

Table 8.8: Functional annotation cluster analysis, cluster 7, disulfide bond. Table showing genes and annotation terms in cluster 7. “Database” indicates where the annotation term was derived, “Count” is the number of genes associated with the annotation term and *q*-value is the Bonferroni adjusted *p*-value.

Table 8.9: Functional annotation cluster analysis, cluster 8, double-stranded RNA binding

CLUSTER 8			
Database	**Annotation Term**	**Count**	***q*-value**
GOTERM_MF_DIRECT	double-stranded RNA binding	10	6.60E-05
UP_KEYWORDS	Antiviral defense	8	1.10E-04
INTERPRO	2'-5'-oligoadenylate synthetase 1, domain 2/C-terminal	5	9.70E-03
INTERPRO	2'-5'-oligoadenylate synthase	5	9.70E-03
GOTERM_MF_DIRECT	2'-5'-oligoadenylate synthetase activity	4	1.40E-02
INTERPRO	2-5-oligoadenylate synthetase, N-terminal	5	1.70E-02

Gene Symbol	**Gene Name**
Oas1i	2 ' -5 ' oligoadenylate synthetase 1I(Oas1i)
Oas2	2'-5' oligoadenylate synthetase 2(Oas2)
Oasl2	2'-5' oligoadenylate synthetase-like 2(Oasl2)
Oasl	2'-5'-oligoadenylate synthetase-like(Oasl)
Oas1b	2-5 oligoadenylate synthetase 1B(Oas1b)
Ddx60	DEXD/H-box helicase 60(Ddx60)
Dhx58	DEXH-box helicase 58(Dhx58)
Ifitm3	interferon induced transmembrane protein 3(Ifitm3)
Ifih1	interferon induced with helicase C domain 1(Ifih1)
Mx1	myxovirus (influenza virus) resistance 1(Mx1)
Rsad2	radical S-adenosyl methionine domain containing 2(Rsad2)
Tlr3	toll-like receptor 3(Tlr3)
Tlr7	toll-like receptor 7(Tlr7)
Zc3hav1	zinc finger CCCH-type containing, antiviral 1(Zc3hav1)

Table 8.9: Functional annotation cluster analysis, cluster 8, double-stranded RNA binding. Table showing genes and annotation terms in cluster 8. “Database” indicates where the annotation term was derived, “Count” is the number of genes associated with the annotation term and *q*-value is the Bonferroni adjusted *p*-value.

Table 8.10: Functional annotation cluster analysis, cluster 9, LPS/nucleoside mediated signalling

CLUSTER 9			
Database	**Annotation Term**	**Count**	***q*-value**
GOTERM_BP_DIRECT	lipopolysaccharide-mediated signaling pathway	9	4.60E-06
GOTERM_BP_DIRECT	cellular response to organic cyclic compound	12	5.30E-04

Gene Symbol	**Gene Name**
Abcb1b	ATP-binding cassette, subfamily B (MDR/TAP), member 1B(Abcb1b)
Ccl2	C-C motif chemokine ligand 2(Ccl2)
Ccl3	C-C motif chemokine ligand 3(Ccl3)
Ccl5	C-C motif chemokine ligand 5(Ccl5)
Cd14	CD14 molecule(Cd14)
Lyn	LYN proto-oncogene, Src family tyrosine kinase(Lyn)
Nfkbia	NFKB inhibitor alpha(Nfkbia)
Cyba	cytochrome b-245 alpha chain(Cyba)
Il1b	interleukin 1 beta(Il1b)
Il18	interleukin 18(Il18)
Msr1	macrophage scavenger receptor 1(Msr1)
P2ry6	pyrimidinergic receptor P2Y6(P2ry6)
Ripk2	receptor-interacting serine-threonine kinase 2(Ripk2)
Serpine1	serpin family E member 1(Serpine1)
Socs1	suppressor of cytokine signaling 1(Socs1)

Table 8.10: Functional annotation cluster analysis, cluster 9, LPS/nucleoside mediated signalling. Table showing genes and annotation terms in cluster 9. "Database" indicates where the annotation term was derived, "Count" is the number of genes associated with the annotation term and *q*-value is the Bonferroni adjusted *p*-value.

Table 8.11: Functional annotation cluster analysis, cluster 10, NOD-like receptor signalling pathway

CLUSTER 10			
Database	**Annotation Term**	**Count**	***q*-value**
KEGG_PATHWAY	NOD-like receptor signaling pathway	13	3.30E-08
INTERPRO	Caspase Recruitment	6	2.30E-03
INTERPRO	Death-like domain	8	2.60E-02

Gene Symbol	**Gene Name**
Ccl2	C-C motif chemokine ligand 2(Ccl2)
Ccl5	C-C motif chemokine ligand 5(Ccl5)
Cxcl1	C-X-C motif chemokine ligand 1(Cxcl1)
Nfkbia	NFKB inhibitor alpha(Nfkbia)
Nlrp1a	NLR family, pyrin domain containing 1A(Nlrp1a)
Pycard	PYD and CARD domain containing(Pycard)
Birc3	baculoviral IAP repeat-containing 3(Birc3)
Casp1	caspase 1(Casp1)
Casp12	caspase 12(Casp12)
Ccl12	chemokine (C-C motif) ligand 12(Ccl12)
Ifih1	interferon induced with helicase C domain 1(Ifih1)
Il1b	interleukin 1 beta(Il1b)
Il18	interleukin 18(Il18)
Nfkb2	nuclear factor kappa B subunit 2(Nfkb2)
Pstpip1	proline-serine-threonine phosphatase-interacting protein 1(Pstpip1)
Ripk2	receptor-interacting serine-threonine kinase 2(Ripk2)

Table 8.11: Functional annotation cluster analysis, cluster 10, NOD-like receptor signalling pathway. Table showing genes and annotation terms in cluster 10. "Database" indicates where the annotation term was derived, "Count" is the number of genes associated with the annotation term and *q*-value is the Bonferroni adjusted *p*-value.

Table 8.12: Functional annotation cluster analysis, cluster 11, positive regulation of interleukin-6 production

CLUSTER 11			
Database	**Annotation Term**	**Count**	***q*-value**
GOTERM_BP_DIRECT	positive regulation of interleukin-6 production	8	3.90E-03

Gene Symbol	**Gene Name**
Pycard	PYD and CARD domain containing(Pycard)
Cyba	cytochrome b-245 alpha chain(Cyba)
Il1a	interleukin 1 alpha(Il1a)
Il1b	interleukin 1 beta(Il1b)
Ripk2	receptor-interacting serine-threonine kinase 2(Ripk2)
Tlr2	toll-like receptor 2(Tlr2)
Tlr3	toll-like receptor 3(Tlr3)
Tlr7	toll-like receptor 7(Tlr7)

Table 8.12: Functional annotation cluster analysis, cluster 11, positive regulation of interleukin-6 production. Table showing genes and annotation terms in cluster 11. "Database" indicates where the annotation term was derived, "Count" is the number of genes associated with the annotation term and *q*-value is the Bonferroni adjusted *p*-value.

Table 8.13: Functional annotation cluster analysis, cluster 12, response to gamma radiation

CLUSTER 12			
Database	**Annotation Term**	**Count**	***q*-value**
GOTERM_BP_DIRECT	response to gamma radiation	7	3.10E-02

Gene Symbol	**Gene Name**
Ccl2	C-C motif chemokine ligand 2(Ccl2)
Ccl7	C-C motif chemokine ligand 7(Ccl7)
Cxcl1	C-X-C motif chemokine ligand 1(Cxcl1)
Cxcl10	C-X-C motif chemokine ligand 10(Cxcl10)
Il1a	interleukin 1 alpha(Il1a)
Il1b	interleukin 1 beta(Il1b)
Sod2	superoxide dismutase 2, mitochondrial(Sod2)

Table 8.13: Functional annotation cluster analysis, cluster 12, response to gamma radiation. Table showing genes and annotation terms in cluster 12. "Database" indicates where the annotation term was derived, "Count" is the number of genes associated with the annotation term and *q*-value is the Bonferroni adjusted *p*-value.

Table 8.14: Functional annotation cluster analysis, cluster 13, CXCR3 chemokine family

CLUSTER 13			
Database	**Annotation Term**	**Count**	***q*-value**
INTERPRO	CXC chemokine	5	2.10E-03
GOTERM_MF_DIRECT	CXCR3 chemokine receptor binding	4	6.90E-03
INTERPRO	CXC chemokine, conserved site	4	4.60E-02

Gene Symbol	**Gene Name**
Cxcl1	C-X-C motif chemokine ligand 1(Cxcl1)
Cxcl10	C-X-C motif chemokine ligand 10(Cxcl10)
Cxcl11	C-X-C motif chemokine ligand 11(Cxcl11)
Cxcl13	C-X-C motif chemokine ligand 13(Cxcl13)
Cxcl9	C-X-C motif chemokine ligand 9(Cxcl9)

Table 8.14: Functional annotation cluster analysis, cluster 13, CXCR3 chemokine family. Table showing genes and annotation terms in cluster 12. “Database” indicates where the annotation term was derived, “Count” is the number of genes associated with the annotation term and *q*-value is the Bonferroni adjusted *p*-value.

8.3 Interferon regulated genes in O4 treated cultures

Table 8.15: List of genes differentially regulated by serum compared to untreated controls

ISG	I	II	ISG	I	II	ISG	I	II	ISG	I	II	ISG	I	II
Aif1			Cxcl11			Il18			Osmr			Slc7a7		
Anxa4			Cxcl13			Il18bp			P2ry6			Slfn1		
Aoah			Cxcl16			Il1b			Parp10			Slfn2		
Apol9a			Cxcl9			Il1rn			Parp12			Slfn3		
Batf2			Cyba			Il7			Pla2g16			Socs1		
Bcl3			Cyp4v3			Irf7			Plek			Sp100		
Birc3			Ddx60			Irf9			Psmb10			Stab1		
C3			Dhx58			Irg1			Psmb8			Stat2		
C3ar1			Ebi3			Isg15			Psmb9			Tap1		
Capg			Emr1			Isg20			Psme1			Tap2		
Casp1			Epsti1			Itgal			Psme2			Tapbp		
Casp12			Exoc3l4			Lcn2			Pycard			Tapbpl		
Casp7			F10			Lgals3bp			Rac2			Tlr2		
Ccl12			Fam46a			Lgals9			Rarres2			Tlr3		
Ccl19			Fbxw17			Lilrb4			Rasa4			Tlr7		
Ccl2			Fyb			Lrrc25			Rbp1			Tmem106a		
Ccl3			Gbp5			Lst1			Relb			Tmem140		
Ccl4			Hck			Ly6e			Rhoh			Tnfrsf1b		
Ccl5			Hcls1			Ly86			Rsad2			Tnfsf10		
Ccl7			Icam1			Lyn			Rtp4			Tor3a		
Cd14			Ifi27			Mov10			Samd9l			Trim21		
Cd274			Ifi35			Mx1			Selplg			Trim25		
Cd69			Ifi44			Ncf1			Serpine1			Tspo		
Cd72			Ifi47			Nfkb2			Serping1			Uba7		
Ch25h			Ifih1			Nfkbia			Siglec1			Ube2l6		
Clec4a2			Ifit2			Nfkbie			Sla			Usp18		
Clec4e			Ifit3			Nkain4			Slamf8			Vcam1		
Cmpk2			Ifitm2			Nmi			Slamf9			Xdh		
Cst7			Ifitm3			Oas1b			Slc11a1			Zbp1		
Cxcl1			Igsf6			Oas2			Slc12a7			Zc3hav1		
Cxcl10			Il13ra1			Oasl2			Slc40a1			Znfx1		

8.5 Genes differentially expressed by O4 in the presence of serum identified as interferon regulated genes

Table 8.16: Genes differentially regulated by serum compared to untreated controls

Gene_assignment	Symbol	Fold change
Lipocalin 2	Lcn2	39.4015
Chemokine (C-X-C motif) ligand 11	Cxcl11	34.8644
Chemokine (C-C motif) ligand 7	Ccl7	28.723
Chemokine (C-X-C motif) ligand 5	Cxcl5	27.1377
Chemokine (C-X-C motif) ligand 1	Cxcl1	23.1209
Chemokine (C-X-C motif) ligand 9	Cxcl9	12.4985
Serpin peptidase inhibitor, clade E	Serpine1	10.0645
Chemokine (C-X-C motif) ligand 2	Cxcl2	9.77588
Chemokine (C-X-C motif) ligand 10	Cxcl10	9.23277
Triggering receptor expressed on myeloid cells 1	Trem1	9.19954
Complement component 3	C3	8.91663
Myxovirus (influenza virus) resistance 1	Mx1	7.94637
Chemokine (C-C motif) ligand 20	Ccl20	7.86449
Argininosuccinate synthase 1	Ass1	7.62619
Interferon-induced protein with tetratricopeptide repeats 3	Ifit3	7.5988
Guanylate binding protein 5	Gbp5	7.52789
Transglutaminase 1	Tgm1	7.01244
Pentraxin 3,	Ptx3	6.96018
Interleukin 1 receptor antagonist	Il1rn	6.73926
Secretory leukocyte peptidase inhibitor	Slpi	6.4941
B-cell CLL/lymphoma 3	Bcl3	6.484
Selectin L	Sell	6.09861
Chemokine (C-C motif) ligand 6	Ccl6	5.88112
Interferon regulatory factor 7	Irf7	5.75687
Zinc finger CCCH type containing 12A	Zc3h12a	5.60029
Baculoviral IAP repeat-containing 3	Birc3	5.36152
CD93 molecule	Cd93	5.3213
Tumor necrosis factor, alpha-induced protein 2	Tnfaip2	5.21248
Macrophage scavenger receptor 1	Msr1	5.05213
Chemokine (C-C motif) ligand 4	Ccl4	5.05035
Interferon-induced protein with tetratricopeptide repeats 2	Ifit2	4.90145
Apolipoprotein L 9a	Apol9a	4.80391
Retinol binding protein 1, cellular	Rbp1	4.80332
ISG15 ubiquitin-like modifier	Isg15	4.71271
Matrix metallopeptidase 9	Mmp9	4.68955
Serine (or cysteine) peptidase inhibitor, clade A, member 3N	Serpina3n	4.68769
Lectin, galactoside-binding, soluble, 9	Lgals9	4.6604

Continued overleaf

Cholesterol 25-hydroxylase	Ch25h	4.64063
Leukemia inhibitory factor	Lif	4.61324
Lymphatic vessel endothelial hyaluronan receptor 1	Lyve1	4.59899
Ubiquitin specific peptidase 18	Usp18	4.59058
Chemokine (C-C motif) ligand 2	Ccl2	4.56506
2'-5'-oligoadenylate synthetase-like	Oasl	4.42442
Orosomucoid 1	Orm1	4.41432
Chemokine (C-C motif) ligand 5	Ccl5	4.39638
Chitinase 3-like 1 (cartilage glycoprotein-39)	Chi3l1	4.18383
CD14 molecule	Cd14	4.14916
RAB32, member RAS oncogene family	Rab32	4.06797
Uridine phosphorylase 1	Upp1	3.97712
Tubulin, beta 6 class V	Tubb6	3.96917
Integrin, alpha M	Itgam	3.96045
Aldo-keto reductase family 1, member B8	Akr1b8	3.9324
Cytochrome P450, family 4, subfamily b, polypeptide 1	Cyp4b1	3.89947
Gliomedin	Gldn	3.83999
Radical S-adenosyl methionine domain containing 2	Rsad2	3.7904
Interleukin 1 receptor, type II	Il1r2	3.7859
Interferon stimulated exonuclease gene 20	Isg20	3.76765
Placental growth factor	Pgf	3.73715
Interferon, alpha-inducible protein 27 like 2B	Ifi27l2b	3.70168
Chemokine (C-X-C motif) ligand 16	Cxcl16	3.67169
RT1 class I, locus CE4	RT1-CE4	3.65233
CD36 molecule (thrombospondin receptor)	Cd36	3.62766
Oncostatin M receptor	Osmr	3.61136
Macrophage activation 2 like	Mpa2l	3.57897
Proteasome (prosome, macropain) subunit, beta type, 8	Psmb8	3.57728
Flavin containing monooxygenase 5	Fmo5	3.55864
Galanin/GMAP prepropeptide	Gal	3.55505
Transferrin	Tf	3.48297
Superoxide dismutase 2, mitochondrial	Sod2	3.47752
Chemokine (C-X-C motif) ligand 13	Cxcl13	3.45391
Histidine rich carboxyl terminus 1	Hrct1	3.42973
Fos-like antigen 1	Fosl1	3.33806
Schlafen 3	Slfn3	3.31485
Proteasome (prosome, macropain) subunit, beta type, 9	Psmb9	3.29754
Caspase 12	Casp12	3.29305
Lymphocyte-specific protein 1	Lsp1	3.23265
Chemokine (C-C motif) ligand 3	Ccl3	3.21824
Gardner-Rasheed feline sarcoma viral (v-fgr) oncogene homolog	Fgr	3.19856
C-type lectin domain family 4, member D	Clec4d	3.15867
Interleukin 17 receptor B	Il17rb	3.07338
Ubiquitin-conjugating enzyme E2L 6	Ube2l6	3.06809
2'-5' oligoadenylate synthetase 2	Oas2	3.06008

Continued overleaf

Serpin peptidase inhibitor, clade G (C1 inhibitor), member 1	Serping1	3.0504
V-set and immunoglobulin domain containing 4	Vsig4	3.0308
Serglycin	Srgn	3.03044
C-type lectin domain family 4, member A2	Clec4a2	3.0274
Guanine deaminase	Gda	3.01562
Piezo-type mechanosensitive ion channel component 1	Piezo1	2.99938
Prolyl 4-hydroxylase, alpha polypeptide III	P4ha3	2.98761
Interleukin 1 alpha	Il1a	2.98759
Fibronectin type III domain containing 3C1	Fndc3c1	2.97898
RT1 class I, locus CE12	RT1-CE12	2.97554
VGF nerve growth factor inducible	Vgf	2.96875
Sprouty homolog 4 (Drosophila)	Spry4	2.9596
TIMP metallopeptidase inhibitor 1	Timp1	2.92779
Regenerating islet-derived 3 beta	Reg3b	2.90819
Colony stimulating factor 2 receptor, beta	Csf2rb	2.90171
Regulator of G-protein signaling 1	Rgs1	2.88144
Alkaline phosphatase, liver/bone/kidney	Alpl	2.86446
tribbles homolog 1 (Drosophila)	Trib1	2.86061
Prostaglandin-endoperoxide synthase 1	Ptgs1	2.8539
ATP-binding cassette, subfamily B (MDR/TAP), member 1B	Abcb1b	2.84233
Leukocyte immunoglobulin-like receptor, subfamily B, member 4	Lilrb4	2.83903
Vascular cell adhesion molecule 1	Vcam1	2.82613
DEXH (Asp-Glu-X-His) box polypeptide 58	Dhx58	2.81698
2-5 oligoadenylate synthetase 1B	Oas1b	2.79921
Ubiquitin-like modifier activating enzyme 7	Uba7	2.786
Chemokine (C-C motif) ligand 12	Ccl12	2.77584
Integrin, alpha X	Itgax	2.75735
Serpin peptidase inhibitor, clade B (ovalbumin), member 2	Serpinb2	2.73469
Integrin, alpha 8 /	Itga8	2.72054
Tubulin, alpha 1C	Tuba1c	2.70866
Immediate early response 3	Ier3	2.664
Signal transducer and activator of transcription 5A	Stat5a	2.63011
Receptor-interacting serine-threonine kinase 3	Ripk3	2.61884
OAF homolog (Drosophila)	Oaf	2.60538
Cytochrome P450, family 1, subfamily a, polypeptide 1	Cyp1a1	2.60027
2 ' -5 ' oligoadenylate synthetase 1I	Oas1i	2.5778
RAB20, member RAS oncogene family	Rab20	2.56437
Guanine deaminase	Gda	2.55489
Transmembrane protein 106A	Tmem106a	2.55236
Intercellular adhesion molecule 1	Icam1	2.53535
Receptor (chemosensory) transporter protein 4	Rtp4	2.5346
Dehydrogenase/reductase (SDR family) member 9	Dhrs9	2.52085
RAB27B, member RAS oncogene family	Rab27b	2.51803
Ring finger protein 125	Rnf125	2.51755

Continued overleaf

Membrane-spanning 4-domains, subfamily A, member 11	Ms4a11	2.50039
Indoleamine 2,3-dioxygenase 2	Ido2	2.49781
SP140 nuclear body protein	Sp140	2.4945
PDZ and LIM domain 1	Pdlim1	2.47942
Developing brain homeobox 2	Dbx2	2.47164
Calcitonin-related polypeptide, beta	Calcb	2.4678
PML-RARA regulated adaptor molecule 1	Pram1	2.44868
Regulator of G-protein signaling 16	Rgs16	2.4457
Solute carrier family 16, member 3	Slc16a3	2.44418
SHC (Src homology 2 domain containing) family, member 4	Shc4	2.43273
Oxidized low density lipoprotein (lectin-like) receptor 1	Olr1	2.42723
Matrix metallopeptidase 3	Mmp3	2.42532
DEAD (Asp-Glu-Ala-Asp) box polypeptide 60	Ddx60	2.4206
Retinol dehydrogenase 5 (11-cis/9-cis)	Rdh5	2.41391
Prostate androgen-regulated mucin-like protein 1	Parm1	2.40699
2'-5' oligoadenylate synthetase-like 2	Oasl2	2.38261
Transporter 1, ATP-binding cassette	Tap1	2.37094
SRY (sex determining region Y)-box 7	Sox7	2.36869
Nuclear factor of kappa light polypeptide gene enhancer in B-cells inhibitor alpha	Nfkbia	2.36723
Follistatin-like 3 (secreted glycoprotein)	Fstl3	2.36325
CDC42 effector protein (Rho GTPase binding) 5	Cdc42ep5	2.36058
Proteasome (prosome, macropain) subunit, beta type 10	Psmb10	2.3563
Pleckstrin homology-like domain, family A, member 1	Phlda1	2.35206
Cytidine monophosphate (UMP-CMP) kinase 2	Cmpk2	2.35083
Ceruloplasmin (ferroxidase)	Cp	2.34437
Eyes absent homolog 2 (Drosophila)	Eya2	2.33427
Complement component 1, r subcomponent	C1r	2.31133
Epithelial membrane protein 3	Emp3	2.30551
Chemokine (C-X-C motif) ligand 17	Cxcl17	2.3029
Solute carrier family 26	Slc26a2	2.29105
Annexin A1	Anxa1	2.29009
Aldehyde dehydrogenase 1 family, member L2	Aldh1l2	2.28533
RT1 class I, locus T24, gene 3	RT1-T24-3	2.28285
UDP-N-acetyl-alpha-D-galactosamine	Galnt3	2.27608
Interferon induced with helicase C domain 1	Ifih1	2.26664
Lectin, galactoside-binding, soluble, 3 binding protein	Lgals3bp	2.26134
Sema domain, immunoglobulin domain (Ig), short basic domain	Sema3a	2.25988
SP100 nuclear antigen	Sp100	2.25669
Transporter 2, ATP-binding cassette, sub-family B	Tap2	2.25141
MICAL-like 2	Micall2	2.24976
TAP binding protein (tapasin)	Tapbp	2.24189
Nuclear factor of kappa light polypeptide gene enhancer in B-cells 2	Nfkb2	2.2404

Continued overleaf

Interleukin 18 binding protein	Il18bp	2.23687
Gamma-secretase activating protein	Gsap	2.2306
Lectin, galactoside-binding, soluble, 3	Lgals3	2.22923
Leucine rich repeat containing 15	Lrrc15	2.22566
Solute carrier family 2	Slc2a9	2.21637
Cardiotrophin-like cytokine factor 1	Clcf1	2.20969
Interferon-induced protein 44	Ifi44	2.20865
Basic leucine zipper transcription factor, ATF-like 3	Batf3	2.19777
Interleukin 1 beta	Il1b	2.18962
Matrix metallopeptidase 13	Mmp13	2.18812
Cd80 molecule	Cd80	2.18612
Interferon induced transmembrane protein 3	Ifitm3	2.17535
SLP adaptor and CSK interacting membrane protein	Scimp	2.16984
Chloride intracellular channel 1	Clic1	2.16693
Poly (ADP-ribose) polymerase family, member 12	Parp12	2.16215
High mobility group AT-hook 2	Hmga2	2.15145
Solute carrier family 35, member D3	Slc35d3	2.14493
FERM and PDZ domain containing 1	Frmpd1	2.14182
S100 calcium binding protein A6	S100a6	2.14177
Proteolipid protein 2 (colonic epithelium-enriched)	Plp2	2.1412
RT1 class I, locus1	RT1-CE1	2.13407
DENN/MADD domain containing 3	Dennd3	2.125
Interleukin 13 receptor, alpha 1	Il13ra1	2.11786
Nyctalopin	Nyx	2.1149
RT1 class Ib, locus S3	RT1-S3	2.10888
Jun B proto-oncogene	Junb	2.10819
RAS-like family 11 member A	Rasl11a	2.10457
Immunity-related GTPase family, M	Irgm	2.10314
Transgelin 2	Tagln2	2.10079
Tumor necrosis factor receptor superfamily	Tnfrsf12a	2.09778
Alpha 1,3-galactosyltransferase 2	A3galt2	2.09756
Chemokine (C-C motif) ligand 24	Ccl24	2.09531
Interleukin 13 receptor, alpha 1	Il13ra1	2.0888
Similar to Hypothetical UPF0184 protein C9orf16 homolog	RGD1561113	2.08105
Heparin-binding EGF-like growth factor	Hbegf	2.07627
Solute carrier family 11	Slc11a1	2.07041
Cholecystokinin B receptor	Cckbr	2.06328
Receptor-interacting serine-threonine kinase 2	Ripk2	2.06232
Solute carrier family 16, member 1	Slc16a1	2.05633
Cytoskeleton associated protein 2	Ckap2	2.05412
Transforming growth factor, beta 3	Tgfb3	2.0521
Met proto-oncogene	Met	2.04972
Galactosidase, beta 1-like 2	Glb1l2	2.04633
HECT domain containing 2	Hectd2	2.04355
Interleukin-1 receptor-associated kinase 2	Irak2	2.03423
Bicaudal C homolog 1 (Drosophila)	Bicc1	2.02515
Proteoglycan 4	Prg4	2.02283

Continued overleaf

Sprouty homolog 1, antagonist of FGF signaling	Spry1	2.02099
Myeloblastosis oncogene-like 2	Mybl2	2.00329
Ttk protein kinase	Ttk	2.00114
Galanin-like peptide	Galp	2.00097
Schlafen family member 13	Slfn13	2.00015
Melanoma cell adhesion molecule	Mcam	-2.00521
Proline dehydrogenase (oxidase) 1	Prodh	-2.01489
Membrane-spanning 4-domains, subfamily A, member 7	Ms4a7	-2.0616
Protein phosphatase 1, regulatory (inhibitor) subunit 14A	Ppp1r14a	-2.06344
G protein-coupled receptor 62	Gpr62	-2.0636
ATPase, class V, type 10B	Atp10b	-2.06416
Insulin-like growth factor binding protein-like 1	Igfbpl1	-2.10622
Cadherin 19, type 2	Cdh19	-2.10862
G protein-coupled receptor 17	Gpr17	-2.12731
Raftlin family member 2	Rftn2	-2.15479
Glutamate receptor, ionotropic, N-methyl D-aspartate 2C	Grin2c	-2.16038
Tolloid-like 2	Tll2	-2.1696
Phosphorylase, glycogen, muscle	Pygm	-2.18117
Tetraspanin 2	Tspan2	-2.1826
Hairy and enhancer of split 5 (Drosophila)	Hes5	-2.19102
Notch 3	Notch3	-2.19601
microRNA mir-3546	Mir3546	-2.19884
Kinase non-catalytic C-lobe domain (KIND) containing 1	Kndc1	-2.25055
microRNA mir-2964	Mir2964	-2.26275
Family with sequence similarity 69, member C	Fam69c	-2.26754
Ecotropic viral integration site 2A	Evi2a	-2.2876
Ventricular zone expressed PH domain-containing 1	Veph1	-2.29932
KN motif and ankyrin repeat domains 4	Kank4	-2.3211
Transmembrane protein 88B	Tmem88b	-2.33569
Tissue inhibitor of metalloproteinase 4	Timp4	-2.39241
Aldehyde oxidase 1	Aox1	-2.3938
3-hydroxy-3-methylglutaryl-CoA synthase 2	Hmgcs2	-2.42918
Coiled-coil domain containing 3	Ccdc3	-2.44957
Acyl-CoA thioesterase 1	Acot1	-2.46253
Myelin-associated glycoprotein	Mag	-2.47678
Myelin regulatory factor	Myrf	-2.49708
Na+/K+ transporting ATPase interacting 4	Nkain4	-2.5055
Solute carrier family 6	Slc6a11	-2.52069
Flavin containing monooxygenase 1	Fmo1	-2.53623
Catenin (cadherin associated protein), alpha 3	Ctnna3	-2.53761
Transmembrane protein 125	Tmem125	-2.5451
Glycerol-3-phosphate dehydrogenase 1 (soluble)	Gpd1	-2.69496
TLR4 interactor with leucine-rich repeats	Tril	-2.70514
G protein-coupled receptor 20	Gpr20	-2.72843
Stabilin 1	Stab1	-2.74075
3'-phosphoadenosine 5'-phosphosulfate synthase 2	Papss2	-2.76069

Continued overleaf

Sphingosine-1-phosphate receptor 5	S1pr5	-2.76994
G protein-coupled receptor 37	Gpr37	-2.78823
Solute carrier family 40 (iron-regulated transporter), member 1	Slc40a1	-2.80307
Purinergic receptor P2Y, G-protein coupled, 12	P2ry12	-2.8223
Hyaluronan and proteoglycan link protein 2	Hapln2	-2.82758
Calmin	Clmn	-2.84941
Myelin oligodendrocyte glycoprotein	Mog	-2.98122
G protein-coupled receptor 34	Gpr34	-3.01264
Solute carrier family 4, sodium bicarbonate cotransporter	Slc4a5	-3.14409
Angiotensinogen	Agt	-3.21964
Toll-like receptor 5	Tlr5	-3.47302
Continued overleaf		
Carbonic anhydrase 14	Car14	-3.69887
Purinergic receptor P2Y, G-protein coupled, 13	P2ry13	-4.13385
Succinate receptor 1	Sucnr1	-4.14632
Oligodendrocytic myelin paranodal and inner loop protein	Opalin	-4.20144
Hedgehog-interacting protein	Hhip	-4.32235
Wingless-type MMTV integration site family, member 2B	Wnt2b	-4.84392
Cholecystokinin A receptor	Cckar	-4.93485
Mal, T-cell differentiation protein	Mal	-5.15403
C1q and tumor necrosis factor related protein 3	C1qtnf3	-5.62722
Apelin receptor	Aplnr	-7.34987

Table 8.16: Genes differentially regulated by serum compared to untreated controls. Table showing genes differentially regulated in serum-treated myelinated cultures compared to untreated controls. Fold change ≥ ±2, FDR adjusted p – value ≤ 0.05.

8.5 Genes differentially expressed by O4 in the presence of serum identified as IFN-regulated genes

Table 8.17 Genes differentially expressed by O4 in the presence of serum identified as interferon regulated genes.

ISG	I	II	ISG	I	II	ISG	I	II	ISG	I	II
Agt	■		Cxcl16	■		Junb	■		Rgs1	■	
Alpl	■		Cxcl9	■		Lcn2	■		Rsad2	■	■
Anxa1	■		Dbx2	■		Lgals3bp	■	■	Rtp4	■	■
Apol9a		■	Ddx60	■		Lgals9	■		Sell	■	
Batf3		■	Dhx58	■		Lilrb4	■		Serpina3n		■
Bcl3	■		Emp3	■		Mag	■		Serpine1	■	
Birc3	■		Evi2a	■		Met	■		Serping1	■	■
C3	■		Fosl1	■		Mmp13	■		Slc11a1	■	
Casp12	■		Gbp5	■	■	Ms4a7	■		Slc16a3	■	
Ccl12	■		Gpd1	■		Mx1	■		Slc40a1	■	
Ccl2	■	■	Hbegf	■		Mybl2	■		Slfn3	■	
Ccl3	■		Hes5	■		Nfkb2	■		Sp100	■	
Ccl4	■	■	Icam1	■	■	Nfkbia	■		Stab1	■	
Ccl5	■		Ifi44	■	■	Nkain4	■		Tagln2	■	
Ccl6	■		Ifih1	■	■	Notch3	■		Tap1	■	■
Ccl7	■	■	Ifit2	■	■	Oas1b	■		Tap2	■	■
Cd14	■		Ifit3	■	■	Oas2	■		Tapbp	■	
Cd93	■		Ifitm3	■	■	Oasl2	■	■	Timp1	■	
Ch25h	■		Igfbpl1	■		Osmr	■	■	Timp4	■	
Cldn11	■		Il13ra1	■		P2ry12	■		Tmem106a	■	
Clec4a2	■		Il18bp	■		Parp12	■	■	Tnfaip2	■	■
Cmpk2	■	■	Il1b	■		Psmb10	■	■	Tnfrsf12a	■	
Cp	■		Il1rn	■		Psmb8	■	■	Uba7	■	■
Cxcl1	■		Irf7	■	■	Psmb9	■	■	Ube2l6	■	
Cxcl10	■	■	Irg1	■		Ptx3	■		Usp18	■	■
Cxcl11	■		Isg15	■	■	Rab20	■		Vcam1	■	
Cxcl13	■		Isg20	■		Rftn2	■				

Table 8.17: Genes differentially expressed by O4 in the presence of serum identified as interferon regulated genes. Genes regulated by type-I and/or -II interferons in cultures treated with O4 in the presence of serum, identified using Interferome. Gold squares indicate positive association, black squares indicate no known association.

8.6 DAPI$^+$ nuclei in cultures used in fluorescence *in situ* hybridisation experiments

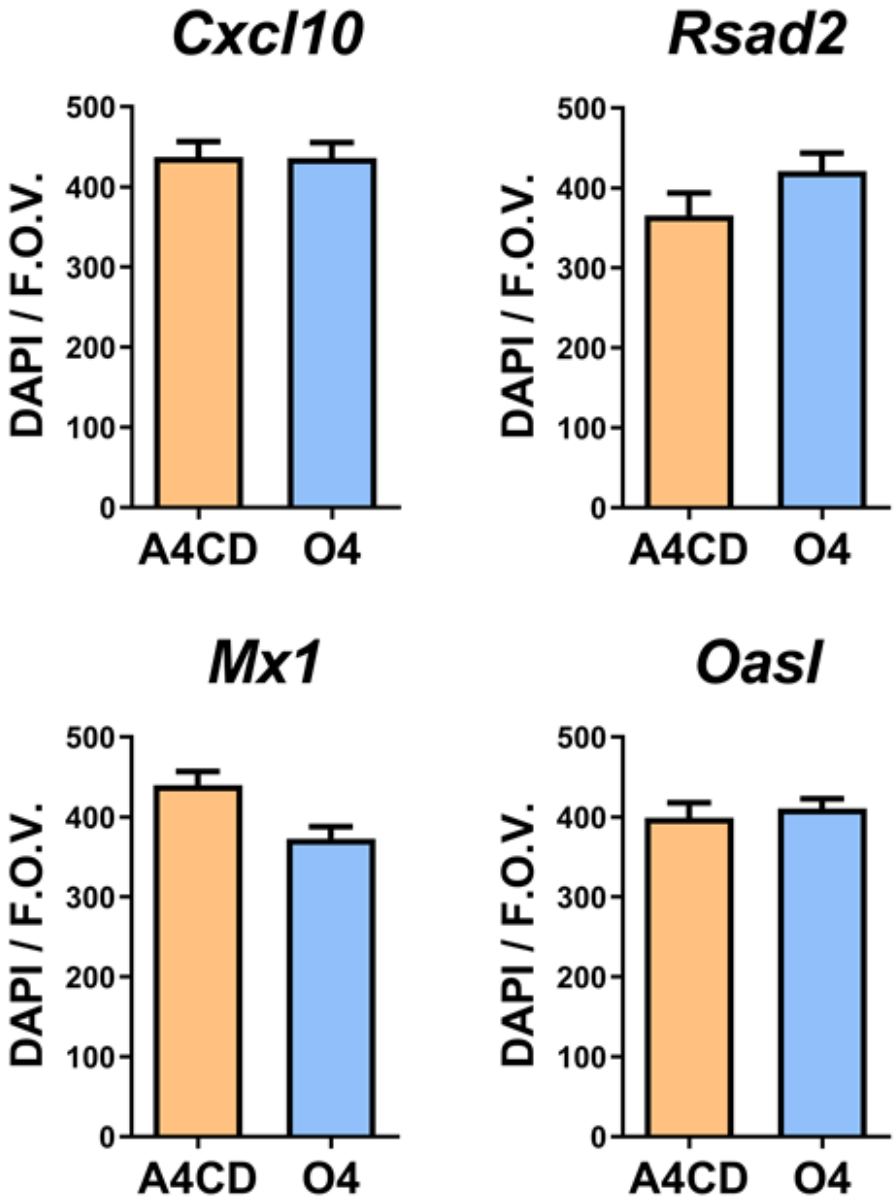

Figure 8.1 DAPI$^+$ nuclei in A4CD and O4-treated cultures used in fluorescence *in situ* hybridisation. Data expressed as mean DAPI counts per field of view (F.O.V.) ± SEM, analysed by paired two-tailed *t*-test, n = 6 for all genes except *Cxcl10* (n = 9).

8.7 Hayden et al. 2020

Lipid-specific IgMs induce antiviral responses in the CNS: implications for progressive multifocal leukoencephalopathy in multiple sclerosis

Lorna Hayden[1], Tiia Semenoff[1], Verena Schultz[1], Simon F Merz[1], Katie J Chapple[1], Moses Rodriguez[2], Arthur E Warrington[2], Xiaohong Shi[1], Clive S McKimmie[3], Julia M Edgar[1], Katja Thümmler[1], Chris Linington[1] & Marieke Pingen[1, *]

Progressive multi-focal leukoencephalopathy (PML) is a potentially fatal encephalitis caused by JC polyomavirus (JCV). PML principally affects people with a compromised immune system, such as patients with multiple sclerosis (MS) receiving treatment with natalizumab. However, intrathecal synthesis of lipid-reactive IgM in MS patients is associated with a markedly lower incidence of natalizumab-associated PML compared to those without this antibody repertoire. Here we demonstrate that a subset of lipid-reactive human and murine IgMs induce a functional anti-viral response that inhibits replication of encephalitic Alpha and Orthobunyaviruses in multi-cellular central nervous system cultures. These lipid-specific IgMs trigger microglia to produce IFN-β in a cGAS-STING-dependent manner, which induces an IFN-α/β-receptor 1-dependent antiviral response in glia and neurons. These data identify lipid-reactive IgM as a mediator of anti-viral activity in the nervous system and provide a rational explanation why intrathecal synthesis of lipid-reactive IgM correlates with a reduced incidence of iatrogenic PML in MS.

[1]Institute of Infection, Immunity and Inflammation, University of Glasgow, Glasgow G12 8TA, UK.
[2]Departments of Neurology and Neurosurgery, Mayo Clinic, Rochester, Minnesota, USA.
[3]Virus Host Interaction Team, Leeds Institute of Medical Research, School of Medicine, Faculty of Medicine and Health, University of Leeds, Leeds LS9 7TF, UK.
[*]Corresponding author: Marieke.Pingen@glasgow.ac.uk

Key words. Type-I interferon, interferon stimulated genes, viral encephalitis, John Cunningham polyomavirus (JCV), microglia, IgM.

Author contributions. Conceptualisation: Christopher Linington, Marieke Pingen; Methodology: Lorna Hayden, Julia M. Edgar, Christopher Linington, Xiaohong Shi, Marieke Pingen, Clive S. McKimmie; Investigation: Lorna Hayden, Tiia Semenoff, Verena Shultz, Simon F. Merz, Katie J. Chapple, Katja Thümmler; Resources: Katja Thümmler, Clive S. McKimmie, Xiaohong Shi, Moses Rodriguez, Arthur E. Warrington; Writing original draft: Lorna Hayden, Christopher Linington, Marieke Pingen; Review and editing: Katja Thümmler, Simon F. Merz, Katie J. Chapple, Moses Rodriguez, Arthur E. Warrington, Xiaohong Shi, Julia M Edgar; Visualisation: Lorna Hayden; Supervision: Julia M. Edgar, Christopher Linington, Marieke Pingen; Funding acquisition: Julia M. Edgar, Christopher Linington, Marieke Pingen.

Acknowledgements. We thank Hugh Willison and Denggao Yao (University of Glasgow, UK) for providing and genotyping the *Cst* knockout mice, and Andres Merits (University of Tartu, Estonia)

for the Semliki Forest Virus construct. This study was funded by generous grants from Hertie Stiftung and the Naomi Bramson Trust to Christopher Linington; several grants from the MS Society UK to Katja Thümmler, Christopher Linington and Julia M. Edgar; PhD studentships from the Medical Research Scotland (PhD-1031-2016) to Lorna Hayden, Medical Research Council to Katie J. Chapple, and the MS Society UK to Tiia Semenoff; an Medical Research Council New Investigator Research Grant (G1001724) to Clive S. McKimmie, and a Glasgow Children Hospital Charity Project Support Grant (GCHC/PSG/2018/01) to Christopher Linington and Marieke Pingen.

Introduction

Neurotropic viral infections pose a major challenge when considering immune modulatory treatment for patients with autoimmune diseases. One of the most devastating of these consequences is progressive multi-focal leukoencephalopathy (PML), a rare demyelinating disease caused by opportunistic infection of the central nervous system (CNS) by JC polyomavirus (JCV; human polyomavirus 2) (Tan and Koralnik 2010; Wollebo et al. 2015). The seroprevalence of JCV in healthy adults is 40-80%, but the vast majority of infections are asymptomatic due to a robust immune response (Knowles 2006; Pietropaolo et al. 2018).

However, immune-suppressed individuals are at an increased risk of developing PML (Jelcic et al. 2015). This has important implications for the clinical management of primary and secondary immune deficiencies, as well as autoimmune diseases in which immunosuppression is a primary treatment option (Pietropaolo et al. 2018). The latter include multiple sclerosis (MS), a chronic inflammatory demyelinating disease of the CNS (Filippi et al. 2018), in which PML can develop in association with immunomodulatory disease modifying therapies including natalizumab (Ho et al. 2017) and fumaric acid esters (Gieselbach et al. 2017).

Natalizumab is a humanised anti-alpha 4 integrin-specific antibody that significantly reduces disease activity by inhibiting migration of immune cells across the blood-brain barrier (BBB) (Rudick et al. 2013). However, its use is limited by the risk of patients developing natalizumab-associated PML, which in JCV-seropositive patients exceeds 10 per 1,000 after a six year treatment period (Ho et al. 2017; Major, Yousry, and Clifford 2018). There are no effective treatments for natalizumab-associated PML, other than plasma exchange to remove natalizumab from the circulation. However, as this itself may trigger immune reconstitution inflammatory syndrome (IRIS) mortality remains high and most survivors are left with severe neurological deficits (Major, Yousry, and Clifford 2018).

Current efforts to counter the threat posed by natalizumab-associated PML focus on risk stratification (Major, Yousry, and Clifford 2018). This is based primarily on JCV serology, but a report identifying intrathecal synthesis of lipid-specific IgM antibodies as a factor associated with a lower probability of developing natalizumab-associated PML suggests an additional strategy (Villar et al. 2015). Here, JCV seropositive patients lacking intrathecal IgM were 60-fold more likely to develop PML than those positive for lipid-specific IgM. Importantly, patients positive for both JCV and intrathecal IgM had similar risk of developing PML as patients seronegative for JCV, suggesting these antibodies substantially contribute to JCV defences in the CNS (Villar et al. 2015). Inspired by reports that disease-associated autoantibodies induce expression of type-I interferons (IFNs) in systemic lupus

erythematosus (Ronnblom, Alm, and Eloranta 2009), we speculated lipid-reactive IgM might act to enhance antiviral activity within the CNS.

We now demonstrate that a subset of human and murine IgM autoantibodies that recognise lipids in the CNS induce interferon-β (IFN-β) in microglia. This response is STING-dependent and mediates IFN-α/β-receptor 1 (IFNAR1)-dependent antiviral activity in all major CNS cell types (neurons, astrocytes, oligodendrocytes and microglia), as demonstrated by inhibition of replication of two unrelated encephalitogenic viruses (Bunyamwera virus (BUNV) and Semliki Forest virus (SVF)) in myelinating cell cultures. Our data provide a logical explanation for the observation intrathecal synthesis of lipid-specific IgM is associated with a reduced incidence of natalizumab-associated PML in MS.

Materials and methods

Myelinated spinal cord cultures from rat. Neurospheres were generated from the striata of post-natal day 1 Sprague-Dawley rats. Striata were mechanically dissociated in Leibovitz's L-15 Medium (Gibco) by glass Pasteur pipette and cultured in neurosphere media [Dulbecco's modified Eagle medium (DMEM)/F12 (Gibco), supplemented with 0.105% $NaHCO_3$, 2 mM glutamine, 1% penicillin-streptomycin (Pen/Strep), 5.0 mM HEPES, 0.0001% bovine serum albumin (BSA), 25 µg/ml insulin, 100 µg/ml apotransferrin, 60 µM putrescine, 20 nM progesterone, and 30 nM sodium selenite (all from Sigma)]. Cultures were supplemented with 20 ng/ml recombinant murine epidermal growth factor (Peprotech) and maintained at 37°C in a humidified atmosphere of 7% CO_2. Cells were fed every 3-4 days by addition of neurosphere medium and EGF. After 7 days, or when cells had formed large round neurospheres, the neurosphere suspension was centrifuged at 86 rcf for 5 mins and resuspended in astrocyte media [DMEM (1g/ml glucose, Gibco) supplemented with 10% foetal bovine serum (FBS) and 2 mM L-glutamine (both Sigma)] before being plated onto poly-L-lysine (13 µg/ml) coated cover slips (13-mm diameter, VWR International). Every 3-4 days, half of the old media was replaced with fresh astrocyte media until cells formed a confluent monolayer.

Sprague-Dawley rats were time-mated. At embryonal development day (E)15.5, spinal cords were extracted from embryos, meninges removed and placed in 1ml Hank's Balanced Salt Solution (Sigma). Up to 6 cords/ml were then enzymatically digested with 2.5% trypsin (100µl/ml) and 1.33% collagenase (100µl/ml) (both Sigma) for 15 mins at 37°C. Enzymatic activity was stopped by adding 2 ml of SD inhibitor [L-15 media supplemented with 0.52 mg/ml soybean trypsin inhibitor, 3.0 mg/ml BSA, and 0.04 mg/ml DNase (all Sigma)] per 1ml HBSS. The cords were then triturated, centrifuged at 196 rcf for 5 mins, resuspended in plating medium [50% DMEM, 25% horse serum, 25% Hank's Balanced Salt Solution (HBSS)] and plated onto the aforementioned neurosphere-derived astrocytes at a density of 150,000 cells per coverslip. Coverslips were contained in 35mm Petri dishes, three 13 mm coverslips per dish, and placed in an incubator for 2 hours. Cells were topped up with 450 µl of plating medium and 600 µl of differentiation medium [DMEM (4.5g/ml glucose), 10 ng/ml biotin, 0.5% N1 supplement, 50 nM hydrocortisone, and 0.1 µg/ml insulin (all from Sigma)]. Cells were fed every 2-3 days by removing 500µl of old media and replacing with 600µl of fresh differentiation media. From DIV13, cells were fed with differentiation media without added insulin (DM^-).

Mouse spinal cord cultures. Myelinating spinal cord cultures were generated from embryos of a number of mouse strains including; C57/Bl6 mice (Jackson Laboratories), *Ifnar1*$^{+/+}$ and *Ifnar1*$^{-/-}$ mice on a 129S7/SvEvBrdBklHprtb-m2 background (B&K Universal) and *Cst*$^{+/+}$, *Cst*$^{+/-}$ and Cst$^{-/-}$ mice on a C57/Bl6 background (Prof. Hugh Willison). Mice were time-mated and pregnant females were killed by CO_2 overdose at E13.5. Spinal cords were extracted from embryos and processed as per rat myelinating culture protocol with some amendments. Cords were enzymatically digested with 2.5% trypsin (100µl/ml) for 15mins at 37°C. Enzymatic activity was stopped by adding 2ml SD inhibitor. Cords were triturated, centrifuged at 181rcf and resuspended in plating medium. Cells were plated onto 13 mm diameter glass coverslips coated with poly-L-lysine (0.1 mg/ml in boric acid buffer, pH 8.4) at a density of 165,000 cells per coverslip. Coverslips were contained in 35mm Petri dishes, 3 coverslips per dish, and incubated for a minimum of 4 hours to attach. Once visibly attached, dishes were topped up with 300µl plating media and 600µl differentiation media. Cells were fed as per the rat culture protocol.

Antibody production. Once proliferating at a stable rate, cells were transferred to a CELLine cell culture flask (BD Biosciences). Cells were seeded in ultra-low endotoxin media [OptiMem supplemented with 10% ultra-low endotoxin FBS (VWR) and 1% Pen/Strep] at a density of 1.5 x 10^6 cells/ml and maintained at a density of maximum 1.5x10^6 cells/ml, supernatants collected and stored at -20°C until antibody purification. O4 and A4CD antibodies were purified under sterile conditions from supernatants using Hi-Trap IgM purification HP columns (GE Healthcare) as per manufacturer's instructions. All buffers were made using sterile ultra-low endotoxin reagents. Eluted protein was dialysed in a Spectra/Por 6 Regenerated Cellulose Dialysis Membrane (Spectrum Labs) against endotoxin tested Dulbecco's phosphate buffered saline (Invitrogen) for 24 hours at 4°C. Final antibody concentration was determined by Nanodrop (Denovix DS-11) and solution diluted to 1mg/ml in DPBS.

Antibody treatment. Cultures were treated at day *in vitro* 24 (DIV24). To treat cultures, 500µl of media was removed and 500µl of treatment added. Treatments were diluted in differentiation media. All antibodies were used at a final concentration of 20µg/ml. Antibodies used in treatments included; IgM from mouse myeloma (Sigma), A4CD, O4, O1 (R&D Systems or in-house produced), A2B5 (Abcam), rhIgM22, shIgM22, rhIgM12, shIgM12, shIgM42 and shIgM201 (kindly provided by MR and AW). Untreated controls were given differentiation media alone. For IFN-β neutralisation, DIV24 rat cultures were treated with media alone, A4CD or O4 in combination with either rabbit anti-rat IFN-β neutralising antibody or normal rabbit IgG control (10µg/ml, R&D Systems) for 24 hours.

Virus infections. BUNVGc-eGFP is a recombinant BUNV, in which the N-terminal 326 amino acid of the viral membrane Gc glycoprotein was replaced by eGFP (Shi et al. 2010). In short, BSR-T7/5 cells were transfected with 1µg pT7riboBUNL(+), pT7riboBUNS(+), and pT7riboBUNMGc-eGFP. After 5 hours, growth media [Glasgow Minimum Essential Medium supplemented with 10% tryptose phosphate broth, 10% FBS, and (Gibco) and 1 mg/ml Geneticin (G418) sulfate (Calbiochem)]. Cells were incubated for 5-11 days at 33°C until cytopathic effect was observed. Supernatant was clarified and stored at -70°C until use. For all eGFP-Semliki Forest Virus (SFV) experiments we used an eGFP expressing variant of the neurovirulent strain SFV4. The eGFP marker gene was inserted in nsP3 via a naturally occurring XhoI site, resulting in plasmid pCMV-SFV4(Xho-EGFP)4 which was generated

and kindly provided by prof Andres Merits (University of Tartu). The backbone of this plasmid has been previously described (Ulper et al. 2008), further details are available from the Lead Author. Virus stocks were generated by electroporating this plasmid in BHK cells and propagated in Glasgow Minimum Essential Medium (Gibco) with 5% FBS, 10% tryptose phosphate broth (Gibco), 1% Pen/Strep at 37°C in 5% CO_2. When severe cytopathic effect was observed, virus-containing supernatant was centrifuged 500xg for 30 minutes to remove cellular debris and cell-free virus stored in small aliquots at -70°C. Stocks were titrated by plaque assay as described below.

DIV24 cultures were treated with either media alone, A4CD or O4 for 24 hours. All media was removed and cells inoculated with 0.75% BSA (Sigma) in PBS alone or with BUNV (MOI 1) for 1 hour at 5% CO_2, shaking gently every 15 minutes or SFV (MOI 1) for 1 hour at room temperature on a plate shaker. Inoculum was removed and fresh differentiation media was added. Cells were then incubated for a further 6-24 hours, at which point supernatant was collected for plaque assay, cells washed with 0.75% BSA-PBS and prepared for further analysis.

To quantify virus stocks and production of BUNV, Vero E6 cell monolayers were incubated with serially diluted supernatant for 1 hour at 37°C then covered with 0.6% Avicel (FMC Biopolymer)-minimum essential medium overlay medium supplemented with 2% FBS. Cells were incubated for 4 days and fixed with 4% formaldehyde-PBS and stained with 0.5% (w/v) methyl violet. Virus titres were calculated and presented as PFU/ml. A similar assay was used for SFV, with the following adaptations: BHK cells were infected and maintained as described, and at 2 days post infection fixed in 10% formaldehyde-PBS and stained with 0.1% toluidine blue (Sigma).

Drug treatment of cultures. To deplete microglia, rat cultures were treated from DIV18-28 with PLX3397 (Selleckchem) or an equivalent volume of dimethyl sulfoxide (DMSO, Sigma) every 2-3 days. Final concentration of PLX3397 in cell culture dish was maintained at 1μM and volume of DMSO maintained at 0.1% of total media volume. For signalling pathway inhibition, DIV24 rat cultures were treated 6 hours with media alone, A4CD or O4 with simultaneous administration of either DMSO or 10μM of one of the following inhibitors; ST2825 (MedChemExpress), RU.521 (Invivogen), C-176 (Biovision) and BX795 (Invivogen).

Fluorescence in situ hybridisation (FISH). FISH was performed on DIV24 rat myelinating cultures treated 24 hours with either A4CD or O4 using the ViewRNA Cell Plus Assay kit (Invitrogen) as per manufacturer's instructions. First, immunocytochemistry was performed against the following antigens; GFAP (1:200, Sigma), NeuN (1:400, Millipore), Olig2 (1:500, Millipore) and Iba1 (1:500, Wako), using secondary antibodies AlexaFluor488 goat anti-rabbit IgG and AlexaFluor568 goat anti-mouse IgG1 (both Invitrogen). ViewRNA cell plus type 6 probe sets against the following genes were used; *Cxcl10*, *Mx1*, *Rsad2* and *Oasl*. Coverslips were mounted onto glass slides using Mowiol 4-88 mounting medium. Mounted slides were stored overnight at 4°C protected from light and imaged.

RNA isolation. RNA was extracted from rat cultures using the RNeasy Plus Micro kit (Qiagen) as per manufacturer's instructions. RNA was extracted from mouse and virally infected cultures by removing all media from cells, adding 1ml TRIzol® Reagent per dish and incubating for 10 minutes. Lysates were transferred to RNase-free tubes (Invitrogen)

and stored at -80°C until use. RNA was isolated using the PureLink™ RNA Mini Kit (Invitrogen) as per manufacturer's instructions. Concentration and quality of RNA was determined by Nanodrop.

Microarray. RNA from treated DIV24 rat myelinating cultures (mock, 20µg/ml O4 or IgM isotype control for 24 hours) was quality checked with the Agilent Bioanalyzer 6000 Nano LabChip platform and biotin labelled using Ambion WT Expression Kit. The labelled RNA was then hybridized to Affymetrix GeneChip Rat Gene 2.1 ST Arrays according to manufaturer's instructions using the Fluidics Station 450 and scanned on Gene Array Scanner 3000-7G. Each treatment group (untreated Control, O4 and IgM treatment) were set up in three replicates, analysed in Partek Genomics Suite (version 6.6, Partek) and deposited in Gene Expression Omnibus database (https://www.ncbi.nlm.nih.gov/geo/) under accession number GSE150331. Probe set level data were normalized using GC-RMA method and One-Step Tukey's Biweight method was used to summarize to transcript cluster level. Differential expression was then calculated by one-way ANOVA comparing O4-treatment vs Control, O4-treatment vs IgM-treatment and IgM-treatment vs Control. Differentially expressed genes (fold-change > ± 1.4, FDR-adjusted p-value < 0.05) were then analysed for enriched KEGG pathways using Partek Pathway and for the presence of interferon regulated genes (IRGs) using the interferome database (v2.01; http://www.interferome.org/interferome/home.jspx) (Rusinova et al. 2013).

cDNA synthesis and quantitative real-time PCR. Primer 3 software (http://biotools.umassmed.edu/bioapps/primer3_www.cgi) (Rozen and Skaletsky 2000) was used to find suitable primer sequences on mRNA sequences from the NCBI nucleotide data base, and checked for specificity using BLAST (http://blast.ncbi.nlm.nih.gov/Blast.cgi). cDNA was synthesized from a maximum of 1µg RNA using a QuantiTect® Reverse Transcription Kit (Qiagen) following the manufacturer's instructions using a Biometra T3 Thermocycler (Thermofisher). Synthesised cDNA was diluted to appropriate volume using RNase-free water (1:200 for 1µg starting RNA). Quantitative real-time PCR was performed in MicroAmp Fast Optical 96-well reaction plates (0.1ml) (Invitrogen) with each sample being run in triplicate. Reagents per well were as follows; 7.5µl Power SYBR™ Green PCR Master Mix (Applied Biosystems), 5.2ul RNase-free water, 0.3ul primer mix (Integrated DNA Technologies, 50µM/primer) and 2µl cDNA. Plates were run in an Applied Biosystems Fast Real-Time PCR System (ABI 7500) and quantified using the comparative CT (ΔΔCT) method or, for human IgM data alone, standard curve method. Cycle settings were as follows; 50°C for 5minutes, 95°C for 10minutes, followed by 40 cycles of 95°C for 15s, 60°C for 1min, and a final dissociation step at 95°C for 15s. *18S* was used as the housekeeping gene for mouse experiments and virus experiments. *Gapdh* was used as the housekeeping gene for all other rat experiments.

Immunocytochemistry. Cultures were fixed with 4% formaldehyde-2% sucrose in PBS for 10 minutes. Fixative was replaced by 0.75% BSA-PBS, and cultures stored at 4°C until immunocytochemistry was performed. Fixed cells were permeabilised with 0.5% Triton X for 10 minutes, washed with PBS, blocked with blocking buffer [1% BSA, 10% horse serum in PBS] for 45 minutes, incubated with primary antibody diluted in blocking buffer for 45 minutes, washed with PBS and incubated in dark with secondary antibody diluted in blocking buffer for 15 minutes. Coverslips were then washed in PBS followed by dH_2O and mounted onto glass slides with Mowiol 4-88 mounting medium [33% w/v Mowiol® 4-88,

13.2% w/v glycerol (both Sigma), 0.05% v/v DAPI (Invitrogen) in 0.13M Tris pH 8.5]. Primary antibodies against the following proteins were used; BUN virions (1:500, Elliott lab), NeuN (1:400, Millipore), Nestin (1:200, Millipore), GFAP (1:200, Sigma), Olig2 (Millipore, 1:200), ED1 (1:100, Abcam), Iba1 (1:500, Wako), A4CD, O4 (both 20µg/ml, both Linington Lab), O1 (20µg/ml, R&D Systems) and A2B5 (20µg/ml, Abcam). All secondary antibodies were purchased from Invitrogen and used at 1:400 including; AlexaFluor488 goat anti-rabbit IgG, AlexaFluor488 goat anti-mouse IgM, AlexaFluor568 goat anti-mouse IgG1 and AlexaFluor568 goat anti-mouse IgG2a. For live-staining of lipid-specific IgM, live cells were incubated with antibody (20µg/ml, 30 minutes, 4°C) and then fixed with 4% PFA. Protocol continues as above.

Image capture and analysis. All imaging and quantification was performed blind. Coverslips from microglia depletion experiments and BUNV infections were imaged on an Olympus BX51 microscope (Olympus Lifescience) using a Retiga R6 camera and Ocular 2.0 software (both Teledyne Qiamging). 10 images were taken per coverslip, 3 coverslips per condition for every biological replicate. Images were saved as 16 bit tif files and converted to 8 bit png files using CellProfiler (Carpenter et al. 2006) pipeline "Ocular.cpproj". Total dapi for each png image was quantified using CellProfiler pipeline "dapi mono.cp". Both pipelines can be found at https://github.com/muecs/cp/tree/v1.1. Iba1-positive cells and BUNV-positive cells were counted manually using cell counter plugin (https://imagej.nih.gov/ij/plugins/cell-counter.html) with ImageJ (Schneider, Rasband, and Eliceiri 2012). Co-localisation of BUNV-positive dapi with other cell markers was also quantified using the cell counter plugin.

Coverslips from FISH experiments were imaged using a Zeiss Axio Imager 2 and Zen 2012 (blue edition) software. To quantify total dapi, images were saved as png files using Zen software and processed using the "dapi mono.cp" CellProfiler pipeline. Cells positive for mRNA of interest were quantified manually using the cell counter plugin in Fiji (Schindelin et al. 2012). Co-localisation of mRNA-positive dapi with other cell markers was also quantified using the cell counter plugin.

Statistical analysis. Statistical details of experiments including statistical tests used, n values and what n represents, definition of centre, dispersion and precision measures are reported in the figure legends. Statistical significance was determined using one of the following tests depending on number of samples and variables; two-tailed t-test for data with one variable and two conditions, one-way ANOVA with Tukey's *post hoc* test for data with one variable and greater than two conditions, and two-way ANOVA with Bonferroni *post hoc* test for data with two variables and two conditions. Data were deemed significant when p-value was less than 0.05 and are denoted in figures as $*p < 0.05$, $**p < 0.01$, $***p < 0.001$. Statistical analysis was performed in GraphPad Prism 8.

Data availability. The microarray data generated for this study are available at the GEO repository under the following accession number GSE150331 and as supplemental information. CellProfiler pipelines can be found at https://github.com/muecs/cp/tree/v1.1
All other data supporting the findings of this study are available in the article, the Supplementary information files, or upon request to the authors. We are happy to provide a source table.

Results

Lipid-specific IgM provides protection against neurotropic viruses in an IFNAR1 - dependent manner. To test the hypothesis that lipid-specific IgMs induce a functional anti-viral response in the CNS, we examined the anti-viral properties of the murine IgM monoclonal antibody (mAb) O4, recognising sulfatide (3-O-sulfogalactosylceramide), a major target of the intrathecal antibody response in MS (Brennan et al. 2011). The antiviral properties of this antibody were tested in rodent myelinated cultures, which replicate much of the cellular and functional complexity of the nervous system *in vivo* in a tractable *in vitro* model (Bijland et al. 2019).

To mimic the situation in MS patients who have intrathecal lipid-specific IgM in their CNS before JCV disseminates to the CNS, rat myelinated cultures were pre-treated for 24 hours with O4 or isotype control A4CD, an IgM mAb specific to myelin oligodendrocyte glycoprotein (MOG) peptide. Both were purified in our laboratory under the same conditions. As JCV is an obligatory human pathogen, we used BUNV as an encephalitic model virus to infect the pre-treated cultures. BUNV, a prototype for both the *orthobunyavirus* genus and *Peribunyaviridae* family, is a tripartite negative sense single-stranded enveloped RNA virus (Hughes et al. 2020) and can induce severe encephalitis in domestic animals (Tauro et al. 2015).

As the cellular tropism of BUNV in rodents is unknown this was first mapped by immune fluorescence microscopy using a GFP-tagged BUNV (BUNVGc-eGFP) (Shi et al. 2010) and a panel of cell type specific markers to reveal that BUNV preferentially infected cells of the neuronal lineage in myelinating cultures (Fig. 1A, B & I). Pre-treatment with O4 had a profound antiviral effect as demonstrated by quantifying BUNVGc-eGFP infected cells by immune fluorescence microscopy ($p < 0.05$) (Fig. 1C, D & J). This finding was corroborated when assessing BUNV RNA expression by RT-PCR, where a >10-fold decrease was observed in *BUNM* transcript in O4-treated cultures ($p = 0.1303$) (Fig. 1K).

Considering our myelinated cultures lack adaptive immune cells, we hypothesised that this antiviral effect might be conferred by the innate antiviral type-I IFN pathway. To investigate this hypothesis, experiments were repeated in myelinated cultures derived from *Ifnar1*$^{-/-}$ mice and wild type controls, resulting in a significant decrease in BUNVGc-eGFP infected cells and supernatant viral titre in O4-treated wild type (WT) cultures only, highlighting the dependency of this response on the type-I IFN pathway (Fig. 1E, F, L & M). Moreover, this also demonstrates the protective effect of O4 is not species-specific as it induced a similar level of antiviral activity to that observed in rat cultures.

To investigate whether this protection can be extended to other viruses with a different cellular tropism and generating different Pattern Associated Molecular Patterns (PAMPs), we investigated the antiviral potential of O4 using SFV. SFV is an encephalitogenic positive-sense single-stranded RNA virus that preferentially infects cells of the oligodendroglial lineage (Fragkoudis et al. 2009) (Fig. 1G & H) (construct kindly provided by Andres Merits). As observed for BUNV, pre-treatment with O4 inhibited replication of SFV in WT cultures ($p<0.001$), but in this case a residual protective effect was observed in *Ifnar1*$^{-/-}$ cultures ($p<0.05$) (Fig. 1N). This may be due to steric hindrance of antibody that is bound to the oligodendrocyte cell surface restricting viral access and/or disruption of receptor-mediated endocytosis but nonetheless, the dominant protective effect is largely IFNAR1-dependent.

Together these results demonstrate that the lipid-specific IgM mAb O4 exhibits antiviral properties that can inhibit virus replication in neurons and glia in an IFNAR1-dependent manner. This supports the idea that intrathecal lipid-specific IgM found in MS patients may contribute to protection against JCV and limit risk of PML.

Lipid-Specific IgM induces an antiviral transcriptional signature *in vitro*. To gain further insight into the mechanistic basis of this antiviral response, a microarray was performed on cultures treated for 24 hours with O4, IgM isotype control or media alone. O4 differentially regulated 543 transcripts compared to the IgM control (431 upregulated, 112 down regulated; fold-change $\geq \pm 1.4$; FDR-adjusted $p \leq 0.05$), whilst no significant differences were observed between untreated and IgM control-treated cultures (Fig. 2A, GSE150331).

The transcriptional response induced by mAb O4 was characterised by increased expression of multiple genes that play important roles in the development of antiviral responses in the CNS (Fig. 2B and Table S1). These include chemokines (chemotactic cytokines) *Cxcl10* and *Ccl5*, the products of which co-ordinate recruitment of immune effector cells into the CNS, (Michlmayr et al. 2014), as well as numerous genes such as *Oasl*, *Mx1* and *Rsad2*, which encode proteins that restrict viral replication (Schoggins and Rice 2011). It is therefore not surprising that pathway enrichment analysis identified viral diseases as the most significantly enriched human disease pathways associated with this response (Table S2). Moreover, the other most significantly enriched organismal system pathways included NOD-like, Toll-like and RIG1-like signaling pathways (Table S3). These observations led us to speculate the IFN-like response triggered by O4 involves activation of one or more Pattern Recognition Receptor (PRR)-dependent pathways; a concept supported by the demonstration that as much as 72% of all differentially regulated genes are interferon-stimulated genes (ISGs) based on the murine interferome database (Fig. 2B and Table S1) (Rusinova et al. 2013).

To validate these microarray data, we selected IFN-β and several top-ranking ISGs for RT-qPCR analysis. *Ifnb1* was rapidly and significantly upregulated within 4 hours of O4 treatment ($p < 0.01$) (Fig. 2C). After 24 hours, we observed a significant upregulation of the chemokine genes *Cxcl10* ($p = 0.0552$) and *Ccl5* ($p < 0.05$), and the antiviral transcripts *Oasl* ($p < 0.0001$), *Mx1* ($p < 0.01$), *Rsad2* ($p < 0.05$), *Ifit2* ($p < 0.01$), *Isg15* ($p < 0.01$), and *Isg20* ($p < 0.05$) (Fig. 2D-G and Suppl. Fig. 1A-D) compared to the IgM and untreated controls.

In summary, these data demonstrate that O4 induces an "IFN-like" response in CNS cells, explaining the potent antiviral effect of O4 against two genetically distinct neurotropic model viruses.

The response induced by O4 is IFN-β- and IFNAR-dependent. To investigate the importance of IFN signalling for this response, we first mapped the kinetics of IFN and ISG expression induced by O4. Expression of *Ifnb1* was detected after 4 hours, peaked at 8 hours and then declined slowly over the following 10 hours (Suppl. Fig. 2A). In contrast, ISG expression increased markedly between 8 and 18 hours post-treatment (Suppl. Fig. 2B-H). Induction of *Ifnb1* and these selected ISGs was not observed in cultures treated with control IgM (Fig. 2C-G).

To assess whether the O4 response was dependent on type-I IFN signalling, WT and *Ifnar1*$^{-/-}$ mouse myelinating cultures were treated with media alone, control IgM (A4CD) or O4 for

24 hours. Induction of ISGs by O4 was abrogated almost completely in *Ifnar1*$^{-/-}$ cultures, showing a significant interaction between the presence of Type I IFN receptors and upregulation of *Cxcl10* ($p<0.0001$), *Mx1* ($p<0.01$), *Rsad2* ($p<0.001$) and *Oasl* ($p<0.001$) (Fig. 3A-D). Induction of ISGs by O4 is therefore mediated predominantly via activation of the type-I IFN pathway.

To confirm the ISG induction was specifically IFN-β-dependent as indicated by the mRNA expression data (Suppl. Fig. 2A), rat myelinating cultures were treated for 24 hours with A4CD or O4 in the presence of an IFN-β neutralising antibody or rabbit IgG as a control. O4-induced ISG expression was attenuated significantly in the presence of the IFN-β neutralising antibody with significant interaction between treatment and neutralisation being observed for mRNA expression of *Cxcl10* ($p< 0.05$), *Mx1* ($p<0.05$) and *Rsad2* ($p<0.05$) (Fig. 3E-G). Expression of *OasI* was also reduced when IFN-β was neutralised but this did not reach statistical significance ($p = 0.1072$) (Fig. 3H).

These data confirm O4-mediated induction of IFN-β is responsible for IFNAR1-dependent expression of antiviral ISGs in these CNS cultures, an observation supporting our hypothesis intrathecal synthesis of lipid-specific IgMs can have antiviral properties in the CNS.

Microglia are the major source of *Ifnb1* in a cGAS-STING-dependent manner. To further elucidate the mechanism of action by O4, we sought to identify those cells responsible for producing IFN-β. Previous studies indicate microglia are a major source of IFN-β (Roth-Cross, Bender, and Weiss 2008; Kocur et al. 2015) and may therefore orchestrate ISG expression in other neural cells. We therefore used the colony-stimulating factor 1 receptor (CSF-1R) inhibitor PLX3397 to deplete microglia prior to treating the cultures with O4 or control IgM (Elmore et al. 2014). PLX3397 reduced Iba-1^{+} microglia by >99% without affecting viability of the other cell types (Fig. 3I-L). This was accompanied by an almost complete abrogation of *Ifnb1* expression in O4-treated cultures (Fig. 3M). We therefore conclude microglia are the major source of O4-induced *Ifnb1* expression in myelinating cultures.

To gain understanding as to how O4 upregulates IFN-β in microglia, we screened a panel of inhibitors that act upstream of known IFN-β-inducing pathways. Rat myelinated cultures were treated for 6 hours with O4 combined with vehicle or inhibitor of interest (10 μM). *Ifnb1* expression was substantially depleted in cultures where cGAS (RU.521) or STING (C-176, $p<0.05$) were inhibited, and completely ablated by inhibition of TBK1/IKKε (BX795, $p<0.05$) (Fig. 3N). This would suggest that *Ifnb1* after O4 treatment is upregulated predominantly by a cGAS-STING-TBK1/IKKε dependent pathway.

O4 induces cell type specific patterns of ISG expression in the CNS. Having identified microglia as the major source of IFN-β, we next asked if IFN-β expression orchestrates ISG expression across all major CNS cell types. For many ISGs there are no suitable antibodies commercially available, so we combined Fluorescent *In Situ* Hybridisation (FISH) with cell-specific antibodies to visualise transcripts encoding candidate ISGs (*Cxcl10*, *Mx1*, *Rsad2* and *Oasl*) in neurons, oligodendroglia, astrocytes and microglia. Compared to A4CD-treated controls, O4 induced a significant increase in cells expressing these candidate ISGs (*Cxcl10* $p<0.001$; *Mx1* $p<0.001$; *Rsad2* $p<0.001$ and *Oasl* $p<0.01$) (Suppl. Fig. 3) and each cell type upregulated at least one ISG (Fig. 4A). Astrocytes upregulated all four ISGs, neurons

upregulated *Rsad2*, *Cxcl10* and *Mx1*, oligodendrocytes upregulated *Cxcl10* and *Mx1* whilst microglia only upregulated *Oasl* in this model of the CNS (Fig. 4).

These observations reinforce our hypothesis that intrathecal synthesis of lipid-specific IgM protects MS patients from natalizumab-associated PML and presumably other viral infections of the CNS.

Lipid-specific IgM-mediated antiviral responses are not sulfatide dependent. We next asked if the STING-dependent induction of IFN-β is dependent on O4 binding sulfatide; a galactosphingolipid highly enriched in myelin. O4 is poly-reactive and not only binds sulfatide but also seminolipid (3-sulfogalactosyl-1-alkyl-2-acyl-sn-glycerol) and a variety of other ligands (Bansal et al. 1989). To differentiate between these targets we used cerebroside sulfotransferase (CST) deficient mice that lack the ability to synthesise sulfatide and seminolipid (Honke et al. 2002), resulting in $CST^{-/-}$ cells to which O4 cannot bind (Fig. 5A & B).

Comparison of cultures from $CST^{+/+}$, $CST^{+/-}$ and $CST^{-/-}$ embryos revealed that specific binding of O4 to sulfatide, seminolipid or any other CST-dependent sulfoglycolipid exposed at the outer surface of myelin and oligodendrocytes was not required for O4 induction of *Ifnb* (Fig. 5A-C). Whilst O4-indued *Ifnb* expression by $CST^{-/-}$ cultures was lower for $CST^{+/+}$ cultures, this difference did not reach statistical significance and could be due to the lower percentage of microglia in the $CST^{-/-}$ cultures (data not shown). Recognition of cell surface sulfogalactolipids by O4 is therefore not an absolute requirement to trigger induction of *Ifnb1*. This was unexpected as our working hypothesis was that induction of antiviral activity involved damage associated molecular patterns (DAMPs) generated in response to O4 binding to the oligodendrocyte/myelin surface.

This observation prompted us to explore whether other glycosphingolipid-reactive IgM mAbs would also induce *Ifnb1* expression in this culture system. This was investigated using O1 which is specific for galactosyl ceramide (Sommer and Schachner 1981) and A2B5 which recognises multiple c-series gangliosides (Saito, Kitamura, and Sugiyama 2001). Immunofluorescence staining confirmed O1 bound extensively to oligodendroglia and myelin (Fig. 5F), whilst A2B5 weakly labelled a population of cells identified tentatively as neural progenitors (Fig. 5G). Strikingly, we found A2B5 upregulated expression of *Cxcl10* and *Mx1* to levels comparable to that in O4 treated cultures, whereas O1 had no such effect (Fig. 5H & I). These data indicate induction of antiviral activity by lipid-reactive IgM is not restricted to O4 but can be mediated by other lipid-reactive IgMs and does not require recognition of CNS myelin.

Screening of human-derived IgM antibodies identifies candidate with antiviral properties. To determine if IgMs with antiviral activity are present in the human antibody repertoire, we investigated a small panel of human IgMs isolated from patients with IgM gammopathies such as Waldenstrom's macroglobulinemia (Warrington et al. 2000). Using mouse myelinated cultures, we found three out of six tested antibodies induced expression of *Ifnb1* at 2 hours (Fig. 5J) and *Cxcl10* at 24 hours (Fig. 5K); shIgM22 (1), 2) rhIgM22 (2) which is a recombinant version of shIgM22 and to a far lesser extent shIgM42 (5). To assess whether induction of *Ifnb1* supported a functional antiviral response we pre-treated cultures with human IgMs for 24 hours and then infected them with SFV. We observed a substantial decrease in the percentage of cells infected with SFV in cultures pre-treated with rhIgM22

and to a lesser extent shIgM22 (Fig. 5L); an effect that correlates with their ability to induce *Ifnb1*. Immunofluorescence staining showed these two antiviral antibodies also bind oligodendrocytes (Suppl. Fig. 4A & B) whilst the remaining antibodies in this screen target neurons (Suppl. Fig. 4C-E) or failed to bind in culture (Suppl. Fig. 4F).

Together, the data indicate a subset of lipid-specific IgM antibodies exists in mice and humans that can induce a functional antiviral response in the CNS. This previously unreported mechanism offers an explanation for the association between intrathecal lipid-specific IgM and protection against JCV in MS patients.

Discussion

Sustained intrathecal antibody synthesis is the most consistent and well-documented immunological abnormality associated with MS; its most obvious manifestation being the presence of oligoclonal immunoglobulins in patient cerebrospinal fluid (Stangel et al. 2013). The specificity profile of this response is complex, but contains a significant component directed against lipid antigens in particular sulfatide (3-O-sulfated galactosyl ceramide) (Kanter et al. 2006; Brennan et al. 2011; Ilyas, Chen, and Cook 2003). It has been suggested this lipid-specific antibody response plays an important role in modulating disease activity in the CNS as intrathecal synthesis of lipid-reactive IgM correlates not only with a more aggressive disease course (Villar, Sadaba, et al. 2005), but also a reduced risk of patients developing natalizumab-associated PML (Villar et al. 2015). Inspired by the latter report, we hypothesised a subset of lipid-reactive IgMs might enhance innate antiviral activity in the CNS. We now demonstrate that several different lipid-reactive IgM mAbs can initiate a functional antiviral response in primary myelinating cultures that reproduce the cellular and functional complexity of the CNS (Thomson et al. 2008; Bijland et al. 2019). This response is dependent on cGAS/STING-mediated upregulation of IFN-β in microglia, which then triggers IFNAR1-dependent expression of antiviral ISGs in oligodendrocytes, neurons, astrocytes and microglia.

Identification of microglia as the source of IFN-β induced by O4 concurs with studies demonstrating microglia are major producers of IFN-β in other inflammatory and viral disease models (Kocur et al. 2015; Roth-Cross, Bender, and Weiss 2008; Pfefferkorn et al. 2016). IFN-β subsequently upregulated expression of ISGs in surrounding neurons and glia via activation of IFNAR, which is expressed ubiquitously by cells throughout the CNS (Y. Zhang et al. 2014). However, the response of individual cells to IFN-β will differ due to intrinsic differences in signalling thresholds and basal levels of proteins regulating the downstream response (Cavanaugh, Holmgren, and Rall 2015; Kapil et al. 2012). Indeed, our comparative analyses of four selected ISGs that are upregulated in response to O4 indicates astrocytes are especially efficient at responding to microglia-derived IFN-β (Fig. 4A).

Astrocytes are the major glial cell type of the CNS and together with microglia are integral components of the BBB (N.J. Abbott et al. 2010). For viruses that enter the CNS by crossing the vascular endothelium, astrocytes are the first cells these viruses encounter. The robust astrocytic response to microglia-derived IFN-β may therefore represent a critical “gate keeper” function that helps protects the CNS compartment from systemic infections (Daniels et al. 2017; Hwang and Bergmann 2018a). However, our data demonstrate O4 not only

initiates antiviral activity in astrocytes but also in oligodendrocytes and neurons. This is important as JCV infects all three cell types in PML (Wuthrich et al. 2016; Darbinyan et al. 2013), and supports our hypothesis that a subset of lipid-reactive IgMs enhance antiviral activity in the CNS, protecting MS patients from natalizumab-associated PML. We were unable to confirm this directly as JCV is an obligate human pathogen. Nonetheless, our identification of human IgMs with similar antiviral properties, together with reports that IFN-β inhibits JCV replication in human glia (O'Hara and Atwood 2008; Co et al. 2007) support this concept.

In addition to providing a logical mechanism linking intrathecal synthesis of lipid-reactive IgM with protection from natalizumab-associated PML (Villar et al. 2015), our data also provide new insight into why this antibody response is also associated with a more aggressive MS disease course (Villar, Sadaba, et al. 2005). In addition to inducing multiple antiviral genes, O4 also upregulated expression of a large number of chemokine genes (Fig. 2B, Table S1). Chemokines are important regulators of immune cell migration and play key roles in the development of inflammatory responses in the CNS (Holman, Klein, and Ransohoff 2011). We therefore interpret this transcriptional response as a mechanism to recruit immune cells across the BBB in response to a perceived viral threat. The observed chemokine response is mainly involved in recruitment of T and B cells, and monocytes, all of which can mediate tissue damage in neuroinflammatory diseases (McManus et al. 1998; W.G. Glass et al. 2004; Mahad and Ransohoff 2003; Renner et al. 2011; Trujillo, Fleming, and Perlman 2013; Metcalf et al. 2013). This multifaceted cellular response is predicted to accelerate clearance of viral pathogens, but in the context of MS may enhance inflammatory activity in the CNS, resulting in a more aggressive disease course.

This is perhaps surprising as IFN-β is a well-recognised treatment for MS. However, we attribute this apparent dichotomy to marked differences in the biological effects of local, endogenous production of IFN-β within the CNS as opposed to those induced by systemic treatment in the periphery. Our data indicate induction of IFN-β by interferogenic IgM's stimulates a co-ordinated but sequestered antiviral response in the CNS that includes a pro-inflammatory component predicted to enhance disease activity in MS. In contrast, the mechanisms responsible for the therapeutic efficacy of IFN-β in MS remain poorly understood. It is unclear if systemic treatment with IFN- β also triggers antiviral activity in the CNS, but its mode of action include effects that reduce leukocyte migration across the blood brain barrier (Kraus et al. 2008; Veldhuis et al. 2003; Daniels and Klein 2015). This is the same mechanism by which natalizumab suppresses immune surveillance of the CNS, a major factor contributing to the risk of patients developing PML. As such, this may explain why some of the first cases of natalizumab-associated PML occurred in MS patients undergoing combinatorial treatment with IFN-β (Langer-Gould et al. 2005; Kleinschmidt-DeMasters and Tyler 2005).

Whilst PML is relatively rare, many other viruses cause life-threatening infections of the CNS, the prevalence of which is increasing due to the continuing emergence of encephalitogenic viruses (Kadambari et al. 2014; Munoz et al. 2018). Moreover, in over half of presumptive cases of viral encephalitis the causative agent is never identified (Kennedy, Quan, and Lipkin 2017), and for most viral pathogens there are no effective antivirals available, as a consequence the clinical outcome is often poor (Tyler 2018). Pan-viral therapeutic strategies that boost innate antiviral activity in the CNS rather than attempting to

target the causative agent specifically may therefore transform treatment of these diseases. Activating skin macrophages at the inoculation site provides pan-viral protection against mosquito-transmitted viruses (Bryden et al. 2020), suggesting a similar outcome might be achieved within the CNS by activating microglia. It would be of interest to determine whether the presence of intrathecal lipid-reactive IgM is correlated to differences in the incidence of complications due to other viruses in the nervous system. Our data obtained using BUNV and SFV as genetically unrelated, model neurotropic viruses support this concept, but there are major challenges associated with using lipid-reactive IgMs to stimulate microglial responses in the CNS.

Challenges of therapeutic use of IgMs include the potential risk of neurological deficits caused by antibodies that can bind to the myelin/oligodendrocyte surface (Kanter et al. 2006; Rosenbluth et al. 2003) and the difficulty achieving sustained high concentrations of IgM in the CNS compartment (Neuwelt et al. 1986; Eisen et al. 2017). Miniaturization of intrathecal pumps may overcome the latter problem, but to develop a safe and more generally accessible pharmacological treatment strategy we must understand how lipid-specific IgMs induce expression of IFN-β in the CNS.

We initially focused on the role of antibody-specificity, as this is the primary factor determining the functional activity of somatically mature antibodies. However, those IgMs inducing an antiviral effect in the CNS are close to germline and polyreactive, features indicating they are natural antibodies (Leslie 2015). As yet no common reactivity was identified that would account for the ability of O4, A2B5 and rhIgM22 to induce IFN-β in the CNS. O4 recognizes sulfatide, seminolipid and other targets (Bansal et al. 1989), A2B5 binds multiple c-series gangliosides (Kundu et al. 1983) and rhIgM22 binds one or more unidentified ligands (B.R. Wright et al. 2009). Notably, O4 and hIgM22 are both natural IgMs with few somatic mutations and we hypothesise their polyreactivity underlies their ability to induce IFN-β in myelinated cultures. Our finding that neither sulfogalactolipids (Fig. 5a-c) nor binding to myelin/oligodendrocytes (Fig. 5f-i) are prerequisites to trigger IFN-β expression by microglia suggest cellular specificity is not a major factor determining their activity. Based on these observations and our demonstration IFN-β induction by O4 involves activation of a cGAS-STING-TBK1/IKKε dependent pathway, we are currently exploring the hypothesis that interferogenic IgMs enhance delivery of an endogenous cGAS/STING agonist to microglia. A precedent which is provided by studies demonstrating that immune complexes can induce type I IFN expression in plasmacytoid dendritic cells by enhancing delivery of host nucleic acids (Båve et al. 2003; Lövgren et al. 2006).

In conclusion, we identify a logical mechanism to explain the association between intrathecal synthesis of lipid reactive IgM and decreased incidence of natalizumab-associated PML in MS. This strengthens the case for using the presence of intrathecal lipid-specific IgM for further risk stratification when deciding on treatment regimens for MS patients. Furthermore, we hope this mechanism can be exploited to guide development of pan-viral treatment strategies for viral encephalitis.

Declaration of interest

rHIgM22 is owned by the Mayo Clinic, Rochester MN USA. Nothing further to declare.

Supplementary information:

Additional file 1: Supplementary figures (.pptx)
Additional file 2: Supplementary tables (.xls)

Figure legends

Fig. 1 Lipid-specific IgM provides protection against neurotropic viruses in an IFNAR1-dependent manner **(a-d, i-k)** Rat cultures pre-treated 24 hrs with A4CD or O4 and infected with BUNV (MOI=1). **(a, b)** BUNV-infected mature neurons and neuronal progenitor. **(c, d)** A4CD and O4-treated cultures infected with BUNV. **(i)** BUNV tropism. **(j, k)** Immunocytochemical and RT-qPCR analysis. Data presented as mean ± SEM and analysed by paired two-tailed *t*-test. **(j)** n = 4 **(k)** n = 3. **(e, f, l, m)** WT and *Ifnar1*$^{-/-}$ mouse cultures treated and infected as above. **(e, f)** BUNV-infected WT and *Ifnar1*$^{-/-}$ cultures pre-treated with O4. **(l, m)** Immunocytochemical and plaque assay analysis. Data presented as mean ± SEM, analysed by two-way ANOVA and significant difference determined by Sidak's *post-hoc* test. **(l)** WT n = 2, *Ifnar1*$^{-/-}$ n = 3 **(m)** n = 2 for all conditions. **(g, h, n**) WT and *Ifnar1*$^{-/-}$ mouse cultures treated as above and infected with SFV. **(g, h)** SFV-infected mature oligodendrocytes and oligodendrocyte progenitors. **(n)** Immunocytochemical analysis. Data presented as mean ± SEM, analysed by two-way ANOVA and significant difference determined by Sidak's *post-hoc* test. n = 4 for all conditions. Significant differences denoted as *$p < 0.05$ and ****$p < 0.0001$.

Fig. 2 Lipid-specific IgM induces anti-viral transcriptional signature in vitro **(a, b)** Microarray analysis of rat myelinating cultures treated 24 hrs with media alone, IgM from mouse myeloma (IgM, Sigma) or O4. **(a)** Cluster analysis of all significant genes (FDR *p*-value < 0.05); heat map shows standardized gene expression level of each gene with high expression in red and low expression in blue. **(b)** Bar graph showing genes most upregulated by O4, interferon stimulated genes denoted by an asterisk. **(c-g)** RT-qPCR analysis of rat cultures treated with media alone, IgM, A4CD or O4 for **(c)** 4 hrs and **(d, g)** 24 hrs. Data analysed by one-way ANOVA and significance determined by Tukey's *post hoc* test. IgM (n = 4), A4CD (n=3) and O4 (n=4). Significant differences denoted as *$p < 0.05$, **$p < 0.01$ and ****$p < 0.0001$.

Fig. 3 O4 response is mediated by *Ifnar1* and microglia-derived interferon-β in a cGAS-STING-TBK1-IKKε dependent manner **(a-h)** RT-qPCR analysis of ISG expression in **(a-d)** WT and *Ifnar1*$^{-/-}$ mouse cultures treated 24 hrs with A4CD or O4 and **(e-h)** rat cultures treated 24 hrs with A4CD or O4 in combination with rabbit IgG or anti-rat IFN-β neutralising antibody. Data presented as mean fold change compared to untreated control ± SEM, analysed by two-way ANOVA, significant interaction denoted *$p < 0.05$, **$p < 0.01$, ***$p < 0.001$ and ****$p < 0.0001$. WT (n = 2), *Ifnar1*$^{-/-}$ (n = 4), IFN-β neutralisation experiment (n = 3 all conditions). **(i-m)** Rat cultures treated 10 days with DMSO or PLX3397 followed by 6 hr treatment with A4CD or O4. **(i, j)** Iba1 staining. **(k, l)** Iba1^{+} and DAPI^{+} cells. Data presented as mean ± SEM, significant difference determined by paired two-tailed *t*-test, *$p < 0.05$. (M) RT-qPCR analysis of *Ifnb1* expression. Data presented as mean fold change compared to untreated control ± SEM, analysed by two-way ANOVA, significant interaction denoted *$p < 0.05$, n = 3 for all conditions. **(n)** *Ifnb1* expression in rat cultures treated 6hrs with O4 alone or in combination with vehicle or inhibitor of interest (10μM). Data presented as mean fold change compared to untreated control ± SEM, analysed by one-way ANOVA with Tukey's *post hoc* test. Significant difference compared to O4 alone denoted as *$p <$

0.05. O4 alone (n = 6), DMSO (n = 6), ST2825 (n = 3), RU.521 (n = 2), C-176 (n = 5) and BX795 (n = 3).

Fig. 4 O4 induces cell type specific patterns of ISG expression in the CNS **(a-i)** DIV24 rat cultures treated 24 hrs with A4CD or O4. **(a)** Table showing differential cellular expression of ISGs. Data analysed by paired two-tailed *t*-test. Significant differences denoted by $*p < 0.05$ and $**p < 0.01$. n = 3. **(b, c)** GFAP (astrocytes) and *Cxcl10* in A4CD and O4-treated cultures respectively. **(d, e)** NeuN (neurons) and *Rsad2* in A4CD and O4-treated cultures respectively. **(f, g)** Olig2 (oligodendrocytes) and *Mx1* in A4CD and O4-treated cultures respectively. **(h, i)** Iba1 and *Oasl* in A4CD and O4-treated cultures respectively.

Fig. 5 Lipid-specific IgM mediated antiviral responses are not sulfatide-dependent and identification of similar antibodies in human repertoire **(a, b)** O4 staining in WT and $Cst^{-/-}$ mouse cultures respectively. **(c)** *Ifnb1* expression in DIV24 $Cst^{+/+}$, $Cst^{+/-}$ and $Cst^{-/-}$ cultures treated 6 hrs with A4CD or O4. Data presented as mean fold change compared to untreated control ± SEM and analysed by two-way ANOVA. **(d-g)** Representative images of binding patterns of A4CD, O4, O1 and A2B5 in DIV24 rat cultures. **(h, i)** ISG expression in DIV24 rat cultures treated 24 hrs with A4CD, O4, O1 and A2B5. Data presented as mean fold change compared to untreated control ± SEM and analysed by one-way ANOVA with Tukey's *post hoc* test. Significant difference compared to A4CD denoted as $*p < 0.05$, n = 3 for all conditions. **(j-l)** Screening of patient-derived human IgM antibodies (hIgM's) **(j)** *Ifnb1* expression 2 hrs post-treatment. **(k)** *Cxcl10* expression 24 hrs post-treatment. Data represent two technical replicates from one biological n (DIV24 mouse cultures) and are presented as mean ± SD. **(l)** Immunocytochemical analysis of DIV24 mouse cultures pre-treated 24 hrs with hIgM's and infected with SFV. Data presented as mean ± SD and represent a biological n of 2 for all conditions except sample 3 (n = 1).

Fig. 1

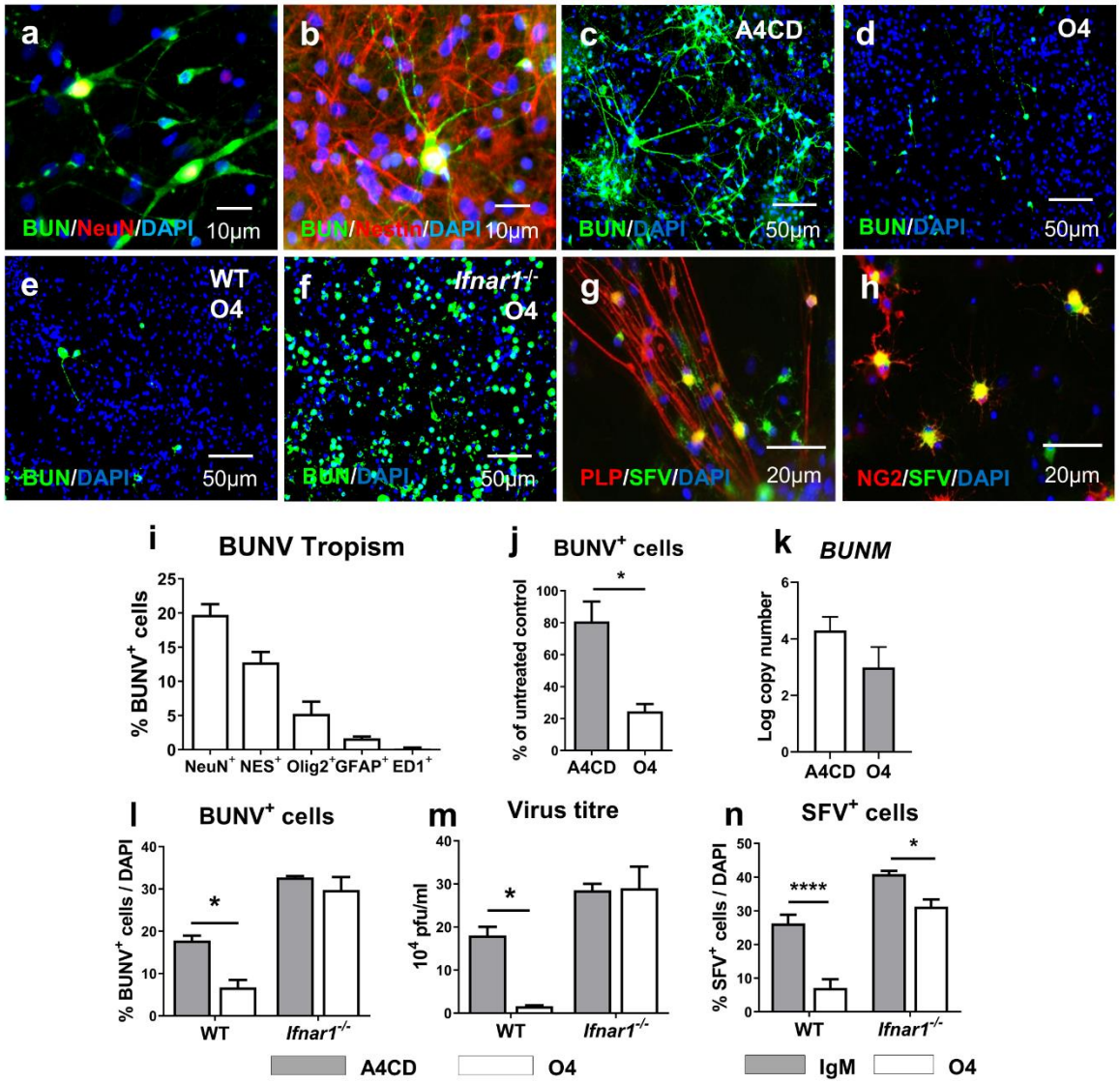
a
BUN/NeuN/DAPI
10μm
b
BUN/NeuN/DAPI
10μm
c
A4CD
BUN/DAPI
50μm
d
O4
BUN/DAPI
50μm
e
WT
O4
BUN/DAPI
50μm
f
Ifnar1-/-
O4
BUN/DAPI
50μm
g
PLP/SFV/DAPI
20μm
h
NG2/SFV/DAPI
20μm
i
BUNV Tropism
% BUNV+ cells
NeuN+ NES+ Olig2+ GFAP+ ED1+
j
BUNV+ cells
% of untreated control
A4CD O4
k
BUNM
Log copy number
A4CD O4
l
BUNV+ cells
% BUNV+ cells / DAPI
WT
Ifnar1-/-
m
Virus titre
10^4 pfu/ml
WT
Ifnar1-/-
n
SFV+ cells
% SFV+ cells / DAPI
WT
Ifnar1-/-
A4CD
O4
IgM
O4

Fig. 2

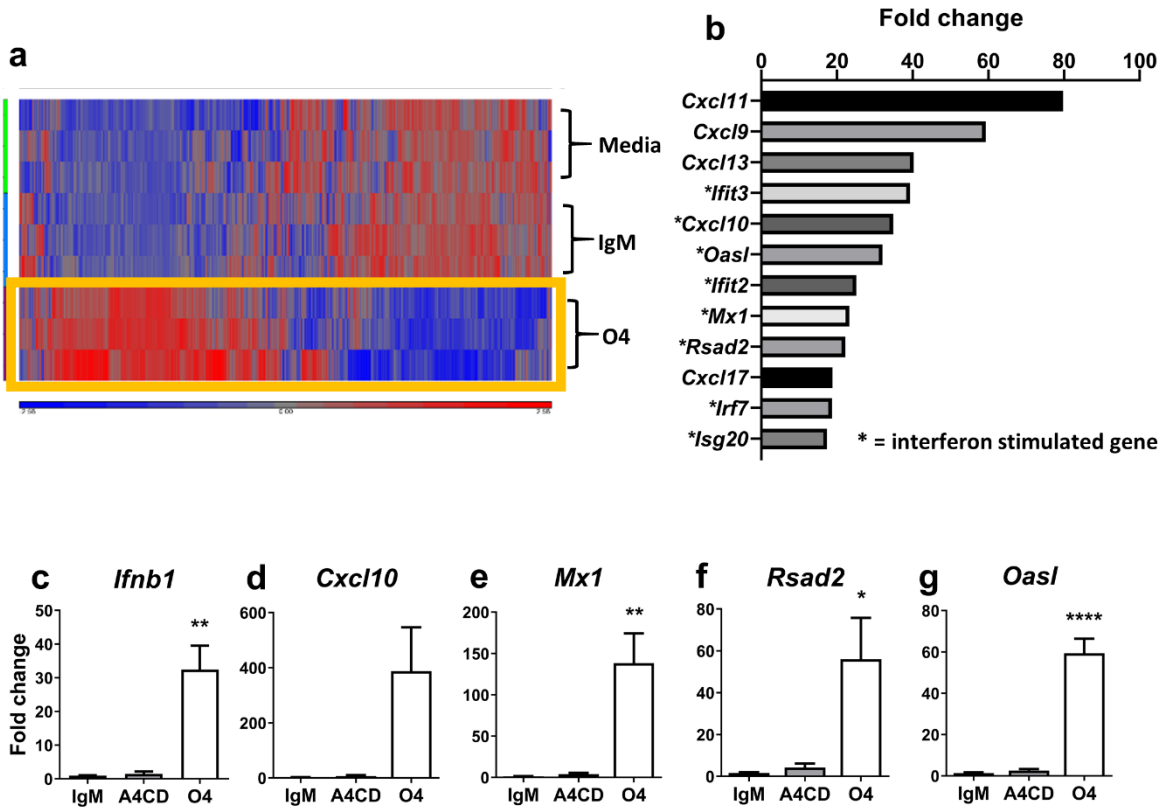
a
Media
IgM
O4
b
Fold change
0
20
40
60
80
100
Cxcl11
Cxcl9
Cxcl13
*Ifit3
*Cxcl10
*Oasl
*Ifit2
*Mx1
*Rsad2
Cxcl17
*Irf7
*Isg20
* = interferon stimulated gene
c
Ifnb1
d
Cxcl10
e
Mx1
f
Rsad2
g
Oasl
Fold change
IgM
A4CD
O4
**
*
****

Fig. 3

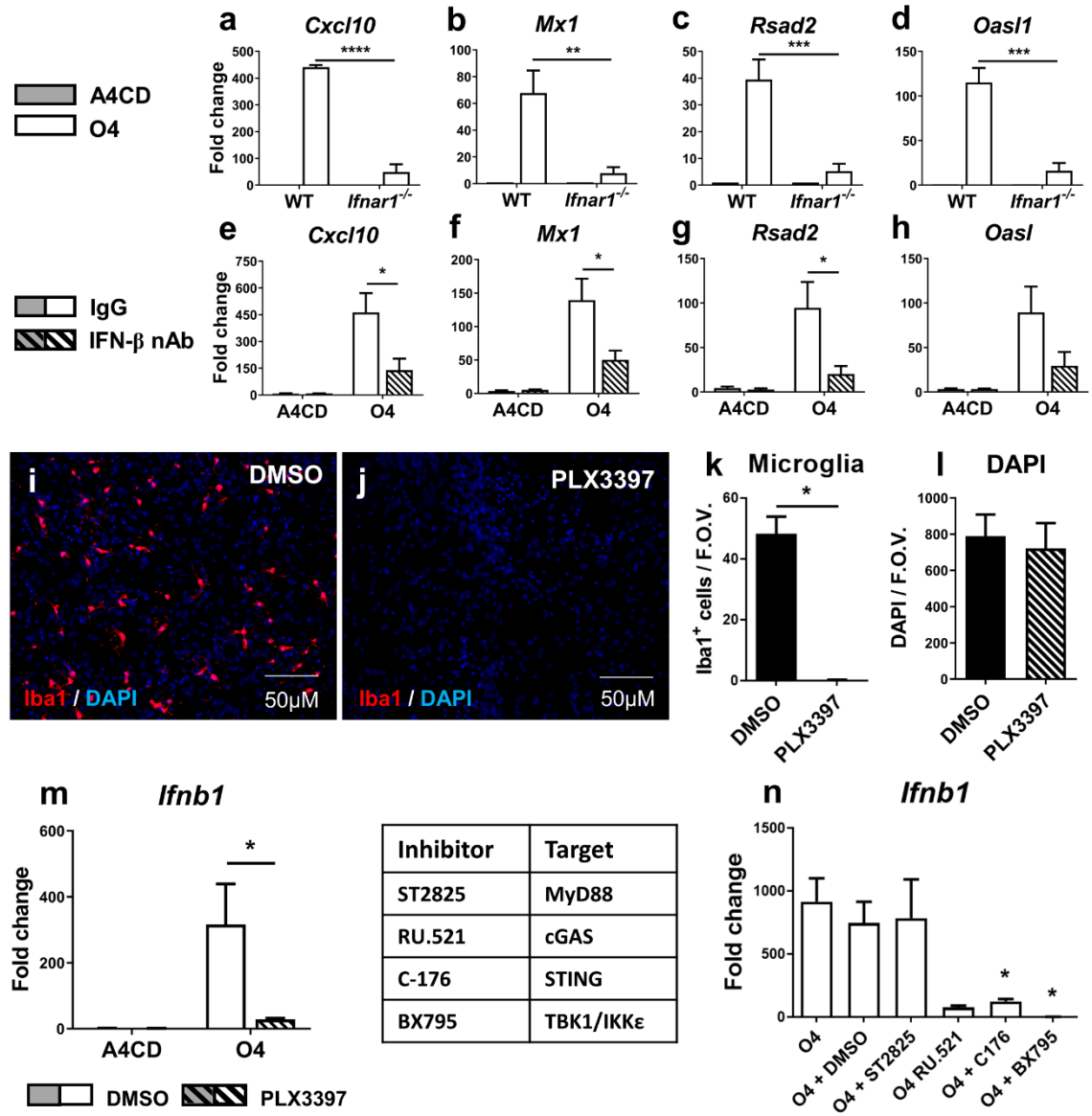

Inhibitor	Target
ST2825	MyD88
RU.521	cGAS
C-176	STING
BX795	TBK1/IKKε

Fig. 4

a	*Cxcl10*		*Rsad2*		*Mx1*		*Oasl*	
	A4CD	O4	A4CD	O4	A4CD	O4	A4CD	O4
Astrocytes	12.9 ± 3.3	50.1 * ± 8.3	5.0 ± 2.2	37.2 * ± 6.5	7.1 ± 1.2	47.0 * ± 4.4	3.4 ± 1.1	31.1 ** ± 1.2
Neurons	1.2 ± 0.3	5.6 * ± 1.3	1.0 ± 0.2	13.3 * ± 2.0	4.5 ± 0.9	11.0 * ± 0.8	0.8 ± 0.3	1.5 ± 0.3
Oligodendrocytes	0.3 ± 0.1	3.7 * ± 0.8	3.1 ± 1.4	4.2 ± 1.2	1.4 ± 0.3	5.3 * ± 0.3	0.6 ± 0.3	1.2 ± 0.1
Microglia	0.6 ± 0.3	1.4 ± 0.7	0.9 ± 0.4	1.3 ± 0.4	3.9 ± 0.1	3.0 ± 0.5	0.4 ± 0.1	5.5 * ± 0.5

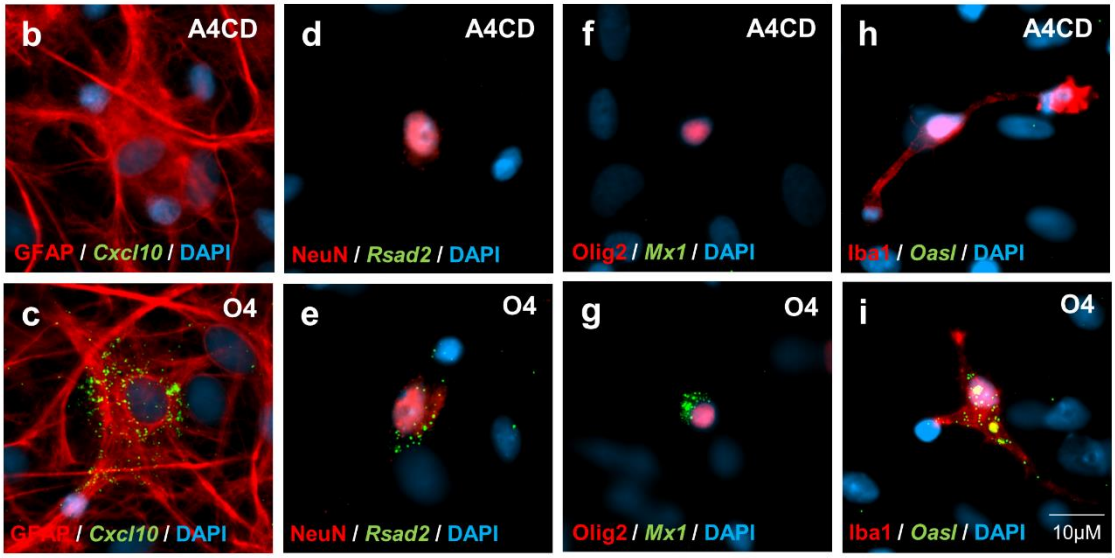

Fig. 5

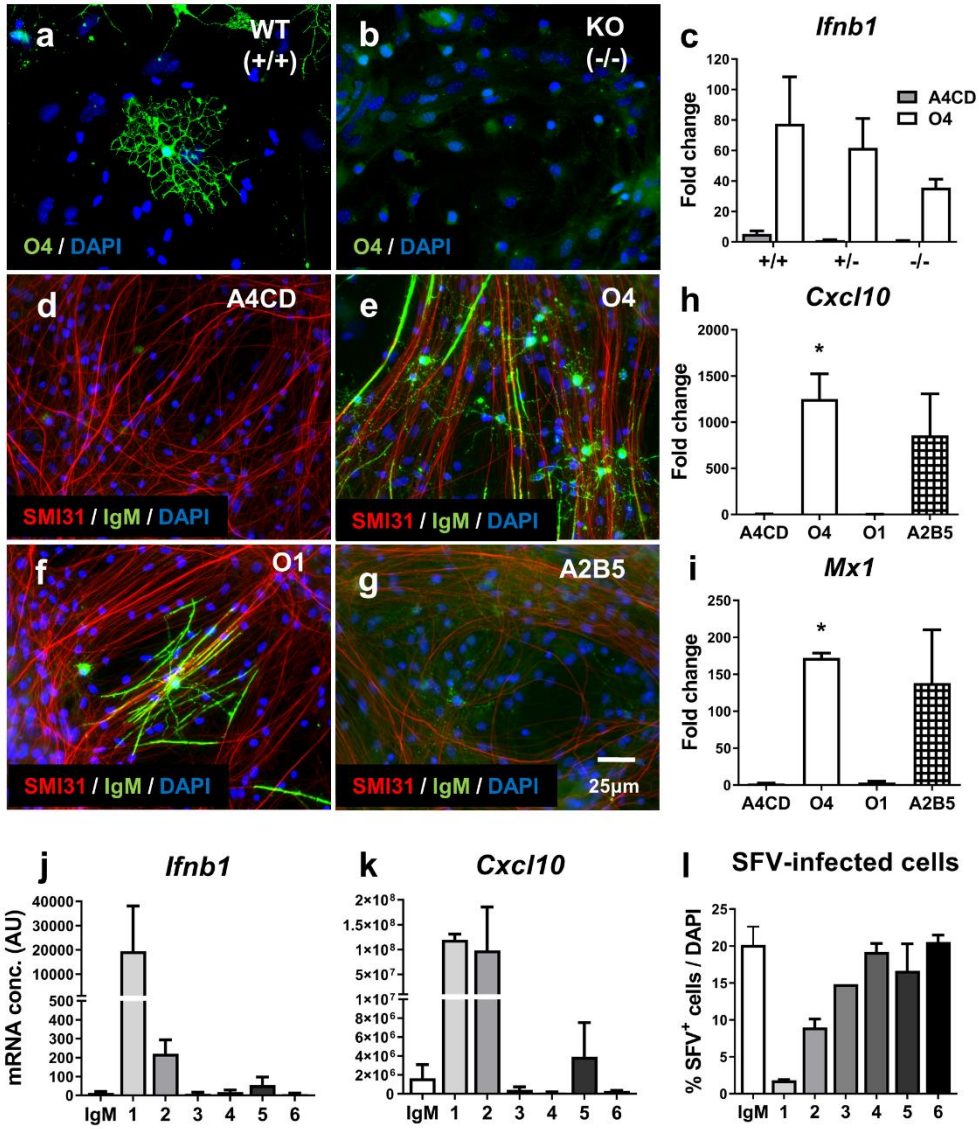
a
WT
(+/+)
O4 / DAPI
b
KO
(-/-)
O4 / DAPI
c
Ifnb1
Fold change
A4CD
O4
+/+
+/-
-/-
d
A4CD
SMI31 / IgM / DAPI
e
O4
SMI31 / IgM / DAPI
h
Cxcl10
Fold change
A4CD
O4
O1
A2B5
f
O1
SMI31 / IgM / DAPI
g
A2B5
SMI31 / IgM / DAPI
25µm
i
Mx1
Fold change
A4CD
O4
O1
A2B5
j
Ifnb1
mRNA conc. (AU)
IgM 1 2 3 4 5 6
k
Cxcl10
IgM 1 2 3 4 5 6
l
SFV-infected cells
% SFV+ cells / DAPI
IgM 1 2 3 4 5 6

References

Abbott, D. W., A. Wilkins, J. M. Asara, and L. C. Cantley. 2004. "The Crohn's disease protein, NOD2, requires RIP2 in order to induce ubiquitinylation of a novel site on NEMO." *Curr Biol* 14 (24): 2217-27. https://doi.org/10.1016/j.cub.2004.12.032.

Abbott, N. J., A. A. Patabendige, D. E. Dolman, S. R. Yusof, and D. J. Begley. 2010. "Structure and function of the blood-brain barrier." *Neurobiol Dis* 37 (1): 13-25. https://doi.org/10.1016/j.nbd.2009.07.030.

Abdou, N. I., and N. L. Abdou. 1973. "Immunoglobulin receptors on human leucocytes. 3. Comparative study of human bone marrow and blood B cells: role of IgM receptors." *Clin Exp Immunol* 13 (1): 45-54.

Abe, T., A. Harashima, T. Xia, H. Konno, K. Konno, A. Morales, J. Ahn, D. Gutman, and G. N. Barber. 2013. "STING recognition of cytoplasmic DNA instigates cellular defense." *Mol Cell* 50 (1): 5-15. https://doi.org/10.1016/j.molcel.2013.01.039.

Afrough, B., S. Dowall, and R. Hewson. 2019. "Emerging viruses and current strategies for vaccine intervention." *Clin Exp Immunol* 196 (2): 157-166. https://doi.org/10.1111/cei.13295.

Aguet, M., F. Belardelli, B. Blanchard, F. Marcucci, and I. Gresser. 1982. "High-affinity binding of 125I-labeled mouse interferon to a specific cell surface receptor. IV. Mouse gamma interferon and cholera toxin do not compete for the common receptor site of alpha / beta interferon." *Virology* 117 (2): 541-4. https://doi.org/10.1016/0042-6822(82)90497-4.

Ahn, E. Y., G. Pan, S. M. Vickers, and J. M. McDonald. 2002. "IFN-gammaupregulates apoptosis-related molecules and enhances Fas-mediated apoptosis in human cholangiocarcinoma." *Int J Cancer* 100 (4): 445-51. https://doi.org/10.1002/ijc.10516.

Ajami, B., J. L. Bennett, C. Krieger, W. Tetzlaff, and F. M. Rossi. 2007. "Local self-renewal can sustain CNS microglia maintenance and function throughout adult life." *Nat Neurosci* 10 (12): 1538-43. https://doi.org/10.1038/nn2014.

Akbar, A. N., N. Borthwick, M. Salmon, W. Gombert, M. Bofill, N. Shamsadeen, D. Pilling, S. Pett, J. E. Grundy, and G. Janossy. 1993. "The significance of low bcl-2 expression by CD45RO T cells in normal individuals and patients with acute viral infections. The role of apoptosis in T cell memory." *J Exp Med* 178 (2): 427-38. https://doi.org/10.1084/jem.178.2.427.

Akiyama, H., K. Ikeda, M. Katoh, E. G. McGeer, and P. L. McGeer. 1994. "Expression of MRP14, 27E10, interferon-alpha and leukocyte common antigen by reactive microglia in postmortem human brain tissue." *J Neuroimmunol* 50 (2): 195-201. https://doi.org/10.1016/0165-5728(94)90046-9.

Akman, L. C., E. N. Silber, and et al. 1949. "Repolarization in the dog ventricle; effects of heating and cooling entire epicardial surface." *Am J Physiol* 159 (3): 492-8. https://doi.org/10.1152/ajplegacy.1949.159.3.492.

Allen, I. C., M. A. Scull, C. B. Moore, E. K. Holl, E. McElvania-TeKippe, D. J. Taxman, E. H. Guthrie, R. J. Pickles, and J. P. Ting. 2009. "The NLRP3

inflammasome mediates in vivo innate immunity to influenza A virus through recognition of viral RNA." *Immunity* 30 (4): 556-65. https://doi.org/10.1016/j.immuni.2009.02.005.

Alvarez, J. I., A. Dodelet-Devillers, H. Kebir, I. Ifergan, P. J. Fabre, S. Terouz, M. Sabbagh, K. Wosik, L. Bourbonnière, M. Bernard, J. van Horssen, H. E. de Vries, F. Charron, and A. Prat. 2011. "The Hedgehog pathway promotes blood-brain barrier integrity and CNS immune quiescence." *Science* 334 (6063): 1727-31. https://doi.org/10.1126/science.1206936.

Amatniek, E., W. Freygang, H. Grundfest, G. Kiebel, and A. Shanes. 1957. "The effect of temperature, potassium, and sodium on the conductance change accompanying the action potential in the squid giant axon." *J Gen Physiol* 41 (2): 333-42. https://doi.org/10.1085/jgp.41.2.333.

Andrews, P. W. 1984. "Retinoic acid induces neuronal differentiation of a cloned human embryonal carcinoma cell line in vitro." *Dev Biol* 103 (2): 285-93. https://doi.org/10.1016/0012-1606(84)90316-6.

Anegon, I., M. C. Cuturi, G. Trinchieri, and B. Perussia. 1988. "Interaction of Fc receptor (CD16) ligands induces transcription of interleukin 2 receptor (CD25) and lymphokine genes and expression of their products in human natural killer cells." *J Exp Med* 167 (2): 452-72. https://doi.org/10.1084/jem.167.2.452.

Angelova, D. M., and D. R. Brown. 2019. "Microglia and the aging brain: are senescent microglia the key to neurodegeneration?" *J Neurochem* 151 (6): 676-688. https://doi.org/10.1111/jnc.14860.

Arai, S., K. Kitada, T. Yamazaki, R. Takai, X. Zhang, Y. Tsugawa, R. Sugisawa, A. Matsumoto, M. Mori, Y. Yoshihara, K. Doi, N. Maehara, S. Kusunoki, A. Takahata, E. Noiri, Y. Suzuki, N. Yahagi, A. Nishiyama, L. Gunaratnam, T. Takano, and T. Miyazaki. 2016. "Apoptosis inhibitor of macrophage protein enhances intraluminal debris clearance and ameliorates acute kidney injury in mice." *Nat Med* 22 (2): 183-93. https://doi.org/10.1038/nm.4012.

Arany, I., M. M. Brysk, K. H. Calhoun, and S. K. Tyring. 1996. "Differentiation and IFN gamma regulate WAF1/CIP1 transcription in p53-independent and p53-dependent pathways in epithelial cells." *In Vivo* 10 (1): 119-23.

Arseni, D. 2020. "GM-CSF licenses microglia to mediate tissue damage in the CNS." Doctoral, College of Medical Veterinary and Life Sciences, Institute of Infection, Immunity, and Inflammation, University of Glasgow (glathesis:2020-79017).

Asch, B. B., D. Medina, and B. R. Brinkley. 1979. "Microtubules and actin-containing filaments of normal, preneoplastic, and neoplastic mouse mammary epithelial cells." *Cancer Res* 39 (3): 893-907.

Ashburner, M., C. A. Ball, J. A. Blake, D. Botstein, H. Butler, J. M. Cherry, A. P. Davis, K. Dolinski, S. S. Dwight, J. T. Eppig, M. A. Harris, D. P. Hill, L. Issel-Tarver, A. Kasarskis, S. Lewis, J. C. Matese, J. E. Richardson, M. Ringwald, G. M. Rubin, and G. Sherlock. 2000. "Gene ontology: tool for the unification of biology. The Gene Ontology Consortium." *Nat Genet* 25 (1): 25-9. https://doi.org/10.1038/75556.

Askew, K., K. Li, A. Olmos-Alonso, F. Garcia-Moreno, Y. Liang, P. Richardson, T. Tipton, M. A. Chapman, K. Riecken, S. Beccari, A. Sierra, Z. Molnár, M. S. Cragg, O. Garaschuk, V. H. Perry, and D. Gomez-Nicola. 2017. "Coupled Proliferation and Apoptosis Maintain the Rapid Turnover of Microglia in the Adult Brain." *Cell Rep* 18 (2): 391-405. https://doi.org/10.1016/j.celrep.2016.12.041.

Aspelund, A., S. Antila, S. T. Proulx, T. V. Karlsen, S. Karaman, M. Detmar, H. Wiig, and K. Alitalo. 2015. "A dural lymphatic vascular system that drains brain interstitial fluid and macromolecules." *J Exp Med* 212 (7): 991-9. https://doi.org/10.1084/jem.20142290.

Astrom, K. E., E. L. Mancall, and E. P. Richardson, Jr. 1958. "Progressive multifocal leuko-encephalopathy; a hitherto unrecognized complication of chronic lymphatic leukaemia and Hodgkin's disease." *Brain* 81 (1): 93-111.

Azuma, M., D. Ito, H. Yagita, K. Okumura, J. H. Phillips, L. L. Lanier, and C. Somoza. 1993. "B70 antigen is a second ligand for CTLA-4 and CD28." *Nature* 366 (6450): 76-9. https://doi.org/10.1038/366076a0.

Babbe, H., A. Roers, A. Waisman, H. Lassmann, N. Goebels, R. Hohlfeld, M. Friese, R. Schröder, M. Deckert, S. Schmidt, R. Ravid, and K. Rajewsky. 2000. "Clonal expansions of CD8(+) T cells dominate the T cell infiltrate in active multiple sclerosis lesions as shown by micromanipulation and single cell polymerase chain reaction." *J Exp Med* 192 (3): 393-404. https://doi.org/10.1084/jem.192.3.393.

Baechler, E. C., F. M. Batliwalla, G. Karypis, P. M. Gaffney, W. A. Ortmann, K. J. Espe, K. B. Shark, W. J. Grande, K. M. Hughes, V. Kapur, P. K. Gregersen, and T. W. Behrens. 2003. "Interferon-inducible gene expression signature in peripheral blood cells of patients with severe lupus." *Proc Natl Acad Sci U S A* 100 (5): 2610-5. https://doi.org/10.1073/pnas.0337679100.

Balfour, H. H., Jr., R. A. Siem, H. Bauer, and P. G. Quie. 1973. "California arbovirus (La Crosse) infections. I. Clinical and laboratory findings in 66 children with meningoencephalitis." *Pediatrics* 52 (5): 680-91.

Baltimore, D. 1971. "Expression of animal virus genomes." *Bacteriol Rev* 35 (3): 235-41.

Bansal, R., A. E. Warrington, A. L. Gard, B. Ranscht, and S. E. Pfeiffer. 1989. "Multiple and novel specificities of monoclonal antibodies O1, O4, and R-mAb used in the analysis of oligodendrocyte development." *J Neurosci Res* 24 (4): 548-57. https://doi.org/10.1002/jnr.490240413.

Barakan, T. H., C. B. Downman, and J. C. Eccles. 1949. "Electric potentials generated by antidromic volleys in quadriceps and hamstring motoneurons." *J Neurophysiol* 12 (6): 393-424. https://doi.org/10.1152/jn.1949.12.6.393.

Baranzini, S. E., and J. R. Oksenberg. 2017. "The Genetics of Multiple Sclerosis: From 0 to 200 in 50 Years." *Trends Genet* 33 (12): 960-970. https://doi.org/10.1016/j.tig.2017.09.004.

Barbey-Martin, C., B. Gigant, T. Bizebard, L. J. Calder, S. A. Wharton, J. J. Skehel, and M. Knossow. 2002. "An antibody that prevents the hemagglutinin low pH fusogenic transition." *Virology* 294 (1): 70-4. https://doi.org/10.1006/viro.2001.1320.

Barbierato, M., M. Borri, L. Facci, M. Zusso, S. D. Skaper, and P. Giusti. 2017. "Expression and Differential Responsiveness of Central Nervous System Glial Cell Populations to the Acute Phase Protein Serum Amyloid A." *Sci Rep* 7 (1): 12158. https://doi.org/10.1038/s41598-017-12529-7.

Barcellos, L. F., S. Sawcer, P. P. Ramsay, S. E. Baranzini, G. Thomson, F. Briggs, B. C. Cree, A. B. Begovich, P. Villoslada, X. Montalban, A. Uccelli, G. Savettieri, R. R. Lincoln, C. DeLoa, J. L. Haines, M. A. Pericak-Vance, A. Compston, S. L. Hauser, and J. R. Oksenberg. 2006. "Heterogeneity at the HLA-DRB1 locus and risk for multiple sclerosis." *Hum Mol Genet* 15 (18): 2813-24. https://doi.org/10.1093/hmg/ddl223.

Barnett, M. H., and J. W. Prineas. 2004. "Relapsing and remitting multiple sclerosis: pathology of the newly forming lesion." *Ann Neurol* 55 (4): 458-68. https://doi.org/10.1002/ana.20016.

Bartholomäus, I., N. Kawakami, F. Odoardi, C. Schläger, D. Miljkovic, J. W. Ellwart, W. E. Klinkert, C. Flügel-Koch, T. B. Issekutz, H. Wekerle, and A. Flügel. 2009. "Effector T cell interactions with meningeal vascular structures in nascent autoimmune CNS lesions." *Nature* 462 (7269): 94-8. https://doi.org/10.1038/nature08478.

Basten, A., N. L. Warner, and T. Mandel. 1972. "A receptor for antibody on B lymphocytes. II. Immunochemical and electron microscopy characteristics." *J Exp Med* 135 (3): 627-42. https://doi.org/10.1084/jem.135.3.627.

Baumann, M., E. M. Hennes, K. Schanda, M. Karenfort, B. Kornek, R. Seidl, K. Diepold, H. Lauffer, I. Marquardt, J. Strautmanis, S. Syrbe, S. Vieker, R. Hoftberger, M. Reindl, and K. Rostasy. 2016. "Children with multiphasic disseminated encephalomyelitis and antibodies to the myelin oligodendrocyte glycoprotein (MOG): Extending the spectrum of MOG antibody positive diseases." *Mult Scler* 22 (14): 1821-1829. https://doi.org/10.1177/1352458516631038.

Baumann, M., K. Sahin, C. Lechner, E. M. Hennes, K. Schanda, S. Mader, M. Karenfort, C. Selch, M. Hausler, A. Eisenkolbl, M. Salandin, U. Gruber-Sedlmayr, A. Blaschek, V. Kraus, S. Leiz, J. Finsterwalder, T. Gotwald, G. Kuchukhidze, T. Berger, M. Reindl, and K. Rostasy. 2015. "Clinical and neuroradiological differences of paediatric acute disseminating encephalomyelitis with and without antibodies to the myelin oligodendrocyte glycoprotein." *J Neurol Neurosurg Psychiatry* 86 (3): 265-72. https://doi.org/10.1136/jnnp-2014-308346.

Baumgarth, N., O. C. Herman, G. C. Jager, L. Brown, and L. A. Herzenberg. 1999. "Innate and acquired humoral immunities to influenza virus are mediated by distinct arms of the immune system." *Proc Natl Acad Sci U S A* 96 (5): 2250-5. https://doi.org/10.1073/pnas.96.5.2250.

Beeson, P. B. 1994. "Age and sex associations of 40 autoimmune diseases." *Am J Med* 96 (5): 457-62. https://doi.org/10.1016/0002-9343(94)90173-2.

Bellizzi, A., C. Nardis, E. Anzivino, D. Rodio, D. Fioriti, M. Mischitelli, F. Chiarini, and V. Pietropaolo. 2012. "Human polyomavirus JC reactivation and pathogenetic mechanisms of progressive multifocal leukoencephalopathy and cancer in the era of monoclonal antibody therapies." *J Neurovirol* 18 (1): 1-11. https://doi.org/10.1007/s13365-012-0080-7.

Berek, C., G. M. Griffiths, and C. Milstein. 1985. "Molecular events during maturation of the immune response to oxazolone." *Nature* 316 (6027): 412-8. https://doi.org/10.1038/316412a0.

Berger, J. R. 2017. "Classifying PML risk with disease modifying therapies." *Mult Scler Relat Disord* 12: 59-63. https://doi.org/10.1016/j.msard.2017.01.006.

Berger, J. R., B. A. Cree, B. Greenberg, B. Hemmer, B. J. Ward, V. M. Dong, and M. Merschhemke. 2018. "Progressive multifocal leukoencephalopathy after fingolimod treatment." *Neurology* 90 (20): e1815-e1821. https://doi.org/10.1212/wnl.0000000000005529.

Bernhard, C. G., and B. Rexed. 1945. "The localization of the premotor interneurons discharging through the peroneal nerve." *J Neurophysiol* 8: 387-92. https://doi.org/10.1152/jn.1945.8.6.387.

Bhangoo, S., D. Ren, R. J. Miller, K. J. Henry, J. Lineswala, C. Hamdouchi, B. Li, P. E. Monahan, D. M. Chan, M. S. Ripsch, and F. A. White. 2007. "Delayed

functional expression of neuronal chemokine receptors following focal nerve demyelination in the rat: a mechanism for the development of chronic sensitization of peripheral nociceptors." *Mol Pain* 3: 38. https://doi.org/10.1186/1744-8069-3-38.

Bianchi, M. E. 2007. "DAMPs, PAMPs and alarmins: all we need to know about danger." *J Leukoc Biol* 81 (1): 1-5. https://doi.org/10.1189/jlb.0306164.

Biber, K., I. Dijkstra, C. Trebst, C. J. De Groot, R. M. Ransohoff, and H. W. Boddeke. 2002. "Functional expression of CXCR3 in cultured mouse and human astrocytes and microglia." *Neuroscience* 112 (3): 487-97. https://doi.org/10.1016/s0306-4522(02)00114-8.

Biberfeld, G., P. Biberfeld, and G. Sterner. 1974. "Cell-mediated immune response following Mycoplasma pneumoniae infection in man. I. Lymphocyte stimulation." *Clin Exp Immunol* 17 (1): 29-41.

Bijland, S., G. Thomson, M. Euston, K. Michail, K. Thummler, S. Mucklisch, C. L. Crawford, S. C. Barnett, M. McLaughlin, T. J. Anderson, C. Linington, E. R. Brown, E. R. Kalkman, and J. M. Edgar. 2019. "An in vitro model for studying CNS white matter: functional properties and experimental approaches." *F1000Res* 8: 117. https://doi.org/10.12688/f1000research.16802.1.

Binder, G. K., and D. E. Griffin. 2001. "Interferon-gamma-mediated site-specific clearance of alphavirus from CNS neurons." *Science* 293 (5528): 303-6. https://doi.org/10.1126/science.1059742.

Binley, J. M., T. Wrin, B. Korber, M. B. Zwick, M. Wang, C. Chappey, G. Stiegler, R. Kunert, S. Zolla-Pazner, H. Katinger, C. J. Petropoulos, and D. R. Burton. 2004. "Comprehensive cross-clade neutralization analysis of a panel of anti-human immunodeficiency virus type 1 monoclonal antibodies." *J Virol* 78 (23): 13232-52. https://doi.org/10.1128/jvi.78.23.13232-13252.2004.

Biogen. 2020. *Physician* Information and Management Guidelines for Patients With Multiple Sclerosis Receiving TYSABRI Therapy*.

Bjorneboe, M., H. Gormsen, and F. Lundquist. 1947. "Further experimental studies on the role of the plasma cells as antibody producers." *J Immunol* 55 (2): 121-9.

Björklund, H., M. Eriksdotter-Nilsson, D. Dahl, and L. Olson. 1984. "Astrocytes in smears of CNS tissues as visualized by GFA and vimentin immunofluorescence." *Med Biol* 62 (1): 38-48.

Blakqori, G., S. Delhaye, M. Habjan, C. D. Blair, I. Sánchez-Vargas, K. E. Olson, G. Attarzadeh-Yazdi, R. Fragkoudis, A. Kohl, U. Kalinke, S. Weiss, T. Michiels, P. Staeheli, and F. Weber. 2007. "La Crosse bunyavirus nonstructural protein NSs serves to suppress the type I interferon system of mammalian hosts." *J Virol* 81 (10): 4991-9. https://doi.org/10.1128/jvi.01933-06.

Blandino, R., and N. Baumgarth. 2019. "Secreted IgM: New tricks for an old molecule." *J Leukoc Biol* 106 (5): 1021-1034. https://doi.org/10.1002/jlb.3ri0519-161r.

Blasi, E., R. Barluzzi, V. Bocchini, R. Mazzolla, and F. Bistoni. 1990. "Immortalization of murine microglial cells by a v-raf/v-myc carrying retrovirus." *J Neuroimmunol* 27 (2-3): 229-37. https://doi.org/10.1016/0165-5728(90)90073-v.

Blatteis, C. M., S. Li, Z. Li, V. Perlik, and C. Feleder. 2004. "Signaling the brain in systemic inflammation: the role of complement." *Front Biosci* 9: 915-31. https://doi.org/10.2741/1297.

Blinzinger, K., and G. Kreutzberg. 1968. "Displacement of synaptic terminals from regenerating motoneurons by microglial cells." *Z Zellforsch Mikrosk Anat* 85 (2): 145-57. https://doi.org/10.1007/bf00325030.

Bode, U., C. Duda, F. Weidner, M. Rodriguez-Palmero, K. Wonigeit, R. Pabst, and J. Westermann. 1999. "Activated T cells enter rat lymph nodes and Peyer's patches via high endothelial venules: survival by tissue-specific proliferation and preferential exit of CD8+ T cell progeny." *Eur J Immunol* 29 (5): 1487-95. https://doi.org/10.1002/(sici)1521-4141(199905)29:05<1487::aid-immu1487>3.0.co;2-1.

Boonpucknavig, S., N. Bhamarapravati, S. Nimmannitya, A. Phalavadhtana, and J. Siripont. 1976. "Immunofluorescent staining of the surfaces of lymphocytes in suspension from patients with dengue hemorrhagic fever." *Am J Pathol* 85 (1): 37-48.

Boos, L., I. L. Campbell, R. Ames, R. A. Wetsel, and S. R. Barnum. 2004. "Deletion of the complement anaphylatoxin C3a receptor attenuates, whereas ectopic expression of C3a in the brain exacerbates, experimental autoimmune encephalomyelitis." *J Immunol* 173 (7): 4708-14. https://doi.org/10.4049/jimmunol.173.7.4708.

Bosco, A., K. Cusato, G. P. Nicchia, A. Frigeri, and D. C. Spray. 2005. "A developmental switch in the expression of aquaporin-4 and Kir4.1 from horizontal to Müller cells in mouse retina." *Invest Ophthalmol Vis Sci* 46 (10): 3869-75. https://doi.org/10.1167/iovs.05-0385.

Bowie, A., E. Kiss-Toth, J. A. Symons, G. L. Smith, S. K. Dower, and L. A. O'Neill. 2000. "A46R and A52R from vaccinia virus are antagonists of host IL-1 and toll-like receptor signaling." *Proc Natl Acad Sci U S A* 97 (18): 10162-7. https://doi.org/10.1073/pnas.160027697.

Bozzali, M., M. Cercignani, M. P. Sormani, G. Comi, and M. Filippi. 2002. "Quantification of brain gray matter damage in different MS phenotypes by use of diffusion tensor MR imaging." *AJNR Am J Neuroradiol* 23 (6): 985-8.

Bradbury, M. W., J. Burden, E. W. Hillhouse, and M. T. Jones. 1974. "Stimulation electrically and by acetylcholine of the rat hypothalamus in vitro." *J Physiol* 239 (2): 269-83. https://doi.org/10.1113/jphysiol.1974.sp010568.

Bramow, S., J. M. Frischer, H. Lassmann, N. Koch-Henriksen, C. F. Lucchinetti, P. S. Sørensen, and H. Laursen. 2010. "Demyelination versus remyelination in progressive multiple sclerosis." *Brain* 133 (10): 2983-98. https://doi.org/10.1093/brain/awq250.

Braun, J. S., R. Novak, K. H. Herzog, S. M. Bodner, J. L. Cleveland, and E. I. Tuomanen. 1999. "Neuroprotection by a caspase inhibitor in acute bacterial meningitis." *Nat Med* 5 (3): 298-302. https://doi.org/10.1038/6514.

Brennan, K. M., F. Galban-Horcajo, S. Rinaldi, C. P. O'Leary, C. S. Goodyear, G. Kalna, A. Arthur, C. Elliot, S. Barnett, C. Linington, J. L. Bennett, G. P. Owens, and H. J. Willison. 2011. "Lipid arrays identify myelin-derived lipids and lipid complexes as prominent targets for oligoclonal band antibodies in multiple sclerosis." *J Neuroimmunol* 238 (1-2): 87-95. https://doi.org/10.1016/j.jneuroim.2011.08.002.

Brettschneider, J., A. Czerwoniak, M. Senel, L. Fang, J. Kassubek, E. Pinkhardt, F. Lauda, T. Kapfer, S. Jesse, V. Lehmensiek, A. C. Ludolph, M. Otto, and H. Tumani. 2010. "The chemokine CXCL13 is a prognostic marker in clinically isolated syndrome (CIS)." *PLoS One* 5 (8): e11986. https://doi.org/10.1371/journal.pone.0011986.

Brettschneider, J., H. Tumani, U. Kiechle, R. Muche, G. Richards, V. Lehmensiek, A. C. Ludolph, and M. Otto. 2009. "IgG antibodies against measles, rubella, and varicella zoster virus predict conversion to multiple sclerosis in clinically isolated syndrome." *PLoS One* 4 (11): e7638. https://doi.org/10.1371/journal.pone.0007638.

Brewer, J. W., T. D. Randall, R. M. Parkhouse, and R. B. Corley. 1994. "Mechanism and subcellular localization of secretory IgM polymer assembly." *J Biol Chem* 269 (25): 17338-48.

Bridgen, A., and R. M. Elliott. 1996. "Rescue of a segmented negative-strand RNA virus entirely from cloned complementary DNAs." *Proc Natl Acad Sci U S A* 93 (26): 15400-4. https://doi.org/10.1073/pnas.93.26.15400.

Brightman, M. W., and T. S. Reese. 1969. "Junctions between intimately apposed cell membranes in the vertebrate brain." *J Cell Biol* 40 (3): 648-77. https://doi.org/10.1083/jcb.40.3.648.

Brooks, B. R., and D. L. Walker. 1984. "Progressive multifocal leukoencephalopathy." *Neurol Clin* 2 (2): 299-313.

Brown, B. A. 2009. "Natalizumab in the treatment of multiple sclerosis." *Ther Clin Risk Manag* 5 (3): 585-94.

Bryden, S. R., M. Pingen, D. A. Lefteri, J. Miltenburg, L. Delang, S. Jacobs, R. Abdelnabi, J. Neyts, E. Pondeville, J. Major, M. Muller, H. Khalid, A. Tuplin, M. Varjak, A. Merits, J. Edgar, G. J. Graham, K. Shams, and C. S. McKimmie. 2020. "Pan-viral protection against arboviruses by activating skin macrophages at the inoculation site." *Sci Transl Med* 12 (527). https://doi.org/10.1126/scitranslmed.aax2421.

Brändle, S. M., B. Obermeier, M. Senel, J. Bruder, R. Mentele, M. Khademi, T. Olsson, H. Tumani, W. Kristoferitsch, F. Lottspeich, H. Wekerle, R. Hohlfeld, and K. Dornmair. 2016. "Distinct oligoclonal band antibodies in multiple sclerosis recognize ubiquitous self-proteins." *Proc Natl Acad Sci U S A* 113 (28): 7864-9. https://doi.org/10.1073/pnas.1522730113.

Bsibsi, M., R. Ravid, D. Gveric, and J. M. van Noort. 2002. "Broad expression of Toll-like receptors in the human central nervous system." *J Neuropathol Exp Neurol* 61 (11): 1013-21. https://doi.org/10.1093/jnen/61.11.1013.

Buller, R. M., K. L. Holmes, A. Hügin, T. N. Frederickson, and H. C. Morse, 3rd. 1987. "Induction of cytotoxic T-cell responses in vivo in the absence of CD4 helper cells." *Nature* 328 (6125): 77-9. https://doi.org/10.1038/328077a0.

Burgert, H. G., and S. Kvist. 1985. "An adenovirus type 2 glycoprotein blocks cell surface expression of human histocompatibility class I antigens." *Cell* 41 (3): 987-97. https://doi.org/10.1016/s0092-8674(85)80079-9.

Båve, U., M. Magnusson, M. L. Eloranta, A. Perers, G. V. Alm, and L. Rönnblom. 2003. "Fc gamma RIIa is expressed on natural IFN-alpha-producing cells (plasmacytoid dendritic cells) and is required for the IFN-alpha production induced by apoptotic cells combined with lupus IgG." *J Immunol* 171 (6): 3296-302. https://doi.org/10.4049/jimmunol.171.6.3296.

Cahoy, J. D., B. Emery, A. Kaushal, L. C. Foo, J. L. Zamanian, K. S. Christopherson, Y. Xing, J. L. Lubischer, P. A. Krieg, S. A. Krupenko, W. J. Thompson, and B. A. Barres. 2008. "A transcriptome database for astrocytes, neurons, and oligodendrocytes: a new resource for understanding brain development and function." *J Neurosci* 28 (1): 264-78. https://doi.org/10.1523/jneurosci.4178-07.2008.

Campodónico, V. L., N. J. Llosa, M. Grout, G. Döring, T. Maira-Litrán, and G. B. Pier. 2010. "Evaluation of flagella and flagellin of Pseudomonas aeruginosa

as vaccines." *Infect Immun* 78 (2): 746-55. https://doi.org/10.1128/iai.00806-09.

Cantin, E. M., D. R. Hinton, J. Chen, and H. Openshaw. 1995. "Gamma interferon expression during acute and latent nervous system infection by herpes simplex virus type 1." *J Virol* 69 (8): 4898-905. https://doi.org/10.1128/jvi.69.8.4898-4905.1995.

Carlton-Smith, C., and R. M. Elliott. 2012. "Viperin, MTAP44, and protein kinase R contribute to the interferon-induced inhibition of Bunyamwera Orthobunyavirus replication." *J Virol* 86 (21): 11548-57. https://doi.org/10.1128/jvi.01773-12.

Carpenter, A. E., T. R. Jones, M. R. Lamprecht, C. Clarke, I. H. Kang, O. Friman, D. A. Guertin, J. H. Chang, R. A. Lindquist, J. Moffat, P. Golland, and D. M. Sabatini. 2006. "CellProfiler: image analysis software for identifying and quantifying cell phenotypes." *Genome Biol* 7 (10): R100. https://doi.org/10.1186/gb-2006-7-10-r100.

Carr, D. J., and I. L. Campbell. 2006. "Herpes simplex virus type 1 induction of chemokine production is unrelated to viral load in the cornea but not in the nervous system." *Viral Immunol* 19 (4): 741-6. https://doi.org/10.1089/vim.2006.19.741.

Carr, D. J. J., J. Ash, T. E. Lane, and W. A. Kuziel. 2006. "Abnormal immune response of CCR5-deficient mice to ocular infection with herpes simplex virus type 1." *J Gen Virol* 87 (Pt 3): 489-499. https://doi.org/10.1099/vir.0.81339-0.

Castelli, J., K. A. Wood, and R. J. Youle. 1998. "The 2-5A system in viral infection and apoptosis." *Biomed Pharmacother* 52 (9): 386-90. https://doi.org/10.1016/s0753-3322(99)80006-7.

Cavanaugh, S. E., A. M. Holmgren, and G. F. Rall. 2015. "Homeostatic interferon expression in neurons is sufficient for early control of viral infection." *J Neuroimmunol* 279: 11-9. https://doi.org/10.1016/j.jneuroim.2014.12.012.

Chandler, W. K., and A. L. Hodgkin. 1965. "The effect of internal sodium on the action potential in the presence of different internal anions." *J Physiol* 181 (3): 594-611. https://doi.org/10.1113/jphysiol.1965.sp007785.

Chaudhuri, A., and P. G. Kennedy. 2002. "Diagnosis and treatment of viral encephalitis." *Postgrad Med J* 78 (924): 575-83. https://doi.org/10.1136/pmj.78.924.575.

Chauhan, M. B., and N. B. Chauhan. 2015. "Brain Uptake of Neurotherapeutics after Intranasal versus Intraperitoneal Delivery in Mice." *J Neurol Neurosurg* 2 (1).

Chen, X., N. Kong, J. Xu, J. Wang, M. Zhang, K. Ruan, L. Li, Y. Zhang, H. Zheng, W. Tong, G. Li, T. Shan, and G. Tong. 2021. "Pseudorabies virus UL24 antagonizes OASL-mediated antiviral effect." *Virus Res* 295: 198276. https://doi.org/10.1016/j.virusres.2020.198276.

Cheng, Y. S., R. J. Colonno, and F. H. Yin. 1983. "Interferon induction of fibroblast proteins with guanylate binding activity." *J Biol Chem* 258 (12): 7746-50.

Chin, K. C., and P. Cresswell. 2001. "Viperin (cig5), an IFN-inducible antiviral protein directly induced by human cytomegalovirus." *Proc Natl Acad Sci U S A* 98 (26): 15125-30. https://doi.org/10.1073/pnas.011593298.

Chinnery, H. R., M. J. Ruitenberg, and P. G. McMenamin. 2010. "Novel characterization of monocyte-derived cell populations in the meninges and choroid plexus and their rates of replenishment in bone marrow

chimeric mice." *J Neuropathol Exp Neurol* 69 (9): 896-909. https://doi.org/10.1097/NEN.0b013e3181edbc1a.

Chiu, Y. H., J. B. Macmillan, and Z. J. Chen. 2009. "RNA polymerase III detects cytosolic DNA and induces type I interferons through the RIG-I pathway." *Cell* 138 (3): 576-91. https://doi.org/10.1016/j.cell.2009.06.015.

Cho, H., S. C. Proll, K. J. Szretter, M. G. Katze, M. Gale, Jr., and M. S. Diamond. 2013. "Differential innate immune response programs in neuronal subtypes determine susceptibility to infection in the brain by positive-stranded RNA viruses." *Nat Med* 19 (4): 458-64. https://doi.org/10.1038/nm.3108.

Choi, S. H., Y. H. Kim, M. Hebisch, C. Sliwinski, S. Lee, C. D'Avanzo, H. Chen, B. Hooli, C. Asselin, J. Muffat, J. B. Klee, C. Zhang, B. J. Wainger, M. Peitz, D. M. Kovacs, C. J. Woolf, S. L. Wagner, R. E. Tanzi, and D. Y. Kim. 2014. "A three-dimensional human neural cell culture model of Alzheimer's disease." *Nature* 515 (7526): 274-8. https://doi.org/10.1038/nature13800.

Christensen, J. E., C. de Lemos, T. Moos, J. P. Christensen, and A. R. Thomsen. 2006. "CXCL10 is the key ligand for CXCR3 on CD8+ effector T cells involved in immune surveillance of the lymphocytic choriomeningitis virus-infected central nervous system." *J Immunol* 176 (7): 4235-43. https://doi.org/10.4049/jimmunol.176.7.4235.

Clifford, D. B., B. Ances, C. Costello, S. Rosen-Schmidt, M. Andersson, D. Parks, A. Perry, R. Yerra, R. Schmidt, E. Alvarez, and K. L. Tyler. 2011. "Rituximab-associated progressive multifocal leukoencephalopathy in rheumatoid arthritis." *Arch Neurol* 68 (9): 1156-64. https://doi.org/10.1001/archneurol.2011.103.

Co, J. K., S. Verma, U. Gurjav, L. Sumibcay, and V. R. Nerurkar. 2007. "Interferon- alpha and - beta restrict polyomavirus JC replication in primary human fetal glial cells: implications for progressive multifocal leukoencephalopathy therapy." *J Infect Dis* 196 (5): 712-8. https://doi.org/10.1086/520518.

Coisne, C., W. Mao, and B. Engelhardt. 2009. "Cutting edge: Natalizumab blocks adhesion but not initial contact of human T cells to the blood-brain barrier in vivo in an animal model of multiple sclerosis." *J Immunol* 182 (10): 5909-13. https://doi.org/10.4049/jimmunol.0803418.

Colombo, M., M. Dono, P. Gazzola, S. Roncella, A. Valetto, N. Chiorazzi, G. L. Mancardi, and M. Ferrarini. 2000. "Accumulation of clonally related B lymphocytes in the cerebrospinal fluid of multiple sclerosis patients." *J Immunol* 164 (5): 2782-9. https://doi.org/10.4049/jimmunol.164.5.2782.

Colucci, M., H. Stöckmann, A. Butera, A. Masotti, A. Baldassarre, E. Giorda, S. Petrini, P. M. Rudd, R. Sitia, F. Emma, and M. Vivarelli. 2015. "Sialylation of N-linked glycans influences the immunomodulatory effects of IgM on T cells." *J Immunol* 194 (1): 151-7. https://doi.org/10.4049/jimmunol.1402025.

Combadiere, C., S. K. Ahuja, and P. M. Murphy. 1995. "Cloning, chromosomal localization, and RNA expression of a human beta chemokine receptor-like gene." *DNA Cell Biol* 14 (8): 673-80. https://doi.org/10.1089/dna.1995.14.673.

Compston, A., and A. Coles. 2008. "Multiple sclerosis." *Lancet* 372 (9648): 1502-17. https://doi.org/10.1016/s0140-6736(08)61620-7.

Confavreux, C., and S. Vukusic. 2006. "Natural history of multiple sclerosis: a unifying concept." *Brain* 129 (Pt 3): 606-16. https://doi.org/10.1093/brain/awl007.

Confavreux, C., S. Vukusic, T. Moreau, and P. Adeleine. 2000. "Relapses and progression of disability in multiple sclerosis." *N Engl J Med* 343 (20): 1430-8. https://doi.org/10.1056/nejm200011163432001.

Creemers, P. C., M. O'Shaughnessy, and W. J. Boyko. 1986. "Increased interleukin-2 receptor expression after mitogen stimulation on CD4- and CD8-positive lymphocytes and decreased interleukin-2 production in HTLV-III antibody-positive symptomatic individuals." *Immunology* 59 (4): 627-9.

Croft, C. L., H. S. Futch, B. D. Moore, and T. E. Golde. 2019. "Organotypic brain slice cultures to model neurodegenerative proteinopathies." *Mol Neurodegener* 14 (1): 45. https://doi.org/10.1186/s13024-019-0346-0.

Cronk, J. C., N. C. Derecki, E. Ji, Y. Xu, A. E. Lampano, I. Smirnov, W. Baker, G. T. Norris, I. Marin, N. Coddington, Y. Wolf, S. D. Turner, A. Aderem, A. L. Klibanov, T. H. Harris, S. Jung, V. Litvak, and J. Kipnis. 2015. "Methyl-CpG Binding Protein 2 Regulates Microglia and Macrophage Gene Expression in Response to Inflammatory Stimuli." *Immunity* 42 (4): 679-91. https://doi.org/10.1016/j.immuni.2015.03.013.

Cumberbatch, M., and I. Kimber. 1992. "Dermal tumour necrosis factor-alpha induces dendritic cell migration to draining lymph nodes, and possibly provides one stimulus for Langerhans' cell migration." *Immunology* 75 (2): 257-63.

Cumberworth, S. L., J. A. Barrie, M. E. Cunningham, D. P. G. de Figueiredo, V. Schultz, A. J. Wilder-Smith, B. Brennan, L. J. Pena, R. Freitas de Oliveira França, C. Linington, S. C. Barnett, H. J. Willison, A. Kohl, and J. M. Edgar. 2017. "Zika virus tropism and interactions in myelinating neural cell cultures: CNS cells and myelin are preferentially affected." *Acta Neuropathol Commun* 5 (1): 50. https://doi.org/10.1186/s40478-017-0450-8.

Cutler, R. W., E. Merler, and J. P. Hammerstad. 1968. "Production of antibody by the central nervous system in subacute sclerosing panencephalitis." *Neurology* 18 (1 Pt 2): 129-32. https://doi.org/10.1212/wnl.18.1_part_2.129.

Cutter, G. R., and O. Stüve. 2014. "Does risk stratification decrease the risk of natalizumab-associated PML? Where is the evidence?" *Mult Scler* 20 (10): 1304-5. https://doi.org/10.1177/1352458514531843.

Cyong, J. C., S. S. Witkin, B. Rieger, E. Barbarese, R. A. Good, and N. K. Day. 1982. "Antibody-independent complement activation by myelin via the classical complement pathway." *J Exp Med* 155 (2): 587-98. https://doi.org/10.1084/jem.155.2.587.

Daffis, S., M. A. Samuel, B. C. Keller, M. Gale, Jr., and M. S. Diamond. 2007. "Cell-specific IRF-3 responses protect against West Nile virus infection by interferon-dependent and -independent mechanisms." *PLoS Pathog* 3 (7): e106. https://doi.org/10.1371/journal.ppat.0030106.

Dale, H. 1934. "CHEMICAL TRANSMISSION OF THE EFFECTS OF NERVE IMPULSES." *Br Med J* 1 (3827): 835-41. https://doi.org/10.1136/bmj.1.3827.835.

Daniels, B. P., D. W. Holman, L. Cruz-Orengo, H. Jujjavarapu, D. M. Durrant, and R. S. Klein. 2014. "Viral pathogen-associated molecular patterns regulate blood-brain barrier integrity via competing innate cytokine signals." *mBio* 5 (5): e01476-14. https://doi.org/10.1128/mBio.01476-14.

Daniels, B. P., H. Jujjavarapu, D. M. Durrant, J. L. Williams, R. R. Green, J. P. White, H. M. Lazear, M. Gale, Jr., M. S. Diamond, and R. S. Klein. 2017. "Regional astrocyte IFN signaling restricts pathogenesis during neurotropic

viral infection." *J Clin Invest* 127 (3): 843-856. https://doi.org/10.1172/jci88720.

Daniels, B. P., and R. S. Klein. 2015. "Knocking on Closed Doors: Host Interferons Dynamically Regulate Blood-Brain Barrier Function during Viral Infections of the Central Nervous System." *PLoS Pathog* 11 (9): e1005096. https://doi.org/10.1371/journal.ppat.1005096.

Darbinyan, A., R. Kaminski, M. K. White, N. Darbinian-Sarkissian, and K. Khalili. 2013. "Polyomavirus JC infection inhibits differentiation of oligodendrocyte progenitor cells." *J Neurosci Res* 91 (1): 116-27. https://doi.org/10.1002/jnr.23135.

Davalos, D., J. Grutzendler, G. Yang, J. V. Kim, Y. Zuo, S. Jung, D. R. Littman, M. L. Dustin, and W. B. Gan. 2005. "ATP mediates rapid microglial response to local brain injury in vivo." *Nat Neurosci* 8 (6): 752-8. https://doi.org/10.1038/nn1472.

De Jager, P. L., X. Jia, J. Wang, P. I. de Bakker, L. Ottoboni, N. T. Aggarwal, L. Piccio, S. Raychaudhuri, D. Tran, C. Aubin, R. Briskin, S. Romano, S. E. Baranzini, J. L. McCauley, M. A. Pericak-Vance, J. L. Haines, R. A. Gibson, Y. Naeglin, B. Uitdehaag, P. M. Matthews, L. Kappos, C. Polman, W. L. McArdle, D. P. Strachan, D. Evans, A. H. Cross, M. J. Daly, A. Compston, S. J. Sawcer, H. L. Weiner, S. L. Hauser, D. A. Hafler, and J. R. Oksenberg. 2009. "Meta-analysis of genome scans and replication identify CD6, IRF8 and TNFRSF1A as new multiple sclerosis susceptibility loci." *Nat Genet* 41 (7): 776-82. https://doi.org/10.1038/ng.401.

De Simoni, A., C. B. Griesinger, and F. A. Edwards. 2003. "Development of rat CA1 neurones in acute versus organotypic slices: role of experience in synaptic morphology and activity." *J Physiol* 550 (Pt 1): 135-47. https://doi.org/10.1113/jphysiol.2003.039099.

de Toledo-Pinto, T. G., A. B. Ferreira, M. Ribeiro-Alves, L. S. Rodrigues, L. R. Batista-Silva, B. J. Silva, R. M. Lemes, A. N. Martinez, F. G. Sandoval, L. E. Alvarado-Arnez, P. S. Rosa, E. J. Shannon, M. C. Pessolani, R. O. Pinheiro, S. L. Antunes, E. N. Sarno, F. A. Lara, D. L. Williams, and M. Ozório Moraes. 2016. "STING-Dependent 2'-5' Oligoadenylate Synthetase-Like Production Is Required for Intracellular Mycobacterium leprae Survival." *J Infect Dis* 214 (2): 311-20. https://doi.org/10.1093/infdis/jiw144.

Dedoni, S., L. A. Campbell, B. K. Harvey, V. Avdoshina, and I. Mocchetti. 2018. "The orphan G-protein-coupled receptor 75 signaling is activated by the chemokine CCL5." *J Neurochem* 146 (5): 526-539. https://doi.org/10.1111/jnc.14463.

Delhaye, S., S. Paul, G. Blakqori, M. Minet, F. Weber, P. Staeheli, and T. Michiels. 2006. "Neurons produce type I interferon during viral encephalitis." *Proc Natl Acad Sci U S A* 103 (20): 7835-40. https://doi.org/10.1073/pnas.0602460103.

Der, S. D., A. Zhou, B. R. Williams, and R. H. Silverman. 1998. "Identification of genes differentially regulated by interferon alpha, beta, or gamma using oligonucleotide arrays." *Proc Natl Acad Sci U S A* 95 (26): 15623-8. https://doi.org/10.1073/pnas.95.26.15623.

Dermietzel, R., and D. C. Spray. 1998. "From neuro-glue ('Nervenkitt') to glia: a prologue." *Glia* 24 (1): 1-7. https://doi.org/10.1002/(sici)1098-1136(199809)24:1<1::aid-glia1>3.0.co;2-a.

Dong, F., Y. Liu, Z. Zhang, R. Guo, L. Ma, X. Qu, H. Yu, H. Fan, and R. Yao. 2017. "Postnatal alteration of monocarboxylate transporter 1 expression in

the rat corpus callosum." *Physiol Res* 66 (2): 345-355. https://doi.org/10.33549/physiolres.933365.

Dong, Y., Y. Gu, Y. Huan, Y. Wang, Y. Liu, M. Liu, F. Ding, and X. Gu. 2013. "HMGB1 protein does not mediate the inflammatory response in spontaneous spinal cord regeneration: a hint for CNS regeneration." *J Biol Chem* 288 (25): 18204-18. https://doi.org/10.1074/jbc.M113.463810.

Dotti, C. G., C. A. Sullivan, and G. A. Banker. 1988. "The establishment of polarity by hippocampal neurons in culture." *J Neurosci* 8 (4): 1454-68. https://doi.org/10.1523/jneurosci.08-04-01454.1988.

Dreiding, P., P. Staeheli, and O. Haller. 1985. "Interferon-induced protein Mx accumulates in nuclei of mouse cells expressing resistance to influenza viruses." *Virology* 140 (1): 192-6. https://doi.org/10.1016/0042-6822(85)90460-x.

DuBois, J. H., C. Bolton, and M. L. Cuzner. 1986. "The production of prostaglandin and the regulation of cell division in neonate rat primary mixed glial cultures." *J Neuroimmunol* 11 (4): 277-85. https://doi.org/10.1016/0165-5728(86)90081-0.

Durán, I., E. M. Martínez-Cáceres, J. Río, N. Barberà, M. E. Marzo, and X. Montalban. 1999. "Immunological profile of patients with primary progressive multiple sclerosis. Expression of adhesion molecules." *Brain* 122 (Pt 12): 2297-307. https://doi.org/10.1093/brain/122.12.2297.

Dutuze, M. F., M. Nzayirambaho, C. N. Mores, and R. C. Christofferson. 2018. "A Review of Bunyamwera, Batai, and Ngari Viruses: Understudied Orthobunyaviruses With Potential One Health Implications." *Front Vet Sci* 5: 69. https://doi.org/10.3389/fvets.2018.00069.

Dörries, K., E. Vogel, S. Günther, and S. Czub. 1994. "Infection of human polyomaviruses JC and BK in peripheral blood leukocytes from immunocompetent individuals." *Virology* 198 (1): 59-70. https://doi.org/10.1006/viro.1994.1008.

Edye, M. E., G. Lopez-Castejon, S. M. Allan, and D. Brough. 2013. "Acidosis drives damage-associated molecular pattern (DAMP)-induced interleukin-1 secretion via a caspase-1-independent pathway." *J Biol Chem* 288 (42): 30485-30494. https://doi.org/10.1074/jbc.M113.478941.

Ehrenstein, M. R., H. T. Cook, and M. S. Neuberger. 2000. "Deficiency in serum immunoglobulin (Ig)M predisposes to development of IgG autoantibodies." *J Exp Med* 191 (7): 1253-8. https://doi.org/10.1084/jem.191.7.1253.

Eid, T., T. S. Lee, M. J. Thomas, M. Amiry-Moghaddam, L. P. Bjørnsen, D. D. Spencer, P. Agre, O. P. Ottersen, and N. C. de Lanerolle. 2005. "Loss of perivascular aquaporin 4 may underlie deficient water and K+ homeostasis in the human epileptogenic hippocampus." *Proc Natl Acad Sci U S A* 102 (4): 1193-8. https://doi.org/10.1073/pnas.0409308102.

Eisen, A., B. M. Greenberg, J. D. Bowen, D. L. Arnold, and A. O. Caggiano. 2017. "A double-blind, placebo-controlled, single ascending-dose study of remyelinating antibody rHIgM22 in people with multiple sclerosis." *Mult Scler J Exp Transl Clin* 3 (4): 2055217317743097. https://doi.org/10.1177/2055217317743097.

Elliott, C., M. Lindner, A. Arthur, K. Brennan, S. Jarius, J. Hussey, A. Chan, A. Stroet, T. Olsson, H. Willison, S. C. Barnett, E. Meinl, and C. Linington. 2012. "Functional identification of pathogenic autoantibody responses in patients with multiple sclerosis." *Brain* 135 (Pt 6): 1819-33. https://doi.org/10.1093/brain/aws105.

Elmore, M. R., A. R. Najafi, M. A. Koike, N. N. Dagher, E. E. Spangenberg, R. A. Rice, M. Kitazawa, B. Matusow, H. Nguyen, B. L. West, and K. N. Green.

2014. "Colony-stimulating factor 1 receptor signaling is necessary for microglia viability, unmasking a microglia progenitor cell in the adult brain." *Neuron* 82 (2): 380-97. https://doi.org/10.1016/j.neuron.2014.02.040.

Eltayeb, S., A. L. Berg, H. Lassmann, E. Wallström, M. Nilsson, T. Olsson, A. Ericsson-Dahlstrand, and D. Sunnemark. 2007. "Temporal expression and cellular origin of CC chemokine receptors CCR1, CCR2 and CCR5 in the central nervous system: insight into mechanisms of MOG-induced EAE." *J Neuroinflammation* 4: 14. https://doi.org/10.1186/1742-2094-4-14.

Endoh, Y., Y. M. Chung, I. A. Clark, C. L. Geczy, and K. Hsu. 2009. "IL-10-dependent S100A8 gene induction in monocytes/macrophages by double-stranded RNA." *J Immunol* 182 (4): 2258-68. https://doi.org/10.4049/jimmunol.0802683.

Engel, A., and T. A. Burch. 1967. "Chronic arthritis in the United States Health Examination Survey." *Arthritis Rheum* 10 (1): 61-2. https://doi.org/10.1002/art.1780100109.

Erecińska, M., and I. A. Silver. 1990. "Metabolism and role of glutamate in mammalian brain." *Prog Neurobiol* 35 (4): 245-96. https://doi.org/10.1016/0301-0082(90)90013-7.

Esen, N., and T. Kielian. 2006. "Central role for MyD88 in the responses of microglia to pathogen-associated molecular patterns." *J Immunol* 176 (11): 6802-11. https://doi.org/10.4049/jimmunol.176.11.6802.

Eyzaguirre, C., and S. W. Kuffler. 1955. "Processes of excitation in the dendrites and in the soma of single isolated sensory nerve cells of the lobster and crayfish." *J Gen Physiol* 39 (1): 87-119. https://doi.org/10.1085/jgp.39.1.87.

Fagioli, C., and R. Sitia. 2001. "Glycoprotein quality control in the endoplasmic reticulum. Mannose trimming by endoplasmic reticulum mannosidase I times the proteasomal degradation of unassembled immunoglobulin subunits." *J Biol Chem* 276 (16): 12885-92. https://doi.org/10.1074/jbc.M009603200.

Fawwaz, R. A., T. S. Tenforde, and W. H. Mehlberg. 1975. "Carbodiimide enhancement of complement-dependent antibody-mediated tumor cell lysis in vitro and antitumor activity in vivo." *Cancer Res* 35 (3): 679-86.

Fazakerley, J. K., C. L. Cotterill, G. Lee, and A. Graham. 2006. "Virus tropism, distribution, persistence and pathology in the corpus callosum of the Semliki Forest virus-infected mouse brain: a novel system to study virus-oligodendrocyte interactions." *Neuropathol Appl Neurobiol* 32 (4): 397-409. https://doi.org/10.1111/j.1365-2990.2006.00739.x.

Fazakerley, J. K., and H. E. Webb. 1987. "Semliki Forest virus induced, immune mediated demyelination: the effect of irradiation." *Br J Exp Pathol* 68 (1): 101-13.

Ferguson, A. D., W. Welte, E. Hofmann, B. Lindner, O. Holst, J. W. Coulton, and K. Diederichs. 2000. "A conserved structural motif for lipopolysaccharide recognition by procaryotic and eucaryotic proteins." *Structure* 8 (6): 585-92. https://doi.org/10.1016/s0969-2126(00)00143-x.

Fernandes-Alnemri, T., J. W. Yu, P. Datta, J. Wu, and E. S. Alnemri. 2009. "AIM2 activates the inflammasome and cell death in response to cytoplasmic DNA." *Nature* 458 (7237): 509-13. https://doi.org/10.1038/nature07710.

Field, A. M., S. D. Gardner, R. A. Goodbody, and M. A. Woodhouse. 1974. "Identity of a newly isolated human polyomavirus from a patient with progressive multifocal leucoencephalopathy." *J Clin Pathol* 27 (5): 341-7. https://doi.org/10.1136/jcp.27.5.341.

Filippi, M., A. Bar-Or, F. Piehl, P. Preziosa, A. Solari, S. Vukusic, and M. A. Rocca. 2018. "Multiple sclerosis." *Nat Rev Dis Primers* 4 (1): 43. https://doi.org/10.1038/s41572-018-0041-4.

Finley, M., D. Fairman, D. Liu, P. Li, A. Wood, and S. Cho. 2004. "Functional validation of adult hippocampal organotypic cultures as an in vitro model of brain injury." *Brain Res* 1001 (1-2): 125-32. https://doi.org/10.1016/j.brainres.2003.12.009.

Fischer, M. T., R. Sharma, J. L. Lim, L. Haider, J. M. Frischer, J. Drexhage, D. Mahad, M. Bradl, J. van Horssen, and H. Lassmann. 2012. "NADPH oxidase expression in active multiple sclerosis lesions in relation to oxidative tissue damage and mitochondrial injury." *Brain* 135 (Pt 3): 886-99. https://doi.org/10.1093/brain/aws012.

Florey, E. 1954. "An inhibitory and an excitatory factor of mammalian central nervous system, and their action of a single sensory neuron." *Arch Int Physiol* 62 (1): 33-53. https://doi.org/10.3109/13813455409145367.

Forthal, D. N. 2014. "Functions of Antibodies." *Microbiol Spectr* 2 (4): Aid-0019-2014. https://doi.org/10.1128/microbiolspec.AID-0019-2014.

Foss, S., R. Watkinson, I. Sandlie, L. C. James, and J. T. Andersen. 2015. "TRIM21: a cytosolic Fc receptor with broad antibody isotype specificity." *Immunol Rev* 268 (1): 328-39. https://doi.org/10.1111/imr.12363.

Fragkoudis, R., N. Tamberg, R. Siu, K. Kiiver, A. Kohl, A. Merits, and J. K. Fazakerley. 2009. "Neurons and oligodendrocytes in the mouse brain differ in their ability to replicate Semliki Forest virus." *J Neurovirol* 15 (1): 57-70. https://doi.org/10.1080/13550280802482583.

Friedman, R. M. 1970. "Studies on the mechanism of interferon action." *J Gen Physiol* 56 (1): 149-71. https://doi.org/10.1085/jgp.56.1.149.

Frisa, P. S., M. N. Goodman, G. M. Smith, J. Silver, and J. W. Jacobberger. 1994. "Immortalization of immature and mature mouse astrocytes with SV40 T antigen." *J Neurosci Res* 39 (1): 47-56. https://doi.org/10.1002/jnr.490390107.

Frischer, J. M., S. Bramow, A. Dal-Bianco, C. F. Lucchinetti, H. Rauschka, M. Schmidbauer, H. Laursen, P. S. Sorensen, and H. Lassmann. 2009. "The relation between inflammation and neurodegeneration in multiple sclerosis brains." *Brain* 132 (Pt 5): 1175-89. https://doi.org/10.1093/brain/awp070.

Fritz, G., H. M. Botelho, L. A. Morozova-Roche, and C. M. Gomes. 2010. "Natural and amyloid self-assembly of S100 proteins: structural basis of functional diversity." *Febs j* 277 (22): 4578-90. https://doi.org/10.1111/j.1742-4658.2010.07887.x.

Fruth, U., F. Sinigaglia, M. Schlesier, J. Kilgus, M. D. Kramer, and M. M. Simon. 1987. "A novel serine proteinase (HuTSP) isolated from a cloned human CD8+ cytolytic T cell line is expressed and secreted by activated CD4+ and CD8+ lymphocytes." *Eur J Immunol* 17 (11): 1625-33. https://doi.org/10.1002/eji.1830171116.

Funch, P. G., and D. S. Faber. 1984. "Measurement of myelin sheath resistances: implications for axonal conduction and pathophysiology." *Science* 225 (4661): 538-40. https://doi.org/10.1126/science.6204382.

Fünfschilling, U., L. M. Supplie, D. Mahad, S. Boretius, A. S. Saab, J. Edgar, B. G. Brinkmann, C. M. Kassmann, I. D. Tzvetanova, W. Möbius, F. Diaz, D. Meijer, U. Suter, B. Hamprecht, M. W. Sereda, C. T. Moraes, J. Frahm, S. Goebbels, and K. A. Nave. 2012. "Glycolytic oligodendrocytes maintain myelin and long-term axonal integrity." *Nature* 485 (7399): 517-21. https://doi.org/10.1038/nature11007.

Gall, B., K. Pryke, J. Abraham, N. Mizuno, S. Botto, T. M. Sali, R. Broeckel, N. Haese, A. Nilsen, A. Placzek, T. Morrison, M. Heise, D. Streblow, and V. DeFilippis. 2018. "Emerging Alphaviruses Are Sensitive to Cellular States Induced by a Novel Small-Molecule Agonist of the STING Pathway." *J Virol* 92 (6). https://doi.org/10.1128/jvi.01913-17.

Gao, P., B. Xiang, Y. Li, M. Sun, Y. Kang, P. Xie, L. Chen, Q. Lin, M. Liao, and T. Ren. 2018. "Therapeutic Effect of Duck Interferon-Alpha Against H5N1 Highly Pathogenic Avian Influenza Virus Infection in Peking Ducks." *J Interferon Cytokine Res* 38 (4): 145-152. https://doi.org/10.1089/jir.2017.0116.

GBD-2016-Multiple-Sclerosis-Collaborators. 2019. "Global, regional, and national burden of multiple sclerosis 1990-2016: a systematic analysis for the Global Burden of Disease Study 2016." *Lancet Neurol* 18 (3): 269-285. https://doi.org/10.1016/s1474-4422(18)30443-5.

Gelderblom, H. R. 1996. "Structure and Classification of Viruses." In *Medical Microbiology*, edited by S. Baron. Galveston (TX): University of Texas Medical Branch at Galveston

Copyright © 1996, The University of Texas Medical Branch at Galveston.

Geller, A. I. 1991. "A system, using neural cell lines, to characterize HSV-1 vectors containing genes which affect neuronal physiology, or neuronal promoters." *J Neurosci Methods* 36 (1): 91-103. https://doi.org/10.1016/0165-0270(91)90142-m.

Gesell, R., J. Hunter, and R. Lillie. 1949. "Electrical and functional activity of motor neurons." *Am J Physiol* 159 (1): 15-28. https://doi.org/10.1152/ajplegacy.1949.159.1.15.

Ghosh, A., L. Shao, P. Sampath, B. Zhao, N. V. Patel, J. Zhu, B. Behl, R. A. Parise, J. H. Beumer, R. J. O'Sullivan, N. A. DeLuca, S. H. Thorne, V. A. K. Rathinam, P. Li, and S. N. Sarkar. 2019. "Oligoadenylate-Synthetase-Family Protein OASL Inhibits Activity of the DNA Sensor cGAS during DNA Virus Infection to Limit Interferon Production." *Immunity* 50 (1): 51-63.e5. https://doi.org/10.1016/j.immuni.2018.12.013.

Gieselbach, R. J., A. H. Muller-Hansma, M. T. Wijburg, M. S. de Bruin-Weller, B. W. van Oosten, D. J. Nieuwkamp, F. E. Coenjaerts, M. P. Wattjes, and J. L. Murk. 2017. "Progressive multifocal leukoencephalopathy in patients treated with fumaric acid esters: a review of 19 cases." *J Neurol* 264 (6): 1155-1164. https://doi.org/10.1007/s00415-017-8509-9.

Gilly, M., M. A. Damore, and R. Wall. 1996. "A promoter ISRE and dual 5' YY1 motifs control IFN-gamma induction of the IRG-47 G-protein gene." *Gene* 179 (2): 237-44. https://doi.org/10.1016/s0378-1119(96)00366-6.

Ginhoux, F., M. Greter, M. Leboeuf, S. Nandi, P. See, S. Gokhan, M. F. Mehler, S. J. Conway, L. G. Ng, E. R. Stanley, I. M. Samokhvalov, and M. Merad. 2010. "Fate mapping analysis reveals that adult microglia derive from primitive macrophages." *Science* 330 (6005): 841-5. https://doi.org/10.1126/science.1194637.

Giulian, D., and T. J. Baker. 1986. "Characterization of ameboid microglia isolated from developing mammalian brain." *J Neurosci* 6 (8): 2163-78. https://doi.org/10.1523/jneurosci.06-08-02163.1986.

Glass, D. N., J. Caffin, R. N. Maini, and J. T. Scott. 1973. "Measurement of DNA antibodies by double antibody precipitation." *Ann Rheum Dis* 32 (4): 342-5. https://doi.org/10.1136/ard.32.4.342.

Glass, W. G., M. J. Hickey, J. L. Hardison, M. T. Liu, J. E. Manning, and T. E. Lane. 2004. "Antibody targeting of the CC chemokine ligand 5 results in diminished leukocyte infiltration into the central nervous system and

reduced neurologic disease in a viral model of multiple sclerosis." *J Immunol* 172 (7): 4018-25. https://doi.org/10.4049/jimmunol.172.7.4018.

Glees, P., and M. Hasan. 1990. "Ultrastructure of human cerebral macroglia and microglia: maturing and hydrocephalic frontal cortex." *Neurosurg Rev* 13 (3): 231-42. https://doi.org/10.1007/bf00313025.

Go, Y. Y., U. B. Balasuriya, and C. K. Lee. 2014. "Zoonotic encephalitides caused by arboviruses: transmission and epidemiology of alphaviruses and flaviviruses." *Clin Exp Vaccine Res* 3 (1): 58-77. https://doi.org/10.7774/cevr.2014.3.1.58.

Goldberg, S. H., P. van der Meer, J. Hesselgesser, S. Jaffer, D. L. Kolson, A. V. Albright, F. González-Scarano, and E. Lavi. 2001. "CXCR3 expression in human central nervous system diseases." *Neuropathol Appl Neurobiol* 27 (2): 127-38. https://doi.org/10.1046/j.1365-2990.2001.00312.x.

Goldman, D. E., and M. P. Blaustein. 1966. "Ions, drugs and the axon membrane." *Ann N Y Acad Sci* 137 (2): 967-81. https://doi.org/10.1111/j.1749-6632.1966.tb50210.x.

Goldmann, T., P. Wieghofer, M. J. Jordão, F. Prutek, N. Hagemeyer, K. Frenzel, L. Amann, O. Staszewski, K. Kierdorf, M. Krueger, G. Locatelli, H. Hochgerner, R. Zeiser, S. Epelman, F. Geissmann, J. Priller, F. M. Rossi, I. Bechmann, M. Kerschensteiner, S. Linnarsson, S. Jung, and M. Prinz. 2016. "Origin, fate and dynamics of macrophages at central nervous system interfaces." *Nat Immunol* 17 (7): 797-805. https://doi.org/10.1038/ni.3423.

Gollins, S. W., and J. S. Porterfield. 1984. "Flavivirus infection enhancement in macrophages: radioactive and biological studies on the effect of antibody on viral fate." *J Gen Virol* 65 (Pt 8): 1261-72. https://doi.org/10.1099/0022-1317-65-8-1261.

Gordon, J., S. Amini, and M. K. White. 2013. "General overview of neuronal cell culture." *Methods Mol Biol* 1078: 1-8. https://doi.org/10.1007/978-1-62703-640-5_1.

Gosert, R., P. Kardas, E. O. Major, and H. H. Hirsch. 2010. "Rearranged JC virus noncoding control regions found in progressive multifocal leukoencephalopathy patient samples increase virus early gene expression and replication rate." *J Virol* 84 (20): 10448-56. https://doi.org/10.1128/jvi.00614-10.

Gosselin, D., D. Skola, N. G. Coufal, I. R. Holtman, J. C. M. Schlachetzki, E. Sajti, B. N. Jaeger, C. O'Connor, C. Fitzpatrick, M. P. Pasillas, M. Pena, A. Adair, D. D. Gonda, M. L. Levy, R. M. Ransohoff, F. H. Gage, and C. K. Glass. 2017. "An environment-dependent transcriptional network specifies human microglia identity." *Science* 356 (6344). https://doi.org/10.1126/science.aal3222.

Grajchen, E., E. Wouters, B. van de Haterd, M. Haidar, K. Hardonnière, T. Dierckx, J. Van Broeckhoven, C. Erens, S. Hendrix, S. Kerdine-Römer, J. J. A. Hendriks, and J. F. J. Bogie. 2020. "CD36-mediated uptake of myelin debris by macrophages and microglia reduces neuroinflammation." *J Neuroinflammation* 17 (1): 224. https://doi.org/10.1186/s12974-020-01899-x.

Green, J., and R. Jotte. 1985. "Interactions between T helper cells and dendritic cells during the rat mixed lymphocyte reaction." *J Exp Med* 162 (5): 1546-60. https://doi.org/10.1084/jem.162.5.1546.

Greenbury, C. L., and D. H. Moore. 1966. "The mechanism of bacterial immobilization by anti-flagellar IgG antibody." *Immunology* 11 (6): 617-25.

Gribkoff, V. K., and L. K. Kaczmarek. 2017. "The need for new approaches in CNS drug discovery: Why drugs have failed, and what can be done to improve outcomes." *Neuropharmacology* 120: 11-19. https://doi.org/10.1016/j.neuropharm.2016.03.021.

Grumet, F. C., A. Coukell, J. G. Bodmer, W. F. Bodmer, and H. O. McDevitt. 1971. "Histocompatibility (HL-A) antigens associated with systemic lupus erythematosus. A possible genetic predisposition to disease." *N Engl J Med* 285 (4): 193-6. https://doi.org/10.1056/nejm197107222850403.

Gu, Z. Y., Q. Li, Y. L. Si, X. Li, H. J. Hao, and H. J. Song. 2003. "Prevalence of BK virus and JC virus in peripheral blood leukocytes and normal arterial walls in healthy individuals in China." *J Med Virol* 70 (4): 600-5. https://doi.org/10.1002/jmv.10436.

Guazzi, S., A. Strangio, A. T. Franzi, and M. E. Bianchi. 2003. "HMGB1, an architectural chromatin protein and extracellular signalling factor, has a spatially and temporally restricted expression pattern in mouse brain." *Gene Expr Patterns* 3 (1): 29-33. https://doi.org/10.1016/s1567-133x(02)00093-5.

Guidotti, L. G., P. Borrow, A. Brown, H. McClary, R. Koch, and F. V. Chisari. 1999. "Noncytopathic clearance of lymphocytic choriomeningitis virus from the hepatocyte." *J Exp Med* 189 (10): 1555-64. https://doi.org/10.1084/jem.189.10.1555.

Guidotti, L. G., R. Rochford, J. Chung, M. Shapiro, R. Purcell, and F. V. Chisari. 1999. "Viral clearance without destruction of infected cells during acute HBV infection." *Science* 284 (5415): 825-9. https://doi.org/10.1126/science.284.5415.825.

Guo, X., J. Ma, J. Sun, and G. Gao. 2007. "The zinc-finger antiviral protein recruits the RNA processing exosome to degrade the target mRNA." *Proc Natl Acad Sci U S A* 104 (1): 151-6. https://doi.org/10.1073/pnas.0607063104.

Gurnik, S., K. Devraj, J. Macas, M. Yamaji, J. Starke, A. Scholz, K. Sommer, M. Di Tacchio, R. Vutukuri, H. Beck, M. Mittelbronn, C. Foerch, W. Pfeilschifter, S. Liebner, K. G. Peters, K. H. Plate, and Y. Reiss. 2016. "Angiopoietin-2-induced blood-brain barrier compromise and increased stroke size are rescued by VE-PTP-dependent restoration of Tie2 signaling." *Acta Neuropathol* 131 (5): 753-73. https://doi.org/10.1007/s00401-016-1551-3.

Hacohen, Y., K. Mankad, W. K. Chong, F. Barkhof, A. Vincent, M. Lim, E. Wassmer, O. Ciccarelli, and C. Hemingway. 2017. "Diagnostic algorithm for relapsing acquired demyelinating syndromes in children." *Neurology* 89 (3): 269-278. https://doi.org/10.1212/wnl.0000000000004117.

Hafler, D. A., A. Compston, S. Sawcer, E. S. Lander, M. J. Daly, P. L. De Jager, P. I. de Bakker, S. B. Gabriel, D. B. Mirel, A. J. Ivinson, M. A. Pericak-Vance, S. G. Gregory, J. D. Rioux, J. L. McCauley, J. L. Haines, L. F. Barcellos, B. Cree, J. R. Oksenberg, and S. L. Hauser. 2007. "Risk alleles for multiple sclerosis identified by a genomewide study." *N Engl J Med* 357 (9): 851-62. https://doi.org/10.1056/NEJMoa073493.

Haider, L., C. Simeonidou, G. Steinberger, S. Hametner, N. Grigoriadis, G. Deretzi, G. G. Kovacs, A. Kutzelnigg, H. Lassmann, and J. M. Frischer. 2014. "Multiple sclerosis deep grey matter: the relation between demyelination, neurodegeneration, inflammation and iron." *J Neurol Neurosurg Psychiatry* 85 (12): 1386-95. https://doi.org/10.1136/jnnp-2014-307712.

Haines, J. L., H. A. Terwedow, K. Burgess, M. A. Pericak-Vance, J. B. Rimmler, E. R. Martin, J. R. Oksenberg, R. Lincoln, D. Y. Zhang, D. R. Banatao, N. Gatto, D. E. Goodkin, and S. L. Hauser. 1998. "Linkage of the MHC to familial multiple sclerosis suggests genetic heterogeneity. The Multiple Sclerosis Genetics Group." *Hum Mol Genet* 7 (8): 1229-34. https://doi.org/10.1093/hmg/7.8.1229.

Halks-Miller, M., M. L. Schroeder, V. Haroutunian, U. Moenning, M. Rossi, C. Achim, D. Purohit, M. Mahmoudi, and R. Horuk. 2003. "CCR1 is an early and specific marker of Alzheimer's disease." *Ann Neurol* 54 (5): 638-46. https://doi.org/10.1002/ana.10733.

Hallström, T., H. Jarva, K. Riesbeck, and A. M. Blom. 2007. "Interaction with C4b-binding protein contributes to nontypeable Haemophilus influenzae serum resistance." *J Immunol* 178 (10): 6359-66. https://doi.org/10.4049/jimmunol.178.10.6359.

Hamilton, S. P., and L. H. Rome. 1994. "Stimulation of in vitro myelin synthesis by microglia." *Glia* 11 (4): 326-35. https://doi.org/10.1002/glia.440110405.

Hashimoto, K., H. Handa, K. Umehara, and S. Sasaki. 1978. "Germfree mice reared on an "antigen-free" diet." *Lab Anim Sci* 28 (1): 38-45.

Hauser, S. L., and B. A. C. Cree. 2020. "Treatment of Multiple Sclerosis: A Review." *Am J Med* 133 (12): 1380-1390.e2. https://doi.org/10.1016/j.amjmed.2020.05.049.

Hauser, S. L., E. Waubant, D. L. Arnold, T. Vollmer, J. Antel, R. J. Fox, A. Bar-Or, M. Panzara, N. Sarkar, S. Agarwal, A. Langer-Gould, and C. H. Smith. 2008. "B-cell depletion with rituximab in relapsing-remitting multiple sclerosis." *N Engl J Med* 358 (7): 676-88. https://doi.org/10.1056/NEJMoa0706383.

Hausmann, J., C. Sauder, M. Wasmer, B. Lu, and P. Staeheli. 2004. "Neurological disorder after Borna disease virus infection in the absence of either interferon-gamma, Fas, inducible NO synthase, or chemokine receptor CXCR3." *Viral Immunol* 17 (1): 79-85. https://doi.org/10.1089/088282404322875476.

Hawke, S., P. G. Stevenson, S. Freeman, and C. R. Bangham. 1998. "Long-term persistence of activated cytotoxic T lymphocytes after viral infection of the central nervous system." *J Exp Med* 187 (10): 1575-82. https://doi.org/10.1084/jem.187.10.1575.

Hawkes, C. A., and J. McLaurin. 2009. "Selective targeting of perivascular macrophages for clearance of beta-amyloid in cerebral amyloid angiopathy." *Proc Natl Acad Sci U S A* 106 (4): 1261-6. https://doi.org/10.1073/pnas.0805453106.

Hayakawa, K., M. Asano, S. A. Shinton, M. Gui, D. Allman, C. L. Stewart, J. Silver, and R. R. Hardy. 1999. "Positive selection of natural autoreactive B cells." *Science* 285 (5424): 113-6. https://doi.org/10.1126/science.285.5424.113.

Hayden, L., T. Semenoff, V. Schultz, S. F. Merz, K. J. Chapple, M. Rodriguez, A. E. Warrington, X. Shi, C. S. McKimmie, J. M. Edgar, K. Thümmler, C. Linington, and M. Pingen. 2020. "Lipid-specific IgMs induce antiviral responses in the CNS: implications for progressive multifocal leukoencephalopathy in multiple sclerosis." *Acta Neuropathol Commun* 8 (1): 135. https://doi.org/10.1186/s40478-020-01011-7.

He, H., J. J. Mack, E. Güç, C. M. Warren, M. L. Squadrito, W. W. Kilarski, C. Baer, R. D. Freshman, A. I. McDonald, S. Ziyad, M. A. Swartz, M. De Palma, and M. L. Iruela-Arispe. 2016. "Perivascular Macrophages Limit

Permeability." *Arterioscler Thromb Vasc Biol* 36 (11): 2203-2212. https://doi.org/10.1161/atvbaha.116.307592.

Heil, F., H. Hemmi, H. Hochrein, F. Ampenberger, C. Kirschning, S. Akira, G. Lipford, H. Wagner, and S. Bauer. 2004. "Species-specific recognition of single-stranded RNA via toll-like receptor 7 and 8." *Science* 303 (5663): 1526-9. https://doi.org/10.1126/science.1093620.

Henning, S., W. M. Lambers, B. Doornbos-van der Meer, W. H. Abdulahad, F. G. M. Kroese, H. Bootsma, J. Westra, and K. de Leeuw. 2020. "Proportions of B-cell subsets are altered in incomplete systemic lupus erythematosus and correlate with interferon score and IgG levels." *Rheumatology (Oxford)* 59 (9): 2616-2624. https://doi.org/10.1093/rheumatology/keaa114.

Henry, S. C., X. G. Daniell, A. R. Burroughs, M. Indaram, D. N. Howell, J. Coers, M. N. Starnbach, J. P. Hunn, J. C. Howard, C. G. Feng, A. Sher, and G. A. Taylor. 2009. "Balance of Irgm protein activities determines IFN-gamma-induced host defense." *J Leukoc Biol* 85 (5): 877-85. https://doi.org/10.1189/jlb.1008599.

Herndon, R. M. 1964. "THE FINE STRUCTURE OF THE RAT CEREBELLUM. II. THE STELLATE NEURONS, GRANULE CELLS, AND GLIA." *J Cell Biol* 23 (2): 277-93. https://doi.org/10.1083/jcb.23.2.277.

Hertz, L., and C. Nissen. 1976. "Differences between leech and mammalian nervous systems in metabolic reaction to K+ as an indication of differences in potassium homeostasis mechanisms." *Brain Res* 110 (1): 182-8. https://doi.org/10.1016/0006-8993(76)90220-1.

Hertz, L., P. H. Wu, and A. Schousboe. 1978. "Evidence for net uptake of GABA into mouse astrocytes in primary cultures--its sodium dependence and potassium independence." *Neurochem Res* 3 (3): 313-23. https://doi.org/10.1007/bf00965577.

Herz, J., A. J. Filiano, A. Smith, N. Yogev, and J. Kipnis. 2017. "Myeloid Cells in the Central Nervous System." *Immunity* 46 (6): 943-956. https://doi.org/10.1016/j.immuni.2017.06.007.

Hickey, M. J., K. S. Held, E. Baum, J. L. Gao, P. M. Murphy, and T. E. Lane. 2007. "CCR1 deficiency increases susceptibility to fatal coronavirus infection of the central nervous system." *Viral Immunol* 20 (4): 599-608. https://doi.org/10.1089/vim.2007.0056.

Hiramoto, E., A. Tsutsumi, R. Suzuki, S. Matsuoka, S. Arai, M. Kikkawa, and T. Miyazaki. 2018. "The IgM pentamer is an asymmetric pentagon with an open groove that binds the AIM protein." *Sci Adv* 4 (10): eaau1199. https://doi.org/10.1126/sciadv.aau1199.

Hisamatsu, T., M. Suzuki, and D. K. Podolsky. 2003. "Interferon-gamma augments CARD4/NOD1 gene and protein expression through interferon regulatory factor-1 in intestinal epithelial cells." *J Biol Chem* 278 (35): 32962-8. https://doi.org/10.1074/jbc.M304355200.

Ho, P. R., H. Koendgen, N. Campbell, B. Haddock, S. Richman, and I. Chang. 2017. "Risk of natalizumab-associated progressive multifocal leukoencephalopathy in patients with multiple sclerosis: a retrospective analysis of data from four clinical studies." *Lancet Neurol* 16 (11): 925-933. https://doi.org/10.1016/s1474-4422(17)30282-x.

Hochmeister, S., R. Grundtner, J. Bauer, B. Engelhardt, R. Lyck, G. Gordon, T. Korosec, A. Kutzelnigg, J. J. Berger, M. Bradl, R. E. Bittner, and H. Lassmann. 2006. "Dysferlin is a new marker for leaky brain blood vessels in multiple sclerosis." *J Neuropathol Exp Neurol* 65 (9): 855-65. https://doi.org/10.1097/01.jnen.0000235119.52311.16.

Hodgkin, P. D., B. E. Castle, and M. R. Kehry. 1994. "B cell differentiation induced by helper T cell membranes: evidence for sequential isotype switching and a requirement for lymphokines during proliferation." *Eur J Immunol* 24 (1): 239-46. https://doi.org/10.1002/eji.1830240138.

Hodgson, N. R., S. G. Bohnet, J. A. Majde, and J. M. Krueger. 2012. "Influenza virus pathophysiology and brain invasion in mice with functional and dysfunctional Mx1 genes." *Brain Behav Immun* 26 (1): 83-9. https://doi.org/10.1016/j.bbi.2011.07.238.

Hofer, M. J., S. L. Carter, M. Müller, and I. L. Campbell. 2008. "Unaltered neurological disease and mortality in CXCR3-deficient mice infected intracranially with lymphocytic choriomeningitis virus-Armstrong." *Viral Immunol* 21 (4): 425-33. https://doi.org/10.1089/vim.2008.0057.

Hohlfeld, R., K. Dornmair, E. Meinl, and H. Wekerle. 2016. "The search for the target antigens of multiple sclerosis, part 2: CD8+ T cells, B cells, and antibodies in the focus of reverse-translational research." *Lancet Neurol* 15 (3): 317-31. https://doi.org/10.1016/s1474-4422(15)00313-0.

Holden, P., and A. D. Hess. 1959. "Cache Valley virus, a previously undescribed mosquito-borne agent." *Science* 130 (3383): 1187-8.

Holman, D. W., R. S. Klein, and R. M. Ransohoff. 2011. "The blood-brain barrier, chemokines and multiple sclerosis." *Biochim Biophys Acta* 1812 (2): 220-30. https://doi.org/10.1016/j.bbadis.2010.07.019.

Hong, S., V. F. Beja-Glasser, B. M. Nfonoyim, A. Frouin, S. Li, S. Ramakrishnan, K. M. Merry, Q. Shi, A. Rosenthal, B. A. Barres, C. A. Lemere, D. J. Selkoe, and B. Stevens. 2016. "Complement and microglia mediate early synapse loss in Alzheimer mouse models." *Science* 352 (6286): 712-716. https://doi.org/10.1126/science.aad8373.

Honjo, K., Y. Kubagawa, D. M. Jones, B. Dizon, Z. Zhu, H. Ohno, S. Izui, J. F. Kearney, and H. Kubagawa. 2012. "Altered Ig levels and antibody responses in mice deficient for the Fc receptor for IgM (FcμR)." *Proc Natl Acad Sci U S A* 109 (39): 15882-7. https://doi.org/10.1073/pnas.1206567109.

Honjo, K., Y. Kubagawa, and H. Kubagawa. 2013. "Is Toso/IgM Fc receptor (FcμR) expressed by innate immune cells?" In *Proc Natl Acad Sci U S A*, E2540-1.

Honke, K., Y. Hirahara, J. Dupree, K. Suzuki, B. Popko, K. Fukushima, J. Fukushima, T. Nagasawa, N. Yoshida, Y. Wada, and N. Taniguchi. 2002. "Paranodal junction formation and spermatogenesis require sulfoglycolipids." *Proc Natl Acad Sci U S A* 99 (7): 4227-32. https://doi.org/10.1073/pnas.032068299.

Horisberger, M. A., O. Haller, and H. Arnheiter. 1980. "Interferon-dependent genetic resistance to influenza virus in mice: virus replication in macrophages is inhibited at an early step." *J Gen Virol* 50 (1): 205-10. https://doi.org/10.1099/0022-1317-50-1-205.

Horisberger, M. A., G. K. McMaster, H. Zeller, M. G. Wathelet, J. Dellis, and J. Content. 1990. "Cloning and sequence analyses of cDNAs for interferon- and virus-induced human Mx proteins reveal that they contain putative guanine nucleotide-binding sites: functional study of the corresponding gene promoter." *J Virol* 64 (3): 1171-81. https://doi.org/10.1128/jvi.64.3.1171-1181.1990.

Hover, S., B. King, B. Hall, E. A. Loundras, H. Taqi, J. Daly, M. Dallas, C. Peers, E. Schnettler, C. McKimmie, A. Kohl, J. N. Barr, and J. Mankouri. 2016. "Modulation of Potassium Channels Inhibits Bunyavirus Infection." *J Biol Chem* 291 (7): 3411-22. https://doi.org/10.1074/jbc.M115.692673.

Howard, J. G., and A. C. Wardlaw. 1958. "The opsonic effect of normal serum on the uptake of bacteria by the reticulo-endothelial system; perfusion studies with isolated rat liver." *Immunology* 1 (4): 338-52.
Howie, S., W. H. McBride, and K. James. 1982. "Distribution of IgM, IgA and IgG secreting cells in the tissues of normal and tumour-bearing mice." *Immunology* 46 (1): 43-8.
Hsieh, M. F., S. L. Lai, J. P. Chen, J. M. Sung, Y. L. Lin, B. A. Wu-Hsieh, C. Gerard, A. Luster, and F. Liao. 2006. "Both CXCR3 and CXCL10/IFN-inducible protein 10 are required for resistance to primary infection by dengue virus." *J Immunol* 177 (3): 1855-63. https://doi.org/10.4049/jimmunol.177.3.1855.
Hu, B. Y., Z. W. Du, and S. C. Zhang. 2009. "Differentiation of human oligodendrocytes from pluripotent stem cells." *Nat Protoc* 4 (11): 1614-22. https://doi.org/10.1038/nprot.2009.186.
Huang da, W., B. T. Sherman, and R. A. Lempicki. 2009. "Systematic and integrative analysis of large gene lists using DAVID bioinformatics resources." *Nat Protoc* 4 (1): 44-57. https://doi.org/10.1038/nprot.2008.211.
Hughes, H. R., S. Adkins, S. Alkhovskiy, M. Beer, C. Blair, C. H. Calisher, M. Drebot, A. J. Lambert, W. M. de Souza, M. Marklewitz, M. R. T. Nunes, X. Shí 石晓宏, and Consortium Ictv Report. 2020. "ICTV Virus Taxonomy Profile: Peribunyaviridae." *J Gen Virol* 101 (1): 1-2. https://doi.org/10.1099/jgv.0.001365.
Hummel, K. B., W. J. Bellini, and M. K. Offermann. 1998. "Strain-specific differences in LFA-1 induction on measles virus-infected monocytes and adhesion and viral transmission to endothelial cells." *J Virol* 72 (10): 8403-7. https://doi.org/10.1128/jvi.72.10.8403-8407.1998.
Hung, J., M. Chansard, S. S. Ousman, M. D. Nguyen, and M. A. Colicos. 2010. "Activation of microglia by neuronal activity: results from a new in vitro paradigm based on neuronal-silicon interfacing technology." *Brain Behav Immun* 24 (1): 31-40. https://doi.org/10.1016/j.bbi.2009.06.150.
Hunter, S., R. Apweiler, T. K. Attwood, A. Bairoch, A. Bateman, D. Binns, P. Bork, U. Das, L. Daugherty, L. Duquenne, R. D. Finn, J. Gough, D. Haft, N. Hulo, D. Kahn, E. Kelly, A. Laugraud, I. Letunic, D. Lonsdale, R. Lopez, M. Madera, J. Maslen, C. McAnulla, J. McDowall, J. Mistry, A. Mitchell, N. Mulder, D. Natale, C. Orengo, A. F. Quinn, J. D. Selengut, C. J. Sigrist, M. Thimma, P. D. Thomas, F. Valentin, D. Wilson, C. H. Wu, and C. Yeats. 2009. "InterPro: the integrative protein signature database." *Nucleic Acids Res* 37 (Database issue): D211-5. https://doi.org/10.1093/nar/gkn785.
Hutter, O. F., and K. Kostial. 1955. "The relationship of sodium ions to the release of acetylcholine." *J Physiol* 129 (1): 159-66. https://doi.org/10.1113/jphysiol.1955.sp005344.
Hwang, M., and C. C. Bergmann. 2018a. "Alpha/Beta Interferon (IFN-alpha/beta) Signaling in Astrocytes Mediates Protection against Viral Encephalomyelitis and Regulates IFN-gamma-Dependent Responses." *J Virol* 92 (10). https://doi.org/10.1128/jvi.01901-17.
---. 2018b. "Alpha/Beta Interferon (IFN-α/ß) Signaling in Astrocytes Mediates Protection against Viral Encephalomyelitis and Regulates IFN-γ-Dependent Responses." *J Virol* 92 (10). https://doi.org/10.1128/jvi.01901-17.
Iannaccone, A., T. J. Hollingsworth, D. Koirala, D. D. New, N. I. Lenchik, S. Beranova-Giorgianni, I. C. Gerling, M. Z. Radic, and F. Giorgianni. 2017. "Retinal pigment epithelium and microglia express the CD5 antigen-like

protein, a novel autoantigen in age-related macular degeneration." *Exp Eye Res* 155: 64-74. https://doi.org/10.1016/j.exer.2016.12.006.

Ibsen, M. S., H. H. Gad, L. L. Andersen, V. Hornung, I. Julkunen, S. N. Sarkar, and R. Hartmann. 2015. "Structural and functional analysis reveals that human OASL binds dsRNA to enhance RIG-I signaling." *Nucleic Acids Res* 43 (10): 5236-48. https://doi.org/10.1093/nar/gkv389.

Ifergan, I., H. Kébir, M. Bernard, K. Wosik, A. Dodelet-Devillers, R. Cayrol, N. Arbour, and A. Prat. 2008. "The blood-brain barrier induces differentiation of migrating monocytes into Th17-polarizing dendritic cells." *Brain* 131 (Pt 3): 785-99. https://doi.org/10.1093/brain/awm295.

Igarashi, Y., H. Utsumi, H. Chiba, Y. Yamada-Sasamori, H. Tobioka, Y. Kamimura, K. Furuuchi, Y. Kokai, T. Nakagawa, M. Mori, and N. Sawada. 1999. "Glial cell line-derived neurotrophic factor induces barrier function of endothelial cells forming the blood-brain barrier." *Biochem Biophys Res Commun* 261 (1): 108-12. https://doi.org/10.1006/bbrc.1999.0992.

Ilyas, A. A., Z. W. Chen, and S. D. Cook. 2003. "Antibodies to sulfatide in cerebrospinal fluid of patients with multiple sclerosis." *J Neuroimmunol* 139 (1-2): 76-80. https://doi.org/10.1016/s0165-5728(03)00131-0.

Isaac, L., and M. Mariano. 1988. "The IgM receptor in mouse peritoneal macrophages." *Clin Exp Immunol* 72 (3): 516-20.

Isaacs, A., and J. Lindenmann. 1957. "Virus interference. I. The interferon." *Proc R Soc Lond B Biol Sci* 147 (927): 258-67. https://doi.org/10.1098/rspb.1957.0048.

Isakson, P. C., E. Puré, E. S. Vitetta, and P. H. Krammer. 1982. "T cell-derived B cell differentiation factor(s). Effect on the isotype switch of murine B cells." *J Exp Med* 155 (3): 734-48. https://doi.org/10.1084/jem.155.3.734.

Ishii, K. J., C. Coban, H. Kato, K. Takahashi, Y. Torii, F. Takeshita, H. Ludwig, G. Sutter, K. Suzuki, H. Hemmi, S. Sato, M. Yamamoto, S. Uematsu, T. Kawai, O. Takeuchi, and S. Akira. 2006. "A Toll-like receptor-independent antiviral response induced by double-stranded B-form DNA." *Nat Immunol* 7 (1): 40-8. https://doi.org/10.1038/ni1282.

Ishikawa, H., and G. N. Barber. 2008. "STING is an endoplasmic reticulum adaptor that facilitates innate immune signalling." *Nature* 455 (7213): 674-8. https://doi.org/10.1038/nature07317.

Ishikawa, H., Z. Ma, and G. N. Barber. 2009. "STING regulates intracellular DNA-mediated, type I interferon-dependent innate immunity." *Nature* 461 (7265): 788-92. https://doi.org/10.1038/nature08476.

Itoyama, Y., H. D. Webster, N. H. Sternberger, E. P. Richardson, Jr., D. L. Walker, R. H. Quarles, and B. L. Padgett. 1982. "Distribution of papovavirus, myelin-associated glycoprotein, and myelin basic protein in progressive multifocal leukoencephalopathy lesions." *Ann Neurol* 11 (4): 396-407. https://doi.org/10.1002/ana.410110414.

Izzy, S., Q. Liu, Z. Fang, S. Lule, L. Wu, J. Y. Chung, A. Sarro-Schwartz, A. Brown-Whalen, C. Perner, S. E. Hickman, D. L. Kaplan, N. A. Patsopoulos, J. El Khoury, and M. J. Whalen. 2019. "Time-Dependent Changes in Microglia Transcriptional Networks Following Traumatic Brain Injury." *Front Cell Neurosci* 13: 307. https://doi.org/10.3389/fncel.2019.00307.

Jacob, A., L. Bao, J. Brorson, R. J. Quigg, and J. J. Alexander. 2010. "C3aR inhibition reduces neurodegeneration in experimental lupus." *Lupus* 19 (1): 73-82. https://doi.org/10.1177/0961203309348978.

Jacobs, L. D., D. L. Cookfair, R. A. Rudick, R. M. Herndon, J. R. Richert, A. M. Salazar, J. S. Fischer, D. E. Goodkin, C. V. Granger, J. H. Simon, J. J.

Alam, D. M. Bartoszak, D. N. Bourdette, J. Braiman, C. M. Brownscheidle, M. E. Coats, S. L. Cohan, D. S. Dougherty, R. P. Kinkel, M. K. Mass, F. E. Munschauer, 3rd, R. L. Priore, P. M. Pullicino, B. J. Scherokman, R. H. Whitham, and et al. 1996. "Intramuscular interferon beta-1a for disease progression in relapsing multiple sclerosis. The Multiple Sclerosis Collaborative Research Group (MSCRG)." *Ann Neurol* 39 (3): 285-94. https://doi.org/10.1002/ana.410390304.

Jacobson, D. L., S. J. Gange, N. R. Rose, and N. M. Graham. 1997. "Epidemiology and estimated population burden of selected autoimmune diseases in the United States." *Clin Immunol Immunopathol* 84 (3): 223-43. https://doi.org/10.1006/clin.1997.4412.

James, L. C., A. H. Keeble, Z. Khan, D. A. Rhodes, and J. Trowsdale. 2007. "Structural basis for PRYSPRY-mediated tripartite motif (TRIM) protein function." *Proc Natl Acad Sci U S A* 104 (15): 6200-5. https://doi.org/10.1073/pnas.0609174104.

Jarius, S., F. Paul, O. Aktas, N. Asgari, R. C. Dale, J. de Seze, D. Franciotta, K. Fujihara, A. Jacob, H. J. Kim, I. Kleiter, T. Kümpfel, M. Levy, J. Palace, K. Ruprecht, A. Saiz, C. Trebst, B. G. Weinshenker, and B. Wildemann. 2018. "MOG encephalomyelitis: international recommendations on diagnosis and antibody testing." *J Neuroinflammation* 15 (1): 134. https://doi.org/10.1186/s12974-018-1144-2.

Jassal, B., L. Matthews, G. Viteri, C. Gong, P. Lorente, A. Fabregat, K. Sidiropoulos, J. Cook, M. Gillespie, R. Haw, F. Loney, B. May, M. Milacic, K. Rothfels, C. Sevilla, V. Shamovsky, S. Shorser, T. Varusai, J. Weiser, G. Wu, L. Stein, H. Hermjakob, and P. D'Eustachio. 2020. "The reactome pathway knowledgebase." *Nucleic Acids Res* 48 (D1): D498-d503. https://doi.org/10.1093/nar/gkz1031.

Jauneau, A. C., A. Ischenko, P. Chan, and M. Fontaine. 2003. "Complement component anaphylatoxins upregulate chemokine expression by human astrocytes." *FEBS Lett* 537 (1-3): 17-22. https://doi.org/10.1016/s0014-5793(03)00060-7.

Jelcic, I., W. Faigle, M. Sospedra, and R. Martin. 2015. "Immunology of progressive multifocal leukoencephalopathy." *J Neurovirol* 21 (6): 614-22. https://doi.org/10.1007/s13365-014-0294-y.

Jerne, N. K. 1974. "Towards a network theory of the immune system." *Ann Immunol (Paris)* 125c (1-2): 373-89.

Ji, J., S. H. Ng, V. Sharma, D. Neculai, S. Hussein, M. Sam, Q. Trinh, G. M. Church, J. D. McPherson, A. Nagy, and N. N. Batada. 2012. "Elevated coding mutation rate during the reprogramming of human somatic cells into induced pluripotent stem cells." *Stem Cells* 30 (3): 435-40. https://doi.org/10.1002/stem.1011.

Johnson, K. P., B. R. Brooks, J. A. Cohen, C. C. Ford, J. Goldstein, R. P. Lisak, L. W. Myers, H. S. Panitch, J. W. Rose, and R. B. Schiffer. 1995. "Copolymer 1 reduces relapse rate and improves disability in relapsing-remitting multiple sclerosis: results of a phase III multicenter, double-blind placebo-controlled trial. The Copolymer 1 Multiple Sclerosis Study Group." *Neurology* 45 (7): 1268-76. https://doi.org/10.1212/wnl.45.7.1268.

Johnson, P., and A. F. Williams. 1986. "Striking similarities between antigen receptor J pieces and sequence in the second chain of the murine CD8 antigen." *Nature* 323 (6083): 74-6. https://doi.org/10.1038/323074a0.

Jonakait, G. M., Y. Wen, Y. Wan, and L. Ni. 2000. "Macrophage cell-conditioned medium promotes cholinergic differentiation of undifferentiated progenitors and synergizes with nerve growth factor action in the

developing basal forebrain." *Exp Neurol* 161 (1): 285-96. https://doi.org/10.1006/exnr.1999.7255.

Joseph, S. B., M. N. Bradley, A. Castrillo, K. W. Bruhn, P. A. Mak, L. Pei, J. Hogenesch, M. O'Connell R, G. Cheng, E. Saez, J. F. Miller, and P. Tontonoz. 2004. "LXR-dependent gene expression is important for macrophage survival and the innate immune response." *Cell* 119 (2): 299-309. https://doi.org/10.1016/j.cell.2004.09.032.

Julander, J. G., V. Siddharthan, L. M. Blatt, K. Schafer, R. W. Sidwell, and J. D. Morrey. 2007. "Effect of exogenous interferon and an interferon inducer on western equine encephalitis virus disease in a hamster model." *Virology* 360 (2): 454-60. https://doi.org/10.1016/j.virol.2006.10.031.

Kabat, E. A., and D. A. Freedman. 1950. "A study of the crystalline albumin, gamma globulin and total protein in the cerebrospinal fluid of 100 cases of multiple sclerosis and in other diseases." *Am J Med Sci* 219 (1): 55-64. https://doi.org/10.1097/00000441-195001000-00009.

Kabelitz, D., K. H. Enssle, B. Fleischer, and J. Reimann. 1987. "Antigen-presenting T cells. II. Clonal responses of alloreactive and virus-specific self-restricted human cytotoxic T cell responses stimulated by T lymphoblasts." *J Immunol* 138 (1): 45-50.

Kadambari, S., I. Okike, S. Ribeiro, M. E. Ramsay, P. T. Heath, M. Sharland, and S. N. Ladhani. 2014. "Seven-fold increase in viral meningo-encephalitis reports in England and Wales during 2004-2013." *J Infect* 69 (4): 326-32. https://doi.org/10.1016/j.jinf.2014.05.012.

Kaisho, T., and S. Akira. 2000. "Critical roles of Toll-like receptors in host defense." *Crit Rev Immunol* 20 (5): 393-405.

Kanehisa, M., and S. Goto. 2000. "KEGG: kyoto encyclopedia of genes and genomes." *Nucleic Acids Res* 28 (1): 27-30. https://doi.org/10.1093/nar/28.1.27.

Kang, D. C., R. V. Gopalkrishnan, Q. Wu, E. Jankowsky, A. M. Pyle, and P. B. Fisher. 2002. "mda-5: An interferon-inducible putative RNA helicase with double-stranded RNA-dependent ATPase activity and melanoma growth-suppressive properties." *Proc Natl Acad Sci U S A* 99 (2): 637-42. https://doi.org/10.1073/pnas.022637199.

Kang, J. S., Y. S. Hwang, L. K. Kim, S. Lee, W. B. Lee, J. Kim-Ha, and Y. J. Kim. 2018. "OASL1 Traps Viral RNAs in Stress Granules to Promote Antiviral Responses." *Mol Cells* 41 (3): 214-223. https://doi.org/10.14348/molcells.2018.2293.

Kanter, J. L., S. Narayana, P. P. Ho, I. Catz, K. G. Warren, R. A. Sobel, L. Steinman, and W. H. Robinson. 2006. "Lipid microarrays identify key mediators of autoimmune brain inflammation." *Nat Med* 12 (1): 138-43. https://doi.org/10.1038/nm1344.

Kapil, P., N. B. Butchi, S. A. Stohlman, and C. C. Bergmann. 2012. "Oligodendroglia are limited in type I interferon induction and responsiveness in vivo." *Glia* 60 (10): 1555-66. https://doi.org/10.1002/glia.22375.

Kappos, L., E. W. Radue, P. O'Connor, C. Polman, R. Hohlfeld, P. Calabresi, K. Selmaj, C. Agoropoulou, M. Leyk, L. Zhang-Auberson, and P. Burtin. 2010. "A placebo-controlled trial of oral fingolimod in relapsing multiple sclerosis." *N Engl J Med* 362 (5): 387-401. https://doi.org/10.1056/NEJMoa0909494.

Kassmann, C. M., C. Lappe-Siefke, M. Baes, B. Brügger, A. Mildner, H. B. Werner, O. Natt, T. Michaelis, M. Prinz, J. Frahm, and K. A. Nave. 2007. "Axonal loss and neuroinflammation caused by peroxisome-deficient

oligodendrocytes." *Nat Genet* 39 (8): 969-76. https://doi.org/10.1038/ng2070.

Kato, A., T. Kitamura, T. Takasaka, T. Tominaga, A. Ishikawa, H. Y. Zheng, and Y. Yogo. 2004. "Detection of the archetypal regulatory region of JC virus from the tonsil tissue of patients with tonsillitis and tonsilar hypertrophy." *J Neurovirol* 10 (4): 244-9. https://doi.org/10.1080/13550280490468663.

Kato, M., S. Kubo, and M. Naiki. 1978. "Complement fixation antibodies to glycosphingolipids in sera of rare blood group p and Pk phenotypes." *J Immunogenet* 5 (1): 31-40. https://doi.org/10.1111/j.1744-313x.1978.tb00628.x.

Katz, D. H., and E. R. Unanue. 1973. "Critical role of determinant presentation in the induction of specific responses in immunocompetent lymphocytes." *J Exp Med* 137 (4): 967-90. https://doi.org/10.1084/jem.137.4.967.

Kawahara, T., H. Ohdan, G. Zhao, Y. G. Yang, and M. Sykes. 2003. "Peritoneal cavity B cells are precursors of splenic IgM natural antibody-producing cells." *J Immunol* 171 (10): 5406-14. https://doi.org/10.4049/jimmunol.171.10.5406.

Kazura, J. W. 1981. "Host defense mechanisms against nematode parasites: destruction of newborn Trichinella spiralis larvae by human antibodies and granulocytes." *J Infect Dis* 143 (5): 712-8. https://doi.org/10.1093/infdis/143.5.712.

Kean, J. M., S. Rao, M. Wang, and R. L. Garcea. 2009. "Seroepidemiology of human polyomaviruses." *PLoS Pathog* 5 (3): e1000363. https://doi.org/10.1371/journal.ppat.1000363.

Kearney, J. F., M. D. Cooper, and A. R. Lawton. 1976. "B cell differentiation induced by lipopolysaccharide. IV. Development of immunoglobulin class restriction in precursors of IgG-synthesizing cells." *J Immunol* 117 (5 Pt 1): 1567-72.

Kehry, M., C. Sibley, J. Fuhrman, J. Schilling, and L. E. Hood. 1979. "Amino acid sequence of a mouse immunoglobulin mu chain." *Proc Natl Acad Sci U S A* 76 (6): 2932-6. https://doi.org/10.1073/pnas.76.6.2932.

Keller, C. W., C. Sina, M. B. Kotur, G. Ramelli, S. Mundt, I. Quast, L. A. Ligeon, P. Weber, B. Becher, C. Münz, and J. D. Lünemann. 2017. "ATG-dependent phagocytosis in dendritic cells drives myelin-specific CD4(+) T cell pathogenicity during CNS inflammation." *Proc Natl Acad Sci U S A* 114 (52): E11228-e11237. https://doi.org/10.1073/pnas.1713664114.

Kenigsberg, R. L., and I. E. Mazzoni. 1995. "Identification of glial cell types involved in mediating epidermal growth factor's effects on septal cholinergic neurons." *J Neurosci Res* 41 (6): 734-44. https://doi.org/10.1002/jnr.490410604.

Kennedy, P. G. E., P. L. Quan, and W. I. Lipkin. 2017. "Viral Encephalitis of Unknown Cause: Current Perspective and Recent Advances." *Viruses* 9 (6). https://doi.org/10.3390/v9060138.

Kesselheim, A. S., T. J. Hwang, and J. M. Franklin. 2015. "Two decades of new drug development for central nervous system disorders." *Nat Rev Drug Discov* 14 (12): 815-6. https://doi.org/10.1038/nrd4793.

Ketelslegers, I. A., D. E. Van Pelt, S. Bryde, R. F. Neuteboom, C. E. Catsman-Berrevoets, D. Hamann, and R. Q. Hintzen. 2015. "Anti-MOG antibodies plead against MS diagnosis in an Acquired Demyelinating Syndromes cohort." *Mult Scler* 21 (12): 1513-20. https://doi.org/10.1177/1352458514566666.

Khorooshi, R., M. T. Morch, T. H. Holm, C. T. Berg, R. T. Dieu, D. Draeby, S. Issazadeh-Navikas, S. Weiss, S. Lienenklaus, and T. Owens. 2015.

"Induction of endogenous Type I interferon within the central nervous system plays a protective role in experimental autoimmune encephalomyelitis." *Acta Neuropathol* 130 (1): 107-18. https://doi.org/10.1007/s00401-015-1418-z.

Kido, G., J. L. Wright, and R. E. Merchant. 1991. "Acute effects of human recombinant tumor necrosis factor-alpha on the cerebral vasculature of the rat in both normal brain and in an experimental glioma model." *J Neurooncol* 10 (2): 95-109. https://doi.org/10.1007/bf00146870.

Kierdorf, K., D. Erny, T. Goldmann, V. Sander, C. Schulz, E. G. Perdiguero, P. Wieghofer, A. Heinrich, P. Riemke, C. Hölscher, D. N. Müller, B. Luckow, T. Brocker, K. Debowski, G. Fritz, G. Opdenakker, A. Diefenbach, K. Biber, M. Heikenwalder, F. Geissmann, F. Rosenbauer, and M. Prinz. 2013. "Microglia emerge from erythromyeloid precursors via Pu.1- and Irf8-dependent pathways." *Nat Neurosci* 16 (3): 273-80. https://doi.org/10.1038/nn.3318.

Kiernan, J. A. 1976. "A comparative survey of the mast cells of the mammalian brain." *J Anat* 121 (Pt 2): 303-11.

Kim, K., A. Doi, B. Wen, K. Ng, R. Zhao, P. Cahan, J. Kim, M. J. Aryee, H. Ji, L. I. Ehrlich, A. Yabuuchi, A. Takeuchi, K. C. Cunniff, H. Hongguang, S. McKinney-Freeman, O. Naveiras, T. J. Yoon, R. A. Irizarry, N. Jung, J. Seita, J. Hanna, P. Murakami, R. Jaenisch, R. Weissleder, S. H. Orkin, I. L. Weissman, A. P. Feinberg, and G. Q. Daley. 2010. "Epigenetic memory in induced pluripotent stem cells." *Nature* 467 (7313): 285-90. https://doi.org/10.1038/nature09342.

Kim, S., M. Davis, E. Sinn, P. Patten, and L. Hood. 1981. "Antibody diversity: somatic hypermutation of rearranged VH genes." *Cell* 27 (3 Pt 2): 573-81. https://doi.org/10.1016/0092-8674(81)90399-8.

Kim, T., S. Pazhoor, M. Bao, Z. Zhang, S. Hanabuchi, V. Facchinetti, L. Bover, J. Plumas, L. Chaperot, J. Qin, and Y. J. Liu. 2010. "Aspartate-glutamate-alanine-histidine box motif (DEAH)/RNA helicase A helicases sense microbial DNA in human plasmacytoid dendritic cells." *Proc Natl Acad Sci U S A* 107 (34): 15181-6. https://doi.org/10.1073/pnas.1006539107.

Kindred, B., and D. C. Shreffler. 1972. "H-2 dependence of co-operation between T and B cells in vivo." *J Immunol* 109 (5): 940-3.

Kitani, H., M. Yamakawa, and H. Ikeda. 2000. "Preferential infection of neuronal and astroglia cells by Akabane virus in primary cultures of fetal bovine brain." *Vet Microbiol* 73 (4): 269-79. https://doi.org/10.1016/s0378-1135(00)00158-9.

Kitley, J., P. Waters, M. Woodhall, M. I. Leite, A. Murchison, J. George, W. Kuker, S. Chandratre, A. Vincent, and J. Palace. 2014. "Neuromyelitis optica spectrum disorders with aquaporin-4 and myelin-oligodendrocyte glycoprotein antibodies: a comparative study." *JAMA Neurol* 71 (3): 276-83. https://doi.org/10.1001/jamaneurol.2013.5857.

Klein, R. S., and C. A. Hunter. 2017. "Protective and Pathological Immunity during Central Nervous System Infections." *Immunity* 46 (6): 891-909. https://doi.org/10.1016/j.immuni.2017.06.012.

Kleinschmidt-DeMasters, B. K., and K. L. Tyler. 2005. "Progressive multifocal leukoencephalopathy complicating treatment with natalizumab and interferon beta-1a for multiple sclerosis." *N Engl J Med* 353 (4): 369-74. https://doi.org/10.1056/NEJMoa051782.

Klugmann, M., M. H. Schwab, A. Pühlhofer, A. Schneider, F. Zimmermann, I. R. Griffiths, and K. A. Nave. 1997. "Assembly of CNS myelin in the absence of

proteolipid protein." *Neuron* 18 (1): 59-70. https://doi.org/10.1016/s0896-6273(01)80046-5.

Knowles, W. A. 2006. "Discovery and epidemiology of the human polyomaviruses BK virus (BKV) and JC virus (JCV)." *Adv Exp Med Biol* 577: 19-45. https://doi.org/10.1007/0-387-32957-9_2.

Koch, K. S., and H. L. Leffert. 1980. "Growth control of differentiated adult rat hepatocytes in primary culture." *Ann N Y Acad Sci* 349: 111-27. https://doi.org/10.1111/j.1749-6632.1980.tb29520.x.

Kocur, M., R. Schneider, A. K. Pulm, J. Bauer, S. Kropp, M. Gliem, J. Ingwersen, N. Goebels, J. Alferink, T. Prozorovski, O. Aktas, and S. Scheu. 2015. "IFNbeta secreted by microglia mediates clearance of myelin debris in CNS autoimmunity." *Acta Neuropathol Commun* 3: 20. https://doi.org/10.1186/s40478-015-0192-4.

Komor, A. C., Y. B. Kim, M. S. Packer, J. A. Zuris, and D. R. Liu. 2016. "Programmable editing of a target base in genomic DNA without double-stranded DNA cleavage." *Nature* 533 (7603): 420-4. https://doi.org/10.1038/nature17946.

Kosugi, A., T. Yoshioka, T. Suda, H. Sano, Y. Takahama, H. Fujiwara, and T. Hamaoka. 1987. "The activation of L3T4+ helper T cells assisting the generation of anti-tumor Lyt-2+ cytotoxic T lymphocytes: requirement of Ia-positive antigen-presenting cells for processing and presentation of tumor antigens." *J Leukoc Biol* 42 (6): 632-41. https://doi.org/10.1002/jlb.42.6.632.

Koszinowski, U., M. J. Gething, and M. Waterfield. 1977. "T-cell cytotoxicity in the absence of viral protein synthesis in target cells." *Nature* 267 (5607): 160-3. https://doi.org/10.1038/267160a0.

Kouadir, M., L. Yang, R. Tan, F. Shi, Y. Lu, S. Zhang, X. Yin, X. Zhou, and D. Zhao. 2012. "CD36 participates in PrP(106-126)-induced activation of microglia." *PLoS One* 7 (1): e30756. https://doi.org/10.1371/journal.pone.0030756.

Kraus, J., K. Voigt, A. M. Schuller, M. Scholz, K. S. Kim, M. Schilling, W. R. Schäbitz, P. Oschmann, and B. Engelhardt. 2008. "Interferon-beta stabilizes barrier characteristics of the blood-brain barrier in four different species in vitro." *Mult Scler* 14 (6): 843-52. https://doi.org/10.1177/1352458508088940.

Kremenchutzky, M., G. P. Rice, J. Baskerville, D. M. Wingerchuk, and G. C. Ebers. 2006. "The natural history of multiple sclerosis: a geographically based study 9: observations on the progressive phase of the disease." *Brain* 129 (Pt 3): 584-94. https://doi.org/10.1093/brain/awh721.

Krencik, R., J. P. Weick, Y. Liu, Z. J. Zhang, and S. C. Zhang. 2011. "Specification of transplantable astroglial subtypes from human pluripotent stem cells." *Nat Biotechnol* 29 (6): 528-34. https://doi.org/10.1038/nbt.1877.

Krieger, M. 1997. "The other side of scavenger receptors: pattern recognition for host defense." *Curr Opin Lipidol* 8 (5): 275-80. https://doi.org/10.1097/00041433-199710000-00006.

Krähenbühl, O., C. Rey, D. Jenne, A. Lanzavecchia, P. Groscurth, S. Carrel, and J. Tschopp. 1988. "Characterization of granzymes A and B isolated from granules of cloned human cytotoxic T lymphocytes." *J Immunol* 141 (10): 3471-7.

Kubagawa, H., S. Oka, Y. Kubagawa, I. Torii, E. Takayama, D. W. Kang, G. L. Gartland, L. F. Bertoli, H. Mori, H. Takatsu, T. Kitamura, H. Ohno, and J. Y. Wang. 2009. "Identity of the elusive IgM Fc receptor (FcmuR) in

humans." *J Exp Med* 206 (12): 2779-93. https://doi.org/10.1084/jem.20091107.

Kumar, S., J. S. Chera, A. Vats, and S. De. 2019. "Nature of selection varies on different domains of IFI16-like PYHIN genes in ruminants." *BMC Evol Biol* 19 (1): 26. https://doi.org/10.1186/s12862-018-1334-7.

Kumaraguru, U., I. A. Davis, S. Deshpande, S. S. Tevethia, and B. T. Rouse. 2001. "Lymphotoxin alpha-/- mice develop functionally impaired CD8+ T cell responses and fail to contain virus infection of the central nervous system." *J Immunol* 166 (2): 1066-74. https://doi.org/10.4049/jimmunol.166.2.1066.

Kundu, S. K., M. A. Pleatman, W. A. Redwine, A. E. Boyd, and D. M. Marcus. 1983. "Binding of monoclonal antibody A2B5 to gangliosides." *Biochem Biophys Res Commun* 116 (3): 836-42. https://doi.org/10.1016/s0006-291x(83)80218-6.

Kurokawa, J., S. Arai, K. Nakashima, H. Nagano, A. Nishijima, K. Miyata, R. Ose, M. Mori, N. Kubota, T. Kadowaki, Y. Oike, H. Koga, M. Febbraio, T. Iwanaga, and T. Miyazaki. 2010. "Macrophage-derived AIM is endocytosed into adipocytes and decreases lipid droplets via inhibition of fatty acid synthase activity." *Cell Metab* 11 (6): 479-92. https://doi.org/10.1016/j.cmet.2010.04.013.

Kurt-Jones, E. A., L. Popova, L. Kwinn, L. M. Haynes, L. P. Jones, R. A. Tripp, E. E. Walsh, M. W. Freeman, D. T. Golenbock, L. J. Anderson, and R. W. Finberg. 2000. "Pattern recognition receptors TLR4 and CD14 mediate response to respiratory syncytial virus." *Nat Immunol* 1 (5): 398-401. https://doi.org/10.1038/80833.

Kurtzke, J. F. 1956. "Course of exacerbations of multiple sclerosis in hospitalized patients." *AMA Arch Neurol Psychiatry* 76 (2): 175-84. https://doi.org/10.1001/archneurpsyc.1956.02330260061002.

Kutzelnigg, A., J. C. Faber-Rod, J. Bauer, C. F. Lucchinetti, P. S. Sorensen, H. Laursen, C. Stadelmann, W. Brück, H. Rauschka, M. Schmidbauer, and H. Lassmann. 2007. "Widespread demyelination in the cerebellar cortex in multiple sclerosis." *Brain Pathol* 17 (1): 38-44. https://doi.org/10.1111/j.1750-3639.2006.00041.x.

Kutzelnigg, A., C. F. Lucchinetti, C. Stadelmann, W. Brück, H. Rauschka, M. Bergmann, M. Schmidbauer, J. E. Parisi, and H. Lassmann. 2005. "Cortical demyelination and diffuse white matter injury in multiple sclerosis." *Brain* 128 (Pt 11): 2705-12. https://doi.org/10.1093/brain/awh641.

Lancaster, K. Z., and J. K. Pfeiffer. 2010. "Limited trafficking of a neurotropic virus through inefficient retrograde axonal transport and the type I interferon response." *PLoS Pathog* 6 (3): e1000791. https://doi.org/10.1371/journal.ppat.1000791.

Lands, A. M. 1951. "An investigation of the molecular configurations favorable for stimulation or blockade of the acetylcholine-sensitive receptors of visceral organs." *J Pharmacol Exp Ther* 102 (4): 219-36.

Lane, J. H., V. G. Sasseville, M. O. Smith, P. Vogel, D. R. Pauley, M. P. Heyes, and A. A. Lackner. 1996. "Neuroinvasion by simian immunodeficiency virus coincides with increased numbers of perivascular macrophages/microglia and intrathecal immune activation." *J Neurovirol* 2 (6): 423-32. https://doi.org/10.3109/13550289609146909.

Langer-Gould, A., S. W. Atlas, A. J. Green, A. W. Bollen, and D. Pelletier. 2005. "Progressive multifocal leukoencephalopathy in a patient treated with natalizumab." *N Engl J Med* 353 (4): 375-81. https://doi.org/10.1056/NEJMoa051847.

Lappe-Siefke, C., S. Goebbels, M. Gravel, E. Nicksch, J. Lee, P. E. Braun, I. R. Griffiths, and K. A. Nave. 2003. "Disruption of Cnp1 uncouples oligodendroglial functions in axonal support and myelination." *Nat Genet* 33 (3): 366-74. https://doi.org/10.1038/ng1095.

Lappin, D. F., G. W. Nakitare, J. W. Palfreyman, and R. M. Elliott. 1994. "Localization of Bunyamwera bunyavirus G1 glycoprotein to the Golgi requires association with G2 but not with NSm." *J Gen Virol* 75 (Pt 12): 3441-51. https://doi.org/10.1099/0022-1317-75-12-3441.

Lassmann, H. 2008. "The pathologic substrate of magnetic resonance alterations in multiple sclerosis." *Neuroimaging Clin N Am* 18 (4): 563-76, ix. https://doi.org/10.1016/j.nic.2008.06.005.

Lassmann, H., C. S. Raine, J. Antel, and J. W. Prineas. 1998. "Immunopathology of multiple sclerosis: report on an international meeting held at the Institute of Neurology of the University of Vienna." In *J Neuroimmunol*, 213-7. Netherlands.

Lawrence, C. W., and T. J. Braciale. 2004. "Activation, differentiation, and migration of naive virus-specific CD8+ T cells during pulmonary influenza virus infection." *J Immunol* 173 (2): 1209-18. https://doi.org/10.4049/jimmunol.173.2.1209.

Lazic, S. E., C. J. Clarke-Williams, and M. R. Munafò. 2018. "What exactly is 'N' in cell culture and animal experiments?" *PLoS Biol* 16 (4): e2005282. https://doi.org/10.1371/journal.pbio.2005282.

Lee, J. C., M. G. Hanna, Jr., J. N. Ihle, and S. A. Aaronson. 1974. "Autogenous immunity to endogenous RNA tumor virus: differential reactivities of immunoglobulins M and G to virus envelope antigens." *J Virol* 14 (4): 773-81. https://doi.org/10.1128/jvi.14.4.773-781.1974.

Lee, Y., B. M. Morrison, Y. Li, S. Lengacher, M. H. Farah, P. N. Hoffman, Y. Liu, A. Tsingalia, L. Jin, P. W. Zhang, L. Pellerin, P. J. Magistretti, and J. D. Rothstein. 2012. "Oligodendroglia metabolically support axons and contribute to neurodegeneration." *Nature* 487 (7408): 443-8. https://doi.org/10.1038/nature11314.

Lemkey-Johnston, N., V. Butler, and W. A. Reynolds. 1976. "Glial changes in the progress of a chemical lesion. An electron microscopic study." *J Comp Neurol* 167 (4): 481-501. https://doi.org/10.1002/cne.901670406.

Leslie, M. 2015. "Cleanup crew." *Science* 347 (6226): 1058-9, 1061. https://doi.org/10.1126/science.347.6226.1058.

Levy, D. E., D. J. Lew, T. Decker, D. S. Kessler, and J. E. Darnell, Jr. 1990. "Synergistic interaction between interferon-alpha and interferon-gamma through induced synthesis of one subunit of the transcription factor ISGF3." *Embo j* 9 (4): 1105-11.

Lewis, D. E., B. E. Gilbert, and V. Knight. 1986. "Influenza virus infection induces functional alterations in peripheral blood lymphocytes." *J Immunol* 137 (12): 3777-81.

Lewis, N. D., J. D. Hill, K. W. Juchem, D. E. Stefanopoulos, and L. K. Modis. 2014. "RNA sequencing of microglia and monocyte-derived macrophages from mice with experimental autoimmune encephalomyelitis illustrates a changing phenotype with disease course." *J Neuroimmunol* 277 (1-2): 26-38. https://doi.org/10.1016/j.jneuroim.2014.09.014.

Li, F., Y. Wang, L. Yu, S. Cao, K. Wang, J. Yuan, C. Wang, M. Cui, and Z. F. Fu. 2015. "Viral Infection of the Central Nervous System and Neuroinflammation Precede Blood-Brain Barrier Disruption during Japanese Encephalitis Virus Infection." *J Virol* 89 (10): 5602-14. https://doi.org/10.1128/jvi.00143-15.

Li, J., H. Wang, C. Du, X. Jin, Y. Geng, B. Han, Q. Ma, Q. Li, Q. Wang, Y. Guo, M. Wang, and B. Yan. 2020. "hUC-MSCs ameliorated CUMS-induced depression by modulating complement C3 signaling-mediated microglial polarization during astrocyte-microglia crosstalk." *Brain Res Bull* 163: 109-119. https://doi.org/10.1016/j.brainresbull.2020.07.004.

Li, Q. Z., J. Zhou, Y. Lian, B. Zhang, V. K. Branch, F. Carr-Johnson, D. R. Karp, C. Mohan, E. K. Wakeland, and N. J. Olsen. 2010. "Interferon signature gene expression is correlated with autoantibody profiles in patients with incomplete lupus syndromes." *Clin Exp Immunol* 159 (3): 281-91. https://doi.org/10.1111/j.1365-2249.2009.04057.x.

Li, R., K. R. Patterson, and A. Bar-Or. 2018. "Reassessing B cell contributions in multiple sclerosis." *Nat Immunol* 19 (7): 696-707. https://doi.org/10.1038/s41590-018-0135-x.

Lian, H., A. Litvinchuk, A. C. Chiang, N. Aithmitti, J. L. Jankowsky, and H. Zheng. 2016. "Astrocyte-Microglia Cross Talk through Complement Activation Modulates Amyloid Pathology in Mouse Models of Alzheimer's Disease." *J Neurosci* 36 (2): 577-89. https://doi.org/10.1523/jneurosci.2117-15.2016.

Liebner, S., R. M. Dijkhuizen, Y. Reiss, K. H. Plate, D. Agalliu, and G. Constantin. 2018. "Functional morphology of the blood-brain barrier in health and disease." *Acta Neuropathol* 135 (3): 311-336. https://doi.org/10.1007/s00401-018-1815-1.

Lien, C. F., S. K. Mohanta, M. Frontczak-Baniewicz, J. D. Swinny, B. Zablocka, and D. C. Górecki. 2012. "Absence of glial α-dystrobrevin causes abnormalities of the blood-brain barrier and progressive brain edema." *J Biol Chem* 287 (49): 41374-85. https://doi.org/10.1074/jbc.M112.400044.

Lilienfeld, A. M. 1973. "Epidemiology of infectious and non-infectious disease: some comparisons." *Am J Epidemiol* 97 (3): 135-47. https://doi.org/10.1093/oxfordjournals.aje.a121494.

Lin, R. J., C. L. Liao, E. Lin, and Y. L. Lin. 2004. "Blocking of the alpha interferon-induced Jak-Stat signaling pathway by Japanese encephalitis virus infection." *J Virol* 78 (17): 9285-94. https://doi.org/10.1128/jvi.78.17.9285-9294.2004.

Lindqvist, R., C. Kurhade, J. D. Gilthorpe, and A. K. Overby. 2018. "Cell-type- and region-specific restriction of neurotropic flavivirus infection by viperin." *J Neuroinflammation* 15 (1): 80. https://doi.org/10.1186/s12974-018-1119-3.

Lindqvist, R., C. Kurhade, J. D. Gilthorpe, and A. K. Överby. 2018. "Cell-type- and region-specific restriction of neurotropic flavivirus infection by viperin." *J Neuroinflammation* 15 (1): 80. https://doi.org/10.1186/s12974-018-1119-3.

Lindsay, R. M., P. C. Barber, M. R. Sherwood, J. Zimmer, and G. Raisman. 1982. "Astrocyte cultures from adult rat brain. Derivation, characterization and neurotrophic properties of pure astroglial cells from corpus callosum." *Brain Res* 243 (2): 329-43. https://doi.org/10.1016/0006-8993(82)90257-8.

Liu, H., C. X. Huang, Q. He, D. Li, M. H. Luo, F. Zhao, and W. Lu. 2019. "Proteomics analysis of HSV-1-induced alterations in mouse brain microvascular endothelial cells." *J Neurovirol* 25 (4): 525-539. https://doi.org/10.1007/s13365-019-00752-z.

Liu, M. T., B. P. Chen, P. Oertel, M. J. Buchmeier, D. Armstrong, T. A. Hamilton, and T. E. Lane. 2000. "The T cell chemoattractant IFN-inducible protein

10 is essential in host defense against viral-induced neurologic disease." *J Immunol* 165 (5): 2327-30. https://doi.org/10.4049/jimmunol.165.5.2327.

Lochhead, J. J., D. J. Wolak, M. E. Pizzo, and R. G. Thorne. 2015. "Rapid transport within cerebral perivascular spaces underlies widespread tracer distribution in the brain after intranasal administration." *J Cereb Blood Flow Metab* 35 (3): 371-81. https://doi.org/10.1038/jcbfm.2014.215.

Loetscher, M., B. Gerber, P. Loetscher, S. A. Jones, L. Piali, I. Clark-Lewis, M. Baggiolini, and B. Moser. 1996. "Chemokine receptor specific for IP10 and mig: structure, function, and expression in activated T-lymphocytes." *J Exp Med* 184 (3): 963-9. https://doi.org/10.1084/jem.184.3.963.

Lokensgard, J. R., M. B. Mutnal, S. Prasad, W. Sheng, and S. Hu. 2016. "Glial cell activation, recruitment, and survival of B-lineage cells following MCMV brain infection." *J Neuroinflammation* 13 (1): 114. https://doi.org/10.1186/s12974-016-0582-y.

Loré, K., M. R. Betts, J. M. Brenchley, J. Kuruppu, S. Khojasteh, S. Perfetto, M. Roederer, R. A. Seder, and R. A. Koup. 2003. "Toll-like receptor ligands modulate dendritic cells to augment cytomegalovirus- and HIV-1-specific T cell responses." *J Immunol* 171 (8): 4320-8. https://doi.org/10.4049/jimmunol.171.8.4320.

Losana, G., C. Bovolenta, L. Rigamonti, I. Borghi, F. Altare, E. Jouanguy, G. Forni, J. L. Casanova, B. Sherry, M. Mengozzi, G. Trinchieri, G. Poli, F. Gerosa, and F. Novelli. 2002. "IFN-gamma and IL-12 differentially regulate CC-chemokine secretion and CCR5 expression in human T lymphocytes." *J Leukoc Biol* 72 (4): 735-42.

Louveau, A., I. Smirnov, T. J. Keyes, J. D. Eccles, S. J. Rouhani, J. D. Peske, N. C. Derecki, D. Castle, J. W. Mandell, K. S. Lee, T. H. Harris, and J. Kipnis. 2015. "Structural and functional features of central nervous system lymphatic vessels." *Nature* 523 (7560): 337-41. https://doi.org/10.1038/nature14432.

Lovato, L., S. N. Willis, S. J. Rodig, T. Caron, S. E. Almendinger, O. W. Howell, R. Reynolds, K. C. O'Connor, and D. A. Hafler. 2011. "Related B cell clones populate the meninges and parenchyma of patients with multiple sclerosis." *Brain* 134 (Pt 2): 534-41. https://doi.org/10.1093/brain/awq350.

Lowenthal, A., and D. Karcher. 1979. "Immune Responses in the Cerebrospinal Fluid." In *Aspects of Slow and Persistent Virus Infections. New Perspectives in Clinical Microbiology*, edited by Tyrrell D.A.J. Dordrecht: Springer.

Lu, F., and B. Kalman. 1999. "Autoreactive IgG to intracellular proteins in sera of MS patients." *J Neuroimmunol* 99 (1): 72-81. https://doi.org/10.1016/s0165-5728(99)00104-6.

Lu, T. M., S. Houghton, T. Magdeldin, J. G. B. Durán, A. P. Minotti, A. Snead, A. Sproul, D. T. Nguyen, J. Xiang, H. A. Fine, Z. Rosenwaks, L. Studer, S. Rafii, D. Agalliu, D. Redmond, and R. Lis. 2021. "Pluripotent stem cell-derived epithelium misidentified as brain microvascular endothelium requires ETS factors to acquire vascular fate." *Proc Natl Acad Sci U S A* 118 (8). https://doi.org/10.1073/pnas.2016950118.

Lublin, F. D., S. C. Reingold, J. A. Cohen, G. R. Cutter, P. S. Sørensen, A. J. Thompson, J. S. Wolinsky, L. J. Balcer, B. Banwell, F. Barkhof, B. Bebo, Jr., P. A. Calabresi, M. Clanet, G. Comi, R. J. Fox, M. S. Freedman, A. D. Goodman, M. Inglese, L. Kappos, B. C. Kieseier, J. A. Lincoln, C. Lubetzki, A. E. Miller, X. Montalban, P. W. O'Connor, J. Petkau, C. Pozzilli, R. A. Rudick, M. P. Sormani, O. Stüve, E. Waubant, and C. H. Polman. 2014.

"Defining the clinical course of multiple sclerosis: the 2013 revisions." *Neurology* 83 (3): 278-86. https://doi.org/10.1212/wnl.0000000000000560.

Lublin, F., D. H. Miller, M. S. Freedman, B. A. C. Cree, J. S. Wolinsky, H. Weiner, C. Lubetzki, H. P. Hartung, X. Montalban, B. M. J. Uitdehaag, M. Merschhemke, B. Li, N. Putzki, F. C. Liu, D. A. Häring, and L. Kappos. 2016. "Oral fingolimod in primary progressive multiple sclerosis (INFORMS): a phase 3, randomised, double-blind, placebo-controlled trial." *Lancet* 387 (10023): 1075-1084. https://doi.org/10.1016/s0140-6736(15)01314-8.

Lucas, M., T. Mashimo, M. P. Frenkiel, D. Simon-Chazottes, X. Montagutelli, P. E. Ceccaldi, J. L. Guénet, and P. Desprès. 2003. "Infection of mouse neurones by West Nile virus is modulated by the interferon-inducible 2'-5' oligoadenylate synthetase 1b protein." *Immunol Cell Biol* 81 (3): 230-6. https://doi.org/10.1046/j.1440-1711.2003.01166.x.

Lucchinetti, C. F., W. Brück, M. Rodriguez, and H. Lassmann. 1996. "Distinct patterns of multiple sclerosis pathology indicates heterogeneity on pathogenesis." *Brain Pathol* 6 (3): 259-74. https://doi.org/10.1111/j.1750-3639.1996.tb00854.x.

Lucius, R., and J. Sievers. 1996. "Postnatal retinal ganglion cells in vitro: protection against reactive oxygen species (ROS)-induced axonal degeneration by cocultured astrocytes." *Brain Res* 743 (1-2): 56-62. https://doi.org/10.1016/s0006-8993(96)01029-3.

Lumsden, C. E. 1971. "The immunogenesis of the multiple sclerosis plaque." *Brain Res* 28 (3): 365-90. https://doi.org/10.1016/0006-8993(71)90052-7.

Lund, J. M., L. Alexopoulou, A. Sato, M. Karow, N. C. Adams, N. W. Gale, A. Iwasaki, and R. A. Flavell. 2004. "Recognition of single-stranded RNA viruses by Toll-like receptor 7." *Proc Natl Acad Sci U S A* 101 (15): 5598-603. https://doi.org/10.1073/pnas.0400937101.

Léonard, V. H., A. Kohl, T. J. Hart, and R. M. Elliott. 2006. "Interaction of Bunyamwera Orthobunyavirus NSs protein with mediator protein MED8: a mechanism for inhibiting the interferon response." *J Virol* 80 (19): 9667-75. https://doi.org/10.1128/jvi.00822-06.

Lövgren, T., M. L. Eloranta, B. Kastner, M. Wahren-Herlenius, G. V. Alm, and L. Rönnblom. 2006. "Induction of interferon-alpha by immune complexes or liposomes containing systemic lupus erythematosus autoantigen- and Sjögren's syndrome autoantigen-associated RNA." *Arthritis Rheum* 54 (6): 1917-27. https://doi.org/10.1002/art.21893.

Ma, D., D. Jiang, M. Qing, J. M. Weidner, X. Qu, H. Guo, J. Chang, B. Gu, P. Y. Shi, T. M. Block, and J. T. Guo. 2009. "Antiviral effect of interferon lambda against West Nile virus." *Antiviral Res* 83 (1): 53-60. https://doi.org/10.1016/j.antiviral.2009.03.006.

Ma, S., H. J. Kwon, and Z. Huang. 2012. "A functional requirement for astroglia in promoting blood vessel development in the early postnatal brain." *PLoS One* 7 (10): e48001. https://doi.org/10.1371/journal.pone.0048001.

Maat-Schieman, M. L., S. G. van Duinen, A. J. Rozemuller, J. Haan, and R. A. Roos. 1997. "Association of vascular amyloid beta and cells of the mononuclear phagocyte system in hereditary cerebral hemorrhage with amyloidosis (Dutch) and Alzheimer disease." *J Neuropathol Exp Neurol* 56 (3): 273-84. https://doi.org/10.1097/00005072-199703000-00006.

MacDonald, J. A., C. P. Wijekoon, K. C. Liao, and D. A. Muruve. 2013. "Biochemical and structural aspects of the ATP-binding domain in

inflammasome-forming human NLRP proteins." *IUBMB Life* 65 (10): 851-62. https://doi.org/10.1002/iub.1210.

MacLennan, I. C., and A. Howard. 1972. "Evidence for correlation between the antigenic specificity and charge of human IgG. A study of antibody-inducing lymphocyte mediated cell damage." *Immunology* 22 (6): 1043-9.

Maehara, N., S. Arai, M. Mori, Y. Iwamura, J. Kurokawa, T. Kai, S. Kusunoki, K. Taniguchi, K. Ikeda, O. Ohara, K. I. Yamamura, and T. Miyazaki. 2014. "Circulating AIM prevents hepatocellular carcinoma through complement activation." *Cell Rep* 9 (1): 61-74. https://doi.org/10.1016/j.celrep.2014.08.058.

Magliozzi, R., O. Howell, A. Vora, B. Serafini, R. Nicholas, M. Puopolo, R. Reynolds, and F. Aloisi. 2007. "Meningeal B-cell follicles in secondary progressive multiple sclerosis associate with early onset of disease and severe cortical pathology." *Brain* 130 (Pt 4): 1089-104. https://doi.org/10.1093/brain/awm038.

Magri, G., L. Comerma, M. Pybus, J. Sintes, D. Lligé, D. Segura-Garzón, S. Bascones, A. Yeste, E. K. Grasset, C. Gutzeit, M. Uzzan, M. Ramanujam, M. C. van Zelm, R. Albero-González, I. Vazquez, M. Iglesias, S. Serrano, L. Márquez, E. Mercade, S. Mehandru, and A. Cerutti. 2017. "Human Secretory IgM Emerges from Plasma Cells Clonally Related to Gut Memory B Cells and Targets Highly Diverse Commensals." *Immunity* 47 (1): 118-134.e8. https://doi.org/10.1016/j.immuni.2017.06.013.

Mahad, D. J., and R. M. Ransohoff. 2003. "The role of MCP-1 (CCL2) and CCR2 in multiple sclerosis and experimental autoimmune encephalomyelitis (EAE)." *Semin Immunol* 15 (1): 23-32. https://doi.org/10.1016/s1044-5323(02)00125-2.

Major, E. O., and J. V. Neel. 1998. "The JC and BK human polyoma viruses appear to be recent introductions to some South American Indian tribes: there is no serological evidence of cross-reactivity with the simian polyoma virus SV40." *Proc Natl Acad Sci U S A* 95 (26): 15525-30. https://doi.org/10.1073/pnas.95.26.15525.

Major, E. O., T. A. Yousry, and D. B. Clifford. 2018. "Pathogenesis of progressive multifocal leukoencephalopathy and risks associated with treatments for multiple sclerosis: a decade of lessons learned." *Lancet Neurol* 17 (5): 467-480. https://doi.org/10.1016/s1474-4422(18)30040-1.

Mallery, D. L., W. A. McEwan, S. R. Bidgood, G. J. Towers, C. M. Johnson, and L. C. James. 2010. "Antibodies mediate intracellular immunity through tripartite motif-containing 21 (TRIM21)." *Proc Natl Acad Sci U S A* 107 (46): 19985-90. https://doi.org/10.1073/pnas.1014074107.

Manivel, V., N. C. Sahoo, D. M. Salunke, and K. V. Rao. 2000. "Maturation of an antibody response is governed by modulations in flexibility of the antigen-combining site." *Immunity* 13 (5): 611-20. https://doi.org/10.1016/s1074-7613(00)00061-3.

Manser, T., L. J. Wysocki, T. Gridley, R. I. Near, and M. L. Gefter. 1985. "The molecular evolution of the immune response." *Immunol Today* 6 (3): 94-101. https://doi.org/10.1016/0167-5699(85)90024-6.

Maoz, B. M., A. Herland, E. A. FitzGerald, T. Grevesse, C. Vidoudez, A. R. Pacheco, S. P. Sheehy, T. E. Park, S. Dauth, R. Mannix, N. Budnik, K. Shores, A. Cho, J. C. Nawroth, D. Segrè, B. Budnik, D. E. Ingber, and K. K. Parker. 2018. "A linked organ-on-chip model of the human neurovascular unit reveals the metabolic coupling of endothelial and neuronal cells." *Nat Biotechnol* 36 (9): 865-874. https://doi.org/10.1038/nbt.4226.

Maroof, A. M., S. Keros, J. A. Tyson, S. W. Ying, Y. M. Ganat, F. T. Merkle, B. Liu, A. Goulburn, E. G. Stanley, A. G. Elefanty, H. R. Widmer, K. Eggan, P. A. Goldstein, S. A. Anderson, and L. Studer. 2013. "Directed differentiation and functional maturation of cortical interneurons from human embryonic stem cells." *Cell Stem Cell* 12 (5): 559-72. https://doi.org/10.1016/j.stem.2013.04.008.

Marques, C. P., P. Kapil, D. R. Hinton, C. Hindinger, S. L. Nutt, R. M. Ransohoff, T. W. Phares, S. A. Stohlman, and C. C. Bergmann. 2011. "CXCR3-dependent plasma blast migration to the central nervous system during viral encephalomyelitis." *J Virol* 85 (13): 6136-47. https://doi.org/10.1128/jvi.00202-11.

Martinon, F., K. Burns, and J. Tschopp. 2002. "The inflammasome: a molecular platform triggering activation of inflammatory caspases and processing of proIL-beta." *Mol Cell* 10 (2): 417-26. https://doi.org/10.1016/s1097-2765(02)00599-3.

Matsumoto, Y., N. Hara, R. Tanaka, and M. Fujiwara. 1986. "Immunohistochemical analysis of the rat central nervous system during experimental allergic encephalomyelitis, with special reference to Ia-positive cells with dendritic morphology." *J Immunol* 136 (10): 3668-76.

Matzinger, P. 2002. "The danger model: a renewed sense of self." *Science* 296 (5566): 301-5. https://doi.org/10.1126/science.1071059.

Mayshar, Y., U. Ben-David, N. Lavon, J. C. Biancotti, B. Yakir, A. T. Clark, K. Plath, W. E. Lowry, and N. Benvenisty. 2010. "Identification and classification of chromosomal aberrations in human induced pluripotent stem cells." *Cell Stem Cell* 7 (4): 521-31. https://doi.org/10.1016/j.stem.2010.07.017.

McCarty, D. J., S. Manzi, T. A. Medsger, Jr., R. Ramsey-Goldman, R. E. LaPorte, and C. K. Kwoh. 1995. "Incidence of systemic lupus erythematosus. Race and gender differences." *Arthritis Rheum* 38 (9): 1260-70. https://doi.org/10.1002/art.1780380914.

McCullough, K. C., C. J. Smale, W. C. Carpenter, J. R. Crowther, E. Brocchi, and F. De Simone. 1987. "Conformational alteration in foot-and-mouth disease virus virion capsid structure after complexing with monospecific antibody." *Immunology* 60 (1): 75-82.

McDonough, A., R. V. Lee, S. Noor, C. Lee, T. Le, M. Iorga, J. L. H. Phillips, S. Murphy, T. Möller, and J. R. Weinstein. 2017. "Ischemia/Reperfusion Induces Interferon-Stimulated Gene Expression in Microglia." *J Neurosci* 37 (34): 8292-8308. https://doi.org/10.1523/jneurosci.0725-17.2017.

McEwan, W. A., J. C. Tam, R. E. Watkinson, S. R. Bidgood, D. L. Mallery, and L. C. James. 2013. "Intracellular antibody-bound pathogens stimulate immune signaling via the Fc receptor TRIM21." *Nat Immunol* 14 (4): 327-36. https://doi.org/10.1038/ni.2548.

McIntosh, B. M., C. B. Worth, and R. H. Kokernot. 1961. "Isolation of Semliki Forest virus from Aedes (Aedimorphus) argenteopunctatus (Theobald) collected in Portuguese East Africa." *Trans R Soc Trop Med Hyg* 55: 192-8. https://doi.org/10.1016/0035-9203(61)90025-6.

McLean, B. N., R. W. Luxton, and E. J. Thompson. 1990. "A study of immunoglobulin G in the cerebrospinal fluid of 1007 patients with suspected neurological disease using isoelectric focusing and the Log IgG-Index. A comparison and diagnostic applications." *Brain* 113 (Pt 5): 1269-89. https://doi.org/10.1093/brain/113.5.1269.

McManus, C., J. W. Berman, F. M. Brett, H. Staunton, M. Farrell, and C. F. Brosnan. 1998. "MCP-1, MCP-2 and MCP-3 expression in multiple sclerosis

lesions: an immunohistochemical and in situ hybridization study." *J Neuroimmunol* 86 (1): 20-9. https://doi.org/10.1016/s0165-5728(98)00002-2.

Medawar, P. B. 1948. "Immunity to homologous grafted skin; the fate of skin homografts transplanted to the brain, to subcutaneous tissue, and to the anterior chamber of the eye." *Br J Exp Pathol* 29 (1): 58-69.

Medgyesi, G. A., G. Fóris, G. Füst, and H. Bazin. 1984. "Regulation of Fc mu receptor-mediated functions of resident and provoked peritoneal macrophages." *Immunobiology* 167 (4): 293-300. https://doi.org/10.1016/s0171-2985(84)80001-7.

Medzhitov, R., P. Preston-Hurlburt, and C. A. Janeway, Jr. 1997. "A human homologue of the Drosophila Toll protein signals activation of adaptive immunity." *Nature* 388 (6640): 394-7. https://doi.org/10.1038/41131.

Mehla, R., S. Bivalkar-Mehla, M. Nagarkatti, and A. Chauhan. 2012. "Programming of neurotoxic cofactor CXCL-10 in HIV-1-associated dementia: abrogation of CXCL-10-induced neuro-glial toxicity in vitro by PKC activator." *J Neuroinflammation* 9: 239. https://doi.org/10.1186/1742-2094-9-239.

Melcher, U., and J. W. Uhr. 1976. "Cell surface immunoglobulin. XVI. Polypeptide chain structure of mouse IgM and IgD-like molecule." *J Immunol* 116 (2): 409-15.

Mendes-Jorge, L., D. Ramos, M. Luppo, C. Llombart, G. Alexandre-Pires, V. Nacher, V. Melgarejo, M. Correia, M. Navarro, A. Carretero, S. Tafuro, A. Rodriguez-Baeza, J. A. Esperança-Pina, F. Bosch, and J. Ruberte. 2009. "Scavenger function of resident autofluorescent perivascular macrophages and their contribution to the maintenance of the blood-retinal barrier." *Invest Ophthalmol Vis Sci* 50 (12): 5997-6005. https://doi.org/10.1167/iovs.09-3515.

Menezes, M. J., F. K. McClenahan, C. V. Leiton, A. Aranmolate, X. Shan, and H. Colognato. 2014. "The extracellular matrix protein laminin α2 regulates the maturation and function of the blood-brain barrier." *J Neurosci* 34 (46): 15260-80. https://doi.org/10.1523/jneurosci.3678-13.2014.

Mercolino, T. J., L. W. Arnold, and G. Haughton. 1986. "Phosphatidyl choline is recognized by a series of Ly-1+ murine B cell lymphomas specific for erythrocyte membranes." *J Exp Med* 163 (1): 155-65. https://doi.org/10.1084/jem.163.1.155.

Metcalf, T. U., V. K. Baxter, V. Nilaratanakul, and D. E. Griffin. 2013. "Recruitment and retention of B cells in the central nervous system in response to alphavirus encephalomyelitis." *J Virol* 87 (5): 2420-9. https://doi.org/10.1128/jvi.01769-12.

Michlmayr, D., C. S. McKimmie, M. Pingen, B. Haxton, K. Mansfield, N. Johnson, A. R. Fooks, and G. J. Graham. 2014. "Defining the chemokine basis for leukocyte recruitment during viral encephalitis." *J Virol* 88 (17): 9553-67. https://doi.org/10.1128/jvi.03421-13.

Mielke, J. G., T. Comas, J. Woulfe, R. Monette, B. Chakravarthy, and G. A. Mealing. 2005. "Cytoskeletal, synaptic, and nuclear protein changes associated with rat interface organotypic hippocampal slice culture development." *Brain Res Dev Brain Res* 160 (2): 275-86. https://doi.org/10.1016/j.devbrainres.2005.09.009.

Migliaccio, A. R., and G. Migliaccio. 1988. "Human embryonic hemopoiesis: control mechanisms underlying progenitor differentiation in vitro." *Dev Biol* 125 (1): 127-34. https://doi.org/10.1016/0012-1606(88)90065-6.

Mildner, A., M. Djukic, D. Garbe, A. Wellmer, W. A. Kuziel, M. Mack, R. Nau, and M. Prinz. 2008. "Ly-6G+CCR2- myeloid cells rather than Ly-6ChighCCR2+ monocytes are required for the control of bacterial infection in the central nervous system." *J Immunol* 181 (4): 2713-22. https://doi.org/10.4049/jimmunol.181.4.2713.

Millefiorini, E., C. Gasperini, C. Pozzilli, F. D'Andrea, S. Bastianello, M. Trojano, S. Morino, V. B. Morra, A. Bozzao, A. Calo, M. L. Bernini, D. Gambi, and M. Prencipe. 1997. "Randomized placebo-controlled trial of mitoxantrone in relapsing-remitting multiple sclerosis: 24-month clinical and MRI outcome." *J Neurol* 244 (3): 153-9. https://doi.org/10.1007/s004150050066.

Miller, D. H., D. T. Chard, and O. Ciccarelli. 2012. "Clinically isolated syndromes." *Lancet Neurol* 11 (2): 157-69. https://doi.org/10.1016/s1474-4422(11)70274-5.

Miller, D. H., B. G. Weinshenker, M. Filippi, B. L. Banwell, J. A. Cohen, M. S. Freedman, S. L. Galetta, M. Hutchinson, R. T. Johnson, L. Kappos, J. Kira, F. D. Lublin, H. F. McFarland, X. Montalban, H. Panitch, J. R. Richert, S. C. Reingold, and C. H. Polman. 2008. "Differential diagnosis of suspected multiple sclerosis: a consensus approach." *Mult Scler* 14 (9): 1157-74. https://doi.org/10.1177/1352458508096878.

Miller, J. D., Y. M. Ganat, S. Kishinevsky, R. L. Bowman, B. Liu, E. Y. Tu, P. K. Mandal, E. Vera, J. W. Shim, S. Kriks, T. Taldone, N. Fusaki, M. J. Tomishima, D. Krainc, T. A. Milner, D. J. Rossi, and L. Studer. 2013. "Human iPSC-based modeling of late-onset disease via progerin-induced aging." *Cell Stem Cell* 13 (6): 691-705. https://doi.org/10.1016/j.stem.2013.11.006.

Mills, E. A., and Y. Mao-Draayer. 2018. "Understanding Progressive Multifocal Leukoencephalopathy Risk in Multiple Sclerosis Patients Treated with Immunomodulatory Therapies: A Bird's Eye View." *Front Immunol* 9: 138. https://doi.org/10.3389/fimmu.2018.00138.

Mirones, I., I. de Prada, A. M. Gómez, A. Luque, R. Martín, MÁ Pérez-Jiménez, L. Madero, J. García-Castro, and M. Ramírez. 2013. "A role for the CXCR3/CXCL10 axis in Rasmussen encephalitis." *Pediatr Neurol* 49 (6): 451-457.e1. https://doi.org/10.1016/j.pediatrneurol.2013.07.019.

Miyashita, M., H. Oshiumi, M. Matsumoto, and T. Seya. 2011. "DDX60, a DEXD/H box helicase, is a novel antiviral factor promoting RIG-I-like receptor-mediated signaling." *Mol Cell Biol* 31 (18): 3802-19. https://doi.org/10.1128/mcb.01368-10.

Miyawaki, T., T. Uehara, R. Nibu, T. Tsuji, A. Yachie, S. Yonehara, and N. Taniguchi. 1992. "Differential expression of apoptosis-related Fas antigen on lymphocyte subpopulations in human peripheral blood." *J Immunol* 149 (11): 3753-8.

Miyoshi, K., K. Obata, T. Kondo, H. Okamura, and K. Noguchi. 2008. "Interleukin-18-mediated microglia/astrocyte interaction in the spinal cord enhances neuropathic pain processing after nerve injury." *J Neurosci* 28 (48): 12775-87. https://doi.org/10.1523/jneurosci.3512-08.2008.

Mizee, M. R., P. G. Nijland, S. M. van der Pol, J. A. Drexhage, B. van Het Hof, R. Mebius, P. van der Valk, J. van Horssen, A. Reijerkerk, and H. E. de Vries. 2014. "Astrocyte-derived retinoic acid: a novel regulator of blood-brain barrier function in multiple sclerosis." *Acta Neuropathol* 128 (5): 691-703. https://doi.org/10.1007/s00401-014-1335-6.

Mongini, P. K., W. E. Paul, and E. S. Metcalf. 1982. "T cell regulation of immunoglobulin class expression in the antibody response to

trinitrophenyl-ficoll. Evidence for T cell enhancement of the immunoglobulin class switch." *J Exp Med* 155 (3): 884-902. https://doi.org/10.1084/jem.155.3.884.

Montalban, X., S. L. Hauser, L. Kappos, D. L. Arnold, A. Bar-Or, G. Comi, J. de Seze, G. Giovannoni, H. P. Hartung, B. Hemmer, F. Lublin, K. W. Rammohan, K. Selmaj, A. Traboulsee, A. Sauter, D. Masterman, P. Fontoura, S. Belachew, H. Garren, N. Mairon, P. Chin, and J. S. Wolinsky. 2017. "Ocrelizumab versus Placebo in Primary Progressive Multiple Sclerosis." *N Engl J Med* 376 (3): 209-220. https://doi.org/10.1056/NEJMoa1606468.

Morikawa, Y., K. Tohya, H. Ishida, N. Matsuura, and K. Kakudo. 1995. "Different migration patterns of antigen-presenting cells correlate with Th1/Th2-type responses in mice." *Immunology* 85 (4): 575-81.

Moriyama, M., M. Nagai, Y. Maruzuru, T. Koshiba, Y. Kawaguchi, and T. Ichinohe. 2020. "Influenza Virus-Induced Oxidized DNA Activates Inflammasomes." *iScience* 23 (7): 101270. https://doi.org/10.1016/j.isci.2020.101270.

Mosmann, T. R., and R. L. Coffman. 1989. "TH1 and TH2 cells: different patterns of lymphokine secretion lead to different functional properties." *Annu Rev Immunol* 7: 145-73. https://doi.org/10.1146/annurev.iy.07.040189.001045.

Mouthon, L., A. Nobrega, N. Nicolas, S. V. Kaveri, C. Barreau, A. Coutinho, and M. D. Kazatchkine. 1995. "Invariance and restriction toward a limited set of self-antigens characterize neonatal IgM antibody repertoires and prevail in autoreactive repertoires of healthy adults." *Proc Natl Acad Sci U S A* 92 (9): 3839-43. https://doi.org/10.1073/pnas.92.9.3839.

Muehlinghaus, G., L. Cigliano, S. Huehn, A. Peddinghaus, H. Leyendeckers, A. E. Hauser, F. Hiepe, A. Radbruch, S. Arce, and R. A. Manz. 2005. "Regulation of CXCR3 and CXCR4 expression during terminal differentiation of memory B cells into plasma cells." *Blood* 105 (10): 3965-71. https://doi.org/10.1182/blood-2004-08-2992.

Mueller, P. 1958. "Prolonged action potentials from single nodes of Ranvier." *J Gen Physiol* 42 (1): 137-62. https://doi.org/10.1085/jgp.42.1.137.

Muffat, J., Y. Li, B. Yuan, M. Mitalipova, A. Omer, S. Corcoran, G. Bakiasi, L. H. Tsai, P. Aubourg, R. M. Ransohoff, and R. Jaenisch. 2016. "Efficient derivation of microglia-like cells from human pluripotent stem cells." *Nat Med* 22 (11): 1358-1367. https://doi.org/10.1038/nm.4189.

Munoz, L. S., M. A. Garcia, E. Gordon-Lipkin, B. Parra, and C. A. Pardo. 2018. "Emerging Viral Infections and Their Impact on the Global Burden of Neurological Disease." *Semin Neurol* 38 (2): 163-175. https://doi.org/10.1055/s-0038-1647247.

Möller, T., C. Nolte, R. Burger, A. Verkhratsky, and H. Kettenmann. 1997. "Mechanisms of C5a and C3a complement fragment-induced [Ca2+]i signaling in mouse microglia." *J Neurosci* 17 (2): 615-24. https://doi.org/10.1523/jneurosci.17-02-00615.1997.

Nagyoszi, P., I. Wilhelm, A. E. Farkas, C. Fazakas, N. T. Dung, J. Haskó, and I. A. Krizbai. 2010. "Expression and regulation of toll-like receptors in cerebral endothelial cells." *Neurochem Int* 57 (5): 556-64. https://doi.org/10.1016/j.neuint.2010.07.002.

Nakamura, M., S. E. Burastero, A. L. Notkins, and P. Casal. 1988. "Human monoclonal rheumatoid factor-like antibodies from CD5 (Leu-1)+ B cells are polyreactive." *J Immunol* 140 (12): 4180-6.

Nautiyal, K. M., C. A. Dailey, J. L. Jahn, E. Rodriquez, N. H. Son, J. V. Sweedler, and R. Silver. 2012. "Serotonin of mast cell origin contributes to

hippocampal function." *Eur J Neurosci* 36 (3): 2347-59. https://doi.org/10.1111/j.1460-9568.2012.08138.x.

Neuwelt, E. A., J. Minna, E. Frenkel, P. A. Barnett, and C. I. McCormick. 1986. "Osmotic blood-brain barrier opening to IgM monoclonal antibody in the rat." *Am J Physiol* 250 (5 Pt 2): R875-83. https://doi.org/10.1152/ajpregu.1986.250.5.R875.

Nguyen, T. T. T., B. A. Graf, T. D. Randall, and N. Baumgarth. 2017. "sIgM-FcμR Interactions Regulate Early B Cell Activation and Plasma Cell Development after Influenza Virus Infection." *J Immunol* 199 (5): 1635-1646. https://doi.org/10.4049/jimmunol.1700560.

Nicholas, C. R., J. Chen, Y. Tang, D. G. Southwell, N. Chalmers, D. Vogt, C. M. Arnold, Y. J. Chen, E. G. Stanley, A. G. Elefanty, Y. Sasai, A. Alvarez-Buylla, J. L. Rubenstein, and A. R. Kriegstein. 2013. "Functional maturation of hPSC-derived forebrain interneurons requires an extended timeline and mimics human neural development." *Cell Stem Cell* 12 (5): 573-86. https://doi.org/10.1016/j.stem.2013.04.005.

Nikolakopoulou, P., R. Rauti, D. Voulgaris, I. Shlomy, B. M. Maoz, and A. Herland. 2020. "Recent progress in translational engineered in vitro models of the central nervous system." *Brain* 143 (11): 3181-3213. https://doi.org/10.1093/brain/awaa268.

Nilaratanakul, V., J. Chen, O. Tran, V. K. Baxter, E. M. Troisi, J. X. Yeh, and D. E. Griffin. 2018. "Germ Line IgM Is Sufficient, but Not Required, for Antibody-Mediated Alphavirus Clearance from the Central Nervous System." *J Virol* 92 (7). https://doi.org/10.1128/jvi.02081-17.

Nilsson, K., and J. Pontén. 1975. "Classification and biological nature of established human hematopoietic cell lines." *Int J Cancer* 15 (2): 321-41. https://doi.org/10.1002/ijc.2910150217.

Nimmerjahn, A., F. Kirchhoff, and F. Helmchen. 2005. "Resting microglial cells are highly dynamic surveillants of brain parenchyma in vivo." *Science* 308 (5726): 1314-8. https://doi.org/10.1126/science.1110647.

Ning, S., J. S. Pagano, and G. N. Barber. 2011. "IRF7: activation, regulation, modification and function." *Genes Immun* 12 (6): 399-414. https://doi.org/10.1038/gene.2011.21.

Noelle, R. J., M. Roy, D. M. Shepherd, I. Stamenkovic, J. A. Ledbetter, and A. Aruffo. 1992. "A 39-kDa protein on activated helper T cells binds CD40 and transduces the signal for cognate activation of B cells." *Proc Natl Acad Sci U S A* 89 (14): 6550-4. https://doi.org/10.1073/pnas.89.14.6550.

Nonkwelo, C., I. K. Ruf, and J. Sample. 1997. "Interferon-independent and -induced regulation of Epstein-Barr virus EBNA-1 gene transcription in Burkitt lymphoma." *J Virol* 71 (9): 6887-97. https://doi.org/10.1128/jvi.71.9.6887-6897.1997.

Nossal, G. J., and O. Makela. 1962. "Autoradiographic studies on the immune response.I. The kinetics of plasma cell proliferation." *J Exp Med* 115 (1): 209-30. https://doi.org/10.1084/jem.115.1.209.

Nussbaum, J. L., A. Espinosa de los Monteros, F. M. Pari, J. Doerr-Schott, G. Roussel, and N. M. Neskovic. 1988. "A morphological and biochemical study of the myelin-like membrane structures formed in cultures of pure oligodendrocytes." *Int J Dev Neurosci* 6 (4): 395-408. https://doi.org/10.1016/0736-5748(88)90022-6.

Nussenzweig, M. C., R. M. Steinman, B. Gutchinov, and Z. A. Cohn. 1980. "Dendritic cells are accessory cells for the development of anti-trinitrophenyl cytotoxic T lymphocytes." *J Exp Med* 152 (4): 1070-84. https://doi.org/10.1084/jem.152.4.1070.

Nyúl-Tóth, Á, M. Kozma, P. Nagyőszi, K. Nagy, C. Fazakas, J. Haskó, K. Molnár, A. E. Farkas, A. G. Végh, G. Váró, P. Galajda, I. Wilhelm, and I. A. Krizbai. 2017. "Expression of pattern recognition receptors and activation of the non-canonical inflammasome pathway in brain pericytes." *Brain Behav Immun* 64: 220-231. https://doi.org/10.1016/j.bbi.2017.04.010.

O'Hara, B. A., and W. J. Atwood. 2008. "Interferon beta1-a and selective anti-5HT(2a) receptor antagonists inhibit infection of human glial cells by JC virus." *Virus Res* 132 (1-2): 97-103. https://doi.org/10.1016/j.virusres.2007.11.002.

Obermeier, B., R. Mentele, J. Malotka, J. Kellermann, T. Kümpfel, H. Wekerle, F. Lottspeich, R. Hohlfeld, and K. Dornmair. 2008. "Matching of oligoclonal immunoglobulin transcriptomes and proteomes of cerebrospinal fluid in multiple sclerosis." *Nat Med* 14 (6): 688-93. https://doi.org/10.1038/nm1714.

Odawara, A., Y. Saitoh, A. H. Alhebshi, M. Gotoh, and I. Suzuki. 2014. "Long-term electrophysiological activity and pharmacological response of a human induced pluripotent stem cell-derived neuron and astrocyte co-culture." *Biochem Biophys Res Commun* 443 (4): 1176-81. https://doi.org/10.1016/j.bbrc.2013.12.142.

Oldstone, M. B., P. Blount, P. J. Southern, and P. W. Lampert. 1986. "Cytoimmunotherapy for persistent virus infection reveals a unique clearance pattern from the central nervous system." *Nature* 321 (6067): 239-43. https://doi.org/10.1038/321239a0.

Omari, K. M., G. R. John, S. C. Sealfon, and C. S. Raine. 2005. "CXC chemokine receptors on human oligodendrocytes: implications for multiple sclerosis." *Brain* 128 (Pt 5): 1003-15. https://doi.org/10.1093/brain/awh479.

Oppenheim, J. J., C. O. Zachariae, N. Mukaida, and K. Matsushima. 1991. "Properties of the novel proinflammatory supergene "intercrine" cytokine family." *Annu Rev Immunol* 9: 617-48. https://doi.org/10.1146/annurev.iy.09.040191.003153.

Orchansky, P. L., and H. S. Teh. 1994. "Activation-induced cell death in proliferating T cells is associated with altered tyrosine phosphorylation of TCR/CD3 subunits." *J Immunol* 153 (2): 615-22.

Ouchida, R., H. Mori, K. Hase, H. Takatsu, T. Kurosaki, T. Tokuhisa, H. Ohno, and J. Y. Wang. 2012. "Critical role of the IgM Fc receptor in IgM homeostasis, B-cell survival, and humoral immune responses." *Proc Natl Acad Sci U S A* 109 (40): E2699-706. https://doi.org/10.1073/pnas.1210706109.

Panayiotou, C., R. Lindqvist, C. Kurhade, K. Vonderstein, J. Pasto, K. Edlund, A. S. Upadhyay, and A. K. Överby. 2018. "Viperin Restricts Zika Virus and Tick-Borne Encephalitis Virus Replication by Targeting NS3 for Proteasomal Degradation." *J Virol* 92 (7). https://doi.org/10.1128/jvi.02054-17.

Paolicelli, R. C., G. Bolasco, F. Pagani, L. Maggi, M. Scianni, P. Panzanelli, M. Giustetto, T. A. Ferreira, E. Guiducci, L. Dumas, D. Ragozzino, and C. T. Gross. 2011. "Synaptic pruning by microglia is necessary for normal brain development." *Science* 333 (6048): 1456-8. https://doi.org/10.1126/science.1202529.

Park, J. S., F. Gamboni-Robertson, Q. He, D. Svetkauskaite, J. Y. Kim, D. Strassheim, J. W. Sohn, S. Yamada, I. Maruyama, A. Banerjee, A. Ishizaka, and E. Abraham. 2006. "High mobility group box 1 protein interacts with multiple Toll-like receptors." *Am J Physiol Cell Physiol* 290 (3): C917-24. https://doi.org/10.1152/ajpcell.00401.2005.

Park, J. S., T. I. Kam, S. Lee, H. Park, Y. Oh, S. H. Kwon, J. J. Song, D. Kim, H. Kim, A. Jhaldiyal, D. H. Na, K. C. Lee, E. J. Park, M. G. Pomper, O. Pletnikova, J. C. Troncoso, H. S. Ko, V. L. Dawson, and T. M. Dawson. 2021. "Blocking microglial activation of reactive astrocytes is neuroprotective in models of Alzheimer's disease." *Acta Neuropathol Commun* 9 (1): 78. https://doi.org/10.1186/s40478-021-01180-z.

Park, J., I. Wetzel, I. Marriott, D. Dréau, C. D'Avanzo, D. Y. Kim, R. E. Tanzi, and H. Cho. 2018. "A 3D human triculture system modeling neurodegeneration and neuroinflammation in Alzheimer's disease." *Nat Neurosci* 21 (7): 941-951. https://doi.org/10.1038/s41593-018-0175-4.

Patel, A., J. Sul, M. L. Gordon, J. Steinklein, S. Sanguinetti, B. Pramanik, D. Purohit, V. Haroutunian, A. Williamson, I. Koralnik, and A. Harel. 2021. "Progressive Multifocal Leukoencephalopathy in a Patient With Progressive Multiple Sclerosis Treated With Ocrelizumab Monotherapy." *JAMA Neurol* 78 (6): 736-740. https://doi.org/10.1001/jamaneurol.2021.0627.

Peachey, N. S., M. Yu, J. Y. S. Han, S. Lengacher, P. J. Magistretti, L. Pellerin, and N. J. Philp. 2018. "Impact of MCT1 Haploinsufficiency on the Mouse Retina." *Adv Exp Med Biol* 1074: 375-380. https://doi.org/10.1007/978-3-319-75402-4_46.

Pekosz, A., C. Griot, N. Nathanson, and F. Gonzalez-Scarano. 1995. "Tropism of bunyaviruses: evidence for a G1 glycoprotein-mediated entry pathway common to the California serogroup." *Virology* 214 (2): 339-48. https://doi.org/10.1006/viro.1995.0043.

Penney, J., W. T. Ralvenius, and L. H. Tsai. 2020. "Modeling Alzheimer's disease with iPSC-derived brain cells." *Mol Psychiatry* 25 (1): 148-167. https://doi.org/10.1038/s41380-019-0468-3.

Perez-Polo, J. R., K. Werbach-Perez, and E. Tiffany-Castiglioni. 1979. "A human clonal cell line model of differentiating neurons." *Dev Biol* 71 (2): 341-55. https://doi.org/10.1016/0012-1606(79)90174-x.

Perlmann, P., and G. Holm. 1969. "Cytotoxic effects of lymphoid cells in vitro." *Adv Immunol* 11: 117-93. https://doi.org/10.1016/s0065-2776(08)60479-4.

Perry, S. W., J. P. Norman, A. Litzburg, D. Zhang, S. Dewhurst, and H. A. Gelbard. 2005. "HIV-1 transactivator of transcription protein induces mitochondrial hyperpolarization and synaptic stress leading to apoptosis." *J Immunol* 174 (7): 4333-44. https://doi.org/10.4049/jimmunol.174.7.4333.

Perry, V. H., and C. Holmes. 2014. "Microglial priming in neurodegenerative disease." *Nat Rev Neurol* 10 (4): 217-24. https://doi.org/10.1038/nrneurol.2014.38.

Pestka, S. 1997. "The interferon receptors." *Semin Oncol* 24 (3 Suppl 9): S9-18-s9-40.

Pestka, S., C. D. Krause, and M. R. Walter. 2004. "Interferons, interferon-like cytokines, and their receptors." *Immunol Rev* 202: 8-32. https://doi.org/10.1111/j.0105-2896.2004.00204.x.

Peterson, L. K., I. Tsunoda, T. Masaki, and R. S. Fujinami. 2007. "Polyreactive myelin oligodendrocyte glycoprotein antibodies: Implications for systemic autoimmunity in progressive experimental autoimmune encephalomyelitis." *J Neuroimmunol* 183 (1-2): 69-80. https://doi.org/10.1016/j.jneuroim.2006.11.024.

Pfefferkorn, C., C. Kallfass, S. Lienenklaus, J. Spanier, U. Kalinke, M. Rieder, K. K. Conzelmann, T. Michiels, and P. Staeheli. 2016. "Abortively Infected Astrocytes Appear To Represent the Main Source of Interferon Beta in the

Virus-Infected Brain." *J Virol* 90 (4): 2031-8. https://doi.org/10.1128/jvi.02979-15.

Phalipon, A., A. Cardona, J. P. Kraehenbuhl, L. Edelman, P. J. Sansonetti, and B. Corthésy. 2002. "Secretory component: a new role in secretory IgA-mediated immune exclusion in vivo." *Immunity* 17 (1): 107-15. https://doi.org/10.1016/s1074-7613(02)00341-2.

Phares, T. W., S. A. Stohlman, D. R. Hinton, and C. C. Bergmann. 2013. "Astrocyte-derived CXCL10 drives accumulation of antibody-secreting cells in the central nervous system during viral encephalomyelitis." *J Virol* 87 (6): 3382-92. https://doi.org/10.1128/jvi.03307-12.

Philips, T., and J. D. Rothstein. 2017. "Oligodendroglia: metabolic supporters of neurons." *J Clin Invest* 127 (9): 3271-3280. https://doi.org/10.1172/jci90610.

Phillips, D. M., and A. S. Bourinbaiar. 1992. "Mechanism of HIV spread from lymphocytes to epithelia." *Virology* 186 (1): 261-73. https://doi.org/10.1016/0042-6822(92)90080-9.

Pierrès, A., M. Lopez, C. Cerdan, J. Nunes, D. Olive, and C. Mawas. 1988. "Triggering CD 28 molecules synergize with CD 2 (T 11.1 and T 11.2)-mediated T cell activation." *Eur J Immunol* 18 (5): 685-90. https://doi.org/10.1002/eji.1830180505.

Pietropaolo, V., C. Prezioso, F. Bagnato, and G. Antonelli. 2018. "John Cunningham virus: an overview on biology and disease of the etiological agent of the progressive multifocal leukoencephalopathy." *New Microbiol* 41 (3): 179-186.

Pinteaux, E., J. C. Copin, M. Ledig, and G. Tholey. 1996. "Modulation of oxygen-radical-scavenging enzymes by oxidative stress in primary cultures of rat astroglial cells." *Dev Neurosci* 18 (5-6): 397-404. https://doi.org/10.1159/000111433.

Polliack, M. L., Y. Barak, and A. Achiron. 2001. "Late-onset multiple sclerosis." *J Am Geriatr Soc* 49 (2): 168-71. https://doi.org/10.1046/j.1532-5415.2001.49038.x.

Polman, C. H., P. W. O'Connor, E. Havrdova, M. Hutchinson, L. Kappos, D. H. Miller, J. T. Phillips, F. D. Lublin, G. Giovannoni, A. Wajgt, M. Toal, F. Lynn, M. A. Panzara, and A. W. Sandrock. 2006. "A randomized, placebo-controlled trial of natalizumab for relapsing multiple sclerosis." *N Engl J Med* 354 (9): 899-910. https://doi.org/10.1056/NEJMoa044397.

Polo, J. M., S. Liu, M. E. Figueroa, W. Kulalert, S. Eminli, K. Y. Tan, E. Apostolou, M. Stadtfeld, Y. Li, T. Shioda, S. Natesan, A. J. Wagers, A. Melnick, T. Evans, and K. Hochedlinger. 2010. "Cell type of origin influences the molecular and functional properties of mouse induced pluripotent stem cells." *Nat Biotechnol* 28 (8): 848-55. https://doi.org/10.1038/nbt.1667.

Porat, A., E. Giat, C. Kowal, M. He, M. Son, E. Latz, I. Ben-Zvi, Y. Al-Abed, and B. Diamond. 2018. "DNA-Mediated Interferon Signature Induction by SLE Serum Occurs in Monocytes Through Two Pathways: A Mechanism to Inhibit Both Pathways." *Front Immunol* 9: 2824. https://doi.org/10.3389/fimmu.2018.02824.

Post, T. W., C. R. Bozic, M. E. Rothenberg, A. D. Luster, N. Gerard, and C. Gerard. 1995. "Molecular characterization of two murine eosinophil beta chemokine receptors." *J Immunol* 155 (11): 5299-305.

Pouliot, P., I. Plante, M. A. Raquil, P. A. Tessier, and M. Olivier. 2008. "Myeloid-related proteins rapidly modulate macrophage nitric oxide production

during innate immune response." *J Immunol* 181 (5): 3595-601. https://doi.org/10.4049/jimmunol.181.5.3595.

Price, M. J., S. L. Hicks, J. E. Bradley, T. D. Randall, J. M. Boss, and C. D. Scharer. 2019. "IgM, IgG, and IgA Influenza-Specific Plasma Cells Express Divergent Transcriptomes." *J Immunol* 203 (8): 2121-2129. https://doi.org/10.4049/jimmunol.1900285.

Préhaud, C., F. Mégret, M. Lafage, and M. Lafon. 2005. "Virus infection switches TLR-3-positive human neurons to become strong producers of beta interferon." *J Virol* 79 (20): 12893-904. https://doi.org/10.1128/jvi.79.20.12893-12904.2005.

Pudifin, D. J., B. Harding, and I. C. MacLennan. 1971. "The differential effect of gamma irradiation on the sensitizing and effector stages of antibody dependent lymphocyte mediated cytotoxicity." *Immunology* 21 (5): 853-60.

Pulendran, B., K. Palucka, and J. Banchereau. 2001. "Sensing pathogens and tuning immune responses." *Science* 293 (5528): 253-6. https://doi.org/10.1126/science.1062060.

Purpura, D. P. 1957. "Experimental analysis of the inhibitory action of lysergic acid diethylamide on cortical dendritic activity." *Ann N Y Acad Sci* 66 (3): 515-36. https://doi.org/10.1111/j.1749-6632.1957.tb40747.x.

Putnam, T. J. 1934. "THE BIOLOGICAL SIGNIFICANCE OF THE LESIONS OF MULTIPLE SCLEROSIS." *Science* 80 (2074): 295-6. https://doi.org/10.1126/science.80.2074.295.

Påhlman, S., A. I. Ruusala, L. Abrahamsson, M. E. Mattsson, and T. Esscher. 1984. "Retinoic acid-induced differentiation of cultured human neuroblastoma cells: a comparison with phorbolester-induced differentiation." *Cell Differ* 14 (2): 135-44. https://doi.org/10.1016/0045-6039(84)90038-1.

Périer, O., and A. Grégoire. 1965. "Electron microscopic features of multiple sclerosis lesions." *Brain* 88 (5): 937-52. https://doi.org/10.1093/brain/88.5.937.

Qian, X., H. N. Nguyen, M. M. Song, C. Hadiono, S. C. Ogden, C. Hammack, B. Yao, G. R. Hamersky, F. Jacob, C. Zhong, K. J. Yoon, W. Jeang, L. Lin, Y. Li, J. Thakor, D. A. Berg, C. Zhang, E. Kang, M. Chickering, D. Nauen, C. Y. Ho, Z. Wen, K. M. Christian, P. Y. Shi, B. J. Maher, H. Wu, P. Jin, H. Tang, H. Song, and G. L. Ming. 2016. "Brain-Region-Specific Organoids Using Mini-bioreactors for Modeling ZIKV Exposure." *Cell* 165 (5): 1238-1254. https://doi.org/10.1016/j.cell.2016.04.032.

Qin, S., J. B. Rottman, P. Myers, N. Kassam, M. Weinblatt, M. Loetscher, A. E. Koch, B. Moser, and C. R. Mackay. 1998. "The chemokine receptors CXCR3 and CCR5 mark subsets of T cells associated with certain inflammatory reactions." *J Clin Invest* 101 (4): 746-54. https://doi.org/10.1172/jci1422.

Qin, Y., P. Duquette, Y. Zhang, P. Talbot, R. Poole, and J. Antel. 1998. "Clonal expansion and somatic hypermutation of V(H) genes of B cells from cerebrospinal fluid in multiple sclerosis." *J Clin Invest* 102 (5): 1045-50. https://doi.org/10.1172/jci3568.

Rae-Grant, A., G. S. Day, R. A. Marrie, A. Rabinstein, B. A. C. Cree, G. S. Gronseth, M. Haboubi, J. Halper, J. P. Hosey, D. E. Jones, R. Lisak, D. Pelletier, S. Potrebic, C. Sitcov, R. Sommers, J. Stachowiak, T. S. D. Getchius, S. A. Merillat, and T. Pringsheim. 2018. "Practice guideline recommendations summary: Disease-modifying therapies for adults with multiple sclerosis: Report of the Guideline Development, Dissemination, and Implementation Subcommittee of the American Academy of

Neurology." *Neurology* 90 (17): 777-788. https://doi.org/10.1212/wnl.0000000000005347.
Raicevic, G., M. Najar, H. Busser, E. Crompot, D. Bron, M. Toungouz, and L. Lagneaux. 2017. "Comparison and immunobiological characterization of retinoic acid inducible gene-I-like receptor expression in mesenchymal stromal cells." *Sci Rep* 7 (1): 2896. https://doi.org/10.1038/s41598-017-02850-6.
Raine, C.S. 1984. "Morphology of Myelin and Myelination." In *Myelin*, edited by P. Morell, 1 - 50. Boston, MA, USA: Springer US.
Rakotoarivelo, C., D. Petite, J. de Weille, S. Lumbroso, A. Privat, C. Sultan, and M. Mersel. 2007. "Mild surfection of neural cells, especially motoneurons, in primary culture and cell lines." *Exp Neurol* 204 (1): 118-30. https://doi.org/10.1016/j.expneurol.2006.09.027.
Ram, S., L. A. Lewis, and P. A. Rice. 2010. "Infections of people with complement deficiencies and patients who have undergone splenectomy." *Clin Microbiol Rev* 23 (4): 740-80. https://doi.org/10.1128/cmr.00048-09.
Ram, S., F. G. Mackinnon, S. Gulati, D. P. McQuillen, U. Vogel, M. Frosch, C. Elkins, H. K. Guttormsen, L. M. Wetzler, M. Oppermann, M. K. Pangburn, and P. A. Rice. 1999. "The contrasting mechanisms of serum resistance of Neisseria gonorrhoeae and group B Neisseria meningitidis." *Mol Immunol* 36 (13-14): 915-28. https://doi.org/10.1016/s0161-5890(99)00114-5.
Ramirez, F., R. C. Williams, Jr., W. L. Sibbitt, Jr., and R. P. Searles. 1986. "Immunoglobulin from systemic lupus erythematosus serum induces interferon release by normal mononuclear cells." *Arthritis Rheum* 29 (3): 326-36. https://doi.org/10.1002/art.1780290304.
Ranvier, L. 1871. "Contributions à l'histologie et à la physiologie des nerfs périphériques." Comptes Rendus de l'Académie des Sciences, 1871.
Reinert, L. S., K. Lopusna, H. Winther, C. Sun, M. K. Thomsen, R. Nandakumar, T. H. Mogensen, M. Meyer, C. Vaegter, J. R. Nyengaard, K. A. Fitzgerald, and S. R. Paludan. 2016. "Sensing of HSV-1 by the cGAS-STING pathway in microglia orchestrates antiviral defence in the CNS." *Nat Commun* 7: 13348. https://doi.org/10.1038/ncomms13348.
Ren, R., and V. R. Racaniello. 1992. "Poliovirus spreads from muscle to the central nervous system by neural pathways." *J Infect Dis* 166 (4): 747-52. https://doi.org/10.1093/infdis/166.4.747.
Renner, N. A., N. S. Ivey, R. K. Redmann, A. A. Lackner, and A. G. MacLean. 2011. "MCP-3/CCL7 production by astrocytes: implications for SIV neuroinvasion and AIDS encephalitis." *J Neurovirol* 17 (2): 146-52. https://doi.org/10.1007/s13365-010-0017-y.
Reymond, A., G. Meroni, A. Fantozzi, G. Merla, S. Cairo, L. Luzi, D. Riganelli, E. Zanaria, S. Messali, S. Cainarca, A. Guffanti, S. Minucci, P. G. Pelicci, and A. Ballabio. 2001. "The tripartite motif family identifies cell compartments." *Embo j* 20 (9): 2140-51. https://doi.org/10.1093/emboj/20.9.2140.
Reynaud, J. M., D. Y. Kim, S. Atasheva, A. Rasalouskaya, J. P. White, M. S. Diamond, S. C. Weaver, E. I. Frolova, and I. Frolov. 2015. "IFIT1 Differentially Interferes with Translation and Replication of Alphavirus Genomes and Promotes Induction of Type I Interferon." *PLoS Pathog* 11 (4): e1004863. https://doi.org/10.1371/journal.ppat.1004863.
Ricciarelli, R., C. D'Abramo, J. M. Zingg, L. Giliberto, W. Markesbery, A. Azzi, U. M. Marinari, M. A. Pronzato, and M. Tabaton. 2004. "CD36 overexpression in human brain correlates with beta-amyloid deposition but not with

Alzheimer's disease." *Free Radic Biol Med* 36 (8): 1018-24. https://doi.org/10.1016/j.freeradbiomed.2004.01.007.

Richter-Landsberg, C., and M. Heinrich. 1996. "OLN-93: a new permanent oligodendroglia cell line derived from primary rat brain glial cultures." *J Neurosci Res* 45 (2): 161-73. https://doi.org/10.1002/(sici)1097-4547(19960715)45:2<161::aid-jnr8>3.0.co;2-8.

Rickinson, A. B., D. J. Moss, L. E. Wallace, M. Rowe, I. S. Misko, M. A. Epstein, and J. H. Pope. 1981. "Long-term T-cell-mediated immunity to Epstein-Barr virus." *Cancer Res* 41 (11 Pt 1): 4216-21.

Ries, M., P. Schuster, S. Thomann, N. Donhauser, J. Vollmer, and B. Schmidt. 2013. "Identification of novel oligonucleotides from mitochondrial DNA that spontaneously induce plasmacytoid dendritic cell activation." *J Leukoc Biol* 94 (1): 123-35. https://doi.org/10.1189/jlb.0612278.

Rinaldo, C. R., Jr., and D. J. Torpey, 3rd. 1993. "Cell-mediated immunity and immunosuppression in herpes simplex virus infection." *Immunodeficiency* 5 (1): 33-90.

Risau, W., B. Engelhardt, and H. Wekerle. 1990. "Immune function of the blood-brain barrier: incomplete presentation of protein (auto-)antigens by rat brain microvascular endothelium in vitro." *J Cell Biol* 110 (5): 1757-66. https://doi.org/10.1083/jcb.110.5.1757.

Rodriguez, M., C. F. Lucchinetti, R. J. Clark, T. L. Yakash, H. Markowitz, and V. A. Lennon. 1988. "Immunoglobulins and complement in demyelination induced in mice by Theiler's virus." *J Immunol* 140 (3): 800-6.

Romero, I. A., M. C. Prevost, E. Perret, P. Adamson, J. Greenwood, P. O. Couraud, and S. Ozden. 2000. "Interactions between brain endothelial cells and human T-cell leukemia virus type 1-infected lymphocytes: mechanisms of viral entry into the central nervous system." *J Virol* 74 (13): 6021-30. https://doi.org/10.1128/jvi.74.13.6021-6030.2000.

Ronnblom, L., G. V. Alm, and M. L. Eloranta. 2009. "Type I interferon and lupus." *Curr Opin Rheumatol* 21 (5): 471-7. https://doi.org/10.1097/BOR.0b013e32832e089e.

Rose, C. E., Jr., J. A. Lannigan, P. Kim, J. J. Lee, S. M. Fu, and S. S. Sung. 2010. "Murine lung eosinophil activation and chemokine production in allergic airway inflammation." *Cell Mol Immunol* 7 (5): 361-74. https://doi.org/10.1038/cmi.2010.31.

Rosenbluth, J., R. Schiff, W. L. Liang, and W. Dou. 2003. "Antibody-mediated CNS demyelination II. Focal spinal cord lesions induced by implantation of an IgM antisulfatide-secreting hybridoma." *J Neurocytol* 32 (3): 265-76. https://doi.org/10.1023/B:NEUR.0000010085.91976.a6.

Rosenstiel, P., M. Fantini, K. Bräutigam, T. Kühbacher, G. H. Waetzig, D. Seegert, and S. Schreiber. 2003. "TNF-alpha and IFN-gamma regulate the expression of the NOD2 (CARD15) gene in human intestinal epithelial cells." *Gastroenterology* 124 (4): 1001-9. https://doi.org/10.1053/gast.2003.50157.

Rosevear, J. W., and E. L. Smith. 1961. "Glycopeptides. I. Isolation and properties of glycopeptides from a fraction of human gamma-globulin." *J Biol Chem* 236: 425-35.

Roth-Cross, J. K., S. J. Bender, and S. R. Weiss. 2008. "Murine coronavirus mouse hepatitis virus is recognized by MDA5 and induces type I interferon in brain macrophages/microglia." *J Virol* 82 (20): 9829-38. https://doi.org/10.1128/jvi.01199-08.

Rottman, J. B., A. J. Slavin, R. Silva, H. L. Weiner, C. G. Gerard, and W. W. Hancock. 2000. "Leukocyte recruitment during onset of experimental

allergic encephalomyelitis is CCR1 dependent." *Eur J Immunol* 30 (8): 2372-7. https://doi.org/10.1002/1521-4141(2000)30:8<2372::aid-immu2372>3.0.co;2-d.

Roulston, A., P. Beauparlant, N. Rice, and J. Hiscott. 1993. "Chronic human immunodeficiency virus type 1 infection stimulates distinct NF-kappa B/rel DNA binding activities in myelomonoblastic cells." *J Virol* 67 (9): 5235-46. https://doi.org/10.1128/jvi.67.9.5235-5246.1993.

Rowe, D. S., I. A. McGregor, S. J. Smith, P. Hall, and K. Williams. 1968. "Plasma immunoglobulin concentrations in a West African (Gambian) community and in a group of healthy British adults." *Clin Exp Immunol* 3 (1): 63-79.

Rozen, S., and H. Skaletsky. 2000. "Primer3 on the WWW for general users and for biologist programmers." *Methods Mol Biol* 132: 365-86. https://doi.org/10.1385/1-59259-192-2:365.

Rozenberg, F. 2013. "Acute viral encephalitis." *Handb Clin Neurol* 112: 1171-81. https://doi.org/10.1016/b978-0-444-52910-7.00038-6.

Rudick, R., C. Polman, D. Clifford, D. Miller, and L. Steinman. 2013. "Natalizumab: bench to bedside and beyond." *JAMA Neurol* 70 (2): 172-82. https://doi.org/10.1001/jamaneurol.2013.598.

Rusinova, I., S. Forster, S. Yu, A. Kannan, M. Masse, H. Cumming, R. Chapman, and P. J. Hertzog. 2013. "Interferome v2.0: an updated database of annotated interferon-regulated genes." *Nucleic Acids Res* 41 (Database issue): D1040-6. https://doi.org/10.1093/nar/gks1215.

Rutherford, M. N., G. E. Hannigan, and B. R. Williams. 1988. "Interferon-induced binding of nuclear factors to promoter elements of the 2-5A synthetase gene." *Embo j* 7 (3): 751-9.

Saab, A. S., I. D. Tzvetanova, and K. A. Nave. 2013. "The role of myelin and oligodendrocytes in axonal energy metabolism." *Curr Opin Neurobiol* 23 (6): 1065-72. https://doi.org/10.1016/j.conb.2013.09.008.

Sabbah, A., T. H. Chang, R. Harnack, V. Frohlich, K. Tominaga, P. H. Dube, Y. Xiang, and S. Bose. 2009. "Activation of innate immune antiviral responses by Nod2." *Nat Immunol* 10 (10): 1073-80. https://doi.org/10.1038/ni.1782.

Sad, S., R. Marcotte, and T. R. Mosmann. 1995. "Cytokine-induced differentiation of precursor mouse CD8+ T cells into cytotoxic CD8+ T cells secreting Th1 or Th2 cytokines." *Immunity* 2 (3): 271-9. https://doi.org/10.1016/1074-7613(95)90051-9.

Saito, M., H. Kitamura, and K. Sugiyama. 2001. "The specificity of monoclonal antibody A2B5 to c-series gangliosides." *J Neurochem* 78 (1): 64-74. https://doi.org/10.1046/j.1471-4159.2001.00365.x.

Salinas, S., C. Proukakis, A. Crosby, and T. T. Warner. 2008. "Hereditary spastic paraplegia: clinical features and pathogenetic mechanisms." *Lancet Neurol* 7 (12): 1127-38. https://doi.org/10.1016/s1474-4422(08)70258-8.

Sampogna, F., M. M. Chren, C. F. Melchi, P. Pasquini, S. Tabolli, and D. Abeni. 2006. "Age, gender, quality of life and psychological distress in patients hospitalized with psoriasis." *Br J Dermatol* 154 (2): 325-31. https://doi.org/10.1111/j.1365-2133.2005.06909.x.

Sapp, D. W., and H. H. Yeh. 1998. "Ethanol-GABAA receptor interactions: a comparison between cell lines and cerebellar Purkinje cells." *J Pharmacol Exp Ther* 284 (2): 768-76.

Saul, S., M. Ferguson, C. Cordonin, R. Fragkoudis, M. Ool, N. Tamberg, K. Sherwood, J. K. Fazakerley, and A. Merits. 2015. "Differences in Processing Determinants of Nonstructural Polyprotein and in the Sequence

of Nonstructural Protein 3 Affect Neurovirulence of Semliki Forest Virus." *J Virol* 89 (21): 11030-45. https://doi.org/10.1128/jvi.01186-15.

Sayah, S., A. M. Ischenko, A. Zhakhov, A. S. Bonnard, and M. Fontaine. 1999. "Expression of cytokines by human astrocytomas following stimulation by C3a and C5a anaphylatoxins: specific increase in interleukin-6 mRNA expression." *J Neurochem* 72 (6): 2426-36. https://doi.org/10.1046/j.1471-4159.1999.0722426.x.

Schaeffer, H. J., L. Beauchamp, P. de Miranda, G. B. Elion, D. J. Bauer, and P. Collins. 1978. "9-(2-hydroxyethoxymethyl) guanine activity against viruses of the herpes group." *Nature* 272 (5654): 583-5. https://doi.org/10.1038/272583a0.

Schafer, D. P., E. K. Lehrman, A. G. Kautzman, R. Koyama, A. R. Mardinly, R. Yamasaki, R. M. Ransohoff, M. E. Greenberg, B. A. Barres, and B. Stevens. 2012. "Microglia sculpt postnatal neural circuits in an activity and complement-dependent manner." *Neuron* 74 (4): 691-705. https://doi.org/10.1016/j.neuron.2012.03.026.

Schindelin, J., I. Arganda-Carreras, E. Frise, V. Kaynig, M. Longair, T. Pietzsch, S. Preibisch, C. Rueden, S. Saalfeld, B. Schmid, J. Y. Tinevez, D. J. White, V. Hartenstein, K. Eliceiri, P. Tomancak, and A. Cardona. 2012. "Fiji: an open-source platform for biological-image analysis." *Nat Methods* 9 (7): 676-82. https://doi.org/10.1038/nmeth.2019.

Schmitz, J., and A. Radbruch. 1992. "Distinct antigen presenting cell-derived signals induce TH cell proliferation and expression of effector cytokines." *Int Immunol* 4 (1): 43-51. https://doi.org/10.1093/intimm/4.1.43.

Schneider, C. A., W. S. Rasband, and K. W. Eliceiri. 2012. "NIH Image to ImageJ: 25 years of image analysis." *Nat Methods* 9 (7): 671-5. https://doi.org/10.1038/nmeth.2089.

Schoggins, J. W., and C. M. Rice. 2011. "Interferon-stimulated genes and their antiviral effector functions." *Curr Opin Virol* 1 (6): 519-25. https://doi.org/10.1016/j.coviro.2011.10.008.

Schreiner, B., E. Romanelli, P. Liberski, B. Ingold-Heppner, B. Sobottka-Brillout, T. Hartwig, V. Chandrasekar, H. Johannssen, H. U. Zeilhofer, A. Aguzzi, F. Heppner, M. Kerschensteiner, and B. Becher. 2015. "Astrocyte Depletion Impairs Redox Homeostasis and Triggers Neuronal Loss in the Adult CNS." *Cell Rep* 12 (9): 1377-84. https://doi.org/10.1016/j.celrep.2015.07.051.

Schultz, J., F. Milpetz, P. Bork, and C. P. Ponting. 1998. "SMART, a simple modular architecture research tool: identification of signaling domains." *Proc Natl Acad Sci U S A* 95 (11): 5857-64. https://doi.org/10.1073/pnas.95.11.5857.

Schultz, V., S. L. Cumberworth, Q. Gu, N. Johnson, C. L. Donald, G. A. McCanney, J. A. Barrie, A. Da Silva Filipe, C. Linington, H. J. Willison, J. M. Edgar, S. C. Barnett, and A. Kohl. 2021. "Zika Virus Infection Leads to Demyelination and Axonal Injury in Mature CNS Cultures." *Viruses* 13 (1). https://doi.org/10.3390/v13010091.

Scolding, N. J., B. P. Morgan, A. Houston, A. K. Campbell, C. Linington, and D. A. Compston. 1989. "Normal rat serum cytotoxicity against syngeneic oligodendrocytes. Complement activation and attack in the absence of anti-myelin antibodies." *J Neurol Sci* 89 (2-3): 289-300. https://doi.org/10.1016/0022-510x(89)90030-0.

Seamer, J. H., E. A. Boulter, and I. Zlotnik. 1971. "Delayed onset of encephalitis in mice passively immunised against Semliki Forest virus." *Br J Exp Pathol* 52 (4): 408-14.

Sehgal, P. B., D. C. Helfgott, U. Santhanam, S. B. Tatter, R. H. Clarick, J. Ghrayeb, and L. T. May. 1988. "Regulation of the acute phase and immune responses in viral disease. Enhanced expression of the beta 2-interferon/hepatocyte-stimulating factor/interleukin 6 gene in virus-infected human fibroblasts." *J Exp Med* 167 (6): 1951-6. https://doi.org/10.1084/jem.167.6.1951.

Semenoff, Tiia. 2014. "Sulfatide-specific antibody-mediated effects on the transcriptional profile of myelinating cultures." MSc(R), Institute of Infection, Immunity and Inflammation, University of Glasgow.

Serafini, B., B. Rosicarelli, R. Magliozzi, E. Stigliano, and F. Aloisi. 2004. "Detection of ectopic B-cell follicles with germinal centers in the meninges of patients with secondary progressive multiple sclerosis." *Brain Pathol* 14 (2): 164-74. https://doi.org/10.1111/j.1750-3639.2004.tb00049.x.

Serot, J. M., B. Foliguet, M. C. Béné, and G. C. Faure. 1997. "Ultrastructural and immunohistological evidence for dendritic-like cells within human choroid plexus epithelium." *Neuroreport* 8 (8): 1995-8. https://doi.org/10.1097/00001756-199705260-00039.

Shank, R. P., and G. L. Campbell. 1984. "Alpha-ketoglutarate and malate uptake and metabolism by synaptosomes: further evidence for an astrocyte-to-neuron metabolic shuttle." *J Neurochem* 42 (4): 1153-61. https://doi.org/10.1111/j.1471-4159.1984.tb12724.x.

Shank, R.P., and M.H. Aprison. 1979. "Biochemical aspects of the neurotransmitter function of glutamate." In *Glutamic. Acid: Advances in Biochemistry and Physiology*, edited by L.J. Jnr. Filer and et al., 139 - 150. New York: Raven Press.

Shi, X., J. T. van Mierlo, A. French, and R. M. Elliott. 2010. "Visualizing the replication cycle of bunyamwera orthobunyavirus expressing fluorescent protein-tagged Gc glycoprotein." *J Virol* 84 (17): 8460-9. https://doi.org/10.1128/jvi.00902-10.

Shibuya, A., N. Sakamoto, Y. Shimizu, K. Shibuya, M. Osawa, T. Hiroyama, H. J. Eyre, G. R. Sutherland, Y. Endo, T. Fujita, T. Miyabayashi, S. Sakano, T. Tsuji, E. Nakayama, J. H. Phillips, L. L. Lanier, and H. Nakauchi. 2000. "Fc alpha/mu receptor mediates endocytosis of IgM-coated microbes." *Nat Immunol* 1 (5): 441-6. https://doi.org/10.1038/80886.

Shinobu, N., T. Iwamura, M. Yoneyama, K. Yamaguchi, W. Suhara, Y. Fukuhara, F. Amano, and T. Fujita. 2002. "Involvement of TIRAP/MAL in signaling for the activation of interferon regulatory factor 3 by lipopolysaccharide." *FEBS Lett* 517 (1-3): 251-6. https://doi.org/10.1016/s0014-5793(02)02636-4.

Silver, N. C., P. S. Tofts, M. R. Symms, G. J. Barker, A. J. Thompson, and D. H. Miller. 2001. "Quantitative contrast-enhanced magnetic resonance imaging to evaluate blood-brain barrier integrity in multiple sclerosis: a preliminary study." *Mult Scler* 7 (2): 75-82. https://doi.org/10.1177/135245850100700201.

Sirén, J., J. Pirhonen, I. Julkunen, and S. Matikainen. 2005. "IFN-alpha regulates TLR-dependent gene expression of IFN-alpha, IFN-beta, IL-28, and IL-29." *J Immunol* 174 (4): 1932-7. https://doi.org/10.4049/jimmunol.174.4.1932.

Sivori, S., M. Falco, M. Della Chiesa, S. Carlomagno, M. Vitale, L. Moretta, and A. Moretta. 2004. "CpG and double-stranded RNA trigger human NK cells by Toll-like receptors: induction of cytokine release and cytotoxicity

against tumors and dendritic cells." *Proc Natl Acad Sci U S A* 101 (27): 10116-21. https://doi.org/10.1073/pnas.0403744101.

Sliwinski, A. J., and N. J. Zvaifler. 1972. "Decreased synthesis of the third component of complement (C3) in hypocomplementemic systemic lupus erythematosus." *Clin Exp Immunol* 11 (1): 21-9.

Smith, J. P., M. Morris-Downes, F. R. Brennan, G. J. Wallace, and S. Amor. 2000. "A role for alpha4-integrin in the pathology following Semliki Forest virus infection." *J Neuroimmunol* 106 (1-2): 60-8. https://doi.org/10.1016/s0165-5728(99)00235-0.

Soares, C., K. F. Lee, W. Nassrallah, and J. C. Béïque. 2013. "Differential subcellular targeting of glutamate receptor subtypes during homeostatic synaptic plasticity." *J Neurosci* 33 (33): 13547-59. https://doi.org/10.1523/jneurosci.1873-13.2013.

Soldner, F., D. Hockemeyer, C. Beard, Q. Gao, G. W. Bell, E. G. Cook, G. Hargus, A. Blak, O. Cooper, M. Mitalipova, O. Isacson, and R. Jaenisch. 2009. "Parkinson's disease patient-derived induced pluripotent stem cells free of viral reprogramming factors." *Cell* 136 (5): 964-77. https://doi.org/10.1016/j.cell.2009.02.013.

Sommer, I., and M. Schachner. 1981. "Monoclonal antibodies (O1 to O4) to oligodendrocyte cell surfaces: an immunocytological study in the central nervous system." *Dev Biol* 83 (2): 311-27. https://doi.org/10.1016/0012-1606(81)90477-2.

Sommereyns, C., S. Paul, P. Staeheli, and T. Michiels. 2008. "IFN-lambda (IFN-lambda) is expressed in a tissue-dependent fashion and primarily acts on epithelial cells in vivo." *PLoS Pathog* 4 (3): e1000017. https://doi.org/10.1371/journal.ppat.1000017.

Sooryanarain, H., G. N. Sapkal, and M. M. Gore. 2012. "Pathogenic and vaccine strains of Japanese encephalitis virus elicit different levels of human macrophage effector functions." *Arch Virol* 157 (10): 1905-18. https://doi.org/10.1007/s00705-012-1386-8.

Sousa, A. D., and M. A. Bhat. 2007. "Cytoskeletal transition at the paranodes: the Achilles' heel of myelinated axons." *Neuron Glia Biol* 3 (2): 169-78. https://doi.org/10.1017/s1740925x07000415.

Srivastava, R., M. Aslam, S. R. Kalluri, L. Schirmer, D. Buck, B. Tackenberg, V. Rothhammer, A. Chan, R. Gold, A. Berthele, J. L. Bennett, T. Korn, and B. Hemmer. 2012. "Potassium channel KIR4.1 as an immune target in multiple sclerosis." *N Engl J Med* 367 (2): 115-23. https://doi.org/10.1056/NEJMoa1110740.

Stacey, G. N., B. J. Bolton, and A. Doyle. 1991. "The quality control of cell banks using DNA fingerprinting." *Exs* 58: 361-70. https://doi.org/10.1007/978-3-0348-7312-3_27.

Stacey, N. H., C. J. Bishop, J. W. Halliday, W. J. Halliday, W. G. Cooksley, L. W. Powell, and J. F. Kerr. 1985. "Apoptosis as the mode of cell death in antibody-dependent lymphocytotoxicity." *J Cell Sci* 74: 169-79.

Stadelmann, C., S. Timmler, A. Barrantes-Freer, and M. Simons. 2019. "Myelin in the Central Nervous System: Structure, Function, and Pathology." *Physiol Rev* 99 (3): 1381-1431. https://doi.org/10.1152/physrev.00031.2018.

Staeheli, P., M. Prochazka, P. A. Steigmeier, and O. Haller. 1984. "Genetic control of interferon action: mouse strain distribution and inheritance of an induced protein with guanylate-binding property." *Virology* 137 (1): 135-42. https://doi.org/10.1016/0042-6822(84)90016-3.

Stangel, M., S. Fredrikson, E. Meinl, A. Petzold, O. Stuve, and H. Tumani. 2013. "The utility of cerebrospinal fluid analysis in patients with multiple

sclerosis." *Nat Rev Neurol* 9 (5): 267-76. https://doi.org/10.1038/nrneurol.2013.41.

Steinman, R. M., G. Kaplan, M. D. Witmer, and Z. A. Cohn. 1979. "Identification of a novel cell type in peripheral lymphoid organs of mice. V. Purification of spleen dendritic cells, new surface markers, and maintenance in vitro." *J Exp Med* 149 (1): 1-16. https://doi.org/10.1084/jem.149.1.1.

Stevens, B., N. J. Allen, L. E. Vazquez, G. R. Howell, K. S. Christopherson, N. Nouri, K. D. Micheva, A. K. Mehalow, A. D. Huberman, B. Stafford, A. Sher, A. M. Litke, J. D. Lambris, S. J. Smith, S. W. John, and B. A. Barres. 2007. "The classical complement cascade mediates CNS synapse elimination." *Cell* 131 (6): 1164-78. https://doi.org/10.1016/j.cell.2007.10.036.

Stewart, C. R., L. M. Stuart, K. Wilkinson, J. M. van Gils, J. Deng, A. Halle, K. J. Rayner, L. Boyer, R. Zhong, W. A. Frazier, A. Lacy-Hulbert, J. El Khoury, D. T. Golenbock, and K. J. Moore. 2010. "CD36 ligands promote sterile inflammation through assembly of a Toll-like receptor 4 and 6 heterodimer." *Nat Immunol* 11 (2): 155-61. https://doi.org/10.1038/ni.1836.

Stiles, L. N., M. T. Liu, J. A. Kane, and T. E. Lane. 2009. "CXCL10 and trafficking of virus-specific T cells during coronavirus-induced demyelination." *Autoimmunity* 42 (6): 484-91. https://doi.org/10.1080/08916930902810708.

Stoppini, L., P. A. Buchs, and D. Muller. 1991. "A simple method for organotypic cultures of nervous tissue." *J Neurosci Methods* 37 (2): 173-82. https://doi.org/10.1016/0165-0270(91)90128-m.

Storch, M. K., S. Piddlesden, M. Haltia, M. Iivanainen, P. Morgan, and H. Lassmann. 1998. "Multiple sclerosis: in situ evidence for antibody- and complement-mediated demyelination." *Ann Neurol* 43 (4): 465-71. https://doi.org/10.1002/ana.410430409.

Streit, W. J., M. B. Graeber, and G. W. Kreutzberg. 1988. "Functional plasticity of microglia: a review." *Glia* 1 (5): 301-7. https://doi.org/10.1002/glia.440010502.

Stuart, L. M., S. A. Bell, C. R. Stewart, J. M. Silver, J. Richard, J. L. Goss, A. A. Tseng, A. Zhang, J. B. E. Khoury, and K. J. Moore. 2007. "CD36 signals to the actin cytoskeleton and regulates microglial migration via a p130Cas complex." *J Biol Chem* 282 (37): 27392-27401. https://doi.org/10.1074/jbc.M702887200.

Sun, L., J. Wu, F. Du, X. Chen, and Z. J. Chen. 2013. "Cyclic GMP-AMP synthase is a cytosolic DNA sensor that activates the type I interferon pathway." *Science* 339 (6121): 786-91. https://doi.org/10.1126/science.1232458.

Sunnemark, D., S. Eltayeb, E. Wallström, L. Appelsved, A. Malmberg, H. Lassmann, A. Ericsson-Dahlstrand, F. Piehl, and T. Olsson. 2003. "Differential expression of the chemokine receptors CX3CR1 and CCR1 by microglia and macrophages in myelin-oligodendrocyte-glycoprotein-induced experimental autoimmune encephalomyelitis." *Brain Pathol* 13 (4): 617-29. https://doi.org/10.1111/j.1750-3639.2003.tb00490.x.

Suri, C., B. P. Fung, A. S. Tischler, and D. M. Chikaraishi. 1993. "Catecholaminergic cell lines from the brain and adrenal glands of tyrosine hydroxylase-SV40 T antigen transgenic mice." *J Neurosci* 13 (3): 1280-91. https://doi.org/10.1523/jneurosci.13-03-01280.1993.

Szakal, A. K., K. L. Holmes, and J. G. Tew. 1983. "Transport of immune complexes from the subcapsular sinus to lymph node follicles on the

surface of nonphagocytic cells, including cells with dendritic morphology." *J Immunol* 131 (4): 1714-27.

Szretter, K. J., J. D. Brien, L. B. Thackray, H. W. Virgin, P. Cresswell, and M. S. Diamond. 2011. "The interferon-inducible gene viperin restricts West Nile virus pathogenesis." *J Virol* 85 (22): 11557-66. https://doi.org/10.1128/jvi.05519-11.

Szuchet, S., D. C. Plachetzki, and R. Karialukas. 2002. "Oligodendrocytes express an alpha/beta-interferon-susceptible Mx gene: molecular characterization of the encoded protein." *Glia* 37 (2): 183-9. https://doi.org/10.1002/glia.10027.

Tag-El-Din-Hassan, H. T., N. Sasaki, K. Moritoh, D. Torigoe, A. Maeda, and T. Agui. 2012. "The chicken 2'-5' oligoadenylate synthetase A inhibits the replication of West Nile virus." *Jpn J Vet Res* 60 (2-3): 95-103.

Taguchi, F., J. Kajioka, and T. Miyamura. 1982. "Prevalence rate and age of acquisition of antibodies against JC virus and BK virus in human sera." *Microbiol Immunol* 26 (11): 1057-64. https://doi.org/10.1111/j.1348-0421.1982.tb00254.x.

Takahashi, K., and S. Yamanaka. 2006. "Induction of pluripotent stem cells from mouse embryonic and adult fibroblast cultures by defined factors." *Cell* 126 (4): 663-76. https://doi.org/10.1016/j.cell.2006.07.024.

Takahashi, Y., H. Mori, M. Mishina, M. Watanabe, N. Kondo, J. Shimomura, Y. Kubota, K. Matsuda, K. Fukushima, N. Shiroma, N. Akasaka, H. Nishida, A. Imamura, H. Watanabe, N. Sugiyama, M. Ikezawa, and T. Fujiwara. 2005. "Autoantibodies and cell-mediated autoimmunity to NMDA-type GluRepsilon2 in patients with Rasmussen's encephalitis and chronic progressive epilepsia partialis continua." *Epilepsia* 46 Suppl 5: 152-8. https://doi.org/10.1111/j.1528-1167.2005.01024.x.

Takaoka, A., Z. Wang, M. K. Choi, H. Yanai, H. Negishi, T. Ban, Y. Lu, M. Miyagishi, T. Kodama, K. Honda, Y. Ohba, and T. Taniguchi. 2007. "DAI (DLM-1/ZBP1) is a cytosolic DNA sensor and an activator of innate immune response." *Nature* 448 (7152): 501-5. https://doi.org/10.1038/nature06013.

Tamassia, N., V. Le Moigne, M. Rossato, M. Donini, S. McCartney, F. Calzetti, M. Colonna, F. Bazzoni, and M. A. Cassatella. 2008. "Activation of an immunoregulatory and antiviral gene expression program in poly(I:C)-transfected human neutrophils." *J Immunol* 181 (9): 6563-73. https://doi.org/10.4049/jimmunol.181.9.6563.

Tan, C. S., and I. J. Koralnik. 2010. "Progressive multifocal leukoencephalopathy and other disorders caused by JC virus: clinical features and pathogenesis." *Lancet Neurol* 9 (4): 425-37. https://doi.org/10.1016/s1474-4422(10)70040-5.

Tang, C. A., A. C. Lee, S. Chang, Q. Xu, A. Shao, Y. Lo, W. T. Spalek, J. A. Pinilla-Ibarz, J. R. Del Valle, and C. A. Hu. 2021. "STING regulates BCR signaling in normal and malignant B cells." *Cell Mol Immunol* 18 (4): 1016-1031. https://doi.org/10.1038/s41423-020-00552-0.

Tarlinton, R. E., E. Martynova, A. A. Rizvanov, S. Khaiboullina, and S. Verma. 2020. "Role of Viruses in the Pathogenesis of Multiple Sclerosis." *Viruses* 12 (6). https://doi.org/10.3390/v12060643.

Tauro, L. B., M. E. Rivarola, E. Lucca, B. Marino, R. Mazzini, J. F. Cardoso, M. E. Barrandeguy, M. R. Teixeira Nunes, and M. S. Contigiani. 2015. "First isolation of Bunyamwera virus (Bunyaviridae family) from horses with neurological disease and an abortion in Argentina." *Vet J* 206 (1): 111-4. https://doi.org/10.1016/j.tvjl.2015.06.013.

Thapa, M., R. S. Welner, R. Pelayo, and D. J. Carr. 2008. "CXCL9 and CXCL10 expression are critical for control of genital herpes simplex virus type 2 infection through mobilization of HSV-specific CTL and NK cells to the nervous system." *J Immunol* 180 (2): 1098-106. https://doi.org/10.4049/jimmunol.180.2.1098.

"The Gene Ontology resource: enriching a GOld mine." 2021. *Nucleic Acids Res* 49 (D1): D325-d334. https://doi.org/10.1093/nar/gkaa1113.

Thompson, A. J., B. L. Banwell, F. Barkhof, W. M. Carroll, T. Coetzee, G. Comi, J. Correale, F. Fazekas, M. Filippi, M. S. Freedman, K. Fujihara, S. L. Galetta, H. P. Hartung, L. Kappos, F. D. Lublin, R. A. Marrie, A. E. Miller, D. H. Miller, X. Montalban, E. M. Mowry, P. S. Sorensen, M. Tintoré, A. L. Traboulsee, M. Trojano, B. M. J. Uitdehaag, S. Vukusic, E. Waubant, B. G. Weinshenker, S. C. Reingold, and J. A. Cohen. 2018. "Diagnosis of multiple sclerosis: 2017 revisions of the McDonald criteria." *Lancet Neurol* 17 (2): 162-173. https://doi.org/10.1016/s1474-4422(17)30470-2.

Thomsen, R., and A. Lade Nielsen. 2011. "A Boyden chamber-based method for characterization of astrocyte protrusion localized RNA and protein." *Glia* 59 (11): 1782-92. https://doi.org/10.1002/glia.21223.

Thomson, C. E., M. McCulloch, A. Sorenson, S. C. Barnett, B. V. Seed, I. R. Griffiths, and M. McLaughlin. 2008. "Myelinated, synapsing cultures of murine spinal cord--validation as an in vitro model of the central nervous system." *Eur J Neurosci* 28 (8): 1518-35. https://doi.org/10.1111/j.1460-9568.2008.06415.x.

Tian, J., A. M. Avalos, S. Y. Mao, B. Chen, K. Senthil, H. Wu, P. Parroche, S. Drabic, D. Golenbock, C. Sirois, J. Hua, L. L. An, L. Audoly, G. La Rosa, A. Bierhaus, P. Naworth, A. Marshak-Rothstein, M. K. Crow, K. A. Fitzgerald, E. Latz, P. A. Kiener, and A. J. Coyle. 2007. "Toll-like receptor 9-dependent activation by DNA-containing immune complexes is mediated by HMGB1 and RAGE." *Nat Immunol* 8 (5): 487-96. https://doi.org/10.1038/ni1457.

Tintoré, M., A. Rovira, J. Río, C. Tur, R. Pelayo, C. Nos, N. Téllez, H. Perkal, M. Comabella, J. Sastre-Garriga, and X. Montalban. 2008. "Do oligoclonal bands add information to MRI in first attacks of multiple sclerosis?" *Neurology* 70 (13 Pt 2): 1079-83. https://doi.org/10.1212/01.wnl.0000280576.73609.c6.

Tornberg, U. C., and D. Holmberg. 1995. "B-1a, B-1b and B-2 B cells display unique VHDJH repertoires formed at different stages of ontogeny and under different selection pressures." *Embo j* 14 (8): 1680-9.

Tran, E. H., K. Hoekstra, N. van Rooijen, C. D. Dijkstra, and T. Owens. 1998. "Immune invasion of the central nervous system parenchyma and experimental allergic encephalomyelitis, but not leukocyte extravasation from blood, are prevented in macrophage-depleted mice." *J Immunol* 161 (7): 3767-75.

Trujillo, J. A., E. L. Fleming, and S. Perlman. 2013. "Transgenic CCL2 expression in the central nervous system results in a dysregulated immune response and enhanced lethality after coronavirus infection." *J Virol* 87 (5): 2376-89. https://doi.org/10.1128/jvi.03089-12.

Tsao, N., H. P. Hsu, C. M. Wu, C. C. Liu, and H. Y. Lei. 2001. "Tumour necrosis factor-alpha causes an increase in blood-brain barrier permeability during sepsis." *J Med Microbiol* 50 (9): 812-821. https://doi.org/10.1099/0022-1317-50-9-812.

Tschen, S. I., S. A. Stohlman, C. Ramakrishna, D. R. Hinton, R. D. Atkinson, and C. C. Bergmann. 2006. "CNS viral infection diverts homing of antibody-

secreting cells from lymphoid organs to the CNS." *Eur J Immunol* 36 (3): 603-12. https://doi.org/10.1002/eji.200535123.

Tur-Kaspa, R., L. Teicher, B. J. Levine, A. I. Skoultchi, and D. A. Shafritz. 1986. "Use of electroporation to introduce biologically active foreign genes into primary rat hepatocytes." *Mol Cell Biol* 6 (2): 716-8. https://doi.org/10.1128/mcb.6.2.716-718.1986.

Tyler, K. L. 2018. "Acute Viral Encephalitis." *N Engl J Med* 379 (6): 557-566. https://doi.org/10.1056/NEJMra1708714.

Uguccioni, M., C. R. Mackay, B. Ochensberger, P. Loetscher, S. Rhis, G. J. LaRosa, P. Rao, P. D. Ponath, M. Baggiolini, and C. A. Dahinden. 1997. "High expression of the chemokine receptor CCR3 in human blood basophils. Role in activation by eotaxin, MCP-4, and other chemokines." *J Clin Invest* 100 (5): 1137-43. https://doi.org/10.1172/jci119624.

Ulper, L., I. Sarand, K. Rausalu, and A. Merits. 2008. "Construction, properties, and potential application of infectious plasmids containing Semliki Forest virus full-length cDNA with an inserted intron." *J Virol Methods* 148 (1-2): 265-70. https://doi.org/10.1016/j.jviromet.2007.10.007.

Unterholzner, L., S. E. Keating, M. Baran, K. A. Horan, S. B. Jensen, S. Sharma, C. M. Sirois, T. Jin, E. Latz, T. S. Xiao, K. A. Fitzgerald, S. R. Paludan, and A. G. Bowie. 2010. "IFI16 is an innate immune sensor for intracellular DNA." *Nat Immunol* 11 (11): 997-1004. https://doi.org/10.1038/ni.1932.

van Marle, G., S. Henry, T. Todoruk, A. Sullivan, C. Silva, S. B. Rourke, J. Holden, J. C. McArthur, M. J. Gill, and C. Power. 2004. "Human immunodeficiency virus type 1 Nef protein mediates neural cell death: a neurotoxic role for IP-10." *Virology* 329 (2): 302-18. https://doi.org/10.1016/j.virol.2004.08.024.

Vanguri, P., and M. L. Shin. 1986. "Activation of complement by myelin: identification of C1-binding proteins of human myelin from central nervous tissue." *J Neurochem* 46 (5): 1535-41. https://doi.org/10.1111/j.1471-4159.1986.tb01773.x.

Veldhuis, W. B., S. Floris, P. H. van der Meide, I. M. Vos, H. E. de Vries, C. D. Dijkstra, P. R. Bär, and K. Nicolay. 2003. "Interferon-beta prevents cytokine-induced neutrophil infiltration and attenuates blood-brain barrier disruption." *J Cereb Blood Flow Metab* 23 (9): 1060-9. https://doi.org/10.1097/01.wcb.0000080701.47016.24.

Venkatesan, A., and O. C. Murphy. 2018. "Viral Encephalitis." *Neurol Clin* 36 (4): 705-724. https://doi.org/10.1016/j.ncl.2018.07.001.

Vernadakis, A. 1988. "Neuron-glia interrelations." *Int Rev Neurobiol* 30: 149-224.

Villar, L. M., L. Costa-Frossard, T. Masterman, O. Fernandez, X. Montalban, B. Casanova, G. Izquierdo, F. Coret, H. Tumani, A. Saiz, R. Arroyo, K. Fink, L. Leyva, C. Espejo, M. Simo-Castello, M. I. Garcia-Sanchez, F. Lauda, S. Llufriu, R. Alvarez-Lafuente, J. Olascoaga, A. Prada, A. Oterino, C. de Andres, M. Tintore, L. Ramio-Torrenta, E. Rodriguez-Martin, C. Picon, M. Comabella, E. Quintana, E. Aguera, S. Diaz, R. Fernandez-Bolanos, J. A. Garcia-Merino, L. Landete, M. Menendez-Gonzalez, L. Navarro, D. Perez, F. Sanchez-Lopez, P. J. Serrano-Castro, A. Tunon, M. Espino, A. Muriel, A. Bar-Or, and J. C. Alvarez-Cermeno. 2015. "Lipid-specific immunoglobulin M bands in cerebrospinal fluid are associated with a reduced risk of developing progressive multifocal leukoencephalopathy during treatment with natalizumab." *Ann Neurol* 77 (3): 447-57. https://doi.org/10.1002/ana.24345.

Villar, L. M., M. Espiño, E. Roldán, N. Marín, L. Costa-Frossard, A. Muriel, and J. C. Alvarez-Cermeño. 2011. "Increased peripheral blood CD5+ B cells

predict earlier conversion to MS in high-risk clinically isolated syndromes." *Mult Scler* 17 (6): 690-4. https://doi.org/10.1177/1352458510396922.

Villar, L. M., J. Masjuan, M. C. Sádaba, P. González-Porqué, J. Plaza, A. Bootello, and J. C. Alvarez-Cermeño. 2005. "Early differential diagnosis of multiple sclerosis using a new oligoclonal band test." *Arch Neurol* 62 (4): 574-7. https://doi.org/10.1001/archneur.62.4.574.

Villar, L. M., M. C. Sadaba, E. Roldan, J. Masjuan, P. Gonzalez-Porque, N. Villarrubia, M. Espino, J. A. Garcia-Trujillo, A. Bootello, and J. C. Alvarez-Cermeno. 2005. "Intrathecal synthesis of oligoclonal IgM against myelin lipids predicts an aggressive disease course in MS." *J Clin Invest* 115 (1): 187-94. https://doi.org/10.1172/jci22833.

Vitner, E. B., T. Farfel-Becker, N. S. Ferreira, D. Leshkowitz, P. Sharma, K. S. Lang, and A. H. Futerman. 2016. "Induction of the type I interferon response in neurological forms of Gaucher disease." *J Neuroinflammation* 13 (1): 104. https://doi.org/10.1186/s12974-016-0570-2.

Volpato, V., J. Smith, C. Sandor, J. S. Ried, A. Baud, A. Handel, S. E. Newey, F. Wessely, M. Attar, E. Whiteley, S. Chintawar, A. Verheyen, T. Barta, M. Lako, L. Armstrong, C. Muschet, A. Artati, C. Cusulin, K. Christensen, C. Patsch, E. Sharma, J. Nicod, P. Brownjohn, V. Stubbs, W. E. Heywood, P. Gissen, R. De Filippis, K. Janssen, P. Reinhardt, J. Adamski, I. Royaux, P. J. Peeters, G. C. Terstappen, M. Graf, F. J. Livesey, C. J. Akerman, K. Mills, R. Bowden, G. Nicholson, C. Webber, M. Z. Cader, and V. Lakics. 2018. "Reproducibility of Molecular Phenotypes after Long-Term Differentiation to Human iPSC-Derived Neurons: A Multi-Site Omics Study." *Stem Cell Reports* 11 (4): 897-911. https://doi.org/10.1016/j.stemcr.2018.08.013.

von Glehn, F., R. P. C. Dias-Carneiro, A. S. Moraes, A. S. Farias, Vapg Silva, F. T. M. Oliveira, Cebg Silva, F. de Carvalho, E. Rahal, C. Baecher-Allan, and L. M. B. Santos. 2018. "Dimethyl fumarate downregulates the immune response through the HCA(2)/GPR109A pathway: Implications for the treatment of multiple sclerosis." *Mult Scler Relat Disord* 23: 46-50. https://doi.org/10.1016/j.msard.2018.04.016.

Wahl, S. M., J. M. Wilton, D. L. Rosenstreich, and J. J. Oppenheim. 1975. "The role of macrophages in the production of lymphokines by T and B lymphocytes." *J Immunol* 114 (4): 1296-301.

Wake, H., A. J. Moorhouse, S. Jinno, S. Kohsaka, and J. Nabekura. 2009. "Resting microglia directly monitor the functional state of synapses in vivo and determine the fate of ischemic terminals." *J Neurosci* 29 (13): 3974-80. https://doi.org/10.1523/jneurosci.4363-08.2009.

Walton, C., R. King, L. Rechtman, W. Kaye, E. Leray, R. A. Marrie, N. Robertson, N. La Rocca, B. Uitdehaag, I. van der Mei, M. Wallin, A. Helme, C. Angood Napier, N. Rijke, and P. Baneke. 2020. "Rising prevalence of multiple sclerosis worldwide: Insights from the Atlas of MS, third edition." *Mult Scler* 26 (14): 1816-1821. https://doi.org/10.1177/1352458520970841.

Wang, C., N. Yosef, J. Gaublomme, C. Wu, Y. Lee, C. B. Clish, J. Kaminski, S. Xiao, G. Meyer Zu Horste, M. Pawlak, Y. Kishi, N. Joller, K. Karwacz, C. Zhu, M. Ordovas-Montanes, A. Madi, I. Wortman, T. Miyazaki, R. A. Sobel, H. Park, A. Regev, and V. K. Kuchroo. 2015. "CD5L/AIM Regulates Lipid Biosynthesis and Restrains Th17 Cell Pathogenicity." *Cell* 163 (6): 1413-27. https://doi.org/10.1016/j.cell.2015.10.068.

Wang, X., E. R. Hinson, and P. Cresswell. 2007. "The interferon-inducible protein viperin inhibits influenza virus release by perturbing lipid rafts." *Cell Host Microbe* 2 (2): 96-105. https://doi.org/10.1016/j.chom.2007.06.009.

Wang, X., M. M. H. Li, J. Zhao, S. Li, M. R. MacDonald, C. M. Rice, X. Gao, and G. Gao. 2016. "Sindbis Virus Can Exploit a Host Antiviral Protein To Evade Immune Surveillance." *J Virol* 90 (22): 10247-10258. https://doi.org/10.1128/jvi.01487-16.

Wardlaw, A. C. 1962. "The complement-dependent bacteriolytic activity of normal human serum. I. The effect of pH and ionic strength and the role of lysozyme." *J Exp Med* 115 (6): 1231-49. https://doi.org/10.1084/jem.115.6.1231.

Warrington, A. E., K. Asakura, A. J. Bieber, B. Ciric, V. Van Keulen, S. V. Kaveri, R. A. Kyle, L. R. Pease, and M. Rodriguez. 2000. "Human monoclonal antibodies reactive to oligodendrocytes promote remyelination in a model of multiple sclerosis." *Proc Natl Acad Sci U S A* 97 (12): 6820-5. https://doi.org/10.1073/pnas.97.12.6820.

Watson, J., E. Trenkner, and M. Cohn. 1973. "The use of bacterial lipopolysaccharides to show that two signals are required for the induction of antibody synthesis." *J Exp Med* 138 (3): 699-714. https://doi.org/10.1084/jem.138.3.699.

Wei, J., Y. Ma, L. Wang, X. Chi, R. Yan, S. Wang, X. Li, X. Chen, W. Shao, and J. L. Chen. 2017. "Alpha/beta interferon receptor deficiency in mice significantly enhances susceptibility of the animals to pseudorabies virus infection." *Vet Microbiol* 203: 234-244. https://doi.org/10.1016/j.vetmic.2017.03.022.

Weih, F., G. Warr, H. Yang, and R. Bravo. 1997. "Multifocal defects in immune responses in RelB-deficient mice." *J Immunol* 158 (11): 5211-8.

Wekerle, H., C. Linington, H. Lassmann, and R. Meyermann. 1986. "Cellular immune reactivity within the CNS." *Trends in Neurosciences* 9: 271-277. https://doi.org/https://doi.org/10.1016/0166-2236(86)90077-9. https://www.sciencedirect.com/science/article/pii/0166223686900779.

Weller, R. O., E. Djuanda, H. Y. Yow, and R. O. Carare. 2009. "Lymphatic drainage of the brain and the pathophysiology of neurological disease." *Acta Neuropathol* 117 (1): 1-14. https://doi.org/10.1007/s00401-008-0457-0.

Werner, H. B., K. Kuhlmann, S. Shen, M. Uecker, A. Schardt, K. Dimova, F. Orfaniotou, A. Dhaunchak, B. G. Brinkmann, W. Möbius, L. Guarente, P. Casaccia-Bonnefil, O. Jahn, and K. A. Nave. 2007. "Proteolipid protein is required for transport of sirtuin 2 into CNS myelin." *J Neurosci* 27 (29): 7717-30. https://doi.org/10.1523/jneurosci.1254-07.2007.

Werner, M. H., and D. Huang. 2016. "Natalizumab-treated patients at high risk for PML persistently excrete JC polyomavirus." *J Neurovirol* 22 (6): 871-875. https://doi.org/10.1007/s13365-016-0449-0.

Wevers, N. R., R. van Vught, K. J. Wilschut, A. Nicolas, C. Chiang, H. L. Lanz, S. J. Trietsch, J. Joore, and P. Vulto. 2016. "High-throughput compound evaluation on 3D networks of neurons and glia in a microfluidic platform." *Sci Rep* 6: 38856. https://doi.org/10.1038/srep38856.

White, L. J., J. G. Wang, N. L. Davis, and R. E. Johnston. 2001. "Role of alpha/beta interferon in Venezuelan equine encephalitis virus pathogenesis: effect of an attenuating mutation in the 5' untranslated region." *J Virol* 75 (8): 3706-18. https://doi.org/10.1128/jvi.75.8.3706-3718.2001.

Whittemore, S. R., H. R. Sanon, and P. M. Wood. 1993. "Concurrent isolation and characterization of oligodendrocytes, microglia and astrocytes from adult human spinal cord." *Int J Dev Neurosci* 11 (6): 755-64. https://doi.org/10.1016/0736-5748(93)90064-k.

Wilhelm, K., J. Ganesan, T. Müller, C. Dürr, M. Grimm, A. Beilhack, C. D. Krempl, S. Sorichter, U. V. Gerlach, E. Jüttner, A. Zerweck, F. Gärtner, P. Pellegatti, F. Di Virgilio, D. Ferrari, N. Kambham, P. Fisch, J. Finke, M. Idzko, and R. Zeiser. 2010. "Graft-versus-host disease is enhanced by extracellular ATP activating P2X7R." *Nat Med* 16 (12): 1434-8. https://doi.org/10.1038/nm.2242.

Wilson, R. P., S. E. McGettigan, V. D. Dang, A. Kumar, M. P. Cancro, N. Nikbakht, W. Stohl, and G. F. Debes. 2019. "IgM Plasma Cells Reside in Healthy Skin and Accumulate with Chronic Inflammation." *J Invest Dermatol* 139 (12): 2477-2487. https://doi.org/10.1016/j.jid.2019.05.009.

Wirasinha, R. C., A. R. Davies, M. Srivastava, J. M. Sheridan, X. Y. X. Sng, O. M. Delmonte, K. Dobbs, K. L. Loh, L. A. Miosge, C. E. Lee, R. Chand, A. Chan, J. Y. Yap, M. D. Keller, K. Chen, J. Rossjohn, N. L. La Gruta, C. G. Vinuesa, H. H. Reid, M. S. Lionakis, L. D. Notarangelo, D. H. D. Gray, C. C. Goodnow, M. C. Cook, and S. R. Daley. 2021. "Nfkb2 variants reveal a p100-degradation threshold that defines autoimmune susceptibility." *J Exp Med* 218 (2). https://doi.org/10.1084/jem.20200476.

Wollebo, H. S., M. K. White, J. Gordon, J. R. Berger, and K. Khalili. 2015. "Persistence and pathogenesis of the neurotropic polyomavirus JC." *Ann Neurol* 77 (4): 560-70. https://doi.org/10.1002/ana.24371.

Wong, G. H., and D. V. Goeddel. 1986. "Tumour necrosis factors alpha and beta inhibit virus replication and synergize with interferons." *Nature* 323 (6091): 819-22. https://doi.org/10.1038/323819a0.

Woolums, B. M., B. A. McCray, H. Sung, M. Tabuchi, J. M. Sullivan, K. T. Ruppell, Y. Yang, C. Mamah, W. H. Aisenberg, P. C. Saavedra-Rivera, B. S. Larin, A. R. Lau, D. N. Robinson, Y. Xiang, M. N. Wu, C. J. Sumner, and T. E. Lloyd. 2020. "TRPV4 disrupts mitochondrial transport and causes axonal degeneration via a CaMKII-dependent elevation of intracellular Ca(2)." *Nat Commun* 11 (1): 2679. https://doi.org/10.1038/s41467-020-16411-5.

Wren, D. R., and M. Noble. 1989. "Oligodendrocytes and oligodendrocyte/type-2 astrocyte progenitor cells of adult rats are specifically susceptible to the lytic effects of complement in absence of antibody." *Proc Natl Acad Sci U S A* 86 (22): 9025-9. https://doi.org/10.1073/pnas.86.22.9025.

Wright, B. R., A. E. Warrington, D. D. Edberg, and M. Rodriguez. 2009. "Cellular mechanisms of central nervous system repair by natural autoreactive monoclonal antibodies." *Arch Neurol* 66 (12): 1456-9. https://doi.org/10.1001/archneurol.2009.262.

Wright, J. F., M. J. Shulman, D. E. Isenman, and R. H. Painter. 1990. "C1 binding by mouse IgM. The effect of abnormal glycosylation at position 402 resulting from a serine to asparagine exchange at residue 406 of the mu-chain." *J Biol Chem* 265 (18): 10506-13.

Wuthrich, C., S. Batson, M. P. Anderson, L. R. White, and I. J. Koralnik. 2016. "JC Virus Infects Neurons and Glial Cells in the Hippocampus." *J Neuropathol Exp Neurol* 75 (8): 712-717. https://doi.org/10.1093/jnen/nlw050.

Xia, M. Q., B. J. Bacskai, R. B. Knowles, S. X. Qin, and B. T. Hyman. 2000. "Expression of the chemokine receptor CXCR3 on neurons and the elevated expression of its ligand IP-10 in reactive astrocytes: in vitro ERK1/2 activation and role in Alzheimer's disease." *J Neuroimmunol* 108 (1-2): 227-35. https://doi.org/10.1016/s0165-5728(00)00285-x.

Xu, J., H. Dong, Q. Qian, X. Zhang, Y. Wang, W. Jin, and Y. Qian. 2017. "Astrocyte-derived CCL2 participates in surgery-induced cognitive

dysfunction and neuroinflammation via evoking microglia activation." *Behav Brain Res* 332: 145-153. https://doi.org/10.1016/j.bbr.2017.05.066.

Yamasaki, R., and J. I. Kira. 2019. "Multiple Sclerosis." *Adv Exp Med Biol* 1190: 217-247. https://doi.org/10.1007/978-981-32-9636-7_14.

Yamasaki, R., H. Lu, O. Butovsky, N. Ohno, A. M. Rietsch, R. Cialic, P. M. Wu, C. E. Doykan, J. Lin, A. C. Cotleur, G. Kidd, M. M. Zorlu, N. Sun, W. Hu, L. Liu, J. C. Lee, S. E. Taylor, L. Uehlein, D. Dixon, J. Gu, C. M. Floruta, M. Zhu, I. F. Charo, H. L. Weiner, and R. M. Ransohoff. 2014. "Differential roles of microglia and monocytes in the inflamed central nervous system." *J Exp Med* 211 (8): 1533-49. https://doi.org/10.1084/jem.20132477.

Yamout, B. I., and R. Alroughani. 2018. "Multiple Sclerosis." *Semin Neurol* 38 (2): 212-225. https://doi.org/10.1055/s-0038-1649502.

Yang, Y., T. Eversole, D. J. Lee, R. D. Sontheimer, and J. D. Capra. 1999. "Protein-protein interactions between native Ro52 and immunoglobulin G heavy chain." *Scand J Immunol* 49 (6): 620-8. https://doi.org/10.1046/j.1365-3083.1999.00547.x.

Yin, X., T. O. Crawford, J. W. Griffin, Ph Tu, V. M. Lee, C. Li, J. Roder, and B. D. Trapp. 1998. "Myelin-associated glycoprotein is a myelin signal that modulates the caliber of myelinated axons." *J Neurosci* 18 (6): 1953-62. https://doi.org/10.1523/jneurosci.18-06-01953.1998.

Yogo, Y., T. Kitamura, C. Sugimoto, T. Ueki, Y. Aso, K. Hara, and F. Taguchi. 1990. "Isolation of a possible archetypal JC virus DNA sequence from nonimmunocompromised individuals." *J Virol* 64 (6): 3139-43. https://doi.org/10.1128/jvi.64.6.3139-3143.1990.

Yoneyama, M., M. Kikuchi, T. Natsukawa, N. Shinobu, T. Imaizumi, M. Miyagishi, K. Taira, S. Akira, and T. Fujita. 2004. "The RNA helicase RIG-I has an essential function in double-stranded RNA-induced innate antiviral responses." *Nat Immunol* 5 (7): 730-7. https://doi.org/10.1038/ni1087.

Young, L. H., L. S. Klavinskis, M. B. Oldstone, and J. D. Young. 1989. "In vivo expression of perforin by CD8+ lymphocytes during an acute viral infection." *J Exp Med* 169 (6): 2159-71. https://doi.org/10.1084/jem.169.6.2159.

Yu, S. P., K. C. Ong, D. Perera, and K. T. Wong. 2019. "Neuronal transcriptomic responses to Japanese encephalitis virus infection with a special focus on chemokine CXCL11 and pattern recognition receptors RIG-1 and MDA5." *Virology* 527: 107-115. https://doi.org/10.1016/j.virol.2018.10.015.

Yun, J. J., M. S. Tsao, and S. D. Der. 2011. "Differential utilization of NF-kappaB RELA and RELB in response to extracellular versus intracellular polyIC stimulation in HT1080 cells." *BMC Immunol* 12: 15. https://doi.org/10.1186/1471-2172-12-15.

Zan, H., Z. Li, K. Yamaji, P. Dramitinos, A. Cerutti, and P. Casali. 2000. "B cell receptor engagement and T cell contact induce Bcl-6 somatic hypermutation in human B cells: identity with Ig hypermutation." *J Immunol* 165 (2): 830-9. https://doi.org/10.4049/jimmunol.165.2.830.

Zetterström, C. K., T. Bergman, B. Rynnel-Dagöö, H. Erlandsson Harris, O. Soder, U. Andersson, and H. G. Boman. 2002. "High mobility group box chromosomal protein 1 (HMGB1) is an antibacterial factor produced by the human adenoid." *Pediatr Res* 52 (2): 148-54. https://doi.org/10.1203/00006450-200208000-00004.

Zhan, Y., R. C. Paolicelli, F. Sforazzini, L. Weinhard, G. Bolasco, F. Pagani, A. L. Vyssotski, A. Bifone, A. Gozzi, D. Ragozzino, and C. T. Gross. 2014. "Deficient neuron-microglia signaling results in impaired functional brain

connectivity and social behavior." *Nat Neurosci* 17 (3): 400-6. https://doi.org/10.1038/nn.3641.

Zhang, B., Y. K. Chan, B. Lu, M. S. Diamond, and R. S. Klein. 2008. "CXCR3 mediates region-specific antiviral T cell trafficking within the central nervous system during West Nile virus encephalitis." *J Immunol* 180 (4): 2641-9. https://doi.org/10.4049/jimmunol.180.4.2641.

Zhang, L. Y., J. Pan, M. Mamtilahun, Y. Zhu, L. Wang, A. Venkatesh, R. Shi, X. Tu, K. Jin, Y. Wang, Z. Zhang, and G. Y. Yang. 2020. "Microglia exacerbate white matter injury via complement C3/C3aR pathway after hypoperfusion." *Theranostics* 10 (1): 74-90. https://doi.org/10.7150/thno.35841.

Zhang, Y., K. Chen, S. A. Sloan, M. L. Bennett, A. R. Scholze, S. O'Keeffe, H. P. Phatnani, P. Guarnieri, C. Caneda, N. Ruderisch, S. Deng, S. A. Liddelow, C. Zhang, R. Daneman, T. Maniatis, B. A. Barres, and J. Q. Wu. 2014. "An RNA-sequencing transcriptome and splicing database of glia, neurons, and vascular cells of the cerebral cortex." *J Neurosci* 34 (36): 11929-47. https://doi.org/10.1523/jneurosci.1860-14.2014.

Zhao, J., R. Vijay, M. Gale, Jr., M. S. Diamond, and S. Perlman. 2016. "MAVS Expressed by Hematopoietic Cells Is Critical for Control of West Nile Virus Infection and Pathogenesis." *J Virol* 90 (16): 7098-7108. https://doi.org/10.1128/jvi.00707-16.

Zhou, L., X. Wang, Y. J. Wang, Y. Zhou, S. Hu, L. Ye, W. Hou, H. Li, and W. Z. Ho. 2009. "Activation of toll-like receptor-3 induces interferon-lambda expression in human neuronal cells." *Neuroscience* 159 (2): 629-37. https://doi.org/10.1016/j.neuroscience.2008.12.036.

Zhou, Y., Y. Wang, M. Tischfield, J. Williams, P. M. Smallwood, A. Rattner, M. M. Taketo, and J. Nathans. 2014. "Canonical WNT signaling components in vascular development and barrier formation." *J Clin Invest* 124 (9): 3825-46. https://doi.org/10.1172/jci76431.

Zhu, J., Y. Zhang, A. Ghosh, R. A. Cuevas, A. Forero, J. Dhar, M. S. Ibsen, J. L. Schmid-Burgk, T. Schmidt, M. K. Ganapathiraju, T. Fujita, R. Hartmann, S. Barik, V. Hornung, C. B. Coyne, and S. N. Sarkar. 2014. "Antiviral activity of human OASL protein is mediated by enhancing signaling of the RIG-I RNA sensor." *Immunity* 40 (6): 936-48. https://doi.org/10.1016/j.immuni.2014.05.007.

Zhuang, H., S. Han, Y. Li, D. Kienhofer, P. Lee, S. Shumyak, R. Meyerholz, K. Rosadzinski, D. Rosner, A. Chan, Y. Xu, M. Segal, E. Sobel, L. J. Yang, M. H. Hoffmann, and W. H. Reeves. 2016. "A Novel Mechanism for Generating the Interferon Signature in Lupus: Opsonization of Dead Cells by Complement and IgM." *Arthritis Rheumatol* 68 (12): 2917-2928. https://doi.org/10.1002/art.39781.

Zimmermann, J., W. Hafezi, A. Dockhorn, E. U. Lorentzen, M. Krauthausen, D. R. Getts, M. Müller, J. E. Kühn, and N. J. C. King. 2017. "Enhanced viral clearance and reduced leukocyte infiltration in experimental herpes encephalitis after intranasal infection of CXCR3-deficient mice." *J Neurovirol* 23 (3): 394-403. https://doi.org/10.1007/s13365-016-0508-6.

Zinkernagel, R. M., and P. C. Doherty. 1975. "H-2 compatability requirement for T-cell-mediated lysis of target cells infected with lymphocytic choriomeningitis virus. Different cytotoxic T-cell specificities are associated with structures coded for in H-2K or H-2D." *J Exp Med* 141 (6): 1427-36. https://doi.org/10.1084/jem.141.6.1427.

Zivadinov, R., L. Uxa, A. Bratina, A. Bosco, B. Srinivasaraghavan, A. Minagar, M. Ukmar, Sy Benedetto, and M. Zorzon. 2007. "HLA-DRB1*1501, -DQB1*0301,

-DQB1*0302, -DQB1*0602, and -DQB1*0603 alleles are associated with more severe disease outcome on MRI in patients with multiple sclerosis." *Int Rev Neurobiol* 79: 521-35. https://doi.org/10.1016/s0074-7742(07)79023-2.